NOV 1 1 1930

U. S. DEPARTMENT OF COMMERCE

BUREAU OF STANDARDS JOURNAL OF RESEARCH

Vol. 5 OCTOBER, 1930 No. 4

CONTENTS

RP. No.	TITLE AND AUTHOR	Page
230.	Strength of welded shelf-angle connections. James H. Edwards, H. L. Whittemore, and A. H. Stang	781
231.	Measurement of surface temperatures. Wm. F. Roeser and E. F. Mueller	793
232.	Stress distribution in welded steel pedestals. James H. Edwards, H. L. Whittemore, and A. H. Stang	803
233.	The X-ray method applied to a study of the constitution of Portland cement. L. T. Brownmiller and R. H. Bogue	813
234.	Photo-ionization of cæsium vapor by absorption between the series lines. C. Boeckner and F. L. Mohler	831
235.	Efficiency of production of X rays. Warren W. Nicholas	843
236.	On the determination of the empirical formula of a hydrocarbon. Edward W. Washburn	867
237.	The importance of particle size in samples of certain metallurgical materials. J. A. Scherrer and G. E. F. Lundell	891
238.	A radiobeacon and receiving system for blind landing of aircraft. H. Diamond and F. W. Dunmore	897
239.	The isolation of the isomers of hexane from petroleum. Johannes H. Bruun and Mildred M. Hicks-Bruun	933
240.	Determination of carbon in high sulphur steels by direct combustion. H. A. Bright and G. E. F. Lundell	943
241.	Surface tension of soap solutions and its relation to the thickness of adsorbed films. Ronald Bulkley and F. G. Bitner	951
242.	The measurement of sound absorption. V. L. Chrisler and W. F. Snyder	957

BUREAU OF STANDARDS JOURNAL OF RESEARCH

CONTENTS OF RECENT NUMBERS

May, 1930 (Vol. 4, No. 5)

RP167. The sensitive surface of the Geiger tube electron counter. L. F. Curtiss. Price 5 cents.

RP168. The calorimetry of a fluid. Nathan S. Osborne. Price 5 cents.

RP169. The calibration of the "fingerhut" ionization chamber. Lauriston S. Taylor and G. Singer. Price 5 cents.

RP170. An apparatus and method for determining the compressibility of a gas and the correction for "super-compressibility." Howard S. Bean. Price 5 cents.

RP171. A new method of analyzing α-ray photographs. L. F. Curtiss. Price 5 cents.

RP172. The arc spectrum of bromine and its structure. C. C. Kiess and T. L. deBruin. Price 10 cents.

RP173. Spectral sensitization of photographic emulsions. Notes on bathing with pinacyanolpinaflavol mixtures. Burt H. Carroll and Donald Hubbard. Price 5 cents.

RP174. Performance of the Fahy simplex permeameter. Raymond L. Sanford. Price 5 cents.

RP175. Light scattering in liquids. R. M. Langer and William F. Meggers. Price 15 cents.

June, 1930 (Vol. 4, No. 6)

RP176. A comparison of the quinhydrone and hydrogen electrodes in solutions containing tannin. E. L. Wallace and John Beek, jr. Price 10 cents.

RP177. A gas analysis pipette for difficult absorptions. Martin Shepherd. Price 5 cents.

RP178. Note on the theory of heat conduction. M. S. Van Dusen. Price 5 cents..

RP179. Blistering phenomena in the enameling of cast iron. A. I. Krynitsky and W. N. Harrison. Price 30 cents.

RP180. On a modified method for decomposing aluminous silicates for chemical analysis. A. N. Finn and J. F. Klekotka. 5 cents.

RP181. Test of composite beams and slabs of hollow tile and concrete. D. E. Parsons and A. H. Stang. Price 15 cents.

RP182. Endurance properties of some special rail steels. John R. Freeman, jr., and R. D. France. Price 10 cents.

July, 1930 (Vol. 5, No. 1)

RP183. A comparison of resolving power and sensitivity of photographic plates with varying development. Burt H. Carroll and Donald Hubbard. Price 5 cents.

RP184. Resonance and quenching of the third principal series line of cæsium. C. Boeckner. Price 5 cents.

RP185. Relationships between Rockwell and Brinell numbers. S. N. Petrenko. Price 10 cents.

RP186. Photo-ionization of cæsium by line absorption. F. L. Mohler and C. Boeckner. Price 10 cents.

RP187. Regularities in the spectra of lutecium. William F. Meggers and Bourdon F. Scribner. Price 5 cents.

RP188. A new consistometer and its application to greases and to oils at low temperatures. Ronald Bulkley and F. G. Bitner. Price 5 cents.

RP189. Method of measuring strains between glazes and ceramic bodies. H. G. Schurecht and G. R. Pole. Price 5 cents.

RP190. The preparation of fiber test sheets. Merle B. Shaw, George W. Bicking, and Leo W. Snyder. Price 10 cents.

RP191. The Geiger tube electron counter. L. F. Curtiss. Price 5 cents.

RP192. Flow characteristics of special Fe-Ni-Cr alloys. H. J. French, William Kahlbaum, and A. A. Peterson. Price 25 cents.

RP193. The characteristics of 2-blade propeller fans. H. L. Dryden and P. S. Ballif. Price 10 cents.

Research papers are available as separates for purchase from the Superintendent of Documents United States Government Printing Office, Washington, D. C.

U. S. DEPARTMENT OF COMMERCE
R. P. LAMONT, Secretary
BUREAU OF STANDARDS
GEORGE K. BURGESS, Director

BUREAU OF STANDARDS JOURNAL OF RESEARCH

October, 1930
Vol. 5, No. 4

UNITED STATES
GOVERNMENT PRINTING OFFICE
WASHINGTON : 1930

For sale by the Superintendent of Documents, Washington, D. C. - - - $2.75 Per Year on Subscription

For a partial list of previous research papers appearing in BUREAU OF STANDARDS JOURNAL OF RESEARCH, see pages 2 and 3 of the cover.

STRENGTH OF WELDED SHELF-ANGLE CONNECTIONS

By James H. Edwards, H. L. Whittemore, and A. H. Stang

ABSTRACT

Shelf angles for transferring loads from floor beams to columns in steel-frame buildings were arc welded to H-section steel columns. The angles on the different specimens varied in width, thickness, and length. In some of the specimens the vertical leg of the shelf angle was placed against the web or flange of the column and fastened with fillet welds along one or more of the edges of contact. These types of specimens were: (A) Single weld at heel of angle; (B) welds at heel and toe of angle; (C) welds at ends of angle; (D) welds at heel and ends of angle; and (E) welds at heel, toe, and ends of angle. However, in the specimens of type F the angle was made of such a length that it filled snugly between the flanges of the column and was fastened to the column with fillet welds at both ends of the angle. The inner face of the vertical leg of the angle was placed 2 inches from the center line of the column web.

The specimens were tested to destruction in the 10,000,000-pound testing machine of the National Bureau of Standards. They were placed in the machine in an inverted position so that the outstanding legs of the angles rested on 6 by 6 inch steel bearing blocks placed on the lower platen of the machine. In testing all of the specimens, except type F, the inside faces of the bearing blocks were placed one-half inch from the face of the column to simulate end clearance in the floor beam. For type F the bearing blocks were placed under the entire width of the horizontal legs of the angles.

Increasing the width of the vertical leg of the angle increased the maximum stress for specimens welded only at the ends, type C. There were no definite indications that the width of the vertical leg of the angles affected the strength of the other types of specimens. Neither the thickness nor the length of the angles appeared to have much effect on the unit strength of the specimens.

Shelf-angle connections in designing which the stresses are those recommended by the Code for Fusion Welding and Gas Cutting in Building Construction, prepared by the American Welding Society, will have a factor of safety of about four, provided the welds are reinforced as much as the welds on these specimens.

CONTENTS

	Page
I. Introduction	782
1. Preliminary	782
2. Purpose	782
3. Acknowledgments	782
II. Specimens	782
1. Make-up	782
2. Welds	785
3. Angles	785
III. Test procedure	785
IV. Test data	786
V. Discussion	787
1. Welds	787
2. Angles	789
(*a*) Width	789
(*b*) Thickness	790
(*c*) Length	791
VI. Conclusions	791

I. INTRODUCTION

1. PRELIMINARY

The increased use of welding in fabricating steel structures has given rise to many questions regarding the strength of welded connections. In the past most of the tests have been made on relatively small specimens in which the distribution of stress is simple and for which there is an exact method of stress analysis. These have served to establish safe values of stress to be used in design as well as methods of supervision and inspection to insure that good welds are produced. There still remains the need of investigating full-sized connections subjected to the more complex conditions of stress which are present in an actual structure. Definite knowledge of their behavior under load makes it possible to design welded connections which are equally strong in resisting the various conditions of stress to which they may be subjected.

2. PURPOSE

These tests were made to determine the strength of welded connections of the seat-angle type for use in steel-frame buildings. In this type of connection, angles are welded to the outside of the flanges or to the inside of the flanges of the rolled steel columns as shown at *A* and *C* in Figure 1. The ends of the beams and girders which carry the floor are supported on these angles. The effect of changing the dimensions of the shelf angles and the location of the welds with respect to the angles were studied.

3. ACKNOWLEDGMENTS

The tests were made at the National Bureau of Standards. The American Bridge Co. furnished the specimens which were designed by James H. Edwards, chief engineer. O. E. Hovey, assistant chief engineer, and other members of the company's engineering staff assisted in making the tests. Prof. Elmer O. Bergman, research associate, made the analysis of the test data and edited the manuscript.

II. SPECIMENS

1. MAKE-UP

A test specimen consisted of a pair of angles welded to opposite faces of an H-section steel column as shown either at *A* or at *C* in Figure 1. The columns were Carnegie beam sections 3 and 8 feet long and 10 (CB104) (CB105), 12 (CB126), or 14 (CB146) inches deep. To reduce the number of columns required, two pairs of angles were welded to each column as shown in Figure 1. As the columns were not, except in a few cases, visibly deformed after the tests, the size of the columns had little effect upon the strength of the shelf angles. As each of the specimens failed through the welds, the properties of the material in the angles did not appear to affect the results of these tests.

According to the manner of attaching the shelf angle to the column, there were two classes of specimens. For class 1, the vertical leg of the angle was placed in contact with the outside of the flange of the column (see *A*–*A*, fig. 1) and attached with various combinations of welds as shown for types A, B, C, D, and E (fig. 2). For class 2,

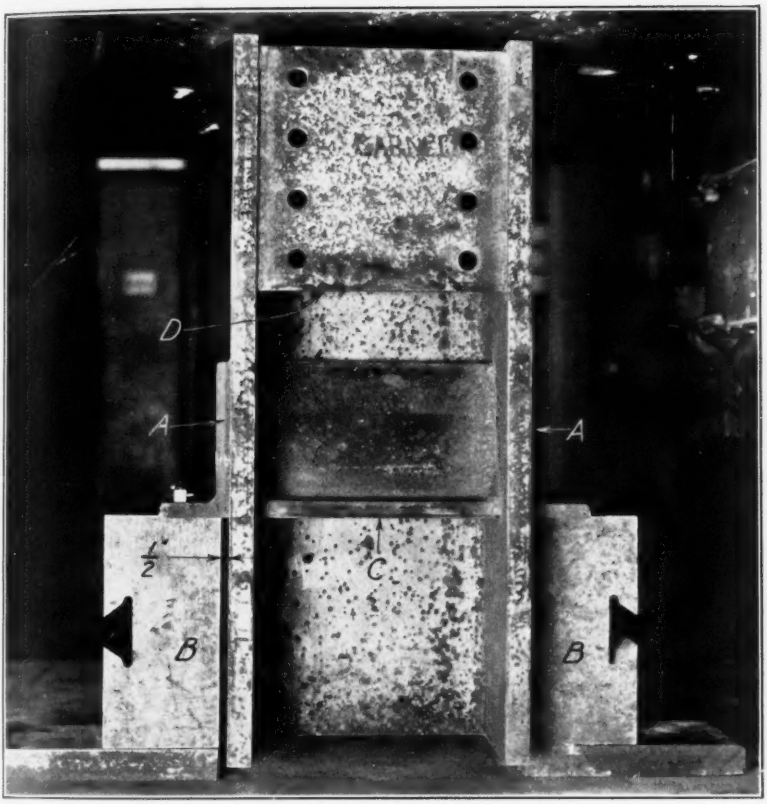

FIGURE 1.—*Column having welded shelf-angle connections*

(Patent No. 1757359, May 6, 1930, James H. Edwards, "Steel Building, Frame Construction.") Specimen in machine ready for testing. *A–A*, Shelf angles welded to the outside of the flange of the H-section. Specimens *A* to *E*, inclusive, were of this type. *B–B*, steel blocks through which the load was applied. As floor beams do not extend over the entire horizontal leg of the angle, spaces were left between the blocks and the column. *C*, shelf angles welded at the ends of the angles to the inside of the flanges of the H-section. Only one is shown as the other angle is on the other side of the column. The distance between the flange and the web ranged from 1⅛ to 1⅝ inches. The steel blocks, *B–B*, were used for loading these angles. They were placed under the entire width of the horizontal legs of the angles. The plate shown at *D* was used in another investigation.

the angle was of such a length that it fitted snugly between the inside faces of the column flanges as shown at *C* (fig. 1), and type F (fig. 2), to which it was fastened by a horizontal and a vertical weld at each

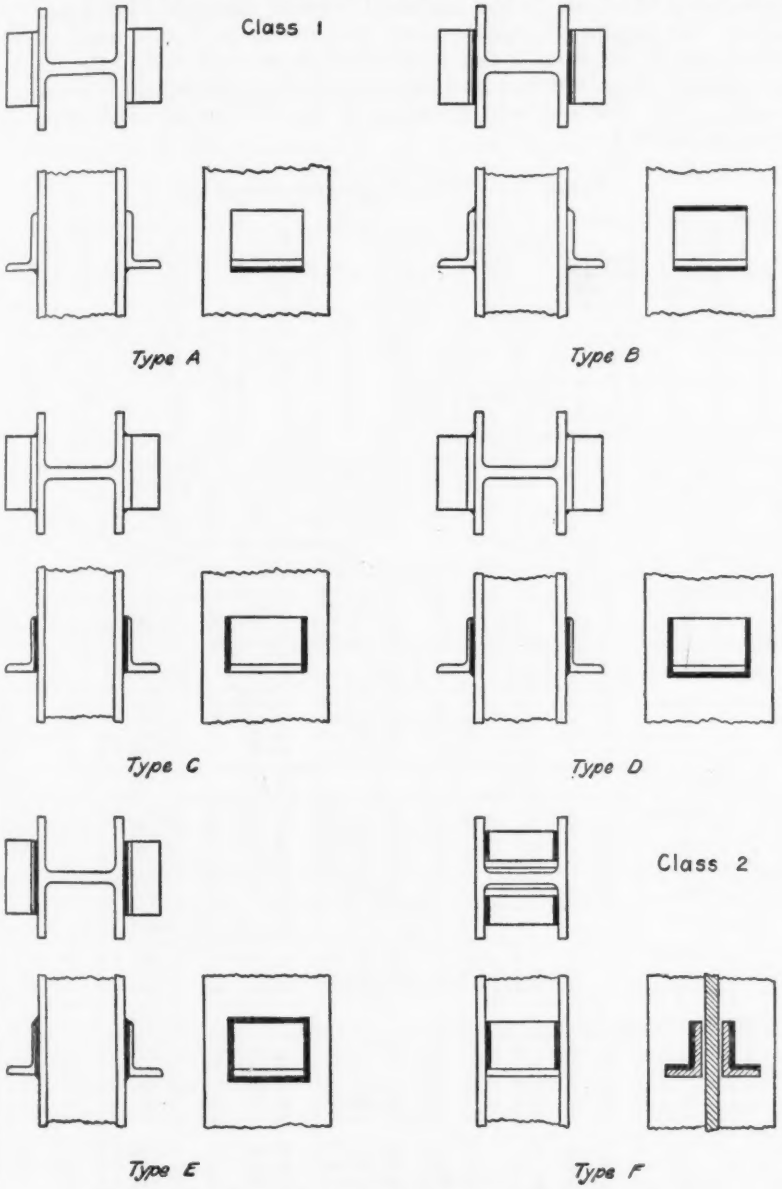

FIGURE 2.—*Drawing of each of the six types of specimens*

end. The inner face of the angle, *C* (fig. 1), was 2 inches from the center line of the web. The distance between the flange of the angle and the web of the column ranged from 1⅛ to 1 ⅝ inches, depending upon the size of the column.

The six types of welds are shown in Figure 2 and may be described as follows: A, horizontal welds along the heels of the angles; B, horizontal welds along the heels and toes of the angles; C, vertical welds along the ends of the angles; D, welds along the heels and the ends of the angles; E, welds along the heels, toes, and ends of the angles; and F, horizontal and vertical welds at each end of the angles, the angles fitting between and being welded to the inside faces of the flanges. The number and position of the welds for each type are given in Table 1.

TABLE 1.—*Tests of shelf-angle connections*

Type and No.	Manner of support	Number of welds on each angle		Dimensions of angles				Total length of weld	Maximum load	Maximum load per unit length	Average throat	Maximum stress on throat area	Factor of safety on throat area [1]	Average width of fracture	Maximum stress on area of fracture
		Horizontal	Vertical	Width— Vertical leg	Width— Horizontal leg	Thickness	Length								
				In.	*In.*	*In.*	*In.*	*In.*	*Lbs.*	*Lbs./in.*	*In.*	*Lbs./in.²*		*In.*	*Lbs./in.²*
A-1	Partial	1	0	4	4	5/8	8	16	363,000	22,700	0.31	[2] 73,000	5.6	7/16	51,900
2	do	1	0	4	4	5/8	8	16	412,500	25,800	.29	[2] 89,000	6.8	1 1/32	75,000
3	do	1	0	6	4	3/4	8	16	421,500	26,300	.27	[2] 98,000	7.5	3/8	70,000
4	do	1	0	6	4	3/4	8	16	353,000	22,100	.27	[2] 82,000	6.3	1 1/32	64,500
Average										24,200		[2] 85,500			65,300
B-1	Partial	2	0	4	4	5/8	8	32	556,000	17,400	0.26	67,000	4.8	7/16	39,800
2	do	2	0	6	4	3/4	8	32	473,000	14,800	.22	67,000	4.8	3/8	39,200
3	do	2	0	7	3 1/2	7/8	10	40	613,000	15,300	.28	55,000	3.9	3/8	40,800
4	do	2	0	8	3 1/2	7/8	10	40	535,000	13,400	.31	43,000	3.1	7/16	30,600
Average										15,200		58,000			37,600
C-1	Partial	0	2	4	4	1/2	8	16	173,000	10,800	0.27	40,000	3.5	1 1/32	31,400
2	do	0	2	6	4	5/8	8	24	313,000	13,000	.24	54,000	4.8	1 1/32	38,100
3	do	0	2	7	3 1/2	3/4	10	28	396,000	14,100	.23	61,000	5.4	3/8	37,600
4	do	0	2	8	3 1/2	3/4	10	32	446,000	13,900	.23	61,000	5.4	5/16	44,800
Average										13,000		54,000			38,000
D-1	Partial	1	2	4	4	3/4	6	28	495,000	17,700	0.31	57,000	4.7	3/8	47,100
2	do	1	2	4	4	3/4	6	28	491,000	17,500	.29	61,000	5.0	1 1/32	51,000
3	do	1	2	4	4	3/4	8	32	514,000	16,100	.28	57,000	4.7	3/8	42,900
4	do	1	2	6	4	7/8	8	40	521,000	13,000	.26	50,000	4.2	3/8	34,700
5	do	1	2	7	3 1/2	3/4	10	48	596,000	12,400	.28	44,000	3.7	3/8	33,100
6	do	1	2	8	3 1/2	1	10	52	689,500	13,300	.27	49,000	4.1	13/32	32,600
Average										15,000		53,000			40,200
E-1	Partial	2	2	4	4	3/4	8	48	676,000	14,100	0.27	52,000	4.0	3/8	37,600
2	do	2	2	6	4	7/8	8	56	799,000	14,300	.27	53,000	4.1	3/8	38,200
3	do	2	2	8	3 1/2	1	10	72	1,062,000	14,800	.26	57,000	4.4	3/8	39,500
Average										14,400		54,000			38,400
F-1	Full	2	2	4	4	5/8	7 3/4	27	316,500	11,700	0.24	49,000	4.0	1 1/32	34,100
2	do	2	2	4	4	3/4	7 3/4	26	359,000	13,800	.24	58,000	4.7	1 1/32	40,200
3	do	2	2	6	4	5/8	7 3/4	35	504,000	14,400	.27	53,000	4.4	13/32	35,400
4	do	2	2	6	4	3/4	8 1/4	34	488,000	14,300	.34	42,000	3.5	13/32	35,300
5	do	2	2	6	4	3/4	8 1/4	34	480,500	14,100	.32	44,000	3.7	13/32	34,800
6	do	2	2	6	4	5/8	9 1/4	35	447,500	12,800	.25	51,000	4.3	1 1/32	37,300
7	do	2	2	6	4	3/4	9 1/4	34	433,000	12,700	.24	53,000	4.4	3/8	33,900
8	do	2	2	8	3 1/2	3/4	12 1/4	40	615,000	15,400	.27	57,000	4.8	5/16	49,300
9	do	2	2	8	3 1/2	7/8	12 1/4	39	526,000	13,500	.27	50,000	4.2	1 1/32	39,300
Average										13,600		51,000			37,700

[1] Shelf angles designed by the method described in IV, Test Data.
[2] These values for maximum stress are much higher than the value found by the analysis given in V-1, Discussion, Welds, which are, in all probability, more nearly the actual stresses in the welds.

2. WELDS

The welder passed the qualification tests of the Structural Steel Welding Committee, American Bureau of Welding.[1] The welding rod was three-sixteenths inch in diameter (carbon 0.17 and manganese 0.52 per cent). The arc characteristics were d.c., average amperes 190, average volts 19. The average ultimate strength of all the 20 qualification specimens was 55,520 lbs./in.[2] and the minimum 43,990 lbs./in.[2] The average strength of the 12 specimens welded in the horizontal position was 56,990 lbs./in.[2] and in the vertical position 53,330 lbs./in.[2] The required average was 45,000 lbs./in.[2] and the minimum was 40,000 lbs./in.[2]

All the welds on these specimens were of the fillet type; that is, they were triangular welds, joining two surfaces approximately perpendicular to each other. The nominal size of the welds was $\frac{5}{16}$ inch, the size of a fillet weld being the designed length of its legs.[2] The actual sizes varied from $\frac{1}{4}$ inch and $\frac{7}{16}$ inch for one weld on specimen F–5 to $\frac{1}{2}$ inch and $\frac{5}{8}$ inch for one weld on specimen F–7. They were reinforced so that the actual throat was about equal to the leg of the weld.

The throat of a fillet weld, as defined in the Code for Fusion Welding and Gas Cutting in Building Construction,[3] is the normal distance from the root of the weld to the hypotenuse of the largest isosceles right triangle that can be constructed in the cross section of the fillet weld. The throat of these specimens was computed by multiplying the width of the narrower side of the weld by 0.707. Measurements on many of the welds showed that the actual throat was equal to the shorter leg of the weld.

The lengths of the welds are the corresponding dimensions of the angles. No deductions were made for craters at the ends of the welds.

3. ANGLES

From stock sizes of rolled steel angles, four sizes, having about the same width of horizontal leg, were selected to obtain a considerable difference in the width of the vertical leg. Angles with 4 and 6 inch vertical legs had 4-inch horizontal legs; those with 7 and 8 inch vertical legs had 3½-inch horizontal legs. The angles varied in length from 6 to 12½ inches and in thickness from ½ to 1 inch. The dimensions of the angles are given in Table 1.

III. TEST PROCEDURE

The specimens were tested to destruction in the 10,000,000 pounds capacity hydraulic testing machine at the National Bureau of Standards. They were placed in the machine in an inverted position so that the outstanding legs of the angles rested on 6 by 6 inch steel bearing blocks, *B–B* (fig. 1) placed on the lower platen of the testing machine. This platen is supported by a spherical bearing. After the specimen was placed in the machine, the lower platen was adjusted to

[1] Specifications for Test Specimens, section B, Qualification of Welders, Part I, Direct Current Metal Arc Process, American Bureau of Welding, 33 West Thirty-ninth Street, New York, N. Y.

[2] Paragraph 75, Weld Size, p. 16, Welding and Cutting Nomenclature, Definitions and Symbols, American Welding Society, 33 West Thirty-ninth Street, New York, N. Y., November, 1929.

[3] Code for Fusion Welding and Gas Cutting in Building Construction, Part A, Structural Steel, Edition 1928, American Welding Society, 33 West Thirty-ninth Street, New York, N. Y.

bring the upper surface of the column parallel with the upper platen; thus, the applied load was distributed approximately uniformly over the column. In all but two specimens (D–1 and D–2) the angles extended beyond the ends of the blocks. Figure 1 shows a specimen in the machine ready for testing.

The methods used in loading the specimens were designed to approximate the loading of a similar connection in an actual structure. In a structure the load on the shelf angle is the end reaction of the floor beam. To facilitate erection, clearance is provided between the ends of the beam and the faces of the columns. Figure 1 shows the method used in loading the specimens, having the vertical leg of the angle against the face of the column (types A, B, C, D, and E). The distance between the face of the bearing block and the face of the column was one-half inch so as to load the angle approximately as it would be loaded by a floor beam having clearance at the ends. This method of loading is referred to in this paper as "partial support."

For specimens of type F, having the angles welded at their ends to the inside faces of the column flanges, the supporting blocks were placed under the entire width of the horizontal legs of the angles, because in an actual structure the clearance at the ends of the beam would be less than the distance between the angle and the web of the column. This method of loading is designated "full support."

IV. TEST DATA

The values of the maximum loads and the corresponding values of the maximum loads per unit length of weld and maximum stresses are given in Table 1. In this table the data for each type of specimen are arranged according to the width of the vertical leg of the angles beginning with the narrowest.

The computed maximum load per unit length of weld is the maximum load divided by the sum of the lengths of all the welds. The computed maximum stress on the throat area is the maximum load divided by the sum of the throat areas of all the welds; that is, the average throat multiplied by the sum of the lengths of all the welds.

For computing the factor of safety, it was assumed that the forces on the shelf angles acted in the faces of the columns. For types A, B, C, D, and E it was assumed that the vertical welds were under shearing stress and the horizontal welds at the heel of the angles under tension and at the toe under compressive stress. Similarly, for type F all the vertical welds were assumed to be under shearing stress and the horizontal welds under tensile stress because the angle deflected.

The stresses recommended by the Code for Fusion Welding were used: that is, shear 11,300, tension 13,000 and compression 15,000 lbs./in.^{2} on the section through the throat of the weld. Dividing the observed maximum load for each specimen by the safe working load computed in this way, a factor of safety was obtained; these values are given in Table 1. A factor of safety of four is usually considered safe for statically loaded steel structures.

This method of design is admittedly the roughest kind of an approximation. Under V–1. Discussion, Welds, a somewhat closer analysis of some of the types of specimens is attempted. These seem to indicate that the computed values of the maximum stress given in Table 1 are higher than the actual stresses, especially for type A specimens.

As the actual throats were in most cases considerably larger than the throat computed in accordance with the Fusion Welding Code, and some of the welds did not rupture through the throat, the actual width of the fracture was measured. These values are given in Table 1. The maximum stress on fractured area was obtained by dividing the maximum load by the sum of the fractured areas of all the welds; that is, the average width of the fracture multiplied by the sum of the lengths of all the welds.

A detailed account of the behavior of the specimens follows.

Type A.—Horizontal welds along the heels of the angles. The angles of specimens 1 and 3 scaled. The specimens failed suddenly by rupture across the throat of the weld at the maximum load.

Type B.—Horizontal welds along the heels and toes of the angles. The heel welds of specimen 4 scaled and those of specimens 1 and 3 cracked. The maximum loads were only slightly greater than those which caused scaling or cracking. The welds at the heel failed across the throat and those at the toe failed along the leg on the column. The horizontal legs of the angles bent, the thickest angles bending the least. The horizontal legs of the angles of specimen 1 started to shear at the corners of the bearing blocks.

Type C.—Vertical welds along the ends of the angles. Failure occurred by rupture of the weld at the throat, fracture beginning at the lower or heel end of the weld. The outstanding legs of the angles bent, the thickest angles bending the least.

Type D.—Welds along the heels and the ends of the angles. The angles of specimens 2, 3, 5, and 6 scaled. The welds along the heel cracked at the maximum load, after which the load decreased very rapidly. Failure occured by rupture of the welds at the throat.

Type E.—Welds along the heels, toes, and ends of the angles. The angles of specimens 1 and 2 and the column flanges of specimen 3 scaled. In general, the welds fractured across the throat at the heel and the ends of the angles and along the leg on the column at the toe of the angles. The outstanding legs of the angles of specimens 1 and 2 bent.

Type F.—Both legs of angles welded to the inside faces of the flanges. The welds scaled and the angles bent. The vertical legs of the angles of specimens 4, 6, 8, and 9 also scaled. Failure of the welds began at the toe of the angles. The column flanges of specimens 1, 2, and 7 bulged outward. One angle of specimen 6 sheared at the heel between the edges of the bearing block and the flanges of the columns. Failure occurred by rupture of the vertical welds at the throat and of the horizontal welds along the leg on the column.

V. DISCUSSION

1. WELDS

The forces acting on the shelf angle for a specimen of type A are shown in Figure 3. The shelf angle on each side of the column is shown to emphasize the fact that the forces are symmetrically arranged with respect to the column. The column and the floor beams are shown by dashed lines. It should be remembered that in this figure the members are shown inverted with respect to the position they would occupy in a structure because the specimens

were tested in this position: P is the force applied by the floor beams, S and T are components of the stress acting across the cut section between the weld and the column, C is the resultant compressive force which the column exerts on the vertical leg of the angle, and F_1 and F_2 are frictional forces. The weld will fail when the stress, of which S and T are the components, becomes greater than the strength of the weld. Both F_1 and F_2 reduce the values which S and T would have if no friction were present.

The authors are indebted to O. E. Hovey for the following analysis of the stresses in the specimens of type A.

As under the action of the force P exerted by the bearing block, the outstanding leg of the angle would deflect, the action line of P is probably outside but close to the outer surface of the vertical leg of the angle about in the position shown in Figure 3.

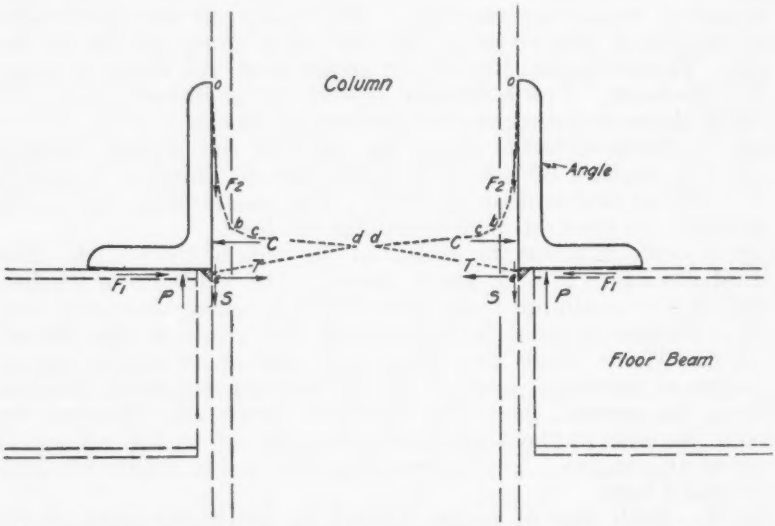

FIGURE 3.—*Free-body diagram showing the forces acting on a shelf angle and the weld of a specimen of type A having a weld at the heel of the angle*

The pressure of the vertical leg of the angle against the flange of the column would cause bending stresses in this leg of the angle which increase from zero at the toe to a maximum at the fillet. Because of the deflection of the vertical leg, the pressures would be expected to vary approximately inversely as the cube of the distance from the fillet. Opposite the fillet the stress distribution is far from simple and need not be discussed. Below the fillet the pressure distribution would be expected to follow closely the compressive stress in a simple beam taking the centroid of the weld as the neutral axis.

An approximate pressure distribution curve is shown at *o b c d e* (fig. 3). The action line of the resultant C is probably slightly above the upper surface of the outstanding leg of the angle as shown.

Knowing, approximately, the action lines of the forces P and C and assuming a coefficient of friction (say 0.3), the values of the forces and of the stress on the weld may be computed. The stress computed in this way is about 60,000 lbs./in^2.

The values of the maximum stress computed on the throat area for specimens of type A given in Table 1 appear to be much higher than the actual stresses and somwehat higher than those computed on the fractured area. A shelf angle designed by the method described in IV, Test Data, would, therefore, be safe. This is indicated, also by the high factors of safety given in Table 1.

The forces acting on a specimen of type B are shown in Figure 4. The forces are similar to those acting on specimens of type A (therefore the notation is the same) with the addition of the shearing force S_T on the toe of the angle. Due to the force S_T, the magnitude of the force S_H is less than in specimens of type A.

The low values of the factor of safety for specimens B–3 and B–4, particularly the latter, raise the question as to the safety of this type of shelf angle when designed in this way. It should be pointed out that if specimen B–4 had been the only one tested, it would have been concluded that the factor of safety of this type of shelf angle was only 3.08.

A discussion of the forces acting on specimens of type C is given later under V–2 (*a*), Angles, Width. For these specimens the stress in the welds is, for the most part, shear. Shelf angles of this type designed as described in IV, Test Data, may be satisfactory, although specimen C–1 showed a low factor of safety.

For types D, E, and F the variation in the number and position of the welds and in the width and length of the angles is too complex to warrant an analysis based on the limited number of tests.

Shelf angles of these types designed as described in IV, Test Data, might be safe, although specimens D–5, E–1, and F–1, 4, and 5 showed factors of safety less than four.

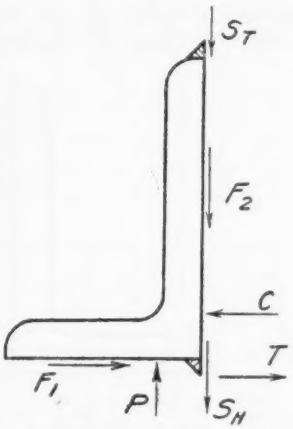

FIGURE 4.—*Free-body diagram showing the forces acting on a shelf angle and the welds of a specimen of type B having welds at the heel and the toe of the angle*

The bending of the shelf angles of type F probably caused high local stresses in the welds resulting in the low factors of safety.

2. ANGLES

(a) WIDTH

There are no definite indications that the width of the vertical leg of the angles affected the strength of the specimens of types A, D, E, and F. For type B there is a decrease and for type C an increase in the maximum stress with an increase in the width of the angle.

For specimens of type B the distribution of the load between the heel and toe welds depends on the stiffness of the vertical leg of the angles. The greater the width of the vertical leg, the larger will be the deformation. As a result the heel weld carries a larger proportion of the load for the lower loads. At and near the maximum load, however, the load must be distributed approximately equally because

the welds in all probability have sufficient ductility to detrude at the maximum load, enough to equalize the loads. Tests upon longitudinal fillet welds, similar to these, showed that the detrusion was about 0.1 inch before the load decreased appreciably from the maximum. For the angles having an 8-inch vertical leg a detrusion in the heel weld of only 0.01 inch more than the toe weld would appear to be all that is necessary to equalize the loads. This detrusion must occur in a direction prependicular to the direction of the weld, and might not reach the value found for the detrusion in the direction of the weld.

The forces acting on a shelf angle of specimens of type C are shown in Figure 5. P is the external force applied to the angle, S is the sum of the friction and the shearing force on the welds, C is the resultant compressive force between the column and the toe of the angle and upper portion of the welds, T is the resultant tensile force on the lower portion of the welds. The angle is in equilibrium under the

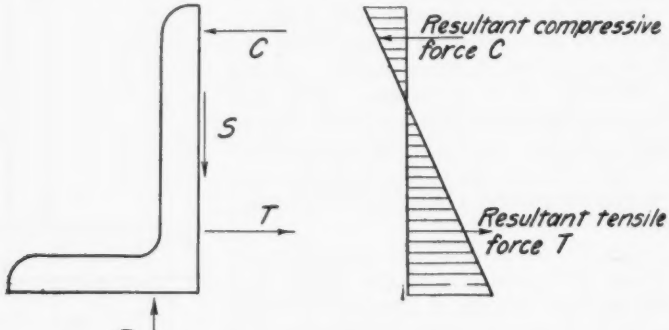

FIGURE 5.—*Free-body diagram showing the forces acting on a shelf angle and the welds of a specimen of type C having welds at the ends of the angle*

action of these forces which form two opposing couples. If the width of the vertical leg of the angle is, for example, doubled and the load P is also doubled (the average shearing stress in the weld remaining the same), the magnitude of the forces T and C will not change since their moment arm is doubled. As a result the tensile stress in the lower portion of the weld will be reduced to one-half its former value, while the shearing stress will remain unchanged. The resultant stress in the lower portion of the weld will, therefore, be decreased as the width of the vertical leg of the angle increases, and a greater maximum load per unit length will be required to cause failure. This is approximately confirmed by the increase in the value of the maximum stress (type C, Table 1) with an increase in the width of the vertical leg of the angle.

(b) THICKNESS

No definite conclusions can be drawn regarding the effect of the thickness of the angles on the strength of the connection. In type C there is an increase in strength with increase of width. The higher loads carried by the wider angles may be due, in part, to their greater thickness.

If we exclude the specimens of type A for which the thickness of the angles, obviously, had little effect upon the maximum stress, we find the following average maximum stresses on the throat area: Angles ½ inch thick, 40,000 lbs/in.^{2}; ⅝ inch thick, 54,800; ¾ inch thick, 55,000; ⅞ inch thick, 50, 200; and 1 inch thick, 53,000. It is evident that the thickness of the angles has practically no effect upon the maximum stress, at least for angles thicker than ½ inch.

(c) LENGTH

Since the length of the angles ranged from 6 to 12 inches and the load was applied only over the middle 6 inches, there were bending stresses in the direction of the length of the angle. These bending stresses might be expected to lower the values of the maximum stresses given in Table 1 for the longer angles.

The angles for specimens of type A were all 8 inches long so no conclusions can be drawn from the results on these specimens. Considering only specimens of types B, C, D, and E, the average maximum stress on the throat area for the angles 6 inches long is 59,000 lbs/in.^{2}; for the angles 8 inches long, 55,000; and for the angles 10 inches long, 52,900. These values tend to confirm the assumed effect of bending stresses, but the differences are small and may have been caused by other variables.

For specimens of type F, the average maximum stress on the throat area for the 7¾-inch angles is 53,300; for the 8¼-inch angles, 43,000; for the 9¼-inch angles, 52,500; and for the 12¼-inch angles, 53,500 lbs./in.^{2} It is evident that for these specimens the length of the angles has very little effect upon the stress. As they were supported only at the ends, the bending stresses were probably higher than in the specimens of the other types. The conclusion seems justified that the maximum stress is practically independent of the length of the angle for all of these specimens.

VI. CONCLUSIONS

Shelf angles for transferring loads from floor beams to columns in steel-frame buildings were arc-welded to H-section columns. The types of weld connections used were: Single weld at heel of shelf angle; welds at heel and toe of angle; welds at ends of angle; welds at heel and ends of angle; welds at heel, toe, and ends of angles; and welds at ends of angles fitted between the flanges of the H-section. The specimens were tested to destruction with the following results:

1. Each specimen failed through the weld. Therefore, the properties of the material in the column and in the angles had little or no effect upon the values of the maximum load.
2. For the specimens having welds only at the ends of the angles the average maximum stress in the welds increased as the width of the vertical leg of the angle was increased.
3. There were no definite indications that the width of the vertical leg of the angles affected the strength of the specimens.
4. Neither the thickness nor the length of the angles appeared to have much effect on the strength of the specimens.
5. Shelf-angle connections similar to those tested in this investigation, with reinforced fillet welds, will have a factor of safety of about

4 if they are designed with the following assumptions: (*a*) The forces act in the face of the column; (*b*) vertical fillet welds are stressed in shear; (*c*) horizontal fillet welds at the heel of the angle are stressed in tension; (*d*) horizontal fillet welds at the toe of the angle are stressed in compression, and (*e*) the allowable stresses are those given in the Code for Fusion Welding and Gas Cutting in Building Construction prepared by the American Welding Society.

WASHINGTON, July 8, 1930.

MEASUREMENT OF SURFACE TEMPERATURES

By Wm. F. Roeser and E. F. Mueller

ABSTRACT

After a brief discussion of some of the methods which have been used for measuring surface temperatures, the paper describes a surface thermometer of the thermocouple type which was successfully used for measuring the temperatures of steel rails during the periods of heating before and after welding. A compensated type of thermocouple, for more precise measurements at temperatures below 400° F., is also described, and results obtained in measuring the temperature of a drying roll are given.

The measurement of the temperature of a surface, when this temperature differs considerably from that of the environment, offers difficulties not encountered in the usual kind of temperature measurements, and many special devices and refinements of technique have been applied in problems of this kind. In this note some of the available methods for measuring surface temperatures are described, with particular reference to two types of contact thermometers which were found to be serviceable in special cases.

The methods which are ordinarily used for measuring surface temperatures fall into four general classes: (1) Those in which substances which undergo visible alterations, such as color change or melting, at a fixed temperature, or within a narrow range of temperature, are placed on the surface; (2) those in which a thermometric device is permanently attached to the surface; (3) those in which the temperature of the surface is inferred from the indication of instruments actuated by the radiation emitted from the surface; and (4) those in which a thermometric device is placed on or near the surface and the temperature of the surface is inferred from the indications of the device.

It is well known that the melting, or still better, the freezing points of pure substances furnish one of the best means available for establishing thermometric fixed points. Under favorable circumstances such thermometric points have been found to be fixed and reproducible to 0.01° or even to 0.001° F. The favorable conditions are purity of material, usually most easily obtained in certain metals or simple inorganic compounds; adequate isolation and protection of the sample during the measurement, and insertion of the thermometer into the material. Under such conditions the accuracy attainable is limited principally by the purity of the material and the sensitivity and accuracy of the temperature-measuring device. Under less favorable conditions the accuracy may be much lower. If the material is impure or becomes contaminated during the measurement, melting or freezing will take place within a range of temperature which, in general, is below the melting point of the pure material.

If a pure material placed upon a heated surface is seen to melt, this gives positive assurance that the temperature of the surface is higher

than the melting point of the material, provided only that there has been no contamination, in which case there is no definite melting point. If the material does not melt, this gives no positive assurance that the temperature of the surface is below the melting point of the material, because the piece placed on the surface is in thermal contact not only with the surface, but also with the surrounding medium, and therefore, assumes a temperature which is the resultant of all the influences to which it is subject. If molten material placed on a surface is seen to freeze, this can be taken to indicate that the temperature of the surface can not be much higher than the freezing point of the material. The method may, therefore, be capable of showing that the temperature of a surface is not below some known temperature, but does not yield other positive information.

The measurement of surface temperatures where the thermometric device is permanently attached is generally limited to the measurement of the temperature of stationary metal surfaces. This is commonly accomplished by drilling two small holes into the surface to a convenient depth and peening the bare end of each wire of a thermocouple into the separate holes. The ordinary welded junction is not employed, the circuit being completed through the metal. If the wires are sufficiently small, the effect due to heat transfer along the wires is negligible. Even when the temperature of the surface is not uniform, the holes can usually be drilled so close together that the indication of the thermocouple will correspond approximately to the temperature of the surface immediately surrounding the place where the couple wires are peened. Several devices to bring the portion of the wires next to the junction to the same temperature as the junction, have been employed. One method which gives very satisfactory results is to run the thermocouple wires along the surface, so that the wires are in good thermal contact with the surface, but electrically insulated from it.

The measurement of the temperature of moving surfaces by thermometric devices which are permanently attached to the surface requires complicated auxiliaries, such as sliding electric contacts. This method is so complicated that it is not ordinarily employed.

Radiation and optical pyrometers whose indications depend upon the radiation received by the instruments are available for measuring surface temperatures. Theoretically the total radiation pyrometer can be used for measuring any temperature, but it is ordinarily not applied for temperatures below 1,200° F. If the surface is exposed to view and above a red heat, the optical pyrometer may be employed and very satisfactory results obtained under favorable conditions.

The apparent temperatures indicated by these pyrometers are always lower than the true temperatures of the surfaces, by an amount depending upon the emission characteristics of the surfaces. Data are available for a large number of materials by means of which approximate corrections for emissivity may be made. The corrections in the case of the radiation pyrometer are much larger than in the case of the optical pyrometer, with a correspondingly larger uncertainty in the temperature found.

Contact thermometers have been made in a great variety of forms. Most of them contain a thermocouple which is so designed that when

the thermometer is brought into contact with a surface, the junction of the thermocouple assumes nearly the temperature of the surface. If such a couple is first calibrated by contact with surfaces of known temperature, it can be used to measure the temperature of any similar surface.

In 1924, at the request of the Joint Committee on Welded Rail Joints, American Bureau of Welding, there was designed and constructed at the National Bureau of Standards a contact pyrometer for determining the temperature of rails during the heating periods before and after the welding operation. This contact pyrometer shown in Figure 1 proved satisfactory for measuring the temperature of stationary metallic surfaces up to 1,300° F. The hot junction of this pyrometer consisted of a gold disk, 1 mm thick and 7 mm in diameter, into which two holes were drilled about 0.5 mm deep. No. 22 gage chromel and alumel thermocouple wires were hard soldered into these holes. The gold disk was backed with mica disks forming a stack 2 or 3 mm thick to provide thermal and electrical insulation between the hot junction and the supporting tube, as well as to cushion the gold disk. The front surface of the gold tip was made smooth to permit good thermal contact with the metallic surfaces.

It was found that when the gold disk was placed in firm contact with a hot metallic surface, the temperature of the disk was consistently lower than that of the surface by approximately 10 per cent of the difference between the air temperature and that of the hot surface. The instrument was calibrated by determining the emfs. when the disk was placed in contact with hot surfaces, the temperatures of which were determined by means of thermocouples peened into the

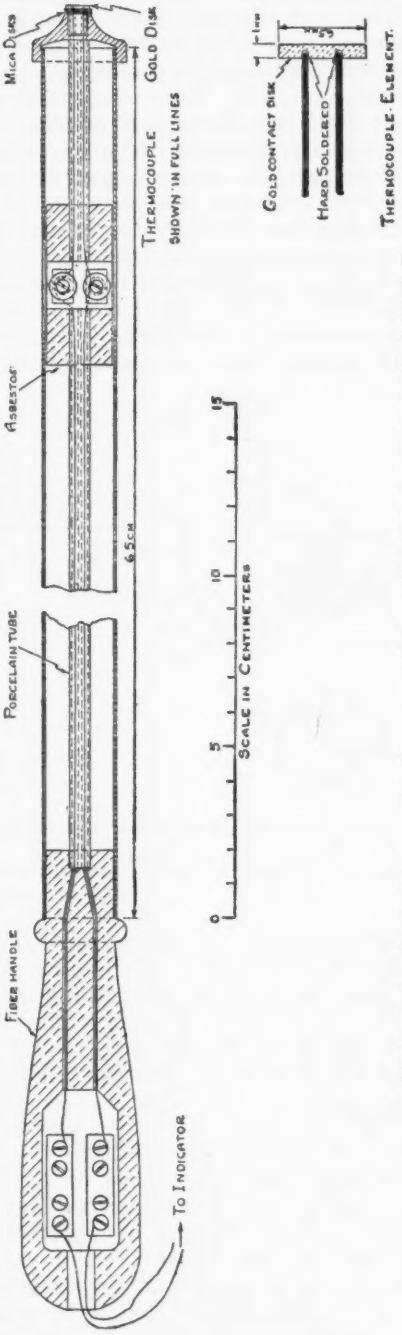

FIGURE 1.—*Contact pyrometer for measuring surface temperatures up to 1,300° F.*

metal. The time required to obtain a reading to an accuracy of ±25° F. at 1,100° F. was approximately 30 seconds.

King and Blackie [1] have described a thermocouple of this general type for measuring surface temperatures up to 200° C. (392° F.). The time required to obtain the surface temperature of a steel slab within 5° C. (9° F.) with this instrument was about six minutes. Neither of the above instruments is very satisfactory for obtaining the surface temperature of materials of very low thermal conductivity.

More recently another type of contact thermometer known as the compensated type has been introduced. One form of this instrument was described by Boyer and Buss.[2] In the compensated type an electric heating coil is placed back of the measuring junction and the heating so regulated that the space back of the measuring thermojunction is brought to the same temperature as this junction. This equality is obtained by regulating the heating until the measuring junction and an auxiliary thermojunction placed between the

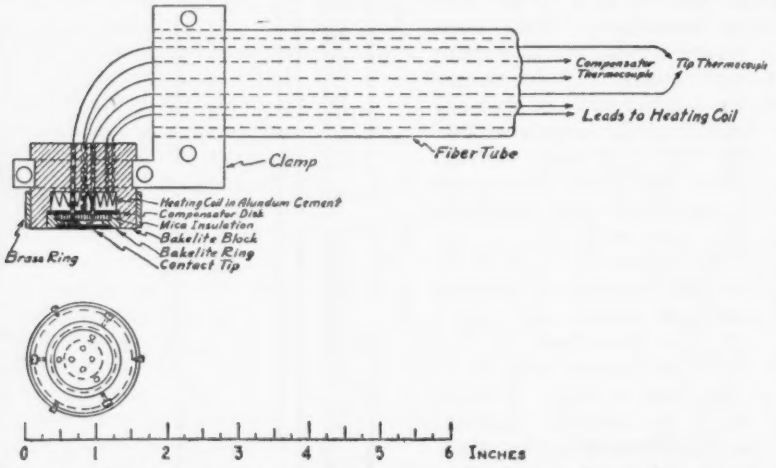

FIGURE 2.—*Compensated contact thermometer for measuring surface temperatures up to 400° F.*

heating coil and measuring junction indicate the same temperature. Under these conditions no heat is conducted away from the measuring junction and the latter, therefore, assumes the temperature of the surface with which it is in contact. Such a contact thermometer need not be calibrated empirically under actual conditions of use, since the measuring junction necessarily assumes the temperature of the surface. Tests on heated surfaces of known temperature are desirable in order to verify the calibration and to determine the adequacy of the compensation.

An important advantage of the compensated thermometer over the simpler type first described lies in the fact that the indications are very little affected by thermal resistance between the surface and the junction, since there is no heat flow from the hot surface to the junction when readings are made. In fact, it should be possible to use a compensated couple to measure surface temperatures with

[1] King and Blackie, J. of Sci. Inst., **2**, p. 260; 1924–25.
[2] Boyer and Buss, Ind. and Eng. Chem., **18**, p. 728; 1926.

considerable accuracy, while maintaining the junction at a small distance away from the heated surface instead of in contact with it.

A compensated contact thermometer is peculiarly adapted for measuring the temperature of a moving surface, when the temperature of the surface passing a given point in space is always the same, as is the case in most continuous processes. Such a thermometer is adapted primarily for measuring constant temperatures, since several minutes are required for the measuring couple to assume the temperature, and for adjusting the compensation and taking the readings.

In 1928 the authors designed and constructed a compensated contact thermometer for measuring the surface temperature of drying rolls in operation. A diagram of this instrument is shown in Figure 2 and the method employed for connecting the thermometer to the indicator is shown in Figure 3. The thermocouple elements are B. & S. gage No. 22 chromel and alumel wire. The contact disk of the thermometer is made of "sumet," a bearing metal, having a

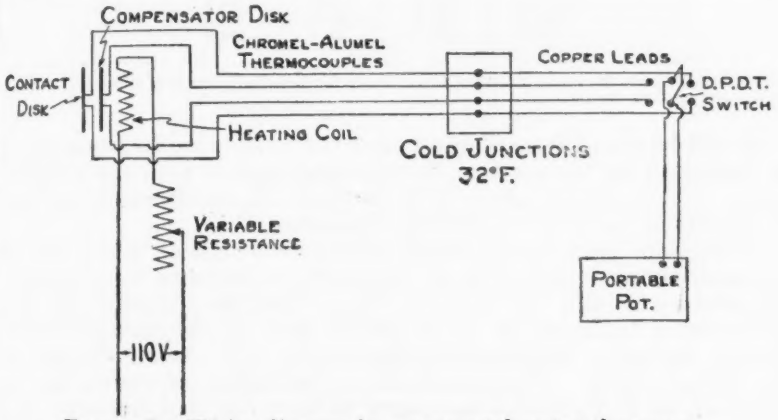

FIGURE 3.—*Wiring diagram for compensated contact thermometer*

low coefficient of friction against smooth steel or cast iron. This minimizes local heating of the contact tip by friction against the moving rolls. The "compensator" disk is made of copper in order to favor a uniform distribution of temperature back of the contact disk. Small holes were drilled into the disks and the thermocouple wires soldered into the holes with silver solder. The thermocouple wires of the contact disk were insulated from the compensator disk by small porcelain tubes.

The accuracy with which the temperature of a moving surface can be measured with such a contact thermometer remained to be determined. This was done by checking the thermometer on moving rolls inside of which known steam pressures were maintained.

The contact thermometer was first checked on paper drying rolls, the results being given in Table 1. A mercury-in-glass thermometer was placed in a thermometer well in the exhaust pipe from the roll on which the tests were made, and the observed temperatures were found to check with those calculated from these thermometer readings and from the steam pressure inside the roll. The particular roll

on which the temperature measurements were made was partially protected from heat losses by other hot rolls below and on the sides. Under such conditions the drop in temperature through the metal wall of the roll was very low. It was estimated that the drop was 0.5° F. and this amount has been subtracted from the steam temperature calculated from the pressure in order to obtain the true surface temperatures given in Table 1.

TABLE 1.—*Checks on contact thermometer on paper drying rolls, 15-inch diameter*

Surface speed of rolls	Contact thermometer temperature	Steam temperature	True surface temperature	Thermometer in well	Difference [1]
Ft. min.	*°F.*	*°F.*	*°F.*	*°F.*	*°F.*
47.5	250.5	252.2	251.7	252.7	−1.2
47.5	253.0	252.5	252.0	252.7	+1.0
47.5	261.0	261.2	260.7	261.7	+.3
47.5	262.0	261.2	260.7	261.7	+1.3
58	268.5	268.4	267.9		+.6
65	268.5	269.1	268.6	270.7	−.1
	265.0	266.9	266.4	264.0	−1.4
	266.0	266.0	265.5	263.5	+.5
	266.5	266.9	266.4	265.0	+.1

[1] This column gives the values of contact thermometer temperature (column 2) minus calculated (true) surface temperature (column 4).

It will be noted from Table 1 that the outside surface temperature as indicated by the contact thermometer agrees with the calculated (true) surface temperature to within 1.5° F., in all cases, and there is no indication of a systematic difference.

Tests were made to determine the error produced when the compensator thermocouple was not adjusted to the same temperature as the contact couple. It was found that when the compensator couple indicated a temperature 5° F. below that of the contact thermocouple, the latter indicated a termperature 1° F. below the true surface temperature. Thus, to obtain an indication of the surface temperature to 1° F. it was necessary to have the compensator couple indicate the same temperature as the contact couple to within 5° F.

The contact thermometer was also checked on milk drying rolls running with known steam pressures with no milk on the rolls. The results of these tests are given in Table 2. The rolls were protected from drafts and, in this case, it was estimated that the drop in temperature in the wall of the roll was 2° F.

TABLE 2.—*Checks on contact thermometer on milk drying rolls*

[The diameter of the rolls was 28 inches. The surface speed of the rolls was 107 feet per minute]

Contact thermometer temperature	Steam temperature	True surface temperature	Difference [1]
°F.	*°F.*	*°F.*	*°F.*
262.5	264.5	262.5	0.0
319.5	319.0	317.0	+2.5
317.0	317.4	315.4	+1.6
320.0	321.3	319.3	+.7

[1] This column gives the values of contact thermometer temperature (column 1) minus the calculated (true) surface temperature (column 3).

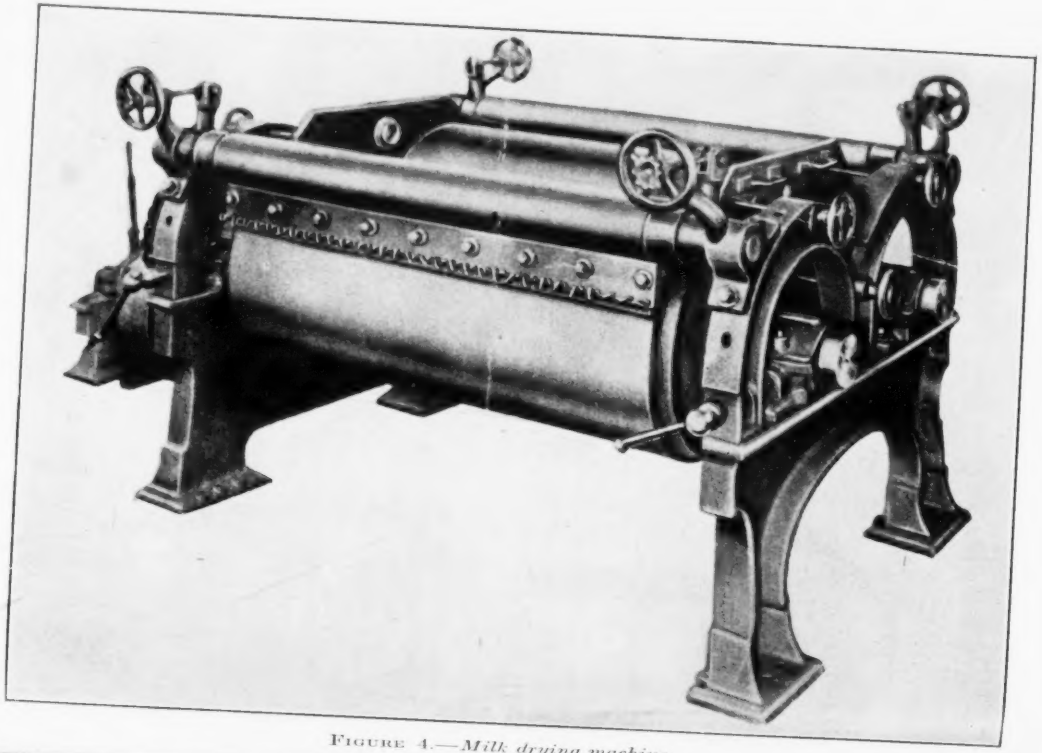

FIGURE 4.—*Milk drying machine*

It will be noted from Table 2 that the outside surface temperature as indicated by the contact thermometer agrees with the calculated (true) surface temperature to within 2.5° F. in all cases, while the average difference is 1.2° F.

As an example of the application of this type of instrument to the measurement of surface temperature and of the magnitude of the temperature variations obtained in drying processes, the results of some measurements on the rolls of a milk drying machine while in operation will be given.

A photograph of a twin-cylinder machine is reproduced in Figure 4. The drying cylinders are made of cast iron and are heated from the inside by steam at a pressure of approximately 75 lbs./in.^{2} (gauge). The cylinders, 28 inches in diameter and 5 feet long, rotate about 14 times per minute. Fresh liquid milk is fed into the V-shaped space between the upper halves of the faces of the two cylinders and a fixed depth of liquid milk is maintained in that space during operation. A small quantity of the milk passes regularly between the cylinders (which are slightly separated from each other) and adheres in the form of a thin film upon the face of each cylinder, is dried thereon, and then removed by stripping knives held in contract with the rotating cylinders.

The temperature measurements on the rolls of the milk drying machines were made at a plant of the Dry Milk Co. For making measurements on the portion of the rolls carrying a milk film, an auxiliary knife was used for scraping the film from the roll. This knife scraped the milk off for a width of about 2 inches. It was placed at various points around the circumference at the middle of the roll and the contact thermometer was placed in a position about 2 inches behind the knife. Under these circumstances, while the rate of heat flow within the cylinder wall was not modified, the rate of heat loss from the portion of the surface at which measurements were being made was very nearly the same as the rate of heat loss from the surface of a clean, dry roll.

The values in Table 3 give the results of tests made on one of the rolls of one machine when operating at an average steam pressure of 64.2 lbs./in.^{2} (gauge). The position at which the contact thermometer was held are expressed as percentages of the circumference from the point of the rolls nearest to contact.

TABLE 3.—*Temperature measurements on milk drying rolls*

[Steam pressure approximately 64 lbs./in.^{2} (gauge). Corresponding steam temperature 311° F.]

Position on roll	Per cent	Steam pressure	Surface temperature
		Lbs./in.^{2}	*°F.*
At top of roll	75.0	64.7	255.0
6 inches above knife	62.0	65.2	251.0
3¼ inches below knife	51.0	64.3	250.0
13¾ inches below knife	39.5	64.7	244.5
At bottom of roll	25.0	63.8	242.0
45° from bottom	12.5	62.5	238.0

The values in Table 4 give the results of the tests on the same roll of the same machine when operating at an average steam pressure of 74.3 lbs./in.^{2} (gauge).

TABLE 4.—*Temperature measurements on milk drying rolls*

[Steam pressure approximately 74 lbs./in.² (gauge). Corresponding steam temperature 319° F.]

Position on roll	Per cent	Steam pressure	Surface temperature
		Lbs./in.²	°F
At top of roll	75.0	74.5	256
6 inches above knife	62.0	74.9	252
3¼ inches below knife	51.0	75.4	250
13¾ inches below knife	39.5	74.4	253
At bottom of roll	25.0	73.0	246
45° from bottom	12.5	73.8	241

The observations given in Tables 3 and 4 are shown graphically in Figures 5 and 6. Figure 5 indicates the cycle of temperature which a point on the roll goes through during each rotation.

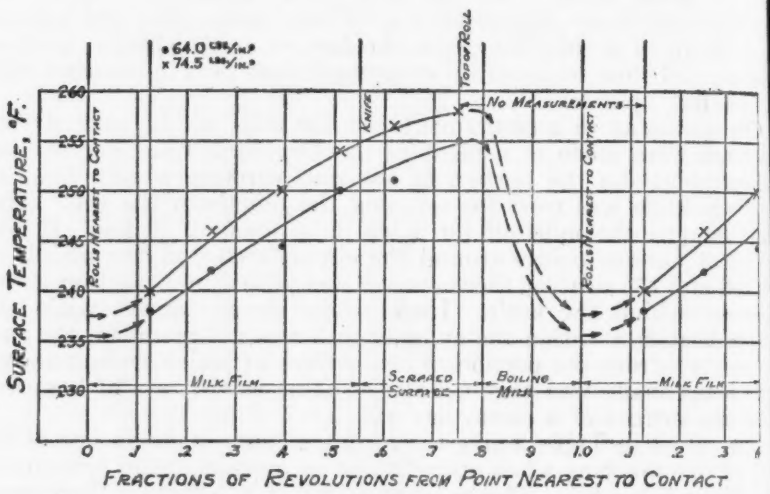

FIGURE 5.—*Cycle of temperature of a point on the surface of the roll*

The following observations were taken at a point just below the knife on one of the rolls to determine the temperature drop in the milk film:

	Steam pressure	Temperature
	Lbs./in.²	°F.
Measurement on scraped roll	68.8	230.0
Measurement on milk film	71.7	268.0

At the point where these measurements were made the milk film was practically free from moisture. Taking into consideration the change in steam pressure the temperature drop in the milk film was of the order of 3° F.

An attempt was made to determine the temperature of the upper surface of one of the rolls by applying fusible substances to the surface. Benzoic acid, pyrogallol, and a number of other substances were used.

In the experiments on the rolls of a paper drying machine very satisfactory results had been obtained on the clean, dry surfaces by applying a small bead of the material, inclosing the head of a pin, to the surface of the moving roll. When the temperature was below the melting point of the material, the bead made no mark on the roll but when the temperature was high enough to melt the material the bead left a wet streak on the roll.

When this method was applied to the milk drying machines under operating conditions it failed to yield definite results because the cylinders were not scraped entirely clean by the stripping knives

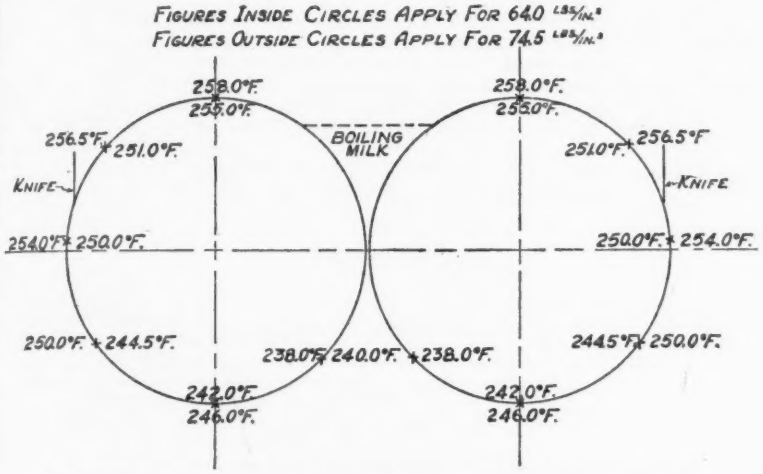

FIGURE 6.—*Temperatures observed at various points on the rolls*

The film of material on the cylinder was of such character that when the beads of various materials were held against the moving surface streaks always appeared. Streaks of practically the same appearance, however, were produced by beads of several fusible materials whose melting points, when pure, were known to be above the temperature of the roll. Even a piece of wood made a similar streak on the roll.

It was found that the rolls of the milk drying machine moved too rapidly to make the determination by placing small pieces of the fusible materials on the cylinder, since it was not possible, with the unaided eye, to observe whether melting took place or not. Stopping the machines long enough to make the observation would have involved a very uncertain extrapolation, since every accessible point on the surface was increasing in temperature by approximately 5° F. per second. We thus have to record one more instance in which the measurement by means of fusible substances has failed to meet expectations.

SUMMARY

Two types of contact thermometers are described in this paper and the results of temperature measurements made on the rolls of paper and milk drying machines with one of the contact thermometers are also given. The surface temperatures of moving rolls have been determined to an accuracy of 2° F. by means of a compensated contact thermometer.

Attempts to determine the approximate temperature of the surface of the moving rolls by employing fusible substances proved successful on clean, dry surfaces but were unsuccessful when applied to surfaces carrying foreign or contaminating materials.

WASHINGTON, June 9, 1930.

STRESS DISTRIBUTION IN WELDED STEEL PEDESTALS

By James H. Edwards, H. L. Whittemore, and A. H. Stang

ABSTRACT

Two welded steel pedestals were tested in compression and a study of the stress distribution was made. These pedestals were designed for the purpose of replacing cast-steel pedestals for bridges because they could be made in a shorter time and without the use of expensive patterns. In one of the pedestals, the inclined plates did not touch the bottom plates, and the parts of the pedestal could be clamped in their proper relative position before welding the inclined plates to the bottom plates. The stress distribution in this pedestal was uniform over the inclined plates and the stiffeners at mid height. The inclined plates of the other pedestal were machined so as to fit directly between the top and base plates and a fillet weld was used to maintain the relative position of the plates. The stresses in the stiffeners of this pedestal were more than twice as great as the stresses in the inclined plates for loads in the designed working range. It was evident that the uniform distribution of stress in the first pedestal was due to the even bearing obtained by the use of the large weld between the inclined and the base plates.

The maximum strengths of the two pedestals were, however, about the same and more than six times the load for which they were designed.

CONTENTS

	Page
I. Introduction	803
II. The pedestals	804
III. Location of strain gage lines	804
IV. Testing procedure	807
V. Results and discussion of the tests	808
1. Stresses computed from the load	808
2. Stresses computed from the strain readings	808
(*a*) Stresses at mid height	809
(*b*) Stresses near top and bottom of the inclined plates	811
(*c*) Stresses in the lower plate	811
3. Maximum load and description of failure	811
VI. Conclusions	811

I. INTRODUCTION

Pedestals are used to support the ends of bridges. They distribute the concentrated load over the top of the masonry or concrete bridge piers. If the lower surface of the pedestal is sufficiently large, the compressive stresses in the pier will be safe.

Bridge pedestals have in the past been either grey iron or steel castings. Cast pedestals have the disadvantages that the patterns are expensive and that the time required to make the castings sometimes delays the completion of the bridge.

Pedestals, especially the smaller sizes, can not be economically made by riveting together pieces of rolled structural steel. As welding is coming into use for the fabrication of steel structures, the American Bridge Co. designed pedestals of rolled steel plates, joining the pieces by electric arc welding. As the use of welded pedestals was a radical departure from present practice, the cooperation of the bureau was obtained in determining the compressive strength.

II. THE PEDESTALS

Drawings of the pedestals are shown in Figure 1. They were designed to carry a load of 350,000 pounds, and represent one size in a series of pedestals for different bridge spans and loadings.

The difference between the pedestals *F1* and *F2* lies wholly in the connection between the bottom plate and the inclined plates. In pedestal *F1*, the inclined plates (*P2*) do not touch the bottom plate and the parts of the pedestal can be truly lined and clamped in their proper relative positions before the weld "A" is made. The corresponding inclined plates (*P6*) of pedestal *F2* must be carefully

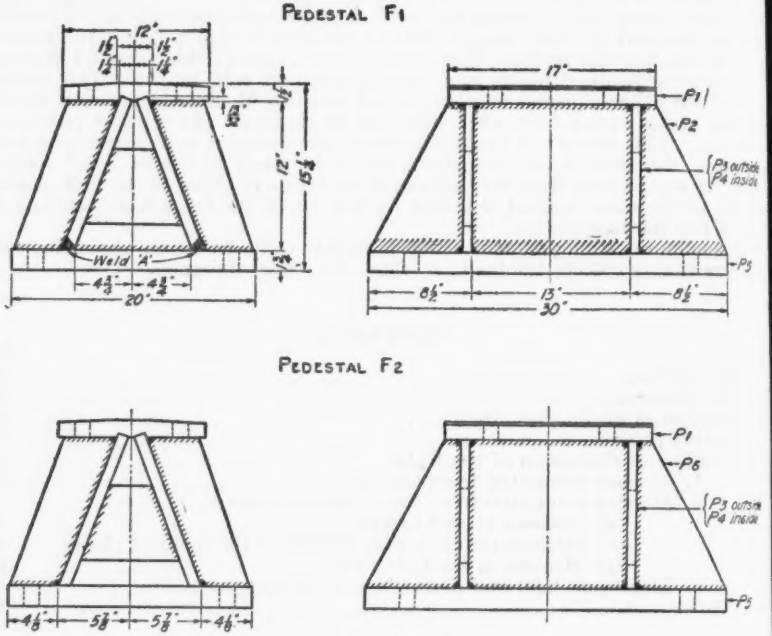

FIGURE 1.—*Drawing of the pedestals*

MATERIAL FOR PEDESTAL F1

P1, one plate 12 by 1½ by 17 inches.
P2, two plates 12 13/16 (finished width) by ⅞ by 30 inches.
P3, four plates 3½ by ¾ by 12 13/16 inches (neat length).
P4, two plates 6 by ¾ by 8 inches.
P5, one plate 20 by 1¾ by 30 inches.

MATERIAL FOR PEDESTAL F2

All material same as that in F1 except plates P6 used instead of plates P2.
P6, two plates 13¼ (finished width) by ⅞ by 30 inches.

NOTE.—All welds ⅜ inch except weld A for pedestal F1.

finished at both the bottom and the top, and any irregularity in any of the plates may result in uneven bearing after the seams are welded.

III. LOCATION OF STRAIN GAGE LINES

Twenty 2-inch gage lines were used for the study of stress distribution on each pedestal. It was recognized that this number was not sufficient to determine fully the stress distribution, but the results show that much was learned which would aid in perfecting the design. The location of the gage lines is shown in Figures 2, 3, and 4.

It was convenient to designate the four sides of the pedestal by the initials of the cardinal points of the compass toward which the sides faced when in the testing machine and the gage lines on each side by an additional number or letter to show the location.

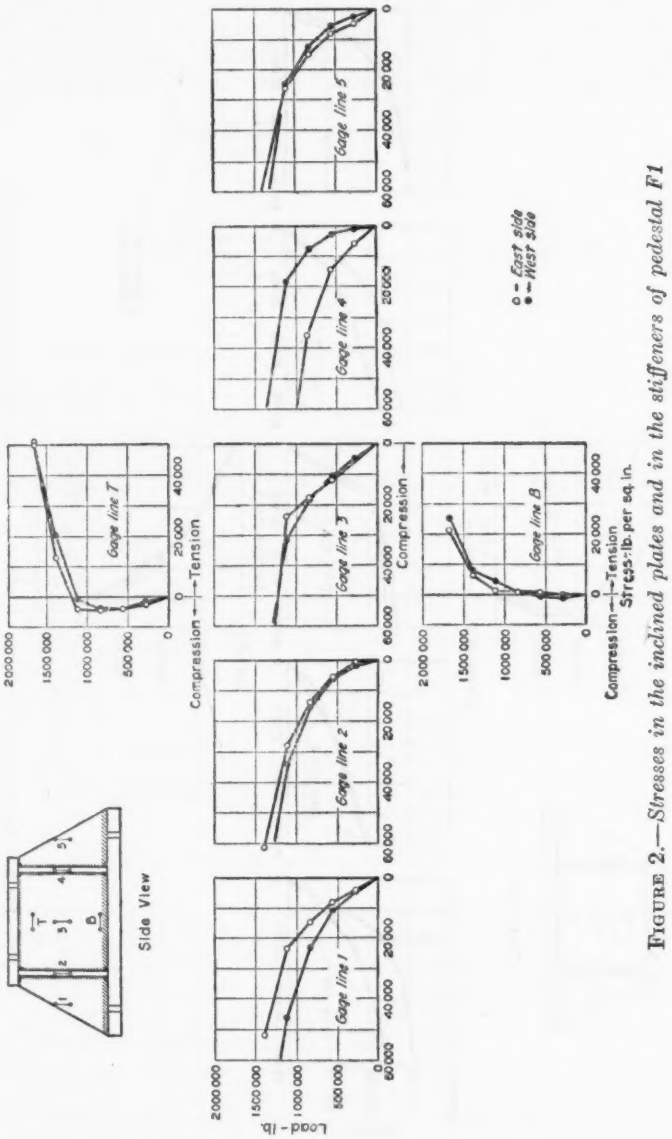

FIGURE 2.—*Stresses in the inclined plates and in the stiffeners of pedestal F1*

On the east and west sides, the five gage lines, 1 to 5, were at mid height between the top and bottom plates. Line *E1* was directly opposite *W1*, and they were near the north side of the pedestal. Other lines having corresponding numbers were also opposite each

other. Lines 1, 3, and 5 were on the inclined plates and lines 2 and 4 on the outer surface of the stiffener plates. The horizontal gage lines *E–T* and *W–T* were near the top, and *E–B* and *W–B* were near the bottom of the inclined plates at mid length.

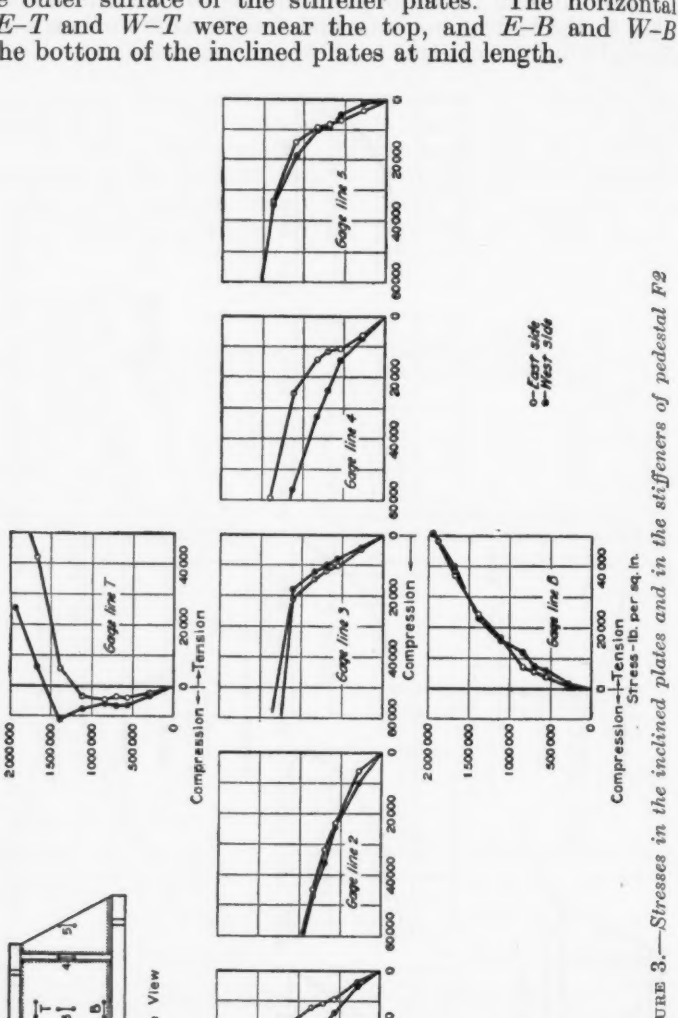

FIGURE 3.—*Stresses in the inclined plates and in the stiffeners of pedestal F2*

Three horizontal gage lines were located on both the north and south edges of the base plates, one-eighth inch below the top surface of this plate. Gage lines *N–A* and *S–A* were directly opposite each other, as were the remaining lines having similar designations.

IV. TESTING PROCEDURE

The pedestals were tested in compression in the 10,000,000-pound capacity testing machine at the bureau. In order to simulate the conditions under which bridge pedestals are used, these specimens were supported in the testing machine on concrete blocks, 3 feet 3 inches long by 2 feet 8 inches wide by 18 inches high, which had been aged one month. The distance between the base of the pedestal and the edge of the block was 6 inches at the sides and the ends.

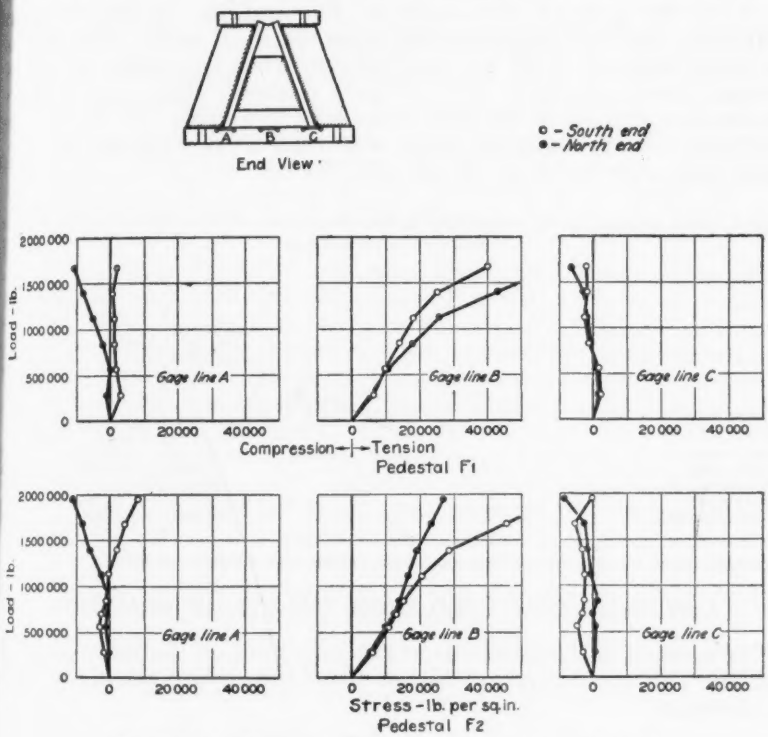

FIGURE 4.—*Stresses in the lower plates of the pedestals*

These concrete blocks were centered on the lower platen of the testing machine and set in a bed of plaster of Paris. The pedestal was then placed on top of the block in another bed of plaster of Paris and loaded through a steel bar 3 inches wide and having a length equal to the top length of the pedestal. Figure 5 shows pedestal *F2* in the testing machine after test.

A Whittemore fulcrum plate strain gage having a 2-inch gage length was used. This gage was provided with a Last Word dial, each division of which was 1/10,000 inch. Readings were estimated to 1/10 division.

V. RESULTS AND DISCUSSION OF THE TESTS

1. STRESSES COMPUTED FROM THE LOAD

The compressive stress in the pedestals at mid height for each load was computed by resolving the load into two components acting parallel to the inclined plates.

Each component was, then, divided by the cross-sectional area of the inclined plate and the two outside stiffeners on one side of the pedestal to obtain the stress. The nominal dimensions (given in fig. 1) of the inclined plates (*P2* or *P6*) and the outside stiffeners (*P3*) were used in computing the cross-sectional area. The area of the inside stiffeners (*P4*) was not included when computing the cross-sectional area because it did not seem probable that it carried any appreciable portion of the components of the load. A section perpendicular to the inclined plates was used in computing the area. These values of the stress are given in Table 1.

TABLE 1.—*Comparison of calculated stress from load with weighted average stress from strain readings*

Load	Calculated stress at mid height	Stress from strain readings	
		Pedestal F1	Pedestal F2
	*Lbs./in.*²	*Lbs./in.*²	*Lbs./in.*²
280,000 pounds	5, 790	3, 900	4, 500
560,000 pounds	11, 580	8, 800	11, 000
700,000 pounds	14, 475		14, 400
840,000 pounds	17, 370	17, 300	18, 000
1,120,000 pounds	23, 160	[1] 30, 000	[1] 30, 200

[1] Probably above the proportional limit and therefore an incorrect value for the stress.

2. STRESSES COMPUTED FROM THE STRAIN READINGS

The stresses in the pedestals at the gage lines on the inclined plates and the stiffeners were calculated from the deformation, by using the formula:

$$S=\frac{e}{l}E$$

where

S = stress, lbs./in.².

e = deformation, inch, indicated by the gage readings.

l = gage length, 2 inches.

and

E = modulus of elasticity of the steel, assumed to be 30,000,000 lbs./in.².

As no coupon specimens of the material in these pedestals were furnished, the interpretation of the strain readings is somewhat unsatisfactory. This formula does not apply for values of the stress above the proportional limit. As the proportional limits are not known for the plates in the pedestals, it is impossible to determine whether the values of the stresses should be computed for the strains at the higher loads.

The calculation of the stresses in the other gage lines does not appear to be practicable for a structure as complicated as these pedestals.

Figures 2, 3, and 4 show curves which have been plotted with the load as ordinates and with the stresses in the gage lines, computed from the strain readings, as abscissas. The tensile stresses are plotted to the right, and the compressive stresses to the left of the vertical axis of each diagram.

(a) STRESSES AT MID HEIGHT

A comparison of the average stresses at mid height in the inclined plates and in the stiffeners can be made from the values given in Table 2. For pedestal F1, having large welds at the base of the inclined plates, the stresses in the inclined plates were practically equal to those in the stiffener plates, showing that in this design the stress was approximately uniform in the compressive members of the pedestal. The stresses in the stiffeners of pedestal F2 were, however, for all loads, more than twice the stresses in the inclined plates.

It is evident that the load was distributed more uniformly in pedestal F1, having closed single bevel T joints[1] between the inclined plates and the lower plate, than in pedestal F2, having the inclined plates machined to fit the lower plate and secured by fillet welds on one side. It seems probable that in other welded steel structures the one having closed single bevel T joints would be more satisfactory as well as cheaper than one in which the members were machined to fit and held in position by a fillet weld on one side.

To obtain an average compressive stress at mid height from the values computed from the strain-gage readings, the stresses given in Table 2 were used. The stress in the inclined plates for a given load was multiplied by the ratio of the cross-sectional area of the inclined plates to the cross-sectional area of both the inclined plates and the outside stiffeners. The stress in the stiffeners was multiplied by the ratio of the cross-sectional area of the outside stiffeners to the cross-sectional area of both the inclined plates and the outside stiffeners. The sum of these results is given in Table 1 for both pedestals.

TABLE 2.—*Comparison of average stress at mid height from strain readings in inclined plates and in stiffeners*

Load	Average stress from strain readings			
	Pedestal F1		Pedestal F2	
	Inclined plates	Stiffeners	Inclined plates	Stiffeners
	Lbs./in.²	*Lbs./in.²*	*Lbs./in.²*	*Lbs./in.²*
280,000 pounds	4,350	2,100	3,750	7,650
560,000 pounds	9,250	7,200	9,100	18,400
700,000 pounds			11,400	26,100
840,000 pounds	17,100	18,300	13,650	35,100
1,120,000 pounds	29,400	32,700	22,800	[a] 59,700

[a] Probably above the proportional limit and therefore an incorrect value for the stress.

[1] Welding and Cutting, Nomenclature, Definitions, and Symbols, Nov. 19, 1929, American Welding Society, 33 West Thirty-ninth Street, New York, N. Y., paragraph 460, 27.

The log sheets, Tables 3 and 4, show that the inclined plate *P2* pedestal *F1* scaled at 840,000 pounds and the inclined plate *P6* pedestal *F2* at a higher load (1,120,000 pounds). Scaling is an indication that the stress in the steel plate has exceeded the yielding point of the material.

As, however, the stress (17,370 lbs./in.^{2}) for the pedestal *F1* under load of 840,000 pounds agrees very closely with the other values in this load in Table 1, it is probable that the amount of material in pedestal *F1* which had reached the yield point was so small that the error in this value is not appreciable.

TABLE 3.—*Log sheet for test of pedestal F1*

Load (in pounds)	Remarks
0	Strain readings taken.
280,000	Do.
560,000	Strain readings taken, some cracks heard.
840,000	Strain readings taken. Scaling on inside surface of *P2*. Scaling on outside surface of *P2* near of *E–T* at upper part of plate.
1,120,000	Strain readings taken.
1,400,000	Do.
1,680,000	Strain readings taken on some.
2,000,000	Top plate visibly bowing down at mid length.
2,119,000	Weld along stiffener scaling.
2,315,000	Plates *P2* visibly buckling. Also stiffener plates *P3*.
2,322,000	Maximum load. Welds on diaphragm *P4* broken at top.

TABLE 4.—*Log sheet for test of pedestal F2*

Load (in pounds)	Remarks
0	Strain readings taken.
280,000	Do.
560,000	Do.
700,000	Do.
840,000	Do.
1,120,000	Strain readings taken. Scaling on top east plate *P6*.
1,400,000	Strain readings taken.
1,680,000	Do.
1,960,000	Do.
2,156,000	Visible buckle in stiffener *P3*.
2,260,000	Top plate bowing down at center.
2,423,000	Maximum load. Welds on diaphragms *P4* broken.

The stresses computed from the strain-gage readings for the 1,120,000 pounds load, however, are, as was to be expected, much greater than the stress computed from the load.

The stresses (Table 1) in pedestal *F1* computed from the strain-gage readings are somewhat lower than for pedestal *F2* which was, in all probabity, due to the more uniform stress distribution in pedestal *F1*.

For pedestal *F2* the stresses from strain-gage reading agree very closely with the stresses computed from the load.

If it is assumed that the stresses computed from the load approximate the actual stresses, the agreement of the stresses from the strain-gage reading with these values is remarkable. It should be remembered that these pedestals were fabricated from many comparatively small pieces and that the stress distribution is far from simple. It is evident that the strain gage is of value in studying the stress distri-

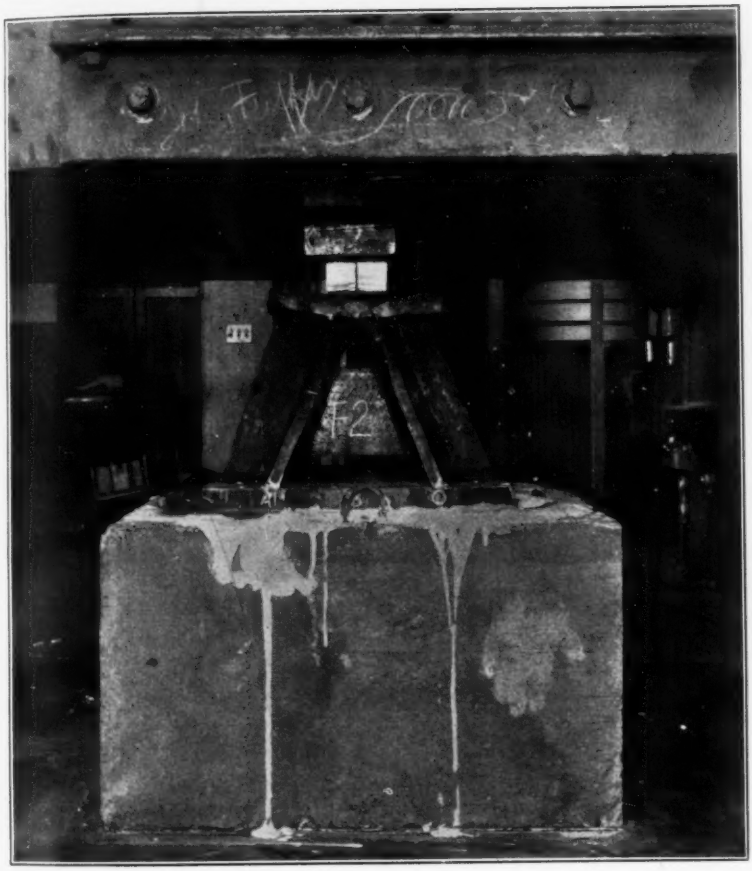

FIGURE 5.—*Pedestal F2 in the 10,000,000-pound capacity testing machine after test*

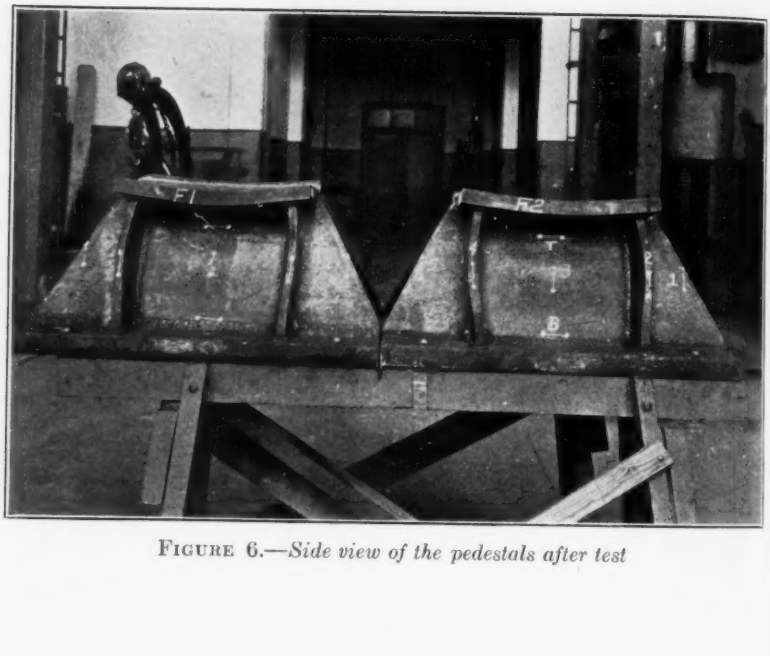

FIGURE 6.—*Side view of the pedestals after test*

bution in structures of this kind for which the usual methods of computing the stresses in engineering structures do not give sufficiently accurate results.

(b) STRESSES NEAR TOP AND BOTTOM OF THE INCLINED PLATES

The stresses in the horizontal gage lines, *T*, near the top and *B*, near the bottom of the inclined plates are shown in Figures 2 and 3. Low loads appeared to induce compressive stresses in the top gage lines, but higher loads caused tensile stresses which rapidly increased beyond the proportional limit of the material. A similar tendency was shown by the bottom gage lines, but the compressive stresses were much less, and tensile stresses occurred at lower loads than was the case for the top of the plate.

(c) STRESSES IN THE LOWER PLATE

Figure 4 shows the stresses in the lower plate of the pedestal. The stresses were low in the gage lines *A* and *C*, which were directly below the inclined plates. Those in gage line *B*, at the center, were comparatively large tensile stresses, induced probably by the horizontal components of the forces exerted by the inclined plates and by bending of the lower plate.

3. MAXIMUM LOAD AND DESCRIPTION OF FAILURE

Tables 3 and 4 are copies of the log sheets for the tests. The maximum loads carried by the two pedestals, notwithstanding the differences in the stress distributions, were very nearly equal. The factor of safety for the design load of 350,000 pounds was 6.6 for pedestal *F1* and 6.9 for pedestal *F2*.

Figures 5 and 6 show that, at failure, the top plate had bowed downward at mid length, the stiffener plates were buckled, and the inclined plates were deformed so that the welds between them and the inside stiffener plates, *P4* (fig. 1), were broken. The base plate was not visibly deformed, although the strain readings represented in Figure 4 showed that the material had been highly stressed at least along the longitudinal center line at the top of the plate.

No strain measurements were taken on the top plate, and consequently the load necessary to cause dangerously high stresses in that plate are unknown.

VI. CONCLUSIONS

1. The compressive tests of two electric arc welded steel pedestals for bridges, designed for a load of 350,000 pounds showed that the factor of safety was more than six.

2. The stress distribution in the inclined plates (subjected to compressive forces) was more uniform in the pedestal having closed single bevel T joints between the inclined plates and the lower (base) plate, than in the pedestal in which the members were machined to fit and held in position by a fillet weld on one side.

3. The compressive stresses in the sides of the pedestal computed from the strain-gage readings were nearly the same as the stresses computed from the loads on the pedestals.

WASHINGTON, July 7, 1930.

11295°—30——3

THE X-RAY METHOD APPLIED TO A STUDY OF THE CONSTITUTION OF PORTLAND CEMENT

By L. T. Brownmiller and R. H. Bogue

ABSTRACT

The X-ray diffraction method has been applied to a study of the constitution of Portland cement clinker.

It has been found that $2CaO.SiO_2$ and CaO combine to form $3CaO.SiO_2$ and not a solid solution of $2CaO.SiO_2 + CaO$; that $8CaO.Al_2O_3.2SiO_2$ does not exist in Portland cement systems; that solid solutions are not formed between the aluminates and silicates of cement systems; and that free CaO is not present generally in commercial cements in amounts as great as 2.5 per cent.

The limiting amounts were determined of each cement compound that could be identified by X-ray means as employed in this study. Twenty-eight commercial cement clinkers were subjected to X-ray examination and $3CaO.SiO_2$ and $2CaO.SiO_2$ were identified in each. $3CaO.Al_2O_3$, $4CaO.Al_2O_3.Fe_2O_3$ and MgO were found in the samples which contained those compounds, by calculation, in amounts great enough to permit identification.

CONTENTS

		Page
I.	Introduction	813
II.	The X-ray method	814
III.	The composition $3CaO + SiO_2$	817
IV.	The composition $8CaO + Al_2O_3 + 2SiO_2$	820
V.	Solid solutions of aluminates in silicates	821
VI.	Free lime	822
VII.	Limiting amounts required for identification	824
VIII.	Examination of commercial cement clinkers	826
IX.	Summary	828
X.	Bibliography	829

I. INTRODUCTION

The investigations by Rankin and Wright (1)[1] on the system $CaO–Al_2O_3–SiO_2$ have shown that there are formed in that system, at equilibrium, in the region of Portland cement clinkers, $3CaO.SiO_2$, $2CaO.SiO_2$, and $3CaO.Al_2O_3$. More recently, other systems have been solved (2), as a result of which the compounds that can be formed at equilibrium, in the region of Portland cement clinker, have been determined for the components CaO, Al_2O_3, SiO_2, Fe_2O_3, and MgO. These compounds are $3CaO.SiO_2$, $2CaO.SiO_2$, $3CaO.Al_2O_3$, $4CaO.Al_2O_3$, Fe_2O_3, and MgO.

Portland cement clinker contains, in addition to the above mentioned components, from 2 to 4 per cent of other material, as alkalies, titania, sulphates, manganese oxides, phosphates, etc. These may have some influence on the proportions of the above-mentioned compounds in the clinker, but it is improbable that they materially affect the major constitution of the commercial product.

[1] The figures in parenthesis here and throughout the text relate to the reference figure in the bibliography at the end of this paper.

The findings on the five-component system referred to are deduced from studies at the condition of equilibrium. The method used in the manufacture of Portland cement leads to the belief that a condition approaching equilibrium is attained in commercial clinker. A failure completely to reach equilibrium, however, may result in the presence of some uncombined lime and a change in the relative proportions of the other compounds, but rarely in the elimination of one of those compounds with the formation of a different compound.

Investigations (3) have been reported from this laboratory which confirm this viewpoint. The methods used in the study of phase equilibria, including thermal, microscopic, and X-ray examinations indicated that the major compounds of Portland cement clinker are $3CaO.SiO_2$, $\beta 2CaO.SiO_2$, $3CaO.Al_2O_3$, $4CaO.Al_2O_3.Fe_2O_3$, and MgO.

Many investigators, however, especially in Europe, have adhered to theories of constitution developed prior to the application of the phase rule, or have advanced other views which are at variance with those expressed above. Prominent among these may be mentioned the view (4) that the lime, in excess of that necessary to form $2CaO.SiO_2$ with the silica, enters essentially into solid solution with the $2CaO.SiO_2$; the contention (5) that $3CaO.SiO_2$ does not exist and that the principal constituent of clinker is $8CaO.Al_2O_3.2SiO_2$; the opinion (6) that the $3CaO.Al_2O_3$ enters into solid solution with the calcium silicates; and the conclusion (7) that Portland cement clinker contains relatively large amounts of uncombined lime.

The X-ray method is peculiarly well adapted to the examination of the above theories, both as they apply in pure systems and in commercial clinkers. This was one of the objectives of this research—to present X-ray evidence bearing directly on each of the above theories to the end that the nature of the compounds in the pure systems and in commercial cement clinker may become generally established.

The second purpose of this study was to examine by X-ray and chemical means a large number of commercial clinkers to ascertain (1) precisely what compounds could be positively identified in each and (2) the nature of the agreement between such X-ray analysis and the constitution as computed from the chemical analysis. Incidental to this part of the work, it was necessary to determine the efficiency of the X-ray method to resolve the pattern of each compound in the presence of the other compounds of the cement.

II. THE X-RAY METHOD

The positive identification of a crystalline compound by the microscope should include the measurement of a number of the optical properties, such as the refractive indices, optic axial angle, pleochroism, etc.; but in the case of Portland cement it is not possible to obtain all of these data for each phase present. The crystals, even of the principal constituents, usually are very fine grained and often too small to permit of satisfactory measurements. Furthermore, the crystals often are surrounded with glass or contain inclusions. For these reasons the microscopic examination of these materials has not proved entirely satisfactory, and this condition has resulted in much difference of opinion in the interpretation of the available observations. The X-ray method, therefore, fills a distinct need, for the results obtained with it are based on criteria which are convincing.

During recent years the powder X-ray method for identifying compounds in the pure state or in mixtures has received considerable attention and development (8). The theoretical considerations of this method have been described in various places (9). When a powdered material is subjected to X-radiation and the resulting spectrum photographed, there is obtained an X-ray diffraction pattern consisting of a series of lines in definite positions which are ordinarily measured from a fixed zero point and recorded as "interplanar spacings" (d_{hkl}). Each crystalline chemical compound has a characteristic diffraction pattern which appears always to be the same whether the compound is present in a pure state or intermixed with other compounds. Even different crystalline forms of the same composition can be distinguished by the method; thus $\gamma-$ and $\beta-$ $2CaO.SiO_2$ have entirely different diffraction patterns (10).

The X-ray method has definite but well-understood limitations. Thus, a diffraction pattern depends on the arrangement of the atoms of a substance in crystal planes. Glass shows no such arrangement, and, hence, can not be detected by the method.

In a mixture of two compounds, it often happens that some of the lines of one pattern coincide with some of the lines of the other pattern. Hence, the greater the number of compounds, the greater the probability of coincidence of lines. Nevertheless such coincidences cause differences in intensity of the resulting lines so that the identity of a pattern may not be entirely obscured.

Of greater significance are the limitations due to the amount of a material present. As the quantity of one crystalline phase decreases, the general intensity of the pattern of that compound decreases. First the least intense lines of the pattern disappear and then the stronger lines until a certain minimum amount of the compound is reached when the strongest lines can no longer be observed. Under the most favorable conditions, quantities of material less than 2 or 3 per cent of the total can rarely be identified. For the detection of such small amounts of material, the crystals should be well developed, possess a high order of symmetry and a simple structure, and give rise to lines which do not conflict with those of the patterns of the other materials present. Only infrequently are these conditions fulfilled, so that, ordinarily, greater amounts than those mentioned above are required for the recognition of a phase.

The relative intensities of the lines as well as their positions are significant in the identification of compounds. If one line of a diffraction pattern is twice as intense as another line of the same pattern, that relation obtains whether the compound is present in a pure state or in a mixture. In a mixture of two compounds, the pattern of one is superimposed on that of the other; the general intensity of each pattern is diminished because of dilution by the other, but the relative intensities of the lines of each pattern remain the same.

Analysis of a sample of an unknown material, therefore, depends upon the recognition, by position and relative intensity, of the lines of the diffraction pattern of a pure material in that of the unknown sample. Hence, before any such analysis can be undertaken, the diffraction patterns of the pure compounds which may occur in the sample must be known. Such information has been published from this laboratory for most of the pure compounds which occur in the oxide systems of Portland cement (11). Recent improvements in

methods and purity of samples have resulted in somewhat more precise measurement of the lines of the diffraction patterns and in more complete diffraction data, but the interplanar spacings are not found to differ essentially from those reported previously.

The apparatus used in this study was the X-ray diffraction photometer of Hull equipped with a Coolidge molybdenum water-cooled target. The cassettes for holding the films were provided with zirconium oxide filters so that the effective wave length of the rays was 0.712 A. U. The radius of the cassettes was 8 inches. Since crystals of clinker are extremely small, the powder method of Debye and Hull (9) was found most suitable and was used exclusively in these studies. By this method the samples of clinker are ground to pass a No. 200 sieve and mounted in lead-free glass tubes of about 0.5 mm. inside diameter. Occasionally the samples were mounted on a silk thread. To do so the finely ground clinker was mixed with collodion and the thread immersed. On withdrawing the thread, sufficient material adhered to permit a satisfactory analysis. Exposure of a sample lasted 50 hours in most cases at a tube current of about 18 milliamperes and a voltage of 30,000.

Diffraction patterns were obtained of 28 samples of clinker, both domestic and foreign. For the complete analysis of any one sample, several exposures were necessary. Normal exposure of 50 hours was sufficient for the identification of most of the lines; occasionally, however, overexposure and overdevelopment of the films were resorted to for the strengthening of the weaker lines. On the other hand, underexposure and underdevelopment sometimes provided a means for the resolution of two lines lying very close to each other, which lines ordinarily merged to form one broad band. In the identification of the patterns of various pure compounds in clinker a capillary tube was filled one half of its length with the samples of clinker and the other half with the compound to be identified. Thereby the patterns of the two were exactly opposite each other on the film and measurement of the lines became more precise, since then irregularities of two films were avoided. Altogether some 200 exposures were made in the course of this study.

The precision of measurement of the interplanar spacing increases as the interplanar spacing decreases. It may be pointed out, however, that weak lines are more difficult to estimate than stronger lines so that measurement in such cases may not be as accurate; often also they lie close to strong lines so that their true position may be misjudged. Measurements were made on the centers of the lines, but in some cases, where a line is broad, the precise allocation of the center is difficult. Many of these broad lines may be found, by special exposures, to consist of two lines. Where such lines occur in the patterns, the position of each component line is recorded in the following tables, together with the reading that ordinarily is obtained where the two lines appear as one broad band.

In order to determine the relative precision of the measurements of the interplanar spacings, 15 films of the diffraction pattern of tricaclium aluminate were examined. Six lines in each film were measured. A summary of the results is given in Table 1. It may be noted that the difference between the extreme values, as measured, diminish from 0.020 at interplanar spacings of 2.690 to 0.004 at interplanar spacings of 1.202. The average deviations from the mean

through the same range diminish from 0.004 to 0.001. This serves as a general indication of the precision of measurements in this study but some variation may occur due to the differences in sharpness or intensity of the lines as above noted.

TABLE 1.—*The precision of measurement of six lines in the X-ray diffraction pattern of* $3CaO.Al_2O_3$

	Line No.					
	1	2	3	4	5	6
Mean (15 films)	2.690	2.202	1.905	1.555	1.346	1.202
Maximum value	2.700	2.210	1.910	1.557	1.348	1.205
Minimum value	2.680	2.195	1.897	1.551	1.344	1.201
Difference between extreme values	.020	.015	.013	.006	.004	.004
Average deviation from mean	.004	.004	.003	.002	.001	.001

The intensity of the lines was measured visually. This is the procedure commonly employed and is satisfactory for qualitative observations. A photodensitometer (12) has been developed in this laboratory, however, for the more precise estimation of the intensities of the lines which will be employed in a later study on the quantitative X-ray determination of the compounds present.

III. THE COMPOSITION $3CaO+SiO_2$

The existence of $3CaO.SiO_2$ in the $CaO–Al_2O_3–SiO_2$ system (1) and in Portland cement clinker (3) has been established by phase equilibria studies combined with microscopic examinations. A number of European investigators, however, have been unable to accept the existence of that compound (5), and the suggestion has been urged (4) that the lime enters into solid solution with dicalcium silicate. The evidence obtained by the X-ray method on this problem is important because of the rigid nature of the criteria in identification of compounds in the X-ray diffraction patterns. These data, set down below, offer impressive confirmation of the existence of the tricalcium silicate in the $CaO–Al_2O_3–SiO_2$ system and in Portland cement clinker.

Samples were prepared of the following compositions: No. 1, $2CaO+SiO_2$; No. 2, $2\frac{1}{3}$ $CaO+SiO_2$; No. 3, $2\frac{1}{2}$ $CaO+SiO_2$; No. 4, $2\frac{3}{4}$ $CaO+SiO_2$; and No. 5, $3CaO+SiO_2$.

These were made from calcium carbonate and quartz of high purity as indicated by the partial analyses (13) of these materials given in Table 2.

TABLE 2.—*Partial analyses of raw materials*

	Calcium carbonate	Quartz
CaO	55.55	0.02
MgO	.07	.00
SiO_2	.03	99.37
Al_2O_3	.01	.50
Fe_2O_3	.00	.03
Cl	.04	.00
SO_3	.00	.00
CO_2	43.63	
Loss on ignition	43.97	.11

The weighed portions of sample No. 1 ($2CaO+SiO_2$), ground to pass completely through the No. 200 sieve, were mixed in a pebble mill for 3 hours, then formed into bars about 10 inches long by 1 inch cross section and heated in an updraft gas furnace for 2½ hours at 1,500° C. The clinker was ground and a sample taken for microscopic and X-ray examination and for the free CaO test. The balance of the sample was then mixed in the pebble mill as before with an additional quantity of calcium carbonate to give the composition of No. 2 ($2⅓\ CaO+SiO_2$), and the mixture again burned for 2½ hours at 1,500° C. This process was repeated with additional increments of calcium carbonate until all of the samples of the different compositions had been obtained. The free CaO test showed that no lime remained uncombined in any of the samples.

Each of the samples was subjected to X-radiation and the diffraction patterns obtained. No. 1 showed only the pattern of $\gamma 2CaO.SiO_2$. No. 2 showed the lines of a new pattern, which we will call x, superimposed upon that of $\gamma 2CaO.SiO_2$. In No. 3, the lines of $\gamma 2CaO.SiO_2$ disappeared and were replaced by the pattern of the beta form of that compound. The pattern of x also was present, and in greater intensity than in No. 2. No. 4 showed the same pattern as No. 3 except that the lines of $\beta 2CaO.SiO_2$ were weaker and the lines of x were stronger. No. 5 showed only the pattern of x. In no case were the lines of CaO observed nor was there found any shift in position of the lines of the dicalcium silicate nor of x following a change in composition.

The formation of a distinctive pattern when the composition $3CaO+SiO_2$ is reached, together with the appearance and position of this pattern in other mixtures, meets the requirements for assigning to that composition an identity as the chemical compound $3CaO.SiO_2$. When larger amounts of CaO are present than represented by the composition $3CaO+SiO_2$ the pattern of CaO is found to be superimposed upon that of the $3CaO.SiO_2$. Between the compositions $3CaO+SiO_2$ and $2CaO+SiO_2$ there always are observed the lines of $3CaO.SiO_2$ and β or γ $2CaO.SiO_2$. The intensities of the two patterns are proportional to the calculated amounts of those compounds that should be present. When sufficient attention is given in the preparation to insure that a condition of equilibrium is reached, the lines of CaO are absent. The failure to observe any shift in position of the lines of those compounds when CaO is added indicates that no solid solution is formed or that the amount of such solution, if there is any at all, is too small to be detected.

The principal interplanar spacings of the patterns of CaO, $3CaO.SiO_2$, and $\beta 2CaO.SiO_2$ are listed in Table 3.

An inspection of the data will show that the pattern of each is distinctive. There are, indeed, several lines which are found to be coincident in two or three of the patterns, but a sufficient dissimilarity is found, both in position and intensity of lines, definitely to preclude any interpretation which would assign to tricalcium silicate the composition of a mixture or solid solution of the other two compounds.

Recently Janecke (14) has interpreted X-ray data reported from this laboratory (10) as indicating that $3CaO.SiO_2$ is a mixture of $\beta 2CaO.SiO_2$ and CaO. In order the better to demonstrate that the pattern of $3CaO.SiO_2$ is quite distinct from that of $\beta 2CaO.SiO_2$ with CaO, X-ray diffraction photographs were made as follows: One

half of a capillary glass tube for exposure was filled with pure tricalcium silicate; the other half was filled with an equimolar mixture of beta dicalcium silicate and calcium oxide. The resulting photograph shows the patterns of the two materials on opposite sides of the same film. X-ray diffraction patterns do not reproduce well for printing, but the reproduction shown in Figure 1 reveals the striking dissimilarity of the two patterns. The upper pattern is that of the mixture of $\beta 2CaO.SiO_2$ and CaO. The lower pattern is that of pure $3CaO.SiO_2$. It is at once apparent that $3CaO.SiO_2$ is not composed of $\beta 2CaO.SiO_2 + CaO$.

A careful measurement of the interplanar spacings shows that the mixture of $\beta 2CaO.SiO_2$ and CaO gives a superimposed pattern of those two compounds. It conforms to a combination of the patterns of those compounds as listed in Tabel 3. The pattern of the $3CaO.SiO_2$ is identical with that listed for $3CaO.SiO_2$ in Table 3.

TABLE 3.—*The principal interplanar spacings of CaO, $3CaO.SiO_2$ and $\beta 2CaO.SiO_2$*[1]

Line No.	CaO	$3CaO.SiO_2$	$\beta 2CaO.SiO_2$
1			3.80 w.
2			3.37 w.
3		3.02 s.	3.03 w–b.
4		2.940 w.	
5			2.870 w.
6	2.765 m.	2.770 ss, 2.730 ss } 2.750.	2.780 ss, 2.730 ss } 2.750.
7		2.600 s.	2.610 s.
8			2.540 w.
9		2.435 ww.	2.440 m, 2.400 m } 2.420.
10	2.390 ss.		
11		2.320 m.	
12			2.278 m.
13		2.178 s.	2.182 s.
14			2.080 w.
15			2.040 w, 2.020 w } 2.030.
16		1.975 m.	1.980 m.
17		1.932 m.	
18			1.895 m–b.
19		1.825 w.	
20			1.800 m.
21		1.762 s.	
22			1.755 w.
23			1.700 w–b.
24	1.695 s.		
25		1.627 s.	1.632 w, 1.610 w } 1.620 w
26			
27			1.575 ww.
28		1.542 m–b.	1.548 ww.
29			1.528 w.
30		1.487 s.	1.482 w.
31		1.458 w.	
32	1.445 m.		1.447 ww.
33			1.415 w.
34	1.385 m.	1.390 ww.	1.393 ww.
35			1.370 w.
36		1.198 w.	
37		1.162 w–b.	
38		1.132 w–b.	
39		1.090 w–b.	
40	1.075 m.		
41		1.020 wwb.	
42	.980 m.		

[1] In this and in subsequent tables, ss=very strong; s=strong; m=medium; w=weak; ww=very weak; b=broad.

IV. THE COMPOSITION $8CaO + Al_2O_3 + 2SiO_2$

In 1912 Jänecke (5) published his first paper setting forth his discovery that the "alite," or principal compound of Portland cement, consists of $8CaO.Al_2O_3.2SiO_2$. This contribution was quickly refuted by Rankin and Wright (15), who pointed out that such a compound did not exist in the $CaO–Al_2O_3–SiO_2$ system and that a mixture of that composition at equilibrium consists of $3CaO.SiO_2$, $2CaO.SiO_2$, and $3CaO.Al_2O_3$. The conclusion of Rankin and Wright has been confirmed in this laboratory (16), but the existence of $8CaO.Al_2O_3.2SiO_2$, designated "Jäneckite," (17) as the "alite" of Portland cement clinker, has been reaffirmed by Jänecke (18).

The X-ray evidence upon which the opinion of this laboratory is based is set down below:

The purported composition $8CaO.Al_2O_3.2SiO_2$ was prepared (16) in the form of fused drops by the method described by Dyckerhoff (4) and found by microscopical examination to consist largely of the elongated fiber-like crystals said to be characteristic of that compound. The drops were crushed and examined by the X-ray method. At the same time a mechanical mixture of $3CaO.SiO_2$, $\beta 2CaO.SiO_2$, and $3CaO.Al_2O_3$ in the same molecular proportion was subjected to X-radiation.

The X-ray data on these materials are given in Table 4, together with the pattern of CaO, which was found also to be present in the fused drops.

TABLE 4.—*Interplanar spacings of the $8CaO+Al_2O_3+2SiO_2$ preparations, mixtures of $3CaO.SiO_2$, $\beta 2CaO.SiO_2$ and $3CaO.Al_2O_3$, and of CaO*

Line No.	Fused drops of $8CaO+SiO_2+2SiO_2$	Mixture of C_3S, βC_2S, and C_3A	CaO	Compounds giving rise to lines in pattern of fused drops
1	3.03 m	3.03 m		C_3S.
2	2.77 ss	2.77 ss	2.765 m	C_3S, βC_2S, CaO.
3	2.69 ss	2.69 ss		C_3A.
4	2.60 m	2.60 m		C_3S.
5	2.39 m		2.390 ss	CaO.
6	2.27 ww	2.26 ww		βC_2S.
7	2.18 s	2.18 s		C_3S, βC_2S, C_3A.
8	2.03 ww	2.04 ww		βC_2S, C_3A.
9	1.975 w	1.970 w		C_3S, C_3A.
10	1.895 s	1.895 s		C_3A.
11	1.755 m	1.758 m		C_3S.
12	1.695 m		1.695 s	CaO.
13	1.627 m	1.630 w		C_3S, βC_2S.
14	1.550 s	1.552 s		C_3A.
15	1.483 m	1.485 w		C_3S.
16	1.450 w		1.445 m	CaO.
17	1.385 ww		1.385 m	CaO.
18	1.345 w	1.342 w		C_3A.
19	1.200 m	1.202 m	1.201 w	C_3A, CaO.
20	1.095 w	1.093 ww	1.101 w	C_3S, CaO.
21	1.076 ww		1.075 m	CaO.
22	1.020 w	1.017 w		C_3A.
23	.980 ww		.980 m	CaO.
24	.900 ww	.896 ww		C_3A.

NOTE: $C_2S=3CaO.SiO_2$; $C_2S=2CaO.Si_2O$; $C_3A=3CaO.Al_2O_3$.

The X-ray pattern of the fused drops is observed to be similar to the pattern of the mechanical mixture of $3CaO.SiO_2$, $\beta 2CaO.SiO_2$, and $3CaO.Al_2O_3$ except that a few additional lines appear in the former which may be noted to be due to free CaO.

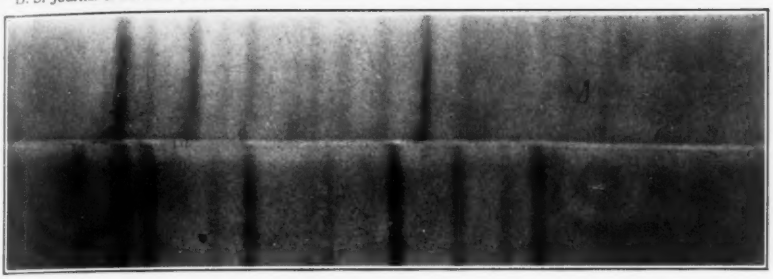

FIGURE 1.—*Upper, pattern of equimolar mixture of $\beta 2CaO.SiO_2$ and CaO. Lower, pattern of pure $3CaO.SiO_2$*

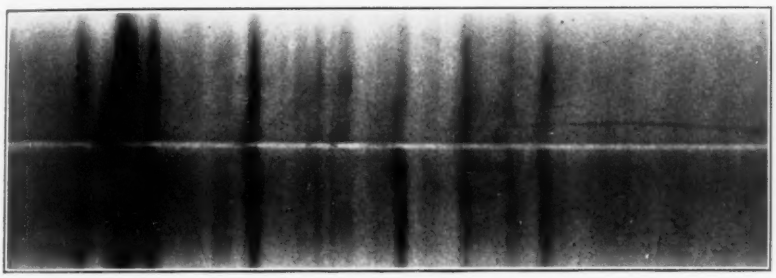

FIGURE 2.—*Upper, mixture of 47 per cent $3CaO.SiO_2$, 47 per cent $\beta 2CaO.SiO_2$, and 6 per cent $3CaO.Al_2O_3$. Lower, composition of same calculated content burned at 1,525° C.*

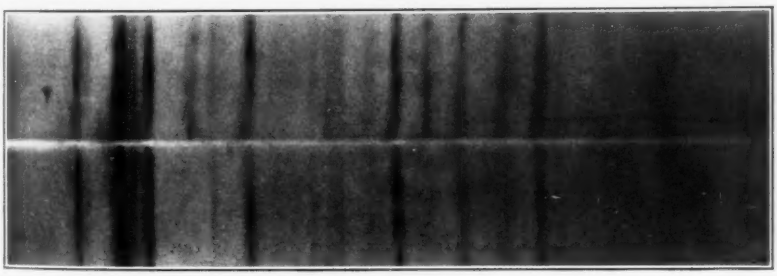

FIGURE 3.—*Upper, clinker burned at 1,435° C. which contains 2.8 per cent free CaO. Lower, clinker burned at 1,500° C. which contains 0.1 per cent free CaO*

In a recent paper, Jänecke (19) presents some information obtained by the X-ray examination of the composition "$8CaO.Al_2O_3.SiO_2$." In the pattern of that composition Jänecke reports that he finds the lines of $\beta 2CaO.SiO_2$, $3CaO.Al_2O_3$, and CaO, together with a few additional lines which he ascribed to "Jäneckite." Unfortunately he makes no attempt at a comparison of those lines with the pattern of tricalcium silicate.

From the evidence presented it appears that Jänecke's compound is a mixture of $3CaO.SiO_2$, $\beta 2CaO.SiO_2$, and $3CaO.Al_2O_3$ with a small amount of CaO.

V. SOLID SOLUTIONS OF ALUMINATES IN SILICATES

It has been reported (6) that $3CaO.SiO_2$ and $3CaO.Al_2O_3$ are capable of entering into solid solution with each other and that they exist as a solid solution in cement clinker. It is extremely difficult by optical methods to identify positively small amounts of $3CaO.Al_2O_3$ in the presence of $3CaO.SiO_2$. The indices of the two compounds (1) are practically identical, 1.710 for $3CaO.Al_2O_3$ and a mean index of 1.715 for $3CaO.SiO_2$. Moreover, in iron-containing systems, the index of $3CaO.Al_2O_3$ may be raised (2), so that its index may be the same or somewhat higher than that of $3CaO.SiO_2$. And, although $3CaO.SiO_2$ is birefracting, yet its birefraction is so low that in small grains it may not be evident. Because of these difficulties, microscopical examinations have only seldom detected $3CaO.Al_2O_3$ in cements and theories, such as solid solution formation, have been advanced to explain this failure of positive identification.

Although optical similarities made the microscopical examination unsatisfactory as a means for the identification of $3CaO.Al_2O_3$ in the presence of $3CaO.SiO_2$, distinct differences in the X-ray diffraction patterns of those two compounds would appear to provide, in the X-ray method, a reliable means for such an identification. If the $3CaO.Al_2O_3$ exists as such in a sintered mixture with $3CaO.SiO_2$ and $2CaO.SiO_2$, the X-ray diffraction patterns of the aluminate will be superimposed upon those of the other two compounds. But if the $3CaO.Al_2O_3$ enters into a solid solution with either of the calcium silicates, the pattern will show the lines of that silicate in a uniformly shifted position with reference to the location they would occupy if the compound were in pure state. Likewise, if either silicate entered into solid solution with the aluminate, the pattern of the aluminate would occupy a shifted position.

To study this problem, a sample of CaO, Al_2O_3, and SiO_2 was mixed to form a composition represented by 47 per cent $3CaO.SiO_2$, 47 per cent $2CaO.SiO_2$, and 6 per cent $3CaO.Al_2O_3$. This sample was burned at 1,500° C., reground, and burned at 1,525° C., following which treatment it showed no free lime by White's test. A mechanical mixture of the pure compounds in the proportion 47 per cent $3CaO.SiO_2$, 47 per cent $\beta 2CaO.SiO_2$, and 6 per cent $3CaO.Al_2O_3$ was then made. These two samples were exposed to X-radiation on the same film, hence, under exactly the same conditions.

The two patterns shown in Figure 2 appear to be identical in every respect, both in the position and in the intensity of the lines. Each of the compounds was definitely identified. Very careful measurement revealed only such slight differences as would obtain

by repeated measurements on the same pattern. Several additional comparisons of the same character were made on compositions containing up to 15 per cent of $3CaO.Al_2O_3$, but the results obtained were similar to those just described. This demonstrates that the pattern of none of those compounds is shifted when sintered preparations are obtained in the system $CaO–Al_2O_3–SiO_2$ in compositions similar to Portland cement clinker. The experiment confirms extensive tests that have been made in this laboratory on commercial and laboratory cements. In a great many of these, tricalcium aluminate has definitely been identified, but in none of them has there been observed any shift in the position of the patterns, either of the aluminate or the silicates. The data constitute convincing evidence that solid solutions are not formed between tricalcium aluminate and either tri-or di-calcium silicate in amounts sufficient to be detected by X-ray means.

VI. FREE LIME

In a study reported from this laboratory (20), it was indicated that free CaO does not occur in Portland cements in amounts exceeding 3 per cent, and that probably the content is generally less than 2 per cent. The method used for determining the free CaO was the ammonium acetate method (21), the results of which were confirmed qualitatively by White's (22) test. Nacken (7), however, has reported that commercial cements may contain significant amounts of fine-grained CaO as determined by the X-ray method.

Nacken obtained his evidence for the presence of free CaO in cements from pinhole diffraction patterns. These diagrams consist of a series of concentric circles; identification of a compound is effected by the measurement of the diameters and relative intensities of the lines of the circles.

As a matter of interest, pinhole photographs were made in this laboratory of a commercial clinker, $3CaO.SiO_2$ and CaO.

The diameters of the circles and relative intensities are recorded in Table 5.

TABLE 5.—*Pinhole X-ray data on a cement clinker, $3CaO.SiO_2$ and CaO*

Clinker	$3CaO.SiO_2$	CaO
3.73 m	3.70 m	
4.08 ss	4.07 ss	4.05 m.
4.35 ss	4.35 s	4.75 ss.
4.95 ww	4.95 ww	
5.25 m	5.23 m	
6.03 ww	6.00 ww	
6.67 sb	6.65 s	
7.35 m	7.34 w	6.95 s.
7.75 w	7.78 w	
8.15 m	8.13 m	
		8.39 m.
		8.90 m.

An examination of these data show that there is no similarity between the patterns of CaO and cement clinker while the patterns of $3CaO.SiO_2$ and this particular clinker correspond within the limit of accuracy by this method. No further studies were made with pinhole diagrams since the method described in this report is a development which gives far superior resolution of the lines from which measurements of greater accuracy may be obtained.

A study was then made of the adaptability of the X-ray method for identifying CaO in cements. A commercial raw mixture was obtained and burned at different temperatures. One portion, burned at 1,435° C. was found, by the ammonium acetate method, to contain 2.8 per cent of free CaO. Another portion, burned at 1,500° C. was found to contain 0.1 per cent of free CaO. The chemical analysis of this clinker and the calculated composition (23) of the clinkers obtained at the two temperatures are given in Table 6.

TABLE 6.—*Chemical analysis and calculated compound composition of a clinker burned at 1,435° and 1,500°C.*

Chemical analysis		Calculated composition at 1,435° C.		Calculated composition at 1,500° C. (Per cent)
Oxides	Per cent	Compounds	Per cent	
CaO	64.7	$3CaO.SiO_2$	26	37
Al_2O_3	5.8	$2CaO.SiO_2$	50	41
Fe_2O_3	2.7	$3CaO.Al_2O_3$	11	11
SiO_2	24.1	$4CaO.Al_2O_3.Fe_2O_3$	8	8
MgO	1.8	MgO	1.8	1.8
		CaO	2.8	.1

Table 7 contains the X-ray diffraction data obtained on the two clinkers, together with the interplanar spacings and intensities of the lines for CaO, $3CaO.SiO_2$, $\beta 2CaO.SiO_2$ and $3CaO.Al_2O_3$.

TABLE 7.—*Interplanar spacings of diffraction patterns of a cement composition burned at two different temperatures, together with the interplanar spacings of the lines of $3CaO.SiO_2$, $\beta 2CaO.SiO_2$, $3CaO.Al_2O_3$ and CaO which may be observed when those compounds are present in mixtures approximating the composition of Portland cement clinker*

Line No.	Cement clinker 1,500° C.	Cement clinker 1,435° C.	C_3S	βC_2S	C_3A	CaO
1	3.02 s	3.02 s	3.02 s			
2	2.955 w	2.950 w	2.940 w			
3	2.755 ssb	2.760 ssb	2.750 ssb	2.750 ssb		2.765 m.
4	2.690 m	2.685 m			2.690 ss	
5	2.610 ss	2.600 ss	2.600 s	2.610 s		
6	2.435 w	2.440 ww		2.440 m		
7	2.395 w	2.390 sb		2.400 m		2.390 ss.
8	2.320 m	2.315 m	2.320 m			
9	2.275 w	2.270 w		2.278 m		
10	2.180 ss	2.175 ss	2.178 s	2.182 s		
11	2.040 wwb	2.035 wwb		2.030 mb		
12	1.980 m	1.978 m	1.975 m	1.980 m		
13	1.932 m	1.932 m	1.932 m			
14	1.905 m	1.905 m		1.895 mb	1.905 s	
15	1.824 wb	1.830 wb	1.825 w	1.800 m		
16	1.763 s	1.765 s	1.762 s			
17		1.698 s				1.695 s.
18	1.624 s	1.629 s	1.627 s			
19	1.554 m	1.557 m			1.555 ss	
20	1.545 mb	1.545 mb	1.542 mb			
21	1.490 s	1.490 s	1.487 s			
22	1.462 w	1.460 wb	1.458 w			1.445 m.
23		1.392 w				1.385 m.
24	1.347 ww	1.348 ww			1.346 m	
25	1.200 wb	1.201 wb	1.198 w			
26	1.159 wb	1.159 wb	1.162 wb			
27	1.133 wb	1.134 wb	1.132 wb			
28	1.092 wb	1.092 wb	1.090 wb			
29		1.077 ww				1.075 m.

It will be observed that the patterns of the two differently burned samples are not identical. The points of difference lie in the lines which are characteristic of CaO. Lines 17, 23, and 29, which are found to be due to CaO and are not found in the pattern of any of the other compounds, are present in the X-ray pattern of the material burned at 1,435° C., but are absent in the pattern of the sample burned at 1,500° C. Furthermore, the strength and breadth of line No. 7 and the breadth of line No. 22 from the low-burned sample indicate that those lines are due to the strong corresponding lines of CaO rather than to the medium and weak corresponding lines of the $\beta 2CaO.SiO_2$ and $3CaO.SiO_2$, respectively. These data show that the free CaO of the low-burned sample can be positively identified by this means.

In Figure 3 the upper pattern is that of the clinker burned at 1,435° C., which contains 2.8 per cent uncombined CaO. The lower pattern is that of the sample burned nearly free of uncombined CaO at 1,500° C. Two lines show up prominently in the upper pattern that are very weak and absent, respectively, in the lower pattern. These are the lines No. 7 and 17 of Table 7. The other differences, noted on the original film, are not observable on the print.

Many other examinations of a similar character indicate that the free CaO may be detected in cements when present to the extent of 2.5 per cent. Of 28 commercial cements examined, however, the lines of free CaO have not been observed in a single case. This is convincing evidence that free CaO does not occur generally in modern rotary kiln clinkers in amounts as high as 2.5 per cent, and confirms the evidence obtained by chemical and microscopical tests.

VII. LIMITING AMOUNTS REQUIRED FOR IDENTIFICATION

In order to determine the effect on the X-ray pattern of varying proportions of compounds, mixtures were made of the pure compounds which have been found to occur in cement. Thus a series of mixtures was prepared which contained various proportions of $3CaO.SiO_2$ and $\beta 2CaO.SiO_2$, and the X-ray diffraction pattern obtained of each mixture. Other series in which $3CaO.Al_2O_3$, $4CaO.Al_2O_3.Fe_2O_3$, and MgO were added to the silicates were included. By a study of these films the minimum amount of each material which could be detected in the presence of the others was determined. Also an idea was obtained of the relative intensities of the lines. Thus in a mixture of 85 per cent $3CaO.SiO_2$ and 15 per cent $2CaO.SiO_2$, only the most intense lines of $2CaO.SiO_2$ appear, whereas only the least intense lines of $3CaO.SiO_2$ disappear. This series furnished a standard to which the films of commercial cements could be compared.

An additional set of standard films was obtained from a series of laboratory cements prepared of various compositions from the pure components: CaO, Al_2O_3, SiO_2, Fe_2O_3, and MgO. It was felt that in mechanical mixtures of pure compounds, crystals are apt to be better developed than in sintered cement clinkers. In the latter, the crystals are very small and intimately mixed so that this series of burned mixtures of known composition should furnish a set of standard films that more closely resemble the conditions met under commercial conditions.

From these studies there was determined under the conditions of test, the minimum amount of one compound which could be detected in the presence of the other compounds of the mixture. These results may be summarized as follows:

It was found by the X-ray method that in the laboratory burns, $\beta 2CaO.SiO_2$ could be identified definitely in the presence of $3CaO.SiO_2$ only when the amount of $\beta 2CaO.SiO_2$ reached 15 per cent. This is due to the circumstances that the more intense lines of $\beta 2CaO.SiO_2$, which are the ones to appear when small amounts of $\beta 2CaO.SiO_2$ are present, nearly or quite coincide with lines of $3CaO.SiO_2$. Only when this minimum amount of $\beta 2CaO.SiO_2$ is reached do the weaker lines of that compound appear whereby it may be identified and its presence confirmed. Under unfavorable conditions; for example, poor crystallization, it is probable that greater amounts may be necessary for identification.

The amount of $3CaO.SiO_2$ which can be identified in the presence of $\beta 2CaO.SiO_2$, or in cement clinkers may be as low as 8 per cent.

Because of the high order of symmetry and relatively simple structure of the crystals of CaO, MgO, and $3CaO.Al_2O_3$, most of the lines in the patterns of these compounds are intense and, therefore, appear when only small percentages of those compounds are present. In mixtures of compounds approaching Portland cement clinker in composition, the minimum amount of MgO which could be detected was about 2.5 per cent; CaO about 2.5 per cent, and $3CaO.Al_2O_3$ about 6 per cent.

$4CaO.Al_2O_3.Fe_2O_3$, like $\beta 2CaO.SiO_2$, gives a diffraction pattern containing only a few intense lines. And in cement like compositions these lines nearly or quite coincide with lines of the other compounds. Therefore, to identify this comopund, especially in the presence of $3CaO.Al_2O_3$ or $\beta 2CaO.SiO_2$, the minimum amount required is about 10 per cent in mixtures of the pure compounds and about 15 per cent in cement clinker. The larger amount required in clinkers may be due to poorer crystal formation; the combination of some of the Fe_2O_3 or Al_2O_3 with alkalies or other minor constituents which can not yet be evaluated in the calculations; or to the failure of some of the $4CaO.Al_2O_3.Fe_2O_3$ to crystallize. Thus Hansen (24) has observed that the iron phase frequently remains as a glass in the presence of silicates. If $3CaO.Al_2O_3$ is absent, or present only in small amounts, the quantity of $4CaO.Al_2O_3.Fe_2O_3$ necessary for identification in clinkers is less than 15 per cent.

To summarize, in laboratory clinkers, the following amounts of crystalline phase must ordinarily be present in order to be susceptible of recognition by the X-ray diffraction method as employed in this study.

	Per cent
$3CaO.SiO_2$	8
$\beta 2CaO.SiO_2$	15
$3CaO.Al_2O_3$	6
$4CaO.Al_2O_3.Fe_2O_3$	15
MgO	2.5
CaO	2.5

VIII. EXAMINATION OF COMMERCIAL CEMENT CLINKERS

Twenty-eight commercial clinkers were examined by the X-ray diffraction method in the attempt definitely to identify the compounds present in them and to correlate the results obtained by X-ray examination with the composition as calculated from chemical analysis. These clinkers represent a variety of types of raw material and methods of manufacture, both domestic and foreign.

Table 8 gives the chemical analyses of three of these commercial clinkers, together with the compounds present as obtained by calculation (23). It should be pointed out that the status of equilibrium is taken into consideration in the calculations by means of the value obtained for the free CaO content.

TABLE 8.—*Chemical analyses and calculated compound composition of three commercial cement clinkers*

Chemical analysis	Clinker No. 1	Clinker No. 2	Clinker No. 3
CaO	63.4	64.5	66.0
Al_2O_3	6.6	6.4	4.4
Fe_2O_3	2.6	2.4	5.1
MgO	4.1	3.1	.6
MnO	.06	.03	
SiO_2	22.8	22.8	24.0
SO_3	.2	.2	.0
Loss	.1	.5	
Free CaO	.0	.4	.0
Compound composition			
$3CaO.SiO_2$	37	41	50
$2CaO.SiO_2$	38	35	31
$3CaO.Al_2O_3$	13	13	3
CaO	0	.4	0
$4CaO.Al_2O_3.Fe_2O_3$	8	7	15
MgO	4.1	3.1	.6
$CaSO_4$	.3	.3	0

Table 9 gives the interplanar spacings and relative intensities of the lines of the X-ray diffraction patterns of these clinkers, together with corresponding data for the compounds to which the lines may be assigned. In the diffraction patterns of the pure compounds, the weakest lines are omitted, since such lines do not appear when the concentrations of the compounds are of the order found to obtain in cements. Complete diffraction data on these compounds have been reported from this laboratory (11).

TABLE 9.—*Interplanar spacings of diffraction patterns of three commercial clinkers, together with the interplanar spacings of the lines of the cement compounds which may be observed when those compounds are present in amounts approximating the quantities predicted in Portland-cement clinker*

Line No.	Clinker No. 1	Clinker No. 2	Clinker No. 3	C_3S	βC_2S	C_3A	MgO	C_4AF
1	3.02 m	3.02 m	3.03 m	3.02 s				
2	2.940 w	2.945 ww	2.950 w	2.940 w				
3	2.755 ssb	2.750 ssb	2.760 ssb	2.750 ssb	2.750 ssb			2.760 m.
4	2.680 w	2.680 w				2.690 ss		
5			2.645 w					2.640 ss.
6	2.605 s	2.595 s	2.590 s	2.600 s	2.610 s			
7	2.435 w	2.430 w	2.435 w		2.440 m			
8	2.405 w	2.390 w	2.400 ww		2.400 m			
9	2.320 w	2.315 w	2.315 w	2.320 m				
10	2.275 w	2.275 w	2.275 w		2.278 m			
11	2.180 s	2.175 s	2.170 s	2.178 s	2.182 s			
12	2.100 m	2.100 w					2.100 ss [1]	
13	2.035wwb	2.035wwb	2.045 w					2.045 m.
14			2.030 wwb		2.030 mb			
15	1.980 w	1.975 w	1.978 w	1.975 m	1.980 m			
16	1.895–1.935 w	1.890–1.935 w	1.924 mb	1.932 m	1.895 mb	1.905 s		1.930 s.
17	1.824 ww	1.824 wwb	1.823 w	1.825 w	1.800 m			
18	1.760 s	1.761 s	1.763 s	1.762 s				
19	1.623 m	1.626 m	1.624 m	1.627 s				
20			1.577 w					1.578 m.
21	1.530–1.560 w	1.540–1.560 w	1.540 mb	1.542 mb		1.555 ss		1.538 m.
22	1.485 s	1.488 s	1.488 s	1.487 s			1.486 ss	
23	1.454 w	1.458 w	1.460 w	1.458 w				
24	1.345 ww	1.345 w				1.346 m		
25			1.318 ww					1.318 m.
26			1.210 w					1.209 w.
27	1.198 w	1.197 w	1.198 w	1.198 w				
28	1.160 wb	1.158 wb	1.159 wb	1.162 wb				
29	1.131 wb	1.132 wb	1.133 wb	1.132 wb				
30	1.092 wb	1.092 wb	1.090 wb	1.090 wb				

[1] A typographical error appeared in a previous publication (*Am. J. Sci.*, **15**, p. 225; 1928) in which the line 2.100 ss for MgO was incorrectly listed 2.01 m.

An examination of the diffraction data shows that there can be identified in clinkers 1 and 2 the compounds $3CaO.SiO_2$, $\beta 2CaO.SiO_2$, $3CaO.Al_2O_3$ and MgO. The compound $4CaO.Al_2O_3.Fe_2O_3$, present (by calculation) to the extent of 8 and 7 per cent, respectively, was not definitely identified in those two clinkers.

In clinker No. 3, which contained (by calculation) 3 per cent of $3CaO.Al_2O_3$, 15 per cent of $4CaO.Al_2O_3.Fe_2O_3$, and 0.6 per cent of MgO, only the lines of $4CaO.Al_2O_3.Fe_2O_3$ were identified in the pattern in addition to those of $3CaO.SiO_2$ and $\beta 2CaO.SiO_2$. The low concentration of the $3CaO.Al_2O_3$ and MgO accounts for the absence of the lines of those compounds in the pattern.

These three clinkers were selected for detailed presentation because they are typical and represent rather widely varying compositions. Twenty-five other commercial-cement clinkers were examined by this method. In all of them, without exception, $3CaO.SiO_2$ and $\beta 2CaO.SiO_2$ were identified. Furthermore, the patterns of those two compounds were always the most prominent, indicating that they are the most abundant constituents of normal cement clinker. One or more of the compounds $3CaO.Al_2O_3$, $4CaO.Al_2O_3.Fe_2O_3$, or MgO were identified in most of the clinkers, but not all of these latter compounds were identified in all clinkers. As previously pointed out, the X-ray method fails to indicate the compounds when they are present in

amounts less than a certain minimum value. In no case, however, has any inconsistency been observed between the computed constitution, due consideration always being given to the free CaO, and the X-ray observations although, to bring out the desired relationships, special exposures and developments have sometimes been necessary.

No one method of approach to the complicated problem of the constitution of Portland cement may be regarded, of itself, as altogether conclusive. The separation of the compounds from a finely ground sample by methods based on differences in specific gravity probably can not be made complete because of the intimate intergrowth of the crystal phases. Microscopical examinations are satisfactory when made on especially prepared laboratory clinkers, but the fine structure and intergrowths of the constituents of commercial clinkers make for difficulties in the interpretation of optical data when applied directly to the commercial material. Calculations based on the phase-rule interpretations of chemical analyses are open to the criticism that the exact state of the equilibrium which obtains and the effect of the minor components are not known precisely. Of itself, the X-ray method also is inconclusive for it is not capable of detecting small amounts of a crystalline phase nor large amounts of an amorphous composition.

Taken together, however, the cogency of the data obtained by phase equilibria, chemical, microscopical, and X-ray methods becomes profoundly impressive. There is in no case a conflict in interpretation and, where one method fails, the other methods usually supply the information to complete the picture. It is especially noteworthy that the X-ray method can be applied directly to commercial clinker. The results obtained by it are not, to as large an extent as in phase equilibria studies, dependent upon a scientific deduction following established laws; but the confirmation of those deductions by the X-ray method, as also by the microscopical method, leads to increased confidence in the findings.

The X-ray technique has not yet been developed to a degree where the method may be employed for the quantitative estimation of the compounds present. This is a problem to be studied in the near future.

IX. SUMMARY

The X-ray method has been applied in recent research to a study of the compounds which may occur in Portland cement clinker. The present investigation is concerned with a number of subjects regarding the constitution of cement clinker and with the identification of the compounds that occur in the commercial material.

An examination of the composition $3CaO+SiO_2$ has shown that $3CaO.SiO_2$ exists and can be formed by the heating together, under the proper conditions, of a properly proportioned mixture of lime and silica. It is shown, furthermore, that CaO does not enter into solid solution with $2CaO.SiO_2$ in appreciable amounts, but that compositions ranging between $2CaO+SiO_2$ and $3CaO+SiO_2$, properly heated, contain at equilibrium a mixture of $3CaO.SiO_2$ and either γ or $\beta 2CaO.SiO_2$.

A study of the composition $8CaO+Al_2O_3+2SiO_2$ has shown that a compound of that composition does not exist in the system

CaO–Al_2O_3–SiO_2 nor in Portland cement. On the contrary, such a mixture, properly heated gives $3CaO.SiO_2$, $\beta 2CaO.SiO_2$ and $3CaO.Al_2O_3$ and, if equilibrium is not complete, a small amount of CaO.

A special examination of the system $3CaO.SiO_2$–$2CaO.SiO_2$–$3CaO.Al_2O_3$ has shown that solid solution does not occur between either of the above silicates and the aluminate in appreciable amounts. The mixtures at equilibrium contain only those three compounds..

Free CaO was not found in commercial cement clinkers by the X-ray method. A study of the identification of that compound indicates that a percentage of CaO of 2.5 could be recognized. Hence, it is demonstrated that free CaO is not commonly present in commercial clinkers in amounts as high as 2.5 per cent.

The minimum amounts of the cement compounds that could be detected in controlled laboratory burns by the X-ray method, as used in this study, were found to be as follows:

	Per cent
$3CaO.SiO_2$	8
$\beta 2CaO.SiO_2$	15
$3CaO.Al_2O_3$	6
$4CaO.Al_2O_3.Fe_2O_3$	15
MgO	2.5
CaO	2.5

The X-ray diffraction patterns of 28 commercial Portland cement clinkers, representing many types of raw material and processes of manufacture, both domestic and foreign, were obtained. $3CaO.SiO_2$ and $\beta 2CaO.SiO_2$ were identified in each as unquestionably the most abundant constituents; $3CaO.Al_2O_3$, $4CaO.Al_2O_3.Fe_2O_3$, and MgO were identified, separately or together, in most of the clinkers but, in many of them, the patterns of one or two of these latter compounds were not observed.

The results obtained in this investigation by X-ray methods are in agreement with those obtained by phase equilibria, chemical and microscopical methods. Each supplements and confirms the other. Taken together, the cogency of their findings becomes convincing. These findings define the major constitution of Portland cement clinker. They indicate that the most abundant constituents are tricalcium silicate and beta dicalcium silicate; that there are normally present, in addition, tricalcium aluminate, tetracalcium alumino ferrite and magnesia; and that free CaO is not normally present in amounts as great as 2.5 per cent.

X. BIBLIOGRAPHY

1. Rankin, G. A., and Wright, F. E., Am. J. Sci., **39,** p. 1; 1915.
2. Rankin, G. A., and Merwin, H. E., The System CaO–Al_2O_3–MgO, J. Am. Chem. Soc., **38,** p. 568; 1916; The System MgO–Al_2O_3–SiO_2, Am. J. Sci., **45,** p. 301; 1916; Ferguson, J. B., and Merwin, H. E., The System CaO–MgO–SiO_2, **48,** p. 81; 1919; Hansen, W. C., and Bogue, R. H., The System CaO–Fe_2O_3–SiO_2, J. Am. Chem. Soc., **48,** p. 1261; 1926; Hansen, W. C., Brownmiller, L. T., and Bogue, R. H., The System CaO–Al_2O_3–Fe_2O_3, **50,** p. 396; 1928; Hansen, W. C., The System $2CaO.SiO_2$–MgO–$5CaO.3Al_2O_3$, **50,** p. 3081; 1928.
3. Hansen, W. C., and Bogue, R. H., Ind. Eng. Chem., **19,** p. 1260; 1927; Hansen, W. C., B. S. Jour. Research, **4,** (RP132); January, 1930.
4. Dyckerhoff, W., Dissertation, 1924; Zement, **16,** p. 731; 1927.
5. Jänecke, E., Z. anorg. Chem., **76,** p. 1357; 1912.
6. Kühl, H., Zement, **13,** p. 512; 1924.

7. Nacken, R., Zement, **16,** p. 1017; 1927.
8. Debye, P., and Scherrer, P., Phys. Z., **17,** p. 277; 1916; Hull, A. W., Phys. Rev., **10,** p. 66; 1917; Davey, W. P., Gen. Elec. Rev., **25,** p. 565; 1922.
9. Bragg, W. H., and W. L., X Rays and Crystal Structure, G. Ball & Sons (London); Wyckoff, R. W. G., The Structure of Crystals, Chemical Catalogue Co., New York, N. Y., Clark, G. L., Applied X Rays, McGraw-Hill Book Co., New York, N. Y.
10. Hansen, W. C., J. Am. Ceram. Soc., **11,** p. 68; 1928.
11. Harrington, E. A., Am. J. Sci., **13,** p. 467; 1927; Hansen, W. C., and Brownmiller, L. T., **15,** p. 225; 1928. See also reference No. 10.
12. Harrington, E. A., J. Opt. Soc. Am., **16,** p. 211; 1928.
13. Analysis by H. C. Stecker.
14. Jänecke, E., Zement, **18,** p. 1345; 1929.
15. Rankin, G. A., and Wright, F. E., Z. anorg. Chem., **75,** p. 63; 1912.
16. Hansen, W. C., Dyckerhoff, W., Ashton, F. W., and Bogue, R. H., J. Phys. Chem., **31,** p. 607; 1927; Zement, **16,** p. 51, 1927.
17. Goebel, H., Zement, **14,** p. 548; 1925.
18. Jänecke, E., Concrete, **35,** p. 105; 1929.
19. Jänecke, E., Zement, **18,** p. 756; 1929.
20. Lerch, Wm., Concrete, C. M. S., **35,** pp. 109, 115; 1929.
21. Lerch, Wm., and Bogue, R. H., Ind. Eng. Chem., Anal. Ed., **2,** p. 296; 1930.
22. White, A. H., Ind. Eng. Chem., **1,** p. 5; 1909.
23. Bogue, R. H., Ind. Eng. Chem., analytical edition, **1,** p. 192; 1929.
24. Hansen, W. C., personal communication.

WASHINGTON, April, 1930.

PHOTO-IONIZATION OF CÆSIUM VAPOR BY ABSORPTION BETWEEN THE SERIES LINES

By C. Boeckner and F. L. Mohler

ABSTRACT

Measurements by the space-charge method have been made on photo-ionization resulting from a small continuous absorption between the series lines. Results are expressed in terms of relative sensitivity I (λ)/I (3,200). At 0.064 mm pressure I (λ)/I (3,200) increases from 0.0003 at 3,750 A to 0.07 at 3,250 A. I (λ)/I (3,200) increases roughly as the square root of the pressure throughout this wave-length range. On the short wave length side of 3,500 A the effect decreases with increasing temperature of the vapor, the effect being reduced to half for a 70° rise in temperature. On the red side of 3,500 A there is little, if any, temperature change. Results other than the temperature effect can be explained on the hypothesis that the absorption between lines is purely atomic as there is some line absorption far from the line center.

However, the temperature variation indicates a molecular origin and leads to an estimate of 0.26 electron volts for the work of dissociation of Cs_2. Other results can be qualitatively explained on the same hypothesis.

CONTENTS

	Page
I. Introduction	831
II. Method and apparatus	833
1. Method	833
2. The space charge tube	833
3. Light sources	833
III. Results	834
1. Ionization as a function of wave length	834
2. Pressure effect	835
3. Temperature effects	835
4. Effects of foreign gases	836
IV. Discussion	839
1. Atomic absorption between lines	840
2. Ionization considered as of molecular origin	840
3. Conclusion	842

I. INTRODUCTION

Measurements of the photo-electric ionization of cæsium vapor have shown that the photo-electric sensitivity is not limited to the region of continuous absorption beyond the principal series limit at 3,184 A, but extends far into the region of line absorption to 3,888 A. Spectral sensitivity curves of the ionization produced by a continuous spectrum dispersed by a monochromator show that most of this effect is in peaks at the positions of the absorption lines with a small background between the lines. A recent paper by the authors gives a quantitative study of the ionization at the lines.[1] The absorption responsible for the peaks is in narrow atomic lines of the order of

[1] Mohler and Boeckner, B. S. Jour. Research, 5, July, 1930 (RP 186). For brevity we will refer to this paper simply by this number.

0.01 A wide and ionization depends upon the collision of the excited atom produced by line absorption with a normal cæsium atom during the life of the excited state. The probability of such a collision depends on the vapor pressure and is independent of the temperature. Results support a theory of Franck's that the excited atom and normal atom can unite to form a molecule ion.

The small background between peaks must be ascribed to a small absorption between lines. Published results indicate the magnitude of this absorption, assuming that it is truly continuous. In paper No. 186, Figure 4, curve 1 obtained in cæsium vapor at 0.14 mm pressure shows a background between the peaks at 3,612 and 3,477 A of about 0.05 times the peak height. The effective width of the monochromator slits was 40 A, while the absorption lines at this pressure gave nearly complete absorption over 0.04 A. Assuming an equal probability for ionization at the lines and between the lines, then the absorption exponent between lines must be about 5×10^{-5}. At lower pressures much higher sensitivity can be obtained and absorption of less than 10^{-7} of the incident light can readily be detected. Photoionization measurements offer the possibility of studying phenomena far beyond the range of more direct methods, but an obvious limitation is set by the low resolving power of monochromators. This can be partly remedied by using in addition to the continuous spectrum selected line sources having isolated strong lines in the spectrum range involved. The mercury arc lines near 3,650 and 3,340 fulfill this requirement. Earlier work indicates some difference of opinion as to whether these lines give any effect. Foote and Mohler [2] give a curve showing a slight effect at 3,340 A while Little [3] observed sensitivities at 3,340 and 3,650 of 0.05 and 0.03 of the sensitivity at 3,130 in saturated vapor at 166° C., but ascribed this to scattered light from the 3,130 line. In the following work relative sensitivities of about 0.006 and 0.003 are observed at this pressure which is not inconsistent with either of the earlier observations.

The following experiments have been guided by the recognition of two possible origins for the absorption between lines. It may be purely atomic since the absorption in a line is not limited to the small width commonly spoken of as the line width and the residual effect to be expected at 50 or more Angstroms from the line center may well be measureable by our methods. On the other hand, a small concentration of cæsium molecules may give rise to this background. It will be seen that the experiments designed to distinguish between these two hypotheses lead to conflicting results. These experiments cover the spectral distribution of the background absorption and its variation with vapor pressure, temperature, and the addition of foreign gases. On the atomic hypothesis we would expect little temperature effect while the concentration of unstable molecules would change greatly. The theories lead to different laws for the variation with cæsium pressure. In another paper the authors [4] describe the modifications in ionization by line absorption produced by foreign gases. The gas modifies the ionization by its effect on the lives of the excited states and the reduction of a peak height in the presence of nitrogen or hydrogen is characteristic of the excited state concerned.

[2] Foote and Mohler, Phys. Rev., **26**, p. 195; 1925.
[3] Little, Phys. Rev., **30**, p. 109; 1927.
[4] Mohler and Boeckner, B. S. Jour. Research, **5** (RP208); August, 1930.

A similar reduction in the background near the peak would give evidence that the same excited state was involved.

II. METHOD AND APPARATUS

1. METHOD

We have followed the experimental procedure described in earlier papers. Ionization is detected by the neutralizing effect of positive ions on a thermionic current limited by electron space charge. The dark current is balanced out and the current change produced by radiation is measured on a sensitive galvanometer. A limit on the attainable sensitivity is set by random fluctuations apparently produced by electro-magnetic disturbances of unknown origin and variable magnitude. The ratio of current change to ion current ranges from 10^4 to 10^6 depending on operating conditions. All observations consist of relative measurements in terms of some standard wave length near the series limit. These can be reduced to an absolute scale on the basis of published results.[5] The absorption coefficient per atom is 1.85×10^{-19} for the 3,130 mercury line, 2.3×10^{-19} at the limit, 3,184 A; and about the same at 3,200 A.

2. THE SPACE CHARGE TUBE

Various tubes used in this work follow the general design described before. A wire cathode is near the axis of a cylindrical anode which electrically incloses it, and light is admitted through a slit in the end or side of the anode. The cæsium is kept in a side tube, and in operation the body of the tube and the side tube are heated by separate heaters so that the vapor pressure and temperature can be controlled independently. In one tube a third heater around the anode chamber made it possible to heat this part of the tube far above the window temperature to avoid discoloring the window.

3. LIGHT SOURCES

A 400-watt Mazda projection lamp served as a continuous spectrum source. Figure 2 of paper No. 186 gives the spectral intensity distribution in quanta per second obtained with our monochromator. It increases about fortyfold in the range 3,150 to 3,800 A.

A 120-volt quartz Uviarc served as a mercury line source. To reduce scattered ultra-violet light a thick plate of pyrex glass was placed near the exit slit of the monochromator. By further reducing the 3,130 A light with wire screens of 6 per cent transmission, the effect of this line was made comparable with the 3,340 and 3,650 A lines. The resulting intensity ratio of 3,130 to 3,340 and to 3,650 was assumed to be 1 to 22 and 1 to 510. An inverted *u* quartz arc containing a mercury cadmium alloy gave the mercury 3,341 line and the unresolved lines 3,261 and 3,253 in the ratio of 2.5 to 1.

The Bausch & Lomb monochromator with both slits, 0.1 mm wide gives a peak about 60 A wide at the base and nearly triangular in shape. Slits as small as 0.03 mm were used, but did not give a proportional increase in resolving power because of imperfect adjustment.

[5] Mohler and Boeckner, B. S. Jour. Research, **1** (RP3), p. 303; 1929.

III. RESULTS

1. IONIZATION AS A FUNCTION OF WAVE LENGTH

Figure 1 shows on a large scale the ionization between lines sa observed with a Mazda lamp at a cæsium pressure of about 0.06 mm. It is a composite curve made up of observations with different slit widths. Table 1 gives values of the effect per unit radiation flux relative to the effect at 3,200 and to the line peaks and includes values based on measurements with mercury and cadmium lines. The small peak at 3,446 A falls within 1 A of the third principal

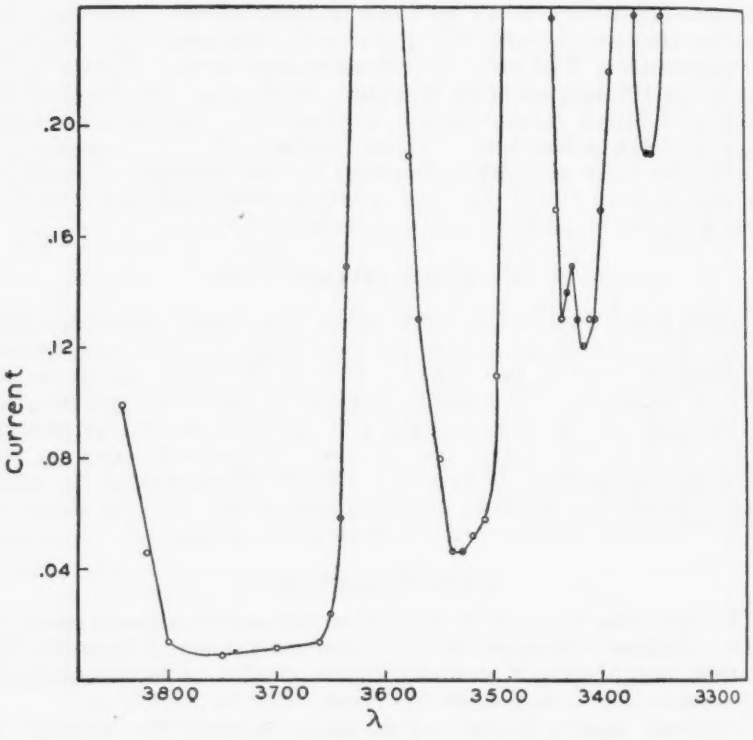

FIGURE 1.—*Ionization as a function of wave length in Cs at 0.064 mm pressure*

On the scale of ordinates the effect at 3,200 A is 1.

series doublet of potassium. It was relatively strong at high pressures and at higher temperatures. Our experiments do not set definite limits to the background except that on the red side of 3,888 it was too small to measure.

In connection with the above, some absorption spectra obtained by Bevan in cæsium vapor may be mentioned. These show that the absorption between the higher series lines remains small relative to the atomic absorption at the limit even at much higher pressures than those used here.[6]

[6] Bevan, Proc. Roy. Soc. A., **83**, p. 421; 1910.

TABLE 1.—*Relative amounts of ionization between absorption lines in cæsium at 0.064 mm pressure*

λ radiation	λ_o Cs lines	I (λ)/I (λ_o)	I (λ)/I (3,200)	Source
3,750	3,612	0.0053	0.00027	Continuous.
3,700	----------	.0065	.00041	Do.
3,660	----------	.0076	.00054	Do.
3,650	----------	----------	.00047	Hg arc.
3,540	3,477	.030	.0032	Continuous.
3,510	----------	.037	.0045	Do.
3,420	3,398	.09	.0165	Do.
3,360	3,347	.165	.035	Do.
3,341	----------	----------	.027	Hg arc.
3,261	3,256	} ----------	.068	Hg-Cd arc.
3,253	3,246			

2. PRESSURE EFFECT

Measurements with a continuous spectrum at various vapor pressures showed a marked increase with vapor pressure in the background relative to either 3,200 or to the peaks, but it was not feasible to get quantitative measurements over a wide pressure range.

Much larger effects could be obtained with the 3,340 and 3,650 lines of the mercury arc. Figure 2 shows the spectral distribution of ionization produced by mercury radiation passed through a plate of glass to reduce scattered ultra-violet light. There are peaks at the mercury lines and peaks at the cæsium lines. The latter come from a continuous background in the arc radiation, and the former from continuous absorption in the cæsium. The two effects are not completely resolved, but are readily separated graphically.

Figure 3 gives some observed ratios of the effect at 3,340 and 3,650 A to that at 3,130 plotted against the square root of the pressure. Some uncontrolled factor made it impossible to reproduce results on the pressure variation within the range of precision suggested in the curves of Figure 2. The absolute sensitivity ratio is obtained by multiplying ordinates of Figure 3 by 4.5×10^{-2} for 3,340 and by 2.0×10^{-3} for 3,650. The change in continuous background with pressure at other wave lengths is comparable with the change at 3 650 and 3.340.

3. TEMPERATURE EFFECTS

During the course of measurements of the pressure effect with the mercury arc wide variations were found in the effect of the 3,340 line as compared with 3,650. The cause was finally found to lie in a large temperature coefficient of the ionization by the former line and to the fact that the furnace temperature had not been kept constant from run to run. Measurement showed that the effect at 3,340 was cut in half by a 70° rise in temperature.

Figure 4 shows a plot of log TI (λ)/I (3,130) against 1/T. The points at the higher temperatures were obtained by superheating the ionization chamber while many of the lower points were obtained by changing the temperature of the whole tube.

Measurements with the cadmium mercury arc were also made, using the unresolved Cd lines 3,252 and 3,261, and the 3,341 mercury

line. The lines at 3,260 and at 3,341 were found to show about the same temperature variation.

By use of the Mazda lamp, it was possible to locate spectral limits of the temperature effect. Figure 5 shows two spectral distribution curves obtained at 320° and 220°, the cæsium pressure being kept at 0. 06 mm. The 3,650 A and 3,550 A regions are seen to have no temperature effects, while at 3,440 and 3,360, there are large effects.

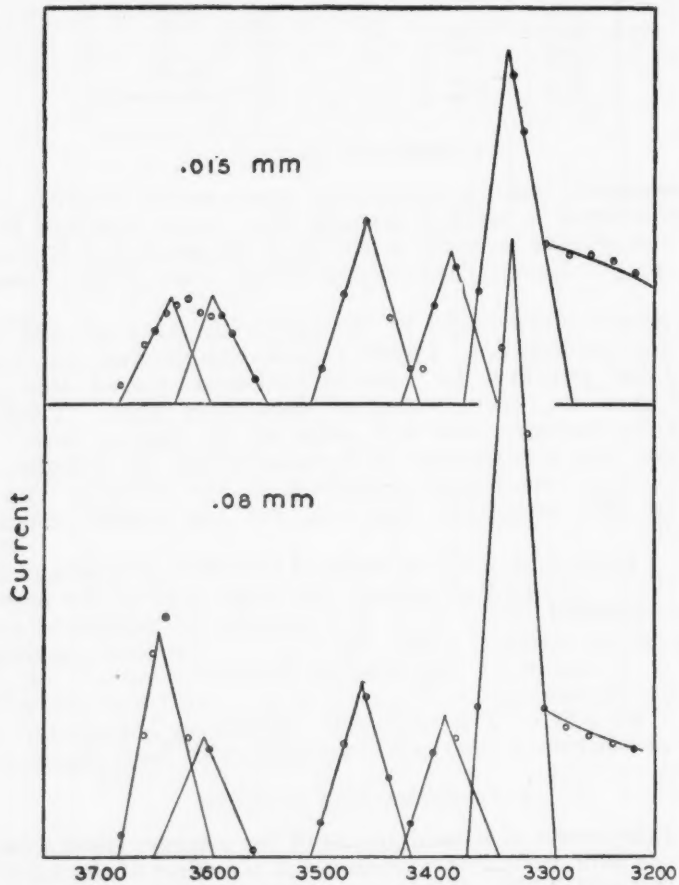

FIGURE 2.—*Ionization produced by mercury arc radiation*
The two extreme peaks are at the position of mercury lines, the others at cæsium lines.

somewhat smaller, however, than those obtained with the Hg arc in the same wave-length region.

4. EFFECTS OF FOREIGN GASES

Figure 6 shows plots of the background with 2 mm of nitrogen and with no foreign gas in the space charge tube. The background at all wave lengths is quenched. Table 2 gives values of the quenching ratio for both the series lines and the background and it is seen that they are approximately the same.

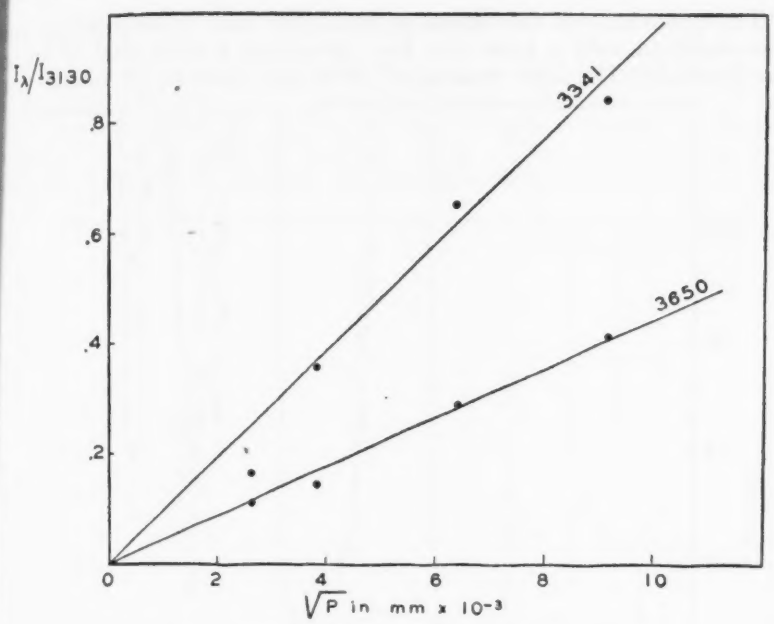

FIGURE 3.—*Ionization as a function of pressure*

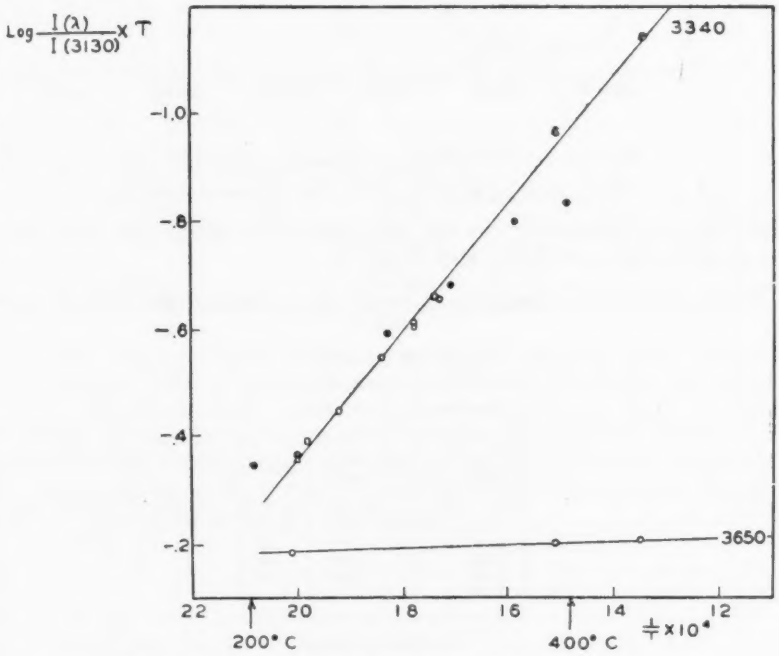

FIGURE 4.—*Variation of ionization with temperature*

The quenching of the effects of the 3,340 and 3,650 mercury lines was obtained with a tube that had developed a good deal of foreign gas (probably H_2) after sealing off from the pumps. It is seen here

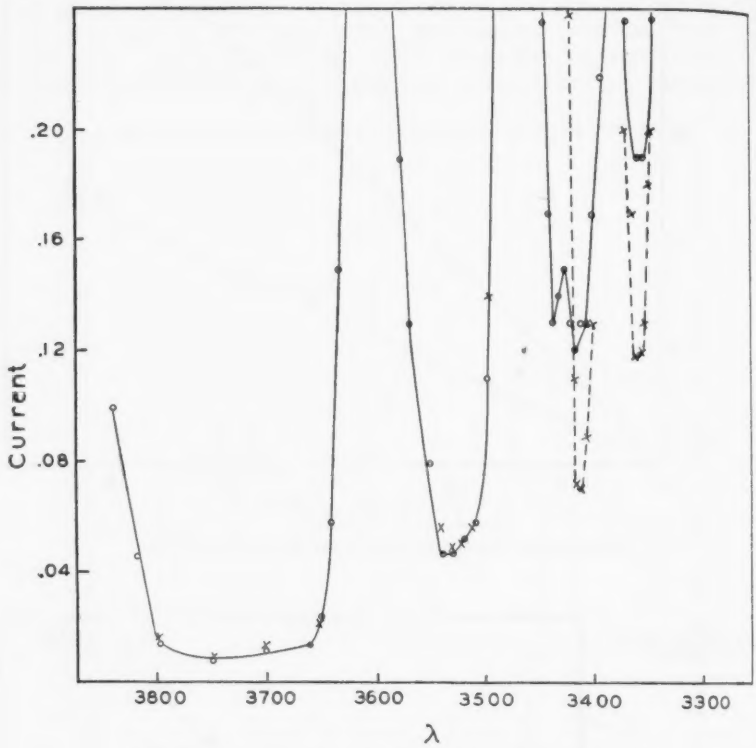

FIGURE 5.—*Ionization of cæsium vapor at 0.06 mm*
Full line and circles at 220° C.; broken lines and crosses at 320° C.

also that the quenching for the background is about the same as for the cæsium lines at 3,612 and 3,347 A.

TABLE 2.—*Reduction of ionization by foreign gas. Ratio of effect with gas to effect without*

2 mm OF NITROGEN

Background		Lines	
Wave length	Ratio	Wave length	Ratio
3,750	0.21	3,612	0.18
3,700	.18	3,477	.20
3,540	.34	3,398	.24
3,430	.25	3,347	.29
3,360	.37		

UNKNOWN GAS

3,650	0.30	3,612	0.29
3,340	.45	3,347	.52

IV. DISCUSSION

We shall consider two possible origins of the absorption between lines which give rise to the photo-ionization. One possibility is that there are some cæsium molecules which have a nearly continuous background of absorption between lines. The other possibility is that the absorption is purely atomic line absorption, for the absorp-

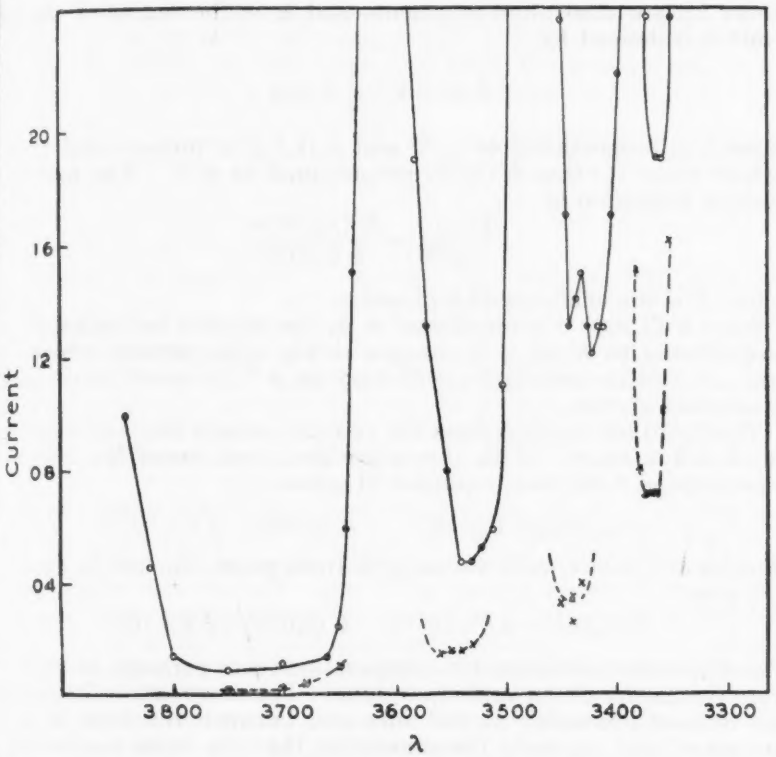

FIGURE 6.—*Full line curve photo-ionization in pure cæsium vapor. Broken curve with 2 mm of nitrogen added*

tion of each line actually extends over an indefinitely large range of wave lengths. Both types of absorption are generally recognized to exist. In the atomic case it seems safe to assume that ionization will result from absorption with the same probability as for light coincident with the center of the line. For the molecular absorption there is no a priori basis for predicting the efficiency of ionization and several mechanisms must be considered.

1. ATOMIC ABSORPTION BETWEEN LINES

We shall assume [7] that the half widths of the lines are proportional to the square root of the pressure and that the absorption far from the line is given by

$$\frac{k\ (\lambda)}{k\ (\lambda_0)}=\frac{\Delta}{(\lambda-\lambda_0)^2} \tag{1}$$

where k's are absorption exponents and λ_0 is the center of the line while Δ is defined by

$$k\ (\lambda \pm \Delta)=\frac{1}{2}\,k\ (\lambda_0)$$

Since Δ is proportional to $p^{1/2}$ and $k\ (\lambda_0)\ \Delta$ is proportional to p it follows from (1) that $k\ (\lambda)$ is proportional to $p^{3/2}$. The measured relative ionization is

$$\frac{I\ (\lambda)}{I\ (3{,}200)}=\frac{E\ (\lambda_0)\ k\ (\lambda)}{k\ (3{,}200)} \tag{2}$$

where E is the efficiency of ionization.

Since $k\ (3{,}200)$ is proportional to p, the relative ionization will be proportional to $E\ p^{1/2}$. E changes slowly with pressure above 0.01 mm., so relative sensitivity will vary as $p^{1/2}$ in accord with results shown in Figure 3.

The 3,650 line is 33 A from the nearest cæsium line and the 3,341 line is 5.9 A away. With absorption data from paper No. 186, with a pressure of 0.064 mm, equation (1) gives

$$k\ (3{,}341)=1.\times 10^{-5} \qquad k\ (3{,}650)=1.1\times 10^{-6}$$

Results of Table 1, with values of E from paper No. 186 in equation (2), give

$$k\ (3{,}341)=4.8\times 10^{-5} \qquad k\ (3{,}650)=2.8\times 10^{-6}$$

The discrepancy between the computations can, perhaps, be expected from the nature of the approximations. The observation that foreign gas reduces ionization at the lines and between the lines in about the same ratio supports the conclusion that the same mechanism is involved. There is only one outstanding objection to the atomic origin of this ionization, the fact that the ionization is reduced at high temperatures.

2. IONIZATION CONSIDERED AS OF MOLECULAR ORIGIN

We assume that the molecules giving rise to the absorption are diatomic. They will exist in relatively low concentration which will depend on the temperature and pressure according to familiar thermodynamical relations. If n_1 is the concentration of cæsium atoms (proportional to vapor density), n_2 the concentration of Cs_2 molecules, Q the heat of dissociation of the molecules at temperature T and K the equilibrium constant of the reaction, $Cs+Cs=Cs_2$, then

$$\log K=\frac{Q}{2,3\ RT}+\text{const} \tag{3}$$

[7] Line widths at the vapor pressures used are determined by the cæsium pressure. Experimental results (Waible, Zeits. f. Phys., **53**, p. 459; 1929) support the square root relation for the half widths. The experiments also give a basis for equation (1).

$$K=\frac{n_2}{{n_1}^2} \tag{4}$$

If we assume that I (3,130) is proportional to n_1 and I (λ) to n_2 (this assumes efficiency of ionization at λ is independent of density and temperature), we see that the form of equation (3) accounts for the observed temperature variation of the ionization at 3,340. (Fig. 4.) The slope of the line in Figure 4 gives a value for Q of 0.26 electron volts. Results shown in Figure 5 indicate that all the background on the short wave-length side of 3,500 A can be ascribed to molecules with a similar value of Q while the background on the red side of 3,500 has a much smaller temperature coefficient and, hence, must have a different origin.

Equation 2 shows that the relative concentrations of molecules n_2/n_1 is directly proportional to the pressure, while observations in Figure 3 indicate that I (λ)/I (3,130) varies more nearly as $p^{1/2}$. There remains the possibility that the probability of ionization of the excited molecule changes with pressure.

The absolute magnitude of n_2 may be computed from relations similar to equation (3) based on statistical considerations.[8] For cæsium at 0.1 mm. pressure and at about 300° C., n_2/n_1 lies between 10^{-5} and 10^{-6}, depending on the values used for Q and other constants.

The estimates of 0.26 volt for the heat dissociation of Cs_2 and 0.7 volt or more for Cs^+_2 set certain limits to the regions in which photo-ionization is to be expected. The ionization potential of the atom is 3.87 volts. The minimum ionization potential of the normal molecule is $3.87-0.7+0.26=3.43$ volts ($\lambda=3{,}600$ A) while the minimum ionization potentials leading to high vibration states of the ion will range to $3.87+0.26=4.13$ volts ($\lambda=3{,}000$). Excited neutral molecules which can spontaneously pass into the ion state can exist in the energy range 3.43 to 4.13 volts. The energy required to ionize a molecule in the normal electronic state, but in a high vibration state may be much as as 0.26 volt less than that required for the normal molecule so that the range of photosensitivity will extend to beyond 3,800 A as observed.

There is, however, an important difference between ionization on the red and violet side of the threshold (3,600 A) for the normal molecule. Photo-electric absorption on the violet side involves normal molecules and will have a temperature coefficient appropriate to Q for the normal molecule. Photo-ionization by longer wave lengths depends on the concentration of molecules in high vibration states and will, therefore, have a much smaller temperature coefficient. The experimental observations of Figure 5 conform roughly to this prediction though the dividing line between high and low temperature coefficients is near 3,500 instead of 3,600 A.

There are at least three possible mechanisms for the photo-ionization process: (1) Direct transition by absorption into the ion state, (2) transition into a discrete state of the neutral molecule with energy greater than 3.4 volts followed by a spontaneous transition into a molecule ion state of the same energy, and (3) transition into a dissociated state giving an excited atom which becomes a molecule ion by a subsequent collision. The most probable transition is the one

[8] Fowler, Phil. Mag., **45**, p. 1; 1923.

which involves the least change in nuclear separation but this is not known for cæsium.

The first and simplest process is ruled out by the fact that ionization is diminished by the presence of a foreign gas. This implies that some time must elapse between the absorption of radiation and the formation of an ion. Both the second and third processes involve a time interval during which a collision may destroy the excited state. The third process of ionization would give identically the same quenching by the foreign gas for the line peaks and for the background, the second a similar but not identical quenching. Another observation seems to favor the second mechanism. We have referred above to evidence that the probability of ionization of the excited molecule decreases with increasing vapor pressure. The results suggest that cæsium vapor, as well as other gases, may quench ionization, and this is to be expected if the excited states are molecular and not atomic.

Whatever the nature of the ionization process may be, it must be highly efficient. This follows from the fact that the observed absorption between the cæsium lines is small compared to that at the limit while the ionization itself is an appreciable fraction of that at the limit.

It may also be concluded that the absorption of the molecule is much greater than that of the atom, since the molecular ionization is comparable to the atomic even though the fraction of atoms associated must be extremely small.

3. CONCLUSION

Our discussion has led to an apparent paradox. Phenomena of ionization between lines can be explained by the assumption that the absorption is purely atomic except for the observed temperature variation of the ionization. The temperature variation clearly indicates a molecular origin of this ionization and all other phenomena are shown to be qualitatively in agreement with this. Results favor the hypothesis that absorption leads to a highly excited neutral molecule which spontaneously passes to a state of the molecule ion.

WASHINGTON, June 17, 1930.

EFFICIENCY OF PRODUCTION OF X RAYS

By Warren W. Nicholas

ABSTRACT

Efficiency.—The various corrections necessary for an estimate of efficiency of production E_c of continuous spectrum X rays are carefully considered. These include corrections for absorption (including absorption in the anticathode), reflection of cathode rays at the focal spot, asymmetric spatial distribution of X-ray intensity, and allowance for characteristic ray energy. Applying these corrections to some data by Rump, E_c for a tungsten anticathode at a voltage $V=40$ kv is found to be 0.0039. It is pointed out that E_c can not yet be accurately estimated for a wide range of voltage. Present knowledge of secondary processes in gas filled tubes is so limited as to make it inadvisable to attempt to use these tubes for an exact estimate of E_c. The bearing of the Thomson-Whiddington constant on the generation of X-ray energy is pointed out, and an explanation given for Ulrey's results indicating a certain degree of periodicity in the dependence of efficiency on atomic number.

Intensities.—It is shown, on the basis of Rump's data, that the continuous spectrum intensity generated inside an anticathode and radiated at an angle $\psi=90°$ with the cathode stream is proportional to $V^{3/2}$, at least for tungsten and $V>40$ kv. A general formula for the spectral intensity distribution of this radiation is given, as well as a means for estimating its variation with ψ; absorption in the anticathode is described quantitatively; the proportion of K characteristic rays for tungsten is found. There is thus obtained a complete description of the intensities obtainable outside X-ray tubes for a wide range of practical conditions.

CONTENTS

	Page
I. Introduction	843
II. Experimental difficulties	845
1. Losses due to stray cathode rays	845
2. Special difficulties with gas-filled tubes	845
3. Losses due to absorption	847
III. Spectral energy distributions	851
IV. Variation of X-ray intensity with voltage	853
V. Intensities in different directions	857
VI. Efficiency of X-ray production	859
VII. Efficiency and the Thomson-Whiddington constant	861
VIII. Discussion	863
IX. Summary	864
X. References	865

I. INTRODUCTION

During some recent work for the International Critical Tables and for the Smithsonian Physical Tables, the author had occasion to review critically the experimental work that has been done on the measurement of the total energy in the X-ray continuous spectrum. There is a surprising range of values obtained in this work. Especially, the recent measurement by Rump (1) [1], who used what seems

[1] The figures given in parentheses here and throughout the text relate to the list of references given at the end of the paper.

to be the best method for measuring X-ray energy, is almost 50 per cent higher than the maximum value estimated by Kulenkampff (2) from a careful consideration of all previous work with unresolved energy. A closer approximation than this is very desirable if for no other reason than to check theoretical estimates of continuous spectrum energy (3). But also the X-ray continuous spectrum is often a very convenient standard source of X-ray energy; for example, it has been used recently by Webster (4) for an estimate of the absolute probability of K emission due to excitation by cathode rays. Further, it is only recently that a fairly complete conception has been obtained of the variation of X-ray intensity in different directions relative to the cathode stream (5). Inasmuch as this variation must be known in order to calculate the total energy emitted (which involves an integration over the whole sphere), it is of interest to apply the new results in an attempt to obtain a more satisfactory estimate of efficiency than it has been possible to obtain previously.

For purposes of definition, let a hypothetical X-ray tube be imagined, the electrodes of which are maintained at a constant d. c. potential difference V, and the current i through which is all carried by the cathode rays. Suppose these cathode rays all enter the target at the focal spot without "reflection"; this insures that all the energy of the cathode rays is converted, in the focal spot, either into heat energy or X-ray energy; that is

$$Vi=H+J \tag{1}$$

where H is the heat energy, and J the X-ray energy, generated per second by the cathode rays within the focal spot in this hypothetical tube.

The quantity J may be divided into several parts. One of these parts, J_c, is associated with the energy of the continuous spectrum X rays, and the remaining parts, J_K, J_L, ... , are associated with the various groups of characteristic rays K, L, . . . respectively. Thus

$$J=J_c+J_K+J_L+ \quad . \quad . \quad .$$

By efficiency of production of X rays is here understood

$$E=J/Vi$$

by efficiency of production of continuous spectrum X rays

$$E_c=J_c/Vi$$

and similarly, the efficiency of production of the various groups of characteristic rays, K, L, ... , may be defined as

$$E_K=J_K/Vi,\ E_L=J_L/Vi, \quad . \quad . \quad . \quad ,$$

respectively. The present paper will deal particularly with an estimation, from experiment, of E_c for a tungsten anticathode, although some data associated with E_K will be obtained incidentally.

II. EXPERIMENTAL DIFFICULTIES

1. LOSSES DUE TO STRAY CATHODE RAYS

In practice, the simple conditions outlined above in connection with the "hypothetical" tube do not hold. With the actual X-ray tube, the cathode rays do not convert all their energy into heat and X rays at the focal spot, but due to a "reflection" (either a single large-angle deflection resulting from a close collision of a cathode ray with an atomic nucleus, or a succession of smaller deflections (6) many of the cathode rays leave the focal spot with a considerable fraction of their initial energy (7, 8, 9, 10). These "stray" rays may strike other parts of the tube (the walls, or parts of the anticathode remote from the focal spot) to generate "off-focus" X rays and heat. On this account, in the actual tube, the X ray and heat energies generated per second at the focal spot are not J and H, but some quantities, say J' and H', where

$$J' < J \text{ and } H' < H$$

(Quantities associated only with the focal spot in the actual X-ray tube will be singly primed.) Similar considerations hold for the quantities J'_c, J'_k, etc., definitions of which are obvious from the above. It may be pointed out that $J-J'$ and $H-H'$ are not measures of the off-focus X ray and heat energies except for the particular case where all the stray cathode rays dissipate their energy in a material in which the efficiency of X-ray production is the same as for the material of the anticathode. The difference between J and J' is not at all negligible, this difference, with a tungsten anticathode, and voltages of the order of 100 kv, being about 20 per cent of J (7, 8).

2. SPECIAL DIFFICULTIES WITH GAS-FILLED TUBES

In gas-filled tubes, some further complicating factors enter; it is desirable to discuss these factors at some length on account of the fact that so many estimates of efficiency have been based on work with this type of tube, and any possibility of comparison of these estimates with the present one should not be overlooked. The considerations discussed here are quite apart from the well-known difficulties of operation of gas-filled tubes, and deal rather with some ambiguities connected with the interpretation of data obtained with these tubes.

With gas-filled tubes, the current i'' (doubly primed quantities will be associated with phenomena in gas-filled tubes) read on a milliammeter in the tube circuit is not equal to the cathode ray current i; this is on account of the fact that a very appreciable part of the tube current i'' is carried by positive ions. In the best work with these tubes, the current i is determined by measuring the amount of heat H'' generated in the anticathode. The true cathode ray current i is then assumed to be H''/V, and the efficiency E'' is taken to be J''/H''. It remains to ascertain how closely this approximates the true efficiency $E = J/Vi =$ (approx.) J/H (since J is very small compared with H).

The difficulties here are again due to the reflection of cathode rays from the target surface, but there is a special uncertainty with gas-

filled tubes on account of not knowing where the stray X rays are produced; for example, if they were produced only on the anode stem as in a Coolidge tube, H'' would include the heat energy produced by the stray cathode rays. However, as is well known, the reason the cathode rays in a well-evacuated tube (Coolidge tube) must eventually dissipate their energy in the anode is that the inner walls of the glass acquire a negative charge due to the accumulation of stray cathode rays, and since the leakage is small, the walls quickly acquire such a potential as will prevent additional stray cathode rays striking them; this is evidenced by the absence of fluorescence on the walls of the Coolidge tube. But in a gas tube the walls do not become charged to the extent they do in the Coolidge tube; this is shown by the fact that they continually exhibit a bright fluorescence. Thus it may be expected that, in a gas tube, an appreciable portion of the cathode rays strike the glass walls with high enough speeds to generate considerable X-ray energy and heat energy there.

Now the effect of these conditions on the comparison of E with E' may be illustrated by some special cases. Suppose first that 20 per cent, say, of the cathode rays are reflected from the target face with their entire energy, and that they all go to the glass walls and stay there. Then it is evident that J'' and H'' will for this case be 80 per cent of J and H, respectively, and that E'' will be equal to E. On the other hand, suppose the reflected cathode rays lose only a negligible amount of energy in the glass walls, and that, due to the field between anode and walls, they are drawn back to the anode striking it at such points as to contribute to H'' but not to J''. In this case E'' will obviously be 80 per cent of E. For the other extreme suppose that a fraction α of the cathode rays first lose a portion of their energy in the focal spot, then reflect to the glass walls and stay there. Had these rays remained in the focal spot, they would have generated there X-ray energy per second $\Delta J = J - J''$ and heat energy $\Delta H = H - H''$ with an efficiency $\Delta J/\Delta H$. This efficiency would have been less than the true efficiency J/H, since efficiency decreases with decreasing cathode ray speed. Thus the loss to the anticathode of these slow-speed stray cathode rays increases the

$$\text{apparent efficiency (that is, } E'' = \frac{J - \Delta J}{H - \Delta H} > \frac{J}{H}, \text{ as may be easily shown}$$

For example, if α were 0.3 and β 0.2, E'' would be about 6 per cent greater than E.

The actual processes occurring in gas-filled tubes are probably a combination of the above. Cathode rays reflect from the focal spot with various portions of their original speeds, and partially charge the walls of the tube. This allows only the faster rays to strike the walls; the slower ones are pulled back to the anode, striking, in general, at points other than the focal spot. So far as the author is aware no data is available for a quantitative estimate of these processes, and therefore, an estimate of the true efficiency E from the apparent efficiency E'' obtained with gas filled tubes can not be relied upon to better than about 10 or 20 per cent of its value. Moreover, it would seem very difficult to ever make a satisfactory estimate of the many experimental errors introduced by these complications. In a Coolidge

tube, on the other hand, the possibility of making satisfactory corrections for the errors introduced by the reflection of cathode rays from the focal spot seems much less remote. For in this case all the reflected rays must eventually return to the anode without loss of speed and the resulting X-ray energy generated there can be estimated. Further, as mentioned above, the tube current as measured with a milliammeter is, with the hot filament tube, presumably a quantity which can be interpreted without ambiguity. For these reasons, it seems preferable to base the present estimate of efficiency entirely on work done with Coolidge tubes; specifically, the work by Rump (1) was chosen as being apparently the most satisfactory from the standpoint of the measurement of the X-ray energy, for the use of fairly steady voltages, and for the use of a range of voltage (40 to 150 kv) which is of especial practical interest at present.

3. LOSSES DUE TO ABSORPTION

J and J' are associated, according to definition, with X-ray energy produced inside the anticathode; thus they can not be measured directly, but must be calculated from quantities which are directly measurable. In measurements of X-ray efficiency the quantity measured is an X-ray intensity gI', the unresolved energy per second incident on some definite area A outside the tube. The slit system limiting the beam to A usually also limits the registered intensity to rays which come from the focal spot; hence gI' must be associated with J' instead of J. Now the rays reaching A must have passed through several materials and lost thereto an appreciable fraction of their initial energy. If I′ is defined as the unresolved intensity which would have been registered at A had these various absorptions not occurred, then g represents that fraction of the initial energy which remains after the various absorptions have taken place. From present knowledge of absorption coefficients, the calculation of that part of g due to the walls of the tube, air path, etc., is perfectly straightforward when the special energy distribution of gI' is known. The calculation of the part of g due to absorption in the anticathode is not so simple, however, since for an adequate estimate a knowledge is required of the depths within the anticathode at which the various wave lengths are produced. It should be possible to calculate the depths indirectly from data on cathode rays involving their losses of speed and deflections on entering the anticathode, together with known laws of X-ray emission. The theoretical difficulties in such a calculation are, however, very great, and such data on cathode rays is not yet complete enough for general use. There is some direct experimental data on the depths in the anticathode at which X rays are produced, but the data dealing with spectrally resolved rays is meager, and most of it is open to some doubt on account of polarization considerations (9) and on account of complications introduced by the roughness of the target face. In view of the fact that the correction for absorption in the anticathode is the one correction in measurements of X-ray efficiency which can not be readily evaluated, it becomes of prime importance to obtain for quantitative estimates of efficiency a satisfactory expression for this correction.

The formula used in the present work for the correction for absorption in the anticathode is the following:

$$\bar{x}=k\frac{V}{bZ^{\frac{1}{2}}}\left\{1-e^{-\frac{VZ^{\frac{1}{2}}}{k}\left(\frac{\nu_0-\nu}{\nu_0}\right)}\right\} \quad (2)$$

where $\bar{x}$ is the effective depth inside a target of atomic number Z at which frequency ν in the continuous spectrum is produced, $\bar{x}$ being measured in the direction in which the cathode beam strikes the target face. V is the voltage applied to the tube, which also determines the frequency ν_0 of the quantum limit, b is the constant of the Thomson-Whiddington-Bohr law in the form

$$\frac{d(V^2)}{dx}=-b \quad (3)$$

e is the base of natural logarithms, and k is a constant probably dependent on the angle at which the cathode rays strike the target face. For the present case this angle was 45° to a close enough approximation;[2] and since the X rays were taken off in the usual direction, the effective path length the X rays must traverse in the anticathode is also $\bar{x}$. V is expressed in kilovolts; $\bar{x}$ is in centimeters; b is calculated from Terrill's formula $b=40\times10^4\rho$ where ρ is the density (in $g\cdot cm^{-3}$) of the anticathode material. The numerical value of k was taken to be 120; this seemed to agree quite satisfactorily with the empirical data, as will be shown below.

The derivation of the formula was based on the following considerations: If the cathode rays penetrated the anticathode without being deflected (or "diffused"), the depth p (measured along the line of the cathode ray beam) to which they would penetrate would be given by the Thomson-Whiddington-Bohr law $p=\frac{V^2}{b}$. Other things being equal, this law will be a measure, for different anticathodes, of the depths to which the cathode rays penetrate in being reduced to zero speed. Thus it may be supposed that the mean depth p to which the cathode rays actually penetrate (that is, now taking account of deflections) will be given by a law of the form

$$p=\frac{V^2}{b}f(Z,V) \quad (4)$$

where $f(Z,V)$ is a factor designed to reduce p to a fraction of p which is dependent on the extent of the deflections of the cathode rays. It should be noted now that the greater the total path length of the cathode rays in the material the more numerous the deflections along the whole path. Accordingly, for very short paths (that is, for low initial speeds), the rays may be expected to be little deflected, and reach depths approximating p, whereas for long paths the fraction $\bar{p}/p$ may be expected to become smaller, since the total number of deflections along the path has increased. Thus a form for $f(Z,V)$ is required which will become unity for very short path lengths, and for long paths will gradually approach some other function $j(Z,V)$

[2] Actually, with the customary arrangement of electrodes, this angle is somewhat smaller than 45° (measured from the normal to the target face) for, as was pointed out by Webster and Hennings (11), the cathode rays are deflected inside the tube to an extent dependent on the arrangement of the electrodes.

which is a measure of the influence of deflections on penetration for the higher voltages. A form for $f(Z,V)$ which fulfills these conditions is

$$f=j\ \{1-e^{-1/j}\} \tag{5}$$

(j is large for short paths, and small for long paths, see below). Substituting in (4) we have for the mean depth of penetration

$$\bar{p}=\frac{V^2}{b}j(Z,\ V)\ \{1-e^{-1/j(Z,\ V)}\} \tag{6}$$

Although the form

$$j=C/VZ^{\frac{1}{2}} \tag{7}$$

was chosen to fit the X-ray data, it is interesting that, choosing the constant $C=35$ kv, this formula gives the order of magnitude of some data by Schonland (12) on cathode ray penetration, and for a very large range of atomic number and voltage. From Schonland's data may be obtained the thickness of metal foil which "reflects" as many cathode rays of a given voltage as it transmits. Half this thickness was taken to be the mean depth of penetration, for if the cathode rays are completely diffused (that is, have random directions) by the time they reach this mean depth, then they have equal probabilities of reaching the two surfaces of the foil. Considering the rough character of this approximation, the comparison with Schonland's data in Table 1 may be regarded as satisfactory.

TABLE 1

Z	V	$\bar{p}$ (calc)	$\bar{p}$ (obs)	Ratio
	kv	μ	μ	
13 (Al)	87	7.8	11.0	1.4
13	41	3.6	3.5	1.0
13	24	2.0	1.3	.64
79 (Au)	20	.10	.09	.9
13	14	.97	.38	.4

Finally, the formula for $\bar{p}$ must be modified in such a manner as to describe the mean depth $\bar{x}$ of production of the X rays, which will depend on frequency ν as well as on V and Z. First it may be pointed out that the rays of very low frequency are produced by the cathode rays all along their paths, according to well-known laws of X-ray emission (13, 9). Thus, $\bar{p}$ may be regarded as a measure of $\bar{x}_{\nu=0}$ except that the latter quantity will be uniformly smaller than $\bar{p}$. This condition was expressed by assuming that for low frequencies the formula for $\bar{x}$ must approximate

$$k\frac{V}{bZ^{\frac{1}{2}}}\{1-e^{-\nu Z^{\frac{1}{2}}/k}\} \tag{8}$$

which is the same as the formula for $\bar{p}$ except for a different numerical value for the constant (the value adopted for k was such as to make $\bar{p}/\bar{x}_{\nu=0}$ about 3 for ordinary conditions, which is reasonable. The higher frequencies, however, must be produced at shallower depths, since it is only in that part of their path for which the cathode rays retain a large fraction of their original speed (and consequently have not penetrated so deeply) that they are allowed by quantum laws to

produce the higher frequencies. For example, a frequency ν_x corresponding to a voltage V_x which is near V, the voltage on the tube, can not be produced at a depth greater than

$$x=\frac{V^2-V_x^2}{b}$$

which is the depth to which a cathode ray can penetrate, according to the Thomson-Whiddington-Bohr law and retain a speed sufficient, by quantum laws, to enable it to produce X rays of frequency ν_x. When $V-V_x$ is small, the cathode rays will not have been much deflected before reaching depth x; also, according to the laws of emission, they will have produced X rays of frequency ν_x with roughly uniform intensity at all depths between zero and x. Thus for this special case, as has been pointed out by Webster and Hennings (11), the mean depth approximates half of x, or

$$\frac{V^2-V_x^2}{2b} \tag{9}$$

and since $(V-V_x)\ll V$ for the case considered, (9) is approximated by

$$\frac{V(V-V_x)}{b} \tag{10}$$

Thus the final formula for $\bar{x}$ should approximate (8) for low frequencies and (10) for high frequencies. The formula (2) adopted does this, since

$$1-e^{-x}\rightarrow x \text{ for } x\rightarrow 0$$

and

$$\frac{\nu_0-\nu}{\nu_0}=\frac{V-V_x}{V}$$

and gives a reasonable distribution of depths for the intermediate frequencies. Some numerical comparisons with experimental results are given in Table 2. The best data for the comparison is that of Webster and Hennings; the calculated values agree excellently for the higher voltages. The disagreement at the lower voltages is believed to be due to a difficulty with the experimental method, since the experimental values for mean depth are greater than the maximum depths allowed by the Thomson-Whiddington-Bohr law if the constant b is calculated according to Terrill's formula. And although b has not yet been obtained directly for molybdenum, there is reason to believe that this formula will apply with good approximation; these questions will be discussed in detail below. The other data, with the exception of the author's, are for unresolved radiation, and are probably complicated by the presence of characteristic rays. On account of fluorescent excitation, these rays have a much greater mean depth of production than the continuous radiation (14); for comparison with this data the value zero was used for ν in formula (2).

TABLE 2

Z	ν	V	Observer	x (calc.)	x (obs.)	Ratio
		kv		μ	μ	
29(Cu)	20	40	Nicholas	1.5	1.0	1.5
	30	60	do	2.8	2.8	1.0
	40	80	do	4.2	6.0	.7
42(Mo)	20	25	Webster and Hennings	.30	1.2	.25
	20	30	do	.65	1.4	.46
	20	50	do	2.1	2.2	.94
	20	70	do	3.3	3.3	1.0
47(Ag)		17	W. P. Davey (15)	.44	.92	.47
78(Pt)		43	L. G. Davey (16)	.65	2.2	.3
82(Pb)		21	W. R. Ham (17)	.51	.64	.8

III. SPECTRAL ENERGY DISTRIBUTIONS

The method used in the present work for an estimate of the factor g above was to assume a spectral energy distribution for I'_c, apply the various corrections for absorption to obtain gI'_c, and by comparing the latter with Rump's experimentally measured gI'_c, obtain an estimate of I'_c.

The spectral energy distribution of I'_c (X-ray continuous spectrum intensity that would have been obtained at 90° with the cathode stream had there been no absorption of X rays in the anticathode, tube walls, etc., compare above) was assumed to follow the formula

$$(I'_c)_\nu = CZ[(\nu_0 - \nu) + aZ\nu_0(1 - e^{-16(\nu_0-\nu)/\nu})] \qquad (11)$$

where C is constant for any one voltage, but must show some variation with voltage to make this formula consistent with the formula for unresolved intensity I'_c (12, below). a is a factor the dependence of which on Z and V will be discussed below; the other quantities have been defined above. This formula is similar to the well-known formula of Kulenkampff (18) except for some modification of the second (and less important) term inside the square brackets. The introduction of the exponential factor is necessary to make the formula fit the observations in the region near the high frequency limit (13, 9); and the a factor is necessary for a satisfactory description of the experimental results at the higher voltages (9). Values of the factor a were taken from the curve drawn in Figure 1, which also contains experimental values obtained by various workers. The rather large divergence of these experimental results is probably due to varying experimental conditions and different correction factors (9). The range of voltage of most importance for present purposes is from 40 to 60 kv; it is fortunate that in this range the values of a would seem by short extrapolations not to be very discordant. Further, on account of the comparative unimportance of the term containing a (formula (11)), the final value of the efficiency does not depend to any great extent on the value of this term; for example, even if a were zero, the final values for efficiency would be modified only about 10 per cent. Actually it is believed that the uncertainty in the estimated efficiency due to the uncertainty in a is only about 3 per cent. In Figure 2 is shown the intensity distribution given by this formula for the continuous spectrum from tungsten at 100 kv. It should be pointed out that while the formula postulates a continuation of the linear portion of the curve to zero frequency, a measurement of the energy at very low frequencies is experimentally impossible on account of absorption.

However, there seems to be no reason at present, either experimental or theoretical, to doubt this extrapolation.

Knowing the spectral intensity distributions for radiation generated inside the anticathode, the distributions obtained outside the anticathode are readily obtained by use of the above formula for effective depth of production, together with known absorption coefficients. The formulas below, which are equivalent to that given by Richtmyer were used for the latter, for wave lengths shorter than the L critical absorption limits:

$$\mu = \frac{\rho}{A}(0.0136\ Z^4\lambda^3 + 0.32\ Z) \quad \ldots \quad \lambda < \lambda_K$$

$$\mu = \frac{\rho}{A}(0.0020\ Z^4\lambda^3 + 0.32\ Z) \quad \ldots \quad \lambda_K < \lambda < \lambda_{L_I}$$

where μ is the absorption coefficient defined in the usual manner, ρ is the density, Z the atomic number, and A the atomic weight of

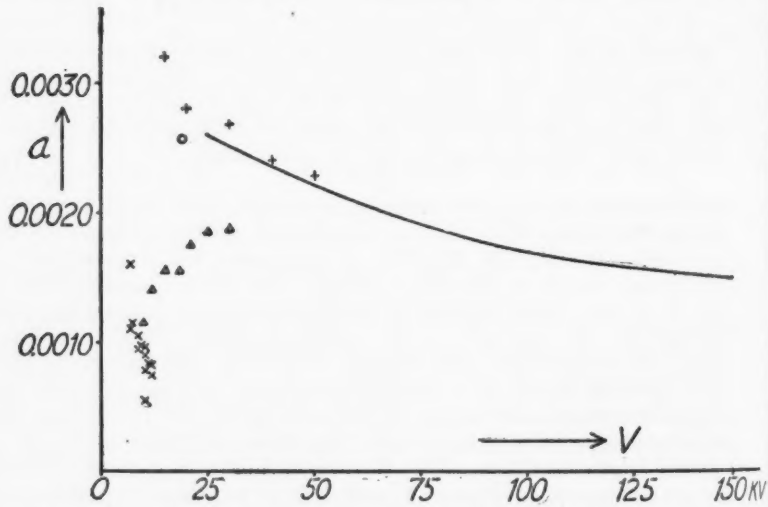

FIGURE 1.—*Values for the quantity a used in the formula for spectral intensity distribution*

× Observations of Kulenkampff (18) for a range of atomic number (Z) from 13 to 78.
△ Webster and Hennings (13) on molybdenum ($Z=42$)
○ Webster (19) on platinum ($Z=78$).
+ Nicholas (9) on copper ($Z=29$).

the absorbing material. The upper formula applies to wave lengths (λ) shorter than the K limit (λ_K), and the lower to the region between the K and the L. For wave lengths longer than λ_{Z_I}, which are really of no importance in the present esimate, the λ^3 formula was used in conjunction with some data by Allen taken from Compton's "X rays and Electrons." Also the spectral intensity distribution for any subsequent filtration is now readily calculated. The distribution (curve *C*) of Figure 2 is the spectrum obtained by Rump in his calorimeter according to present calculations; the filtration in tube walls, air path, calorimeter walls, etc., was closely equivalent to 1.23 mm aluminum according to data given by Rump in his paper. The ratio

(area under curve C)/(area under curve A) of Figure 2 is the factor g above in case the measured radiation consists entirely of continuous spectrum rays. In the same manner, spectra can be drawn for different tube voltages, the corrections for absorption carried through in the same way, and the value of g obtained as a function of the voltage applied to the tube; the continuous curve of Figure 3 represents this dependence of g on voltage. It should be noted that g is simply a ratio of intensities, and thus is independent of the actual amount of energy produced or measured.

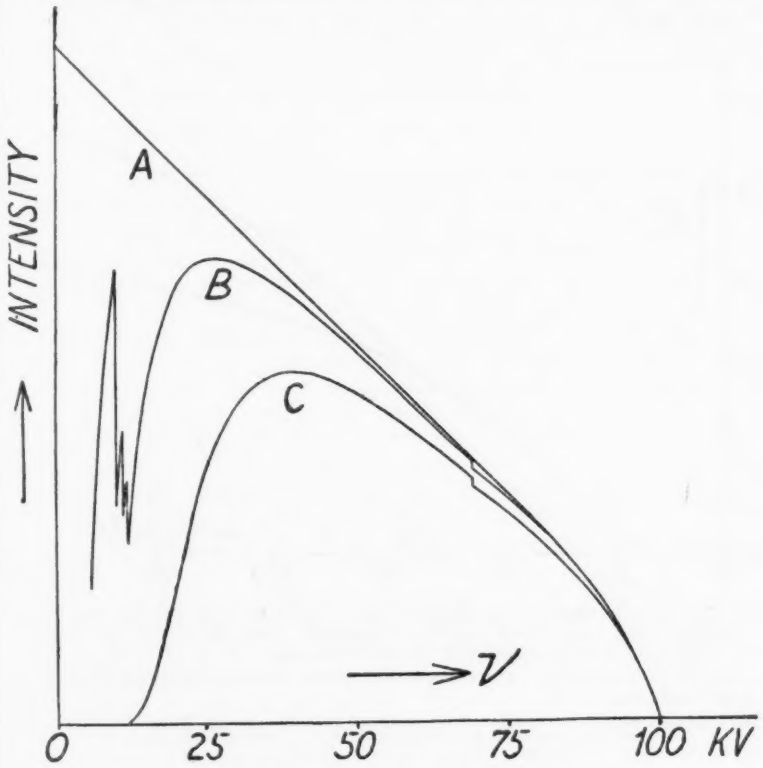

FIGURE 2.—*Intensity distribution*

A, spectral intensity distribution in the continuous radiation from tungsten at 100 kv, as produced within the anticathode, according to formula (11). Plotted on a frequency scale, with frequencies expressed in equivalent excitation potentials.
B, intensities outside the anticathode.
C, same after passing through tube walls, etc., equivalent to 1.23 mm aluminum.
The factor g of Figure 3 (full line) is the ratio (area under C)/(area under A).

IV. VARIATION OF X-RAY INTENSITY WITH VOLTAGE

Experimentally, Rump measured an amount of energy corresponding to gI' and its variation with voltage. Knowing g we can thus calculate I' from Rump's results and determine its variation with voltage (V). It is usually accepted from the work at relatively high voltages that I'_c is closely proportional to V^2 in the high voltage region, but in none of this work have corrections for absorption been so carefully considered as at present. A neglect of absorption will

lead, in general, to too large an apparent value of the exponent, so it will not be surprising to find in the present work a somewhat less rapid increase of I'_c with voltage. At low voltages, Kulenkampff has found that I'_c increases somewhat less rapidly than V^2, as an integration of his formula will show. At high voltages his formula would lead to a variation of I'_c approaching proportionality with V^2, but it has been shown (9) that this formula can not be extended to higher voltages without modification. In the present work, the calculations of I'_c based on Rump's data and the present values of g lead to a variation of I'_c which is much more nearly proportional to $V^{3/2}$ than to V^2

FIGURE 3.—*Comparison of Rump's data (crosses) with calculations which assume total continuous spectrum intensity produced inside the tungsten anticathode to be proportional not to V^2 (as has usually been assumed) but to $V^{3/2}$, and allowing for a considerable proportion of energy in the K characteristic rays*

The unbroken curve corresponds to the continuous radiation (see fig. 2) and the broken curve represents a correction for characteristic rays. Compare with Figure 4.

$$I'_c = KV^{3/2} \ldots (40\ kv < V < 150\ kv) \tag{12}$$

It should be stressed that it can not be concluded from the present work that this formula has general validity; indeed the indications are that the formula predicts too much energy for the region of 10 kv. However, there can be little doubt that, for a tungsten anticathode and for voltages between 40 and 150 kv (and these are conditions of comparatively great practical importance), the formula closely approximates actual conditions. The numerical value adopted for K was 0.043 where V is in kilovolts and I'_c is in ergs/sec. cm² at a distance of 1 m from the focal spot, for 1 milliampere tube current.

From formula (12) for I'_c and from Rump's experimentally measured values for gI' may be obtained values for the quantity g; these values are plotted in Figure 3. The observed points agree well with the predicted curve below 69 kv, at which voltage the characteristic

rays are produced. Above 69 kv the difference between the observed and calculated values may be regarded as a measure of the energy contained in the K characteristic rays of tungsten. For example, it is indicated in Figure 3 that at 140 kv nearly one-third of the energy obtained in the calorimeter is due to K characteristic radiation. This is considered not to be unreasonable in view of some unpublished work by the author (20) which indicated a considerable prominence of the K lines from tungsten at high voltages. A rough check on the amount of the characteristic radiation may be obtained by a use of the known fact that the characteristic ray energy increases approximately with $(V-V_0)^{3/2}$ for voltages V which are not large in comparison with the excitation voltage V_0. The dotted line of Figure 3 was calculated on the assumption that the intensity I'_K of the K characteristic rays obtained in the calorimeter followed the formula

$$I'_K = H(V-V_0)^{1.3} \ldots (V_0 < V < 150\ kv) \tag{13}$$

where H is 0.085 if V, V_0, and I'_K are in the same units as were used in formula (12). The agreement is considered very satisfactory.[3] It should be emphasized that the present methods are by no means adequate to distinguish between the exponents 1.3 and 1.5; the former, however, seemed to be somewhat more satisfactory in Figure 3. It may also be noted that, while $(\Delta g)\ KV^{3/2}$ gives the characteristic ray intensity in the calorimeter (where Δg is the difference between the unbroken and the broken curves of fig. 3), no attempt is made here to obtain an expression for characteristic ray energy generated inside the anticathode, which would involve an estimation of the effective depth of production of the characteristic radiation (see Section II, 3, above).

In Figure 4 are plotted the experimental values of g which would result if I'_c were taken to be proportional to V^2, as has usually been assumed, instead of $V^{3/2}$. The values for efficiency previously published by the author (21, 22) was based on the V^2 law, and it was believed at the time that the errors necessary to account for the inconsistencies, which are, after all, not considerable for this type of work, were due, perhaps, partly to experimental error and partly to insufficiently accurate formulas for spectral intensity distribution and absorption in the anticathode. However, it is believed that in the present paper these estimates are made as satisfactorily as present experimental data will permit. It is readily seen in Figure 4 that below 69 kv the agreement with the calculated curve is not nearly so satisfactory as in Figure 3 where $V^{3/2}$ was assumed, and that also in Figure 4 there is obtained no indication of an adequate amount of characteristic ray intensity above the excitation potential $V_0 = 69$ kv.

More confidence in the assumed spectral energy distributions and the proportion of characteristic ray energy (and thus in the $V^{3/2}$ assumption) may be gained by calculating the decrease of intensity which should be observed for the addition of various thicknesses of copper filter, on which Rump obtained some measurements. The top curve of Figure 5 is identical with Figure 3; the other curves

[3] The disagreement with the observed value for 114 kv is probably due to a typographical error, of which several exist in Rump's paper. This is borne out by the curves plotted in Figure 5, which show good agreement with the calculations for this voltage when various filters are used.

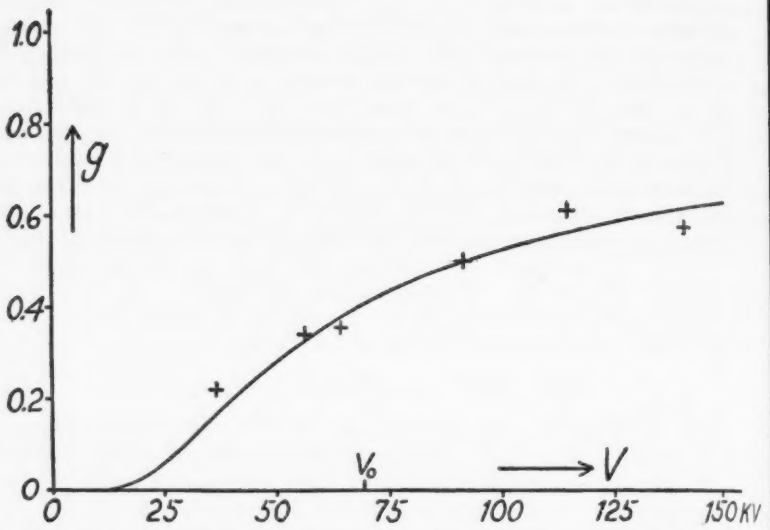

FIGURE 4.—*Assuming continuous spectrum intensity proportional to V*

Note that the agreement is not so good as in Figure 3 at low voltages, and that above the excitation potential (V_0) of the K lines there is not adequate allowance here for characteristic ray intensity.

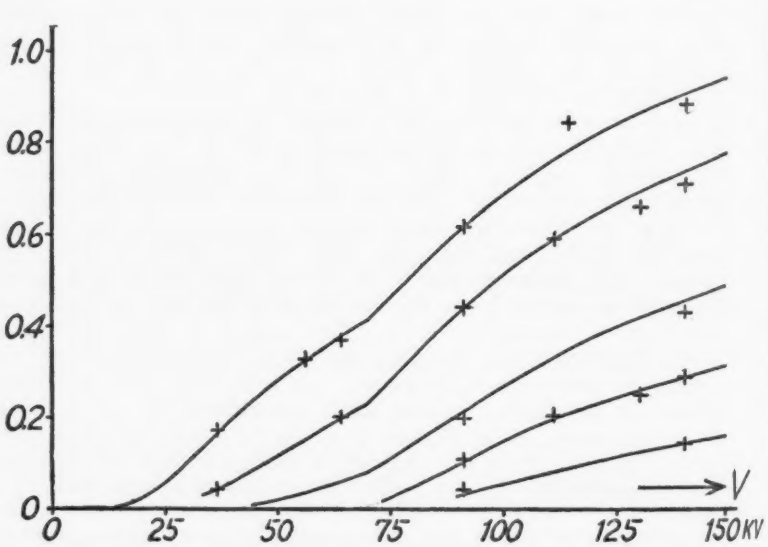

FIGURE 5.—*Use of various thicknesses of copper filter—a test of the assumed spectral intensity distributions and proportion of characteristic ray intensity*

are similar calculations, for filtrations of 0.1, 0.5, 1.0, and 2.0 mm copper. The irregular distribution of observed points (crosses) about the calculated curves indicates that the disagreements are probably mostly due to experimental errors. However, this is not a very sensitive test, considering the experimental uncertainties, and its value as a check on the assumptions must not be overestimated. An estimate of its value as a check may be obtained from Figure 6, where Rump's values for the intensity at 140 kv (effective) [4] are plotted. Curve *A* was calculated on the assumption that the radiation at 140 kv consisted entirely of continuous spectrum, curve *C*

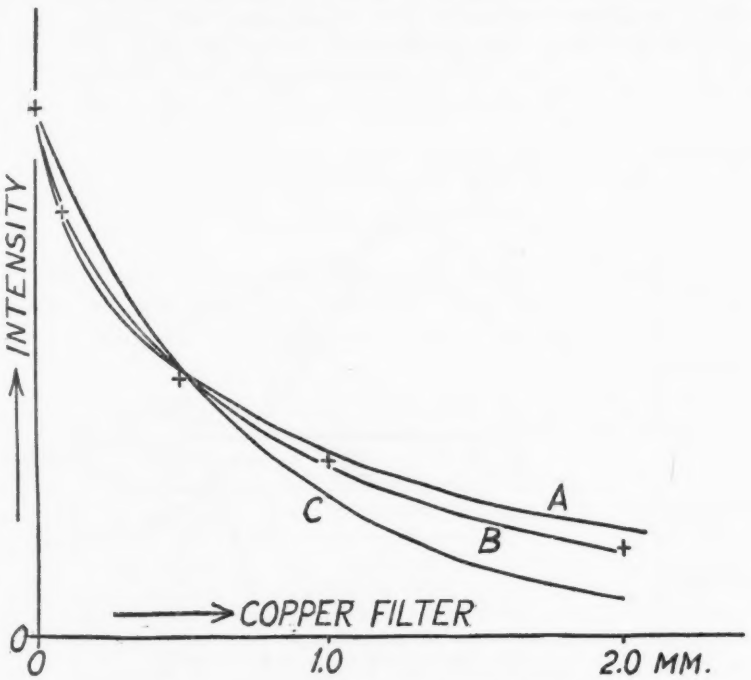

FIGURE 6.—*Absorption curve for the radiation at 140 kv*

A, calculated on assumption radiation all continuous rays.
B, assuming radiation after absorption in anticathode and the equivalent of 1.23 mm aluminum is one-third characteristic rays and two-thirds continuous.
C, assuming radiation entirely characteristic rays.

assumed the radiation to be all *K* characteristic rays, and curve *B* assumed a proportion of two-thirds continuous rays and one-third characteristic, for the radiation reaching the calorimeter with no copper filter.

V. INTENSITIES IN DIFFERENT DIRECTIONS

In previous estimates of efficiency it has usually been assumed that the X-ray energy produced inside the anticathode is radiated equally in all directions. It is well known that this is not actually

[4] Due to the limited capacity of the condensers in the filter system used by Rump, the voltage varied between limits which were about 7 per cent from the mean at 140 kv.

the case, but on account of a lack of experimental work for the various directions, and especially the impossibility, on account of absorption in the target, of ever measuring the energy which is emitted in one hemisphere (that is, into the target), no adequate basis has been available for a better estimate. However, on account of the recent work on thin targets, a satisfactory method of making these corrections seems now to be available.

As previously pointed out (5), a thick target spectrum may be regarded roughly as being composed of two parts (*A*) a part similar to a thin target spectrum and showing the same kind of variation with direction relative to the cathode stream, and (*B*) a part due to completely diffused cathode rays, which, therefore, shows no variation with direction. On this basis it was shown that the variation with direction of the thick target spectrum may be described by permitting the constant a of formula (11) to vary with direction

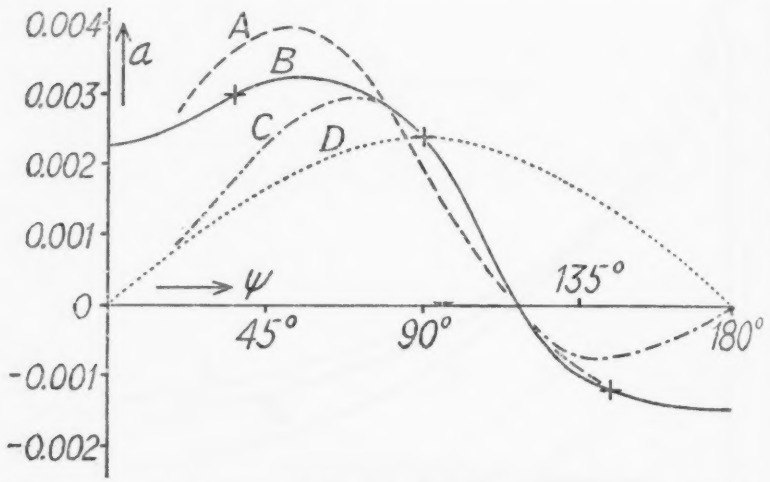

FIGURE 7.—*Calculations used for correcting for variation of X-ray intensity with direction relative to the cathode stream*

The variation of a is not expected to be capable of being predicted solely from the thin target work, however, on account of the fact that part *A* is considerably contributed to by cathode rays that are partly diffused. It is unfortunate, therefore, that data on tungsten is not available to guide the assumption about the quantitative variation of a. However, due to the minor importance of the correction, the variation may be guided with sufficient accuracy for present purposes by the author's work on copper (9), and a more satisfactory correction can be made directly data on tungsten become available. At 40 kv, the highest voltage at which the above-mentioned work is reliable, the values thus selected for a for $\psi=36°$, 90°, and 144° (ψ being the angle between cathode beam and measured X rays) were 0.0030, 0.0024, and −0.0012, respectively; these values are plotted in Figure 7 (crosses). Curve *B* of Figure 7 was selected for the continuous variation of a with ψ; this selection was partly guided by curve *A*, which is the variation of intensity with ψ (but plotted here with a different zero of intensity) observed by Kulenkampff

(23) at 38 kv for a thin target of aluminum (it is indicated in some work by the author (5) that a similar variation holds for heavier elements). Curve B, being contributed to by partially diffused cathode rays, is chosen with broader maxima and minima than curve A. Curve D is proportional to sin ψ, and curve C is proportional to the product of sin ψ and curve B. These curves will be of use below.

VI. EFFICIENCY OF X-RAY PRODUCTION

If X-ray intensity were independent of the direction of emission, and if there were no complications due to reflection of cathode rays from the focal spot, the efficiency of production of continuous spectrum X rays would be calculable directly from formula (12) as follows: The total amount of continuous spectrum X-ray energy given out over the whole sphere would be

$$4\pi \times 100^2 \times 0.043\ V^{3/2}\ i = 5{,}400\ V^{3/2}\ i \text{ ergs/sec.}$$

where V is in kilovolts and i is tube current in milliamperes. Using the same units, the energy supplied to the tube is

$$10^7\ V\ i \text{ ergs/sec.}$$

The ratio of these two quantities may be termed the "apparent efficiency" for the continuous radiation; that is,

$$\text{Apparent efficiency} = 540 \times 10^{-6}\ V^{\frac{1}{2}} \ \ldots\ (Z=74);\ (40\ kv < V < 150\ kv) \tag{14}$$

this is the quantity which is of importance in practical work, since it is a measure of the intensity obtainable for the experimental arrangement which is usually used.

The quantity of importance theoretically, in that it is a measure of the amount of continuous spectrum energy (J_c) radiated in all directions in the hypothetical tube described in Section I, may be called the "true efficiency" (E_c); this has been defined above as J_c/Vi. It is E_c which should be compared with calculations such as those of Kramers (3) and Neunhoffer (24). To obtain E_c two further corrections are necessary: (1) Integration of intensities for all directions, and (2) allowance for reflection of cathode rays at the target face. On account of the small magnitude of each of the corrections, the order of making them is inconsequential.

The integration for the various directions may be carried out according to the formula

$$\int_0^{\pi} I'_c(\psi) \sin \psi\ d\psi \tag{15}$$

where the factor sin ψ is introduced on account of the fact that I'_c is an intensity per unit solid angle instead of a quantity of energy per unit $\Delta\psi$. Now $I'_c\ (\psi)$ may be regarded as being composed of two parts, I'_{c1} and I'_{c2}, which correspond to the two terms on the right-hand side of formula (11); that is

$$I'_{c1} = CZ(\nu_0 - \nu)$$

$$I'_{c2} = CZ^2\nu_0(1 - e^{-16\,(\nu_0-\nu)/\nu})\,a(\psi)$$

(Primed quantities are used in order to be consistent with the definitions in Section II, in which energies associated with the focal spot were denoted by primed quantities.) According to Section V I'_{c1} does not vary with ψ, but I'_{c2} does on account of the variation of a with ψ. Accordingly, the integral (15) becomes

$$I'_{c1}\int_0^{\pi}\sin\psi d\psi+\int_0^{\pi}I'_{c2}\sin\psi d\psi=2I'_{c1}+\int_0^{\pi}I'_{c2}\sin\psi d\psi \qquad (16)$$

Now the calculation of the apparent efficiency (formula (14)) was really equivalent to integrating equation (16) with a constant value of I'_{c2} equal to the value $(I'_{c2})_{90°}$ observed for this quantity at $\psi=90°$; the integral would then turn out to be

$$2\,I'_{c1}+2\,(I'_{c2})_{90°} \qquad (17)$$

and the factor by which the apparent efficiency must be corrected to allow for the variation of intensity with ψ is the ratio (16) to (17). In evaluating this ratio, it may be noted that $I'_{c1}/(I'_{c2})_{90°}$ may be obtained from an integration of formula (11), and that $2\,(I'_{c2})_{90°}$ $\int_0^{\pi}I'_{c2}\sin\psi d\psi$ is the ratio of areas under curves D and C of Figure

7. It turns out that the correction factor for 40 kv is 0.91.

Finally we consider the correction for reflection of cathode rays from the target face. Unfortunately, this effect has been only incompletely investigated, and apparently the best that can be done as a correction for the effect is to suppose, as Rump did, that 20 per cent of the total X-ray energy becomes "off-focus" radiation. Coolidge (7) has estimated the amount of radiation coming from the back of the target to be about one-ninth of the radiation from the focal spot, and allowing for both front and back of target and stem, this seems a reasonable correction. Thus we find the efficiency E_c of production of continuous spectrum X rays in tungsten at 40 kv to be

$$E_c=0.91\times1.25\times540\times10^{-6}\times40^{\frac{1}{2}}=0.0039 \quad . \quad . \quad (\mathrm{V}=40\,kv);\ (Z=74).$$

On account of a lack of knowledge of the variation of intensity with ψ for voltages higher than 40 kv, not much can be said at present about the value of E_c for other voltages. However, on account of the increasing concentration of intensity in the forward angles (values of ψ less than 90°) for higher voltages, the total continuous spectrum energy J_c may be expected to increase somewhat faster than $V^{3/2}$. Supposing it to increase proportional to V^2, making the efficiency proportional to V, and assuming E_c proportional to Z (as is usually accepted), we should have for the efficiency, using the value just found at 40 kv to determine the constant,

$$E_c=13\times10^{-7}\,ZV \qquad (18)$$

where V is in kilovolts. Rump's value (1) for the constant in this formula was about 15×10^{-7}; Kulenkampff's values (2) were $(9.5\pm3)\times10^{-7}$, based on his own work with resolved radiation at 7 to 12 kv, and $(8\pm2)\times10^{-7}$, based on other work with unresolved radiation; Kramers (3) obtained 9.2×10^{-7} from a theoretical calculation of the radiation from electrons in hyperbolic orbits.

VII. EFFICIENCY AND THE THOMSON-WHIDDINGTON CONSTANT

It appears not to be generally appreciated that the X–ray energy generated by cathode rays in penetrating matter is dependent on the value of the constant b in the Thomson-Whiddington-Bohr law (equation (3)). This fact follows at once from an analysis by Webster (25), and may also be shown as follows: According to current theory, a cathode ray can generate an X ray only when it has a close encounter with an atomic nucleus; that is, when the path of the cathode ray as it approaches an atom is such that an extension of this path lies within a certain small area τ surrounding the nucleus. The probability that a cathode ray will have one of these close encounters in a path length dx is

$$\tau N dx$$

where N is the number of atoms per unit volume. Or, utilizing equation (3) above, the probability of a close encounter while the cathode ray is losing an amount of speed corresponding to dV (kilovolts) is

$$\frac{2\tau N V dV}{b}$$

Thus, if the constant b could be made smaller for an X-ray anticathode (strictly b/N must be made smaller) the cathode rays would penetrate a great number of atoms before being slowed by a given amount, the total number of close encounters with nuclei would be increased, and the number of X-ray quanta generated would be greater. Such a change of b/N (but in any case probably only a very small change) may be readily imagined to be associated with a change of crystal structure for example.

The above conception has some interesting applications. It is generally accepted that the intensity of continuous spectrum X rays obtained from various anticathodes increases regularly with the atomic number (Z) of the material of the anticathode, being approximately proportional to Z. Ulrey's experimental results (26), however, indicated that the intensity did not increase regularly, but showed small periodic fluctuations correlating with the periodic variation of chemical properties; these fluctuations have often been thought to be due to some kind of experimental error. If the production of X-ray energy were simply dependent on the collisions between cathode rays and nuclei, there would, indeed, be no basis for assuming any periodicity here, since the electrical properties of the region immediately surrounding the nucleus of atoms should increase in a regular manner with atomic number. However, since the X-ray energy generated is indirectly influenced by b/N, any atomic property which influences the magnitude of b/N may also influence the X-ray energy. Now b/N is a measure of the energy lost by the cathode rays in passing through the material; this energy is used chiefly to ionize and excite the outer energy levels of the atoms, and depends to a considerable extent not only on the number of loosely bound electrons in the atoms, but also on their energy of binding. As is well known, this energy of binding does not increase regularly with atomic number, but shows a periodic variation coinciding with the periodic variation of chemical

properties; for example, the valence electrons of the alkalies and alkali earths are much less firmly bound than the outer electrons of the halogens. Thus a small periodic variation with atomic number, such as was observed by Ulrey, may be expected for the X-ray intensity obtained from various anticathodes. It is interesting in this connection that a comparison (2) of Ulrey's with Kaye's (27) results indicates that the two pieces of work, which were done under entirely different conditions are in agreement as to the position and magnitude of these variations.

It may be remarked incidentally that, as is obvious from the above discussion, a measurement of the X-ray intensity from a material may be used for an indirect determination of the Thomson-Whiddington constant b. Now the value of b has been determined by direct methods for only a very few elements (on account of the requirement that the element be capable of being rolled or beaten into very thin foils) and these have of necessity been in only certain chemical groups. However, the X-ray emission has been measured from a comparatively large number of elements, covering other chemical groups. The fact that the X-ray emission from all these elements has shown only the minor irregularities noted above is adequate evidence that b/N will show, with varying atomic number, only corresponding minor fluctuations. This was the basis, in Section II, 3, above for not questioning the application to molybdenum and tungsten of Terrill's formula for b, although b has not yet been observed directly for these elements.

The relation between X-ray intensities and the quantity b also has application to the anomaly mentioned above (Sec. II, 3) with regard to the observations of Webster and Hennings on the effective depth of production ($\bar{x}$) of continuous spectrum X rays. Their method depends on the measurement of the discontinuity in the continuous spectrum from an anticathode, the discontinuity being observed at a critical absorption frequency (ν_a) of the target material. As they pointed out, in order to deduce $\bar{x}$, it must be assumed that the continuous spectrum as emitted has no discontinuity at ν_a; that is, that the entire observed discontinuity must be due to the absorption of the rays in their path through the target material. Now there are several conceivable ways of producing just such a discontinuity prior to the absorption along the path: One possibility is a process (somewhat similar to Auger's compound photoelectric effect (28) with fluorescent rays) in which the continuous spectrum quanta may have an especially high probability of being absorbed in the atoms within which they are produced. Another possibility is that b may undergo a sudden change for cathode ray speeds which will just excite frequency ν_a; Schonland (29) has speculated on the possibility of such a change and has searched for it experimentally, but under such conditions as would probably not have allowed the detection of so small a change as is necessary to explain the present anomaly. The reason for renewing the discussion of the point at the present time is, of course, to justify the use of the formula for $\bar{x}$ proposed above. However, it seems also that such a change in b would have some very fundamental

[8] The above considerations are entirely apart from the fact that Terrill's formula must itself introduce into b some small irregularities which are due to the fact that atomic weight is not a perfectly regular function of atomic number. From a theoretical standpoint, a more satisfactory expression would be $b=f(\rho Z/A)$ where A is the atomic weight of the material, and f is a function to be determined; this causes b to be dependent on atomic number instead of atomic weight. It turns out, however, that b is closely proportional to ρ and rather than use a form for f which is less simple than the liner form, the formula $b=40\times10^{4}\rho$ is generally given.

theoretical consequences, and experiments designed to test the point are now in progress in the author's laboratory.

VIII. DISCUSSION

Probably the greatest degree of uncertainty in the above calculations is the 20 per cent correction for stray cathode rays; this estimate was made by a photographic method, and not much is known about its variation with tube voltage. However, it should be pointed out that this concerns only the calculation of the "true," or theoretical efficiency E_c; the equations of practical importance (11, 12, 13, and 2), in that they describe the intensity I' actually obtainable from the focal spot, are independent of the 20 per cent correction; and of course, when better measurements on the stray energy are available, they can be applied directly to the present work in order to obtain a better estimate of E_c.

Another uncertainty which affects only E_c and not I' is in the correction for the intensity obtained in various directions. A serious estimate of the adequacy of the present correction for this effect can not be made until work is available for a target of atomic number in the vicinity of tungsten, but it is scarcely conceivable that the error in the present work due to this cause can be over a few per cent. It may be pointed out that whatever uncertainty now exists with regard to this correction is due simply to a lack of experimental data, and is not due to the fact that intensities radiated into the massive target can never be measured.

An uncertainty which applies to both E_c and I' is due to the fact that the voltages used by Rump were not so steady as could be desired, but varied about 10 kv from the mean. It is difficult to estimate the possible errors introduced by this variation, on account of the fact that the voltage wave form of a circuit of the type used by Rump is not a simple one. Supposing a sinusoidal variation, however, it is readily shown [6] that at 40 kv, for example, the correction would be only about 5 per cent; at higher voltages the correction is even less serious. If the observed points below V_o on the curve of Figure 3 were corrected on this basis, the observations would more closely parallel the calculated curve than they do at present. This small correction has, as a matter of fact, already been applied to the numerical results above involving low voltages (equations (12), (14), (18)), and the value of E_c for 40 kv.

---

[6] At 40 kv g (fig. 3) is roughly proportional to $V^2\beta$, making gI' proportional to V^3. Also, at this voltage, the variation from the mean voltage was about 7 kv. Therefore the variation of voltage may be described by

$$V = 40 + 7 \sin y$$

where y is a variable increasing linearly with time. The intensity actually obtained inside the calorimeter is

$$P\int_0^{2\pi} (40+7 \sin y)^3 \, dy \qquad (19)$$

where P is a constant, and the intensity which would have been obtained if the voltage had been steady at 40 kv is

$$P\int_0^{2\pi} (40)^3 \, dy \qquad (20)$$

Thus the correction factor by which an observed point (fig. 3) at 40 kv should be multiplied is the ratio of (20) to (19), which turns out to be 0.954.

The other uncertainties, associated with correction for absorption in the anticathode, and spectral intensity distribution, are probably comparatively minor; the formulas set up for these corrections are believed to be quite satisfactory from the standpoint of present experimental data.[7] Moreover these formulas are of sufficient generality to be of use in future work on X-ray efficiency, at least until better experimental data is available for making these difficult corrections.

IX. SUMMARY

1. The physical conditions inside gas filled tubes are discussed, and it is concluded that, for definite interpretation of results, hot cathode tubes should be used for experimental estimates of X-ray efficiency.

2. A general formula (formula (2)) for absorption of continuous spectrum radiation in the anticathode is set up and compared with available experimental data.

3. A general formula (formula (11)) is given which describes the spectral intensity distribution in the general radiation emitted at an angle (ψ) of 90° from the direction of the cathode stream.

4. Calculations based on some experimental work by Rump lead to the conclusion that, between 40 and 150 kv. and for $\psi = 90°$, the unresolved intensity in the general radiation generated inside a tungsten anticathode is proportional to the 3/2 power of the voltage (V) instead of to V^2 as has usually been assumed (formula (12)).

5. A basis for estimating absolute intensities and spectral intensity distributions for any value of ψ is provided (fig. 7).

6. The intensity of the K characteristic radiation obtainable from tungsten at voltages up to 150 kv is described quantitatively (formula (13)).

7. Formulas (2), (11), (12), and (13), together with Figure 7, provide a means for describing quantitatively the absolute intensity and spectral intensity distribution (including in the case of tungsten the proportion of K characteristic rays) of the continuous radiation for any direction (ψ) obtainable from an X-ray tube under a wide range of practical conditions.

8. The efficiency E_c of production of continuous spectrum X rays inside a tungsten anticathode is estimated for 40 kv. It is pointed out that there is not yet adequate basis for extending the estimate of E_c over a wide range of voltage.

9. The bearing of the Thomson-Whiddington constant on the generation of X-ray energy is pointed out, and its application made to the explanation of some results by Ulrey which indicated that X-ray efficiency showed a periodic variation with atomic number.

The following tabulation may be of interest for purposes of illustration and numerical comparisons:

---

[7] There remains an apparent minor difficulty in this connection: Formula (11) (spectral intensity distribution) was derived (13, 9) from data of the isochromat type assuming the V^2 law for unresolved intensity. Consequently, a discrepancy appears when a $V^{3/2}$ law is found above (formula (12)). However, it may be recalled that in the derivation of formula (11) an approximation was made (neglect of a term corresponding to the exponential term of formula (11)) which was in the direction of assuming $V^{3/2}$ instead of V^2. This, together with the consideration that any remaining differences would probably not be detectable experimentally, removes the apparent discrepancy.

Tungsten anticathode; Constant potential; 1 milliampere tube current

	40 kv	69 kv	100 kv	150 kv
Total continuous spectrum energy produced inside anticathode, allowing 20 per cent for cathode-ray reflection losses. (ergs/sec.)	1.23 $\times 10^6$	3.66 $\times 10^6$	7.70 $\times 10^6$	17.3 $\times 10^6$
Continuous spectrum intensity which would have been obtained outside of tube in the usual 90° position if all absorptions (including that in anticathode) had been negligible. (ergs/sec. cm² at 1 m from focal spot)	10.9	24.6	43.0	79.1
Continuous spectrum intensity actually obtained outside tube for which the walls and other filtration (except anticathode) are equivalent to 1.23 mm aluminum. (ergs/sec. cm² at 1 m from focal spot)	2.18	10.0	22.5	50.0
Intensity in K characteristic radiation actually obtained outside above tube (same units)	0	0	7.3	24.2

X. REFERENCES

1. W. Rump, Zeits. für Physik, **43,** p. 254; 1927.
2. H. Kulenkampff, Handbuch der Physik, **23.**
3. H. A. Kramers, Phil. Mag., **46,** p. 869; 1923.
4. D. L. Webster, P. N. A. S., **14,** p. 339; 1928.
5. W. W. Nicholas, B. S. Jour. Research, **2,** p. 837; 1929.
6. W. Bothe, Handbuch der Physik, **24,** p. 1.
7. W. D. Coolidge, Am. J. Roentgen, **1,** p. 115; 1914.
8. Ledoux-Lebard and Dauvillier, Physique des Rayons X, p. 45; 1921.
9. W. W. Nicholas, Phys. Rev., **29,** p. 619; 1927.
10. E. Lorenz, P. N. A. S., **14,** p. 582; 1928.
11. D. L. Webster and A. E. Hennings, Phys. Rev., **21,** p. 301; 1923.
12. B. F. J. Schonland, Roy. Soc. Proc., **104,** p. 235; 1923; **108,** p. 187; 1925.
13. D. L. Webster and A. E. Hennings, Phys. Rev., **21,** p. 312; 1923.
14. D. L. Webster, P. N. A. S., **14,** p. 330; 1928.
15. W. P. Davey, J. Frank. Inst., **171,** p. 277; 1911.
16. L. G. Davey, Phys. Rev., **4,** p. 217; 1914.
17. W. R. Ham, Phys. Rev., **30,** p. 96; 1910.
18. H. Kulenkampff, Ann. der Physik, **69,** p. 548; 1922.
19. D. L. Webster, P. N. A. S., **5,** p. 163; 1919.
20. W. W. Nicholas, "Spectrum of X-Rays used in Deep Therapy," M. A. thesis, Stanford University.
21. International Critical Tables, **6.**
22. W. W. Nicholas, Phys. Rev., **35,** p. 128; 1930.
23. Kulenkampff, Ann. der Physik, **87,** p. 597; 1928.
24. M. Neunhoffer, Ann. der Physik, **81,** p. 493; 1926.
25. D. L. Webster, Phys. Rev., **9,** p. 220; 1917.
26. C. T. Ulrey, Phys. Rev., **11,** p. 401; 1918.
27. G. W. C. Kaye, Phil. Trans. A., **209,** p. 237; 1908.
28. P. Auger, J. de Phys. et Radium, **6,** p. 205; 1925.
29. B. F. J. Schonland, Proc. Roy. Soc. A., **108,** p. 187; 1925.

WASHINGTON, February 21, 1930.

ON THE DETERMINATION OF THE EMPIRICAL FORMULA OF A HYDROCARBON [1]

By Edward W. Washburn

ABSTRACT

This paper discusses the precision aspects of the problem of determining the molecular weight and hydrogen content of a hydrocarbon and of combining the results so as to obtain the empirical formula. In certain cases the formula can be deduced from the molecular weight alone, in others from the combustion analysis alone. Where both are required, the accuracy necessary in one or both is, in many cases, adjustable within rather wide limits and is determinable in any case. A definite laboratory procedure is outlined for obtaining the desired result with the minimum of effort and inconvenience. By following this procedure it should be possible to determine the empirical formula of any pure hydrocarbon containing not more than 100 carbon atoms. A determination of the bromine- (or other-) addition number may, in some instances be substituted for the molecular weight determination or for the combustion analysis, or may be utilized to decrease the accuracy which would otherwise be required in either or both of these determinations. The requirements necessary for the determination of a reliable "average formula" of a mixture of hydrocarbons are formulated. The influence of impurities and of polymerization is discussed.

CONTENTS

	Page
I. Introduction	868
1. The problem	868
2. Laboratory procedure	868
II. Symbols and abbreviations	869
III. The molecular weight	869
1. Mathematical relations	869
2. Deductions from the molecular weight	870
(*a*) Evalution of M	870
(*b*) Evaluation of n and x	873
(*c*) Illustrative examples	874
IV. The combustion analysis	875
1. General considerations	875
2. Mathematical relations	876
3. Classification into type groups	877
4. Group I. Saturated hydrocarbons. C_nH_{2n+2}	877
5. Group II. Hydrocarbons of the type C_nH_{2n}	879
6. Group III. Hydrocarbons of the type C_nH_{2n-x}	879
7. Evaluation of n and x from combustion analysis alone	879
(*a*) Evaluation of x	879
(*b*) Evaluation of n	880
(*c*) Evaluation of n and x	880
8. Procedure for Group III	880

[1] This discussion has been prepared in order to establish a procedure for use with the hydrocarbons which are in course of fractionation from petroleum under Project No. 6 of the American Petroleum Institute entitled "The Separation, Identification, and Determination of the Chemical Constituents of Commercial Petroleum Fractions." Financial assistance in this project has been received from a research fund of the American Petroleum Institute donated by John D. Rockefeller. This fund is being administered by the Institute with the cooperation of the Central Petroleum Committee of the National Research Council.

Page
V. Possible substitutes for the combustion analysis or the molecular weight determination 884
1. General considerations 884
2. Utilization of the bromine-addition number 885
3. Conclusions 887
VI. Résumé and general procedure 888
VII. Effects of impurities 888
VIII. The "average formula" of a mixture of hydrocarbons 888
IX. Effects of polymerization 889
X. Other chemical compounds 889
XI. Conclusions 889

I. INTRODUCTION

1. THE PROBLEM

The determination of the empirical formula of a hydrocarbon ordinarily involves (1) a combustion analysis in order to ascertain the hydrogen content; together with (2) a molecular weight determination. The purpose of this paper is to present a critical discussion of the precision aspects of the problems involved in measuring these two quantities and in combining them so as to obtain the empirical formula of the hydrocarbon.

The precision aspects present certain unusual and interesting features owing to the fact that the functions which connect the molecular weight and the hydrogen content with the values of n and x in the general formula, C_nH_{2n+x} are not continuous functions and are consequently not amenable to treatment by the methods ordinarily employed in precision-of-measurement discussions. This lack of continuity arises from the conditions (1) that n must be a whole number and (2) that x must be an even whole number. These two conditions, together with the character of the atomic weights of carbon and hydrogen, require further that the molecular weight, except when n is very large, must also be close to an even whole number. The whole-number relations thus involved call for the application of certain new principles of measurement and calculation. A general treatment of these principles has been given in a previous paper,[2] to which frequent reference will be made in the course of the application of these principles to the problems before us.

2. LABORATORY PROCEDURE

Given a sample of a pure hydrocarbon whose formula is desired, the first problem which presents itself is the laboratory procedure to be followed; that is, which of the two quantities, (*a*) molecular weight and (*b*) hydrogen content, should be determined first and how accurately should this determination be made?

The answer to this question in any specific instance is likely to depend upon attendant circumstances. For example, if the problem arose in a laboratory already equipped with, and operating, an accurate combustion apparatus, the most convenient procedure might be to make an accurate combustion analysis first. With this accurate value available it might be found that the molecular weight determination could be dispensed with or that a very rough determination would suffice.

[2] The principles of Measurement and of Calculation in their Application to the Determination of Diophantine Quantities. B. S. Jour. Research, **4** p. 221; 1930.

On the other hand, if the laboratory had no combustion apparatus in working condition but was instead equipped with suitable apparatus for exact molecular weight determinations, the investigator would perhaps prefer to determine the molecular weight accurately, since by so doing he might be able to dispense entirely with the combustion analysis or at worst would require only a rough value for the hydrogen content of his hydrocarbon.

A third case would be represented by a laboratory in which neither of the above outfits happened to be available so that, if required, both would have to be constructed (or assembled) and standardized. In the following treatment we shall assume a situation corresponding to this third case. The procedure appropriate to each of the other cases will, however, be brought out in the course of the discussion.

If now the investigator has at hand and in working order neither an accurate molecular weight apparatus nor an accurate combustion equipment (or indeed, if he has both of them), it will usually be advantageous to first make a rapid and approximate molecular weight determination.

As soon as the molecular weight is known approximately, one can determine (*a*) whether a combustion analysis is required and, if so, with what degree of accuracy and/or (*b*) whether a more accurate molecular weight determination may be needed or preferred, and if so, with what degree of accuracy.

II. SYMBOLS AND ABBREVIATIONS

$\left.\begin{matrix} n \\ x \end{matrix}\right\}$, defined by the formula C_nH_{2n+x}.

M the true molecular weight $= 14.0156n + 1.0078x$.

$r = \frac{n}{x}$.

$h = \frac{1.0078\ (2n+x)}{M} = \frac{\%\mathrm{H}}{100}$.

max., maximum.

min., minimum.

h_a, any experimental value found for h.

$(\delta h)_{max.}$, maximum absolute error for the technic employed.[3]

M_a, any experimental value found for M.

$p_{max.} = \frac{(\delta M)_{max.}}{M}$, maximum fractional error for the technic employed.[3]

$\Delta = 0.0078\ (2n+x)$.

(I), one of the positive integers.

III. THE MOLECULAR WEIGHT

1. MATHEMATICAL RELATIONS

The laws of valency and of atomic proportions give us the following relations:

1. n is a positive integer.

[3] See p. 223 of reference 2.

2. x is an even whole number lying between $+2$ and $\frac{14-M}{6}$, the latter value being the one which makes the formula of the hydrocarbon C_nH_2.

3. $$M=14.0156\,n+1.0078\,x \quad (1)$$

For convenience it is sometimes desirable to express M as a whole number plus the quantity Δ introduced by the fact that the atomic weight of hydrogen is not exactly unity: that is,

$$M=14n+x+\Delta \quad (2)$$

where

$$\Delta=0.0078\ \ (2n+x) \quad (3)$$

Eliminating n from (2) and (3) and solving for Δ

$$\Delta=0.0011\,M+0.0067x \quad (4)$$

The maximum value of x is 2, hence the maximum value of Δ is

$$\Delta_{max.}=0.0011M+0.0133 \quad (5)$$

or

$$\frac{100\Delta_{max.}}{M}=\left(0.11+\frac{1.33}{M}\right)\text{ per cent} \quad (6)$$

The minimum value of Δ is obviously 0.0156, which is that for all hydrocarbons of the formula C_nH_2.

Stated in another way, the molecular weight of a hydrocarbon is greater than some even whole number by an amount which is never more than 0.19 per cent of the number and, as will appear later, is too small to be significant in connection with the problem of determining the empirical formula. Δ may therefore be neglected in practically all cases.

2. DEDUCTIONS FROM THE MOLECULAR WEIGHT

(a) EVALUATION OF M

Add to the observed value (M_a) of M the maximum error in making the determination (or divide it by $1-p_{max.}$ where $p_{max.}$ is the maximum fractional error) and take the nearest even whole number which is smaller. This is an upper limit for $M-\Delta$. Subtract from the observed value of M the maximum error (or divide it by $1+p_{max.}$) and take the nearest even whole number which is larger. This is a lower limit for $M-\Delta$. The true value of $M-\Delta$ will be an even whole number lying between these limits. Column 1 of the "M-table" (Table 1) shows all of the possible values of $M-\Delta$ up to 310. It will be noted that while above 60, all even integers are possible values of $M-\Delta$, below 60 only certain ones are possibilities.

If $M-\Delta$ is to be definitely evaluated by the above procedure alone from any possible observed value of M, it is obvious that (with the single exception of methane) the molecular weight must be determined with a maximum error of less than one unit.[4]

[4] With an error considerably larger than this, evaluation may result for certain values of $M-\Delta$ less than 60, if the actual error is in a favorable direction. On this point see further pp. 231 and 232 of reference 1.

TABLE 1.—*The M-table*

[Formula of hydrocarbon, C_nH_{2n+x}. Molecular weight, $M=14n+x+\Delta$.[1]
[Percentage of hydrogen=100*h*. The table includes all hydrocarbons with molecular weight less than 312.]

$M-\Delta$[1]	*n*	*h*	$2n+x$	$M-\Delta$[1]	*n*	*h*	$2n+x$
16	1	0.2514	4	136	10	0.1184	16
					11	.0296	4
26	2	.0775	2	138	10	.1313	18
28	2	.1438	4		11	.0438	6
30	2	.2012	6	140	10	.1438	20
					11	.0576	8
38	3	.0530	2	142	10	.1559	22
40	3	.1007	4		11	.0709	10
42	3	.1438	6				
44	3	.1830	8	**144**	11	.0839	12
50	4	.0403	2	146	11	.0966	14
52	4	.0775	4		12	.0138	2
54	4	.1079	6	148	11	.1089	16
56	4	.1438	8		12	.0272	4
58	4	.1735	10	150	11	.1208	18
					12	.0403	6
62	5	.0325	2	152	11	.1325	20
64	5	.0630	4		12	.0530	8
66	5	.0915	6	154	11	.1438	22
68	5	.1184	8		12	.0654	10
70	5	.1438	10	156	11	.1548	24
72	5	.1677	12		12	.0775	12
74	6	.0272	2	158	12	.0892	14
76	6	.0530	4		13	.0128	2
78	6	.0775	6	160	12	.1007	16
80	6	.1007	8		13	.0252	4
82	6	.1228	10	162	12	.1079	18
84	6	.1438	12		13	.0373	6
				164	12	.1228	20
86	6	.1638	14		13	.0491	8
	7	.0234	2	166	12	.1334	22
					13	.0607	10
88	7	.0458	4	168	12	.1438	24
90	7	.0672	6		13	.0719	12
92	7	.0876	8				
94	7	.1071	10	170	12	.1539	26
96	7	.1258	12		13	.0829	14
					14	.0119	2
98	7	.1438	14	172	13	.0941	16
	8	.0206	2		14	.0234	4
100	7	.1610	16	174	13	.1041	18
	8	.0403	4		14	.0347	6
				176	13	.1144	20
102	8	.0593	6		14	.0458	8
104	8	.0775	8	178	13	.1244	22
106	8	.0950	10		14	.0566	10
108	8	.1079	12	180	13	.1343	24
					14	.0672	12
110	8	.1281	14				
	9	.0183	2	182	13	.1438	26
112	8	.1438	16		14	.0775	14
	9	.3598	4		15	.0111	2
114	8	.1589	18	184	13	.1532	28
	9	.0530	6		14	.0876	16
					15	.0219	4
116	9	.0695	8	186	14	.0974	18
118	9	.0853	10		15	.0325	6
120	9	.1007	12	188	14	.1071	20
					15	.0429	8
122	9	.1155	14	190	14	.1166	22
	10	.0165	2		15	.0530	10
124	9	.1299	16	192	14	.1258	24
	10	.0325	4		15	.0630	12
126	9	.1438	18				
	10	.0480	6	194	14	.1349	26
128	9	.1573	20		15	.0727	14
	10	.0630	8		16	.0104	2
					14	.1438	28
130	10	.0775	10	196	15	.0822	16
132	10	.0915	12		16	.0206	4
					14	.1525	30
134	10	.1052	14	198	15	.0915	18
	11	.0150	2		16	.0305	6

[1] $\Delta=0.0078\ (2n+x)$.

TABLE 1.—*The M-table*—Continued

$M-\Delta$	n	h	$2n+x$	$M-\Delta$	n	h	$2n+x$
200	15	0.1007	20	254	18	0.1506	38
	16	.0403	8		19	.1031	26
202	15	.1097	22		20	.0555	14
	16	.0499	10		21	.0079	2
204	15	.1184	24	256	19	.1101	28
	16	.0593	12		20	.0630	16
206	15	.1271	26		21	.0157	4
	16	.0685	14	258	19	.1171	30
	17	.0098	2		20	.0703	18
208	15	.1355	28		21	.0234	6
	16	.0775	16	260	19	.1239	32
	17	.0194	4		20	.0775	20
210	15	.1438	30		21	.0310	8
	16	.0863	18	262	19	.1306	34
	17	.0288	6		20	.0846	22
212	15	.1519	32		21	.0385	10
	16	.0950	20	264	19	.1373	36
	17	.0380	8		20	.0915	24
214	16	.1035	22		21	.0458	12
	17	.0471	10	266	19	.1438	38
216	16	.1079	24		20	.0984	26
	17	.0560	12		21	.0530	14
218	16	.1200	26		22	.0076	2
	17	.0647	14	268	19	.1502	40
	18	.0092	2		20	.1052	28
220	16	.1281	28		21	.0601	16
	17	.0733	16		22	.0150	4
	18	.0183	4	270	20	.1119	30
222	16	.1360	30		21	.0672	18
	17	.0816	18		22	.0224	6
	18	.0272	6	272	20	.1184	32
224	16	.1438	32		21	.0741	20
	17	.0899	20		22	.0296	8
	18	.3598	8	274	20	.1249	34
226	16	.1514	34		21	.0809	22
	17	.0980	22		22	.0368	10
	18	.0446	10	276	20	.1313	36
228	17	.1060	24		21	.0876	24
	18	.0530	12		22	.0438	12
230	17	.1138	26	278	20	.1376	38
	18	.0613	14		21	.0942	26
	19	.0088	2		22	.0507	14
232	17	.1215	28		23	.0072	2
	18	.0695	16	280	20	.1438	40
	19	.0174	4		21	.1007	28
234	17	.1291	30		22	.0576	16
	18	.0775	18		23	.0144	4
	19	.0258	6	282	20	.1499	42
236	17	.1365	32		21	.1071	30
	18	.0853	20		22	.0643	18
	19	.0342	8		23	.0214	6
238	17	.1438	34	284	21	.1135	32
	18	.0931	22		22	.0709	20
	19	.0423	10		23	.0284	8
240	17	.1510	36	286	21	.1197	34
	18	.1007	24		22	.0775	22
	19	.0504	12		23	.0352	10
242	18	.1082	26	288	21	.1258	36
	19	.0583	14		22	.0839	24
	20	.0083	2		23	.0420	12
244	18	.1155	28	290	21	.1319	38
	19	.0661	16		22	.0902	26
	20	.0165	4		23	.0486	14
246	18	.1228	30		24	.0069	2
	19	.0737	18	292	21	.1072	40
	20	.0246	6		22	.0966	28
248	18	.1298	32		23	.0552	16
	19	.0812	20		24	.0138	4
	20	.0325	8	294	21	.1438	42
250	18	.1369	34		22	.1028	30
	19	.0886	22		23	.0617	18
	20	.0403	10		24	.0206	6
252	18	.1438	36	296	21	.1496	44
	19	.0959	24		22	.1089	32
	20	.0480	12		23	.0681	20
					24	.0272	8

TABLE 1.—*The M-table*—Continued

$M-\Delta$	n	h	$2n+x$	$M-\Delta$	n	h	$2n+x$
298	22	0.1149	34	306	22	0.1382	42
	23	.0744	22		23	.0987	30
	24	.0034	10		24	.0592	18
300	22	.1208	36		25	.0198	6
	23	.0806	24	308	22	.1438	44
	24	.0403	12		23	.1046	32
302	22	.1267	38		24	.0654	20
	23	.0867	26		25	.0262	8
	24	.0467	14	310	22	.1494	46
	25	.0067	2		23	.1104	34
304	22	.1325	40		24	.0715	22
	23	.0927	28		25	.0325	10
	24	.0530	16				
	25	.0134	4				

(b) EVALUATION OF n AND x

Equation 1 may be written—

$$n=\frac{M-1.0078x}{14.0156} \tag{7}$$

If limiting values of M and x are known, they may be put into the equation to determine limiting values for n. Thus $n_{min.}$ is obtained by substituting $M_{min.}$ and $x_{max.}$ and taking the nearest integer which is larger. $n_{max.}$ is obtained by substituting $M_{max.}$ and $x_{min.}$ and taking the nearest integer which is smaller. If nothing is known about the value of x, $x_{max.}$ should be taken as $+2$ and $x_{min.}$ as $\frac{14-M_{max.}}{6}$. The possible values of n are the integers lying between $n_{min.}$ and $n_{max.}$

For the complete evaluation of n by the above procedure when x is unknown, the following condition, which is both necessary and sufficient, must be fulfilled. (See the M-table.)

The values of $M-\Delta$ falling within the range $M_{min.}$ to $M_{max.}$, inclusive, must be wholly within one of the following inclusive ranges: 16 to 16, 26 to 30, 38 to 44, 50 to 58, 62 to 72, 74 to 84, 88 to 96, 102 to 108, 116 to 120, 130 to 132, or 144 to 144. These values of $M-\Delta$ are printed in bold-face type in Table 1.

From equation (1) x can obviously be computed, if M and n are known, hence, a definite evaluation of $M-\Delta$ as one of the numbers in bold-face type completely determines the empirical formula of the compound.

If the molecular weight can not be identified as one of those corresponding to a single formula, a combustion analysis (or substitute therefor) will always be required except in the following special cases:

In the M-table two hydrocarbons appear with the molecular weight 86. One of these is the saturated hydrocarbon, C_6H_{14}. The other has the formula C_7H_2. This very unsaturated hydrocarbon is not known, and perhaps does not exist. In any event its properties would readily distinguish it from C_6H_{14}. For all practical purposes, therefore, the value 86 might be added to the list of bold-face values in the table. For similar reasons the same statement can be made

with respect to the molecular weights 98, 110, 122, 134, 146, and 158 and, with somewhat less confidence, with respect to a number of other values. In other words, whenever the M-table is used, certain of the hydrocarbons there shown may be eliminated as possibilities in a given case on the grounds that they could not have the properties possessed by the given hydrocarbon.

(c) ILLUSTRATIVE EXAMPLES

Example 1

Given: $M_a = 91$, $p_{max.} = 0.03$.

The true value of $M - \Delta$ must be an even integer lying between the limits

$$M_{max.} - \Delta > 91/0.97 > 93.8 = 92$$
$$M_{min.} - \Delta < 91/1.03 < 88.4 = 90$$

Hence, it is 90 or 92.

From the M-table it is obvious that $n = 7$ and that the hydrocarbon is C_7H_6 or C_7H_8. If we repeat the molecular weight determination without increase of accuracy and find $M_a = 93$, the possible values of $M - \Delta$ are now 92 and 94. The true value must, therefore, be 92 and the hydrocarbon is C_7H_8.

If we prefer to make the evaluation with the aid of a combustion analysis, we note (Table 1) that the possible values for h are 0.0672 and 0.0876. Hence, a combustion analysis accurate to better than $\frac{1}{2}(0.0876 - 0.0672) = 0.01$ unit will suffice to definitely evaluate h.

Example 2

Given: Two determinations of M, $M_1 = 91$, $M_2 = 87$; and $p_{max.} = 0.1$.

$$M_{max.} - \Delta > 87/0.9 > 96.5 = 96$$
$$M_{min.} - \Delta < 91/1.1 < 82.7 = 84$$

From the M-table we find that n is either 6 or 7 and, if the hydrocarbon C_7H_2 is ruled out, definite evaluation is possible, if we redetermine M with sufficient accuracy. If, however, we prefer to make the evaluation from combustion analysis we prepare the following table:

$M-\Delta$	86	88	90	92	94	96	84	80
h	0.0234	0.0458	0.0672	0.0876	0.1071	0.1258	0.1438	0.1608
Δh	0.0224	0.0214	0.0204	0.0195	0.0187	0.0180	0.0200	

The smallest value for Δh is 0.018. Hence, it will suffice, if $(\delta h)_{max.} < 0.009$.

Example 3

Given:

$M_a = 301$ and $p_{max.} = 0.02$

$M_{max.} - \Delta > 301/98 > 306 = 306$

$M_{min.} - \Delta < 301/1.02 < 295 = 296$

The possible values of n are evidently 21, 22, 23, 24, and 25.

Arranging the corresponding values of h in the M-table in ascending order and computing the differences, we find the smallest difference to be $\Delta h = 0.0008$ for the hydrocarbons $C_{25}H_6$ and $C_{24}H_6$. These are very improbable hydrocarbons and might perhaps be ruled out. The next smallest value for Δh is 0.0024 for the hydrocarbons $C_{24}H_{18}$ and $C_{23}H_{18}$. To distinguish between these the error in the combustion analysis should preferably be less than $(\delta h)_{max.} = \frac{0.0024}{2} = 0.0012$. In other words, a careful combustion analysis must be made. Suppose the result is $h_a = 0.149 \pm 0.001$. Obviously $h = 0.1496$ and the hydrocarbon must be $C_{21}H_{44}$.

For all hydrocarbons with molecular weights of the order of 300 or larger, a careful combustion analysis is usually unavoidable. Whenever, therefore, $M_a/(1-p_{max.}) > 300$, it is best to proceed immediately with the combustion analysis and to use the methods to be explained below in place of the M-table for deducing the formula of the hydrocarbon.

We shall now take up the consideration of the combustion analysis and the conclusions which can be derived therefrom.

IV. THE COMBUSTION ANALYSIS

1. GENERAL CONSIDERATIONS

The purpose of the combustion analysis is to determine what fraction of the compound, by weight, is hydrogen. This fraction is represented by $h = \frac{\%H.}{100}$

This can be obtained (1) from the percentage of hydrogen alone, (2) from the percentage of carbon alone, or (3) by combining both values.

Method (1), which requires only a determination of the percentage of hydrogen, is the best of the three methods, if the sample is a pure hydrocarbon. Under these circumstances the carbon determination is unnecessary and of no value.

Method (2) would require an absolute accuracy in the carbon determination equal to that required in method (1) for the hydrogen determination. This practically eliminates this method from consideration.

Method (3) has the following advantages: (*a*) It is not necessary to know the mass of the sample used; (*b*) the result is not affected by the presence of impurities in the sample, except such as give volatile products which are absorbed; (*c*) it is also not affected by a partial oxidation of the sample, provided all of the oxidation products are retained by the sample; (*d*) through an almost exact compensation of air-buoyancy effects, it is unnecessary to correct the weighings to vacuum, if NaOH (or "Ascarite") is used to absorb the carbon dioxide and $MgClO_4.3H_2O$ ("Dehydrite") followed by P_2O_5 to absorb the water.

A comparison of the values of h as given by the three methods in the case of combustion analyses of naphthalene and of a petroleum fraction respectively, is shown in Table 2.[5]

[5] The data in this table are taken from the combustion analyses made by Bruun, B. S. Jour. Research, **2**, 487; 1929.

TABLE 2.—*Illustrating the value of* $h=\frac{\%H}{100}$ *as obtained by three different methods of calculation*

1. NAPHTHALENE

Run	$h_1=\frac{\%H}{100}$	Deviation	$h_2=\frac{100-\%C}{100}$	Deviation	$h_3=\frac{\%H}{\%H+\%C}$	Deviation
1	0.0627	0.0002	0.0639	0.0002	0.0627_7	0.000
2	.0621	.0004	.0634	.0003	$.0621_8$	.000
3	.0626	.0001	.0639	.0002	$.0626_8$	.000
Average	.0625	.0002	.0637	.0002	$.0625_1$	.000
Theoretical	.0629		.0629		.0629	

2. GAS-OIL FRACTION

1	0.1366	0.0002	0.1390	0.0002	0.1369	0.000
2	.1364	.0000	.1395	.0003	.1368	.000
3	.1361	.0003	.1392	.0001	.1365	.000
Average	.1364	$.0001_7$	.1392	.0002	.1367	.000
h_1	.1364	±.0002				
h_3	.1367	±.0002				
Difference	.0003	±.0003				

From these data it would appear to be a conservative conclusion to state that the value of h can, if necessary, be determined within ± 0.0005 unit; also a reasonable and safe value of the "maximum error of the method," $(\delta h)_{max.}$, is ± 0.001. This is obviously a degree of accuracy attainable without much difficulty and it will be found ample for practically all cases.[6]

2. MATHEMATICAL RELATIONS

From the formula, C_nH_{2n+x}, molecular weight $=M$, together with the values 12.000 and 1.0078 for the atomic weights of carbon and hydrogen, respectively, a number of mathmetical relations connecting h, n, x, and M can be easily derived by purely algebraic processes. Those which will be employed [7] in the following discussion are

$$h=\frac{\%\ \mathrm{H}}{100}\ \text{(definition)}$$

$$r=\frac{n}{x}=\frac{1/2\left(\frac{1}{h}-1\right)}{6.95535-1/h} \qquad (8$$

$$x=M(1.15893h-0.16666) \qquad (9$$

[6] On this point see further Sec. XI, p. 890.

[7] Other relations, such as $n=\frac{(1-h)M}{12}$ and $2n+x=\frac{Mh}{1.0078}$ might alternatively be employed, and in some instances would be shorter and more direct. The ones adopted, however, and the procedures based upon them are applicable to all situations and yield the maximum amount of information with little chance of going astray.

3. CLASSIFICATION INTO TYPE GROUPS

In discussing the calculation of n and x from the experimentally determined quantities h and M, the various cases which present themselves fall naturally into three groups which can be defined as follows:

Group I, r is a positive quantity, $x=+2$.
Group II, r is infinite, $x=0$.
Group III, r and x are negative quantities.

The characteristics of each group, together with illustrative examples will be discussed in order. In this discussion $(\delta h)_{\text{max.}}$ will be taken as equal to ± 0.001 for the reasons explained above. The discussion can, therefore, be generalized by substituting $(\delta h)_{\text{max.}}$ for ± 0.001 wherever it is used.

4. Group I. SATURATED HYDROCARBONS, C_nH_{2n+2}

(r is positive, $x=+2$)

While this group is characterized by a positive value for r, it is not necessary to calculate r in order to determine whether or not a given case belongs to the group. This can be determined directly from the value of h as follows: (1) It is obvious that $r\left(=\frac{n}{x}\right)$ can be a positive quantity only when $x=+2$; that is, only for a saturated hydrocarbon. (2) Every saturated hydrocarbon will have a larger value of h than any unsaturated hydrocarbon. (3) The highest value of h for an unsaturated hydrocarbon occurs in the hydrocarbon type, C_nH_{2n}, and is equal to $\frac{2\times 1.0078n}{14.0156n}=0.1438$.

Group I is therefore completely defined by the relation

$$h>0.1438$$

Whenever, therefore, the value of h is greater than 0.1438, the hydrocarbon must be a saturated one; that is, $x=+2$ and $n=2r$.

Example 1

Given, h (found) $=0.1559$, $(\delta h)_{\text{max.}}=0.001$.
Substituting in equation (8) gives

$$11>(2r=n)>9.3$$

The true value of n must, therefore, be 10 and the hydrocarbon is $C_{10}H_{22}$. No molecular weight determination is necessary.

Example 2

Given the following two experimental values for h, $h_1=0.1521$, $h_2=0.1508$, and $(\delta h)_{\text{max.}}=0.001$. Evidently we may write

$$h_{\text{max.}}=h_2+0.001=0.1518$$

$$h_{\text{min.}}=h_1-0.001=0.1511$$

From these two values and equation (8) we find

$$2r_{max.} = n_{max.} \nearrow 16.16 = 16$$

$$2r_{min} = n_{min.} \swarrow 15.2 = 16$$

Hence, $n = 16$ and the hydrocarbon is $C_{16}H_{34}$.

If $(\delta h)_{max.} = 0.001$, no possible single value of h will lead to the evaluation of n for saturated hydrocarbons containing more than 1 carbon atoms, but if more than one determination of h is available such evaluation may result, if n does not exceed about 17.[8]

Example 3

Given

$$h \text{ (found)} = 0.1464, \ (\delta h)_{max.} = 0.001$$

Hence

$$75.0 > (2r = n) > 33.8$$

n must, therefore, be a whole number lying between 75 and 34 inclusive. To find its value a molecular weight determination is required.

The facts concerning saturated hydrocarbons may be summed up as follows:

1. If $(\delta h)_{max.}$ does not exceed 0.001, the formula of the hydrocarbon can always be derived from the combustion analysis alone for all hydrocarbons up to and including C_7; and if a sufficiently favorable value of h is obtained, evaluation is possible up to and including C_{10}.

2. For saturated hydrocarbons between C_{10} and C_{17} the formula of the hydrocarbon may be derived from the combustion analysis alone if two sufficiently favorable values of h are obtained. In general, however, a molecular weight determination will be desirable for all hydrocarbons above C_8 and will be required for all above C_{17}.

3. If it is known that the hydrocarbon is saturated, a combustion analysis is unnecessary, since the formula can be calculated from the molecular weight determination alone. (See equation (7).) Or stated in another way, the combustion analysis need only be accurate enough to show that h is definitely greater than 0.1438. A greater degree of accuracy is ordinarily of no real value (unless it is desired to avoid, where possible, the necessity of a molecular weight determination since (*a*) for saturated hydrocarbons of low molecular weight, only a moderate degree of accuracy in the molecular weight is required in order to determine n by means of equation (7) alone; and since (*b*) for higher molecular weights the accuracy required in the molecular weight determination is not materially diminished by a more accurate knowledge of h.

Procedure for Group I

Compute $r_{min.}$ and $r_{max.}$ with the aid of equation (8). Then find

$$n_{min.} \swarrow 2r_{min.} = (I)_{min.} \quad (10)$$

and

$$n_{max.} \nearrow 2r_{max.} = (I)_{max.} \quad (11)$$

[8] On this point see further the discussion on pp. 233 and 234 of reference 2.

If $(I)_{min.} = (I)_{max.}$, n is completely evaluated.

If $(I)_{max.} > (I)_{min.}$, and a molecular weight determination is required, the accuracy in M should be $(\delta M)_{max.} < 7$ units, in order to be certain of evaluating n from a single determination of M.

5. Group II. HYDROCARBONS OF THE TYPE C_nH_{2n}

$$(x = 0,\ r = \infty)$$

This group includes only, but all, hydrocarbons of the type C_nH_{2n}. For all members of the group $h = 0.1438$. If, therefore, the value 0.1438 is included within the limits

$$h \text{ (found)} \pm [(\delta h)_{max.} = 0.001]$$

the hydrocarbon in all probability has the formula C_nH_{2n}. The only possible alternative is a hydrocarbon containing more than 62 carbon atoms.[9]

For all hydrocarbons belonging to this group the formula must be determined from the molecular weight. The combustion analysis is of no further help.

Procedure for Group II

Determine M and compute n from the relation

$$\frac{M_{max.}}{14.0156} > (n = I) > \frac{M_{min.}}{14.0156} \qquad (12)$$

In order to be certain of evaluating n from a single determination of M, the accuracy in M should be $(\delta M)_{max.} < 7$ units. If n is found to be greater than 62, the combustion analysis must be repeated with an accuracy sufficient to identify the group type with certainty.

6. Group III. HYDROCARBONS OF THE TYPE C_nH_{2n+x}

(x is negative, r is negative)

This group includes all hydrocarbons having negative values of x. The group is completely defined also by the relation

$$h < 0.1438$$

In order to determine n and x for members of this group both M and h are determined and utilized in the calculation. The details of the calculation are discussed in 8 below.

EVALUATION OF n AND x FROM CUMBUSTION ANALYSIS ALONE

(a) EVALUATION OF x

The complete evaluation of x from combustion analysis alone is, in general, possible only when $h \geq 0.1438$. As we have shown above (p. 877), when $h = 0.1438$, $x = 0$ and when $h > 0.1438$, $x = +2$. In particular cases it is possible also for other values of h, provided some

[9] For $(\delta h)_{max.} = 0.0005$ the only alternative is a hydrocarbon with more than 123 carbon atoms.

limitation can be placed upon n. Since, however, the knowledge of such a limitation is practically equivalent to an approximate knowledge of the molecular weight, or at all events of an upper limit for it, such cases are best treated in connection with molecular weight data.

(b) EVALUATION OF n

Complete evaluation of n from combustion analysis alone is possible only when $h>0.1438$ and when n is less than a fixed value determined by and calculable from $(\delta h)_{max.}$ as in the examples already discussed (p. 878, *supra*).

(c) COMBINATION VALUES OF n AND x

If no limitation is placed upon the molecular weight, values of $h<0.1438$ give an infinite number of possible values for n and x. If, however, we agree to limit our field to hydrocarbons for which n is not greater than some fixed value, say 100, then for each value of h or in practice, for each value of $h \pm (\delta h)_{max.}$, there is only a finite number of combination values possible for n and x and these are all calculable.[10] The calculation is made by computing $r_{max.}$ and $r_{min.}$ with the aid of equation (8) and then determining the possible combination values of n and x by Diophantine analysis. Since, however, this set of possible combination values is usually rather large, if M only is known, it is of practical interest only when M can not be determined. The more restricted set which is limited by an approximate knowledge of M is readily calculable by the methods which will now be described.

8. PROCEDURE FOR GROUP III

1. Determine $M_{max.}$ and $M_{min.}$ as directed in Section III, 2 (a).
2. Determine $x_{max.}$ and $x_{min.}$ from relation (9) which gives

$$-x_{max.} \gtrless M_{max.}\,[0.16666-1.1589\,(h-(\delta h)_{max.})]=2\ (I) \qquad (13)$$

$$-x_{min.} \lessgtr M_{min.}\,[0.16666-1.1589\,(h+(\delta h)_{max.})]=2\ (I) \qquad (14)$$

3. Determine $n_{max.}$ and $n_{min.}$ from equation (7) which gives with sufficient accuracy

$$n_{max.} \gtrless \frac{M_{max.}-x_{min.}}{14}=(I)_{max.} \qquad (15)$$

$$n_{min.} \lessgtr \frac{M_{min.}-x_{max.}}{14}=(I)_{min.} \qquad (16)$$

4. If n and x are not evaluated at this point, determine $-r_{max.}$ and $-r_{min.}$ from relation (8).
5. Using in turn each possible value of x as obtained from relations (13) and (14) above, determine the integers lying between $x\times r_{max.}$ and $x\times r_{min.}$ These integers, together with their corresponding values of x, constitute possible combination values of n and x.
6. From the set of combination values thus obtained strike out any which are inconsistent with relations (15) and (16) and tabulate the hydrocarbon formulas of the remainder, together with their molecular weights and values of h.

[10] See p. 241 of reference 2.

7. Determine by inspection of this table the next step in the procedure.

This next step is rather difficult to set forth in explicit terms, since it varies so greatly with the nature of the table obtained in (6) and with the desires of the investigator. It can best be presented by means of concrete examples.

If more than one experimental value of M and/or of h is available, the procedure just outlined may be modified accordingly. This can also best be presented by means of concrete examples.

Example 1

Given:

$M_a = 513$; $p_{max} = 0.1$

$h_a = 0.1398$; $(\delta h)_{max.} = 0.001$

$M_{min.} \lessdot 513/1.1 \lessdot 466 = 466 + \Delta$

$M_{max.} \gtrdot 513/0.9 \gtrdot 570 = 570 + \Delta$

The small quantity Δ may be neglected.

$$-x_{max.} \gtrdot 570\ [0.1666 - 1.1589 \times 0.1388] \gtrdot 3.2 = 2$$

$$-x_{min.} \lessdot 466\ [0.1666 - 1.1589 \times 0.1408] \lessdot 0.98 = 2$$

Hence $x = -2$

$$n_{min.} \lessdot \frac{466+2}{14} \lessdot 33.4 = 34$$

$$n_{max.} \gtrdot \frac{570+2}{14} \gtrdot 40.8 = 40$$

$$-r_{min.} = -1/2\left(\frac{1}{0.1388} - 1\right) \Big/ \left(6.955 - \frac{1}{0.1388}\right) = 12.4$$

$$-r_{max.} = -1/2\left(\frac{1}{0.1408} - 1\right) \Big/ \left(6.955 - \frac{1}{0.1408}\right) = 20.6$$

For $x = -2$ these give $n_{max.} = 41$ and $n_{min.} = 25$, which are wider limits than the above. The hydrocarbon, therefore, belongs to the type C_nH_{2n-2} and n must be between 34 and 40, inclusive. For this type the interval, ΔM, is constant and equal to 14.0156.

The possible hydrocarbons are therefore the following:

F	M	h
$C_{34}H_{66}$	474.508	0.1402
$C_{35}H_{68}$	488.523	.1404
$C_{36}H_{70}$	502.539	.1405
$C_{37}H_{72}$	516.554	.1405
$C_{38}H_{74}$	530.570	.1405
$C_{39}H_{76}$	544.585	.1406
$C_{40}H_{78}$	558.600	.1406

There is evidently nothing to be gained by repeating the combustion analysis. To be certain of identifying the hydrocarbon from one additional M determination it is evident that $(\delta M)_{max.}$ must be < 7 units, or, for the most unfavorable case, $p_{max.}$ must be less than 1.27 per cent. This is obtained from equation (32), page 235 of the preceding paper,[11] which for this case yields

[11] See footnote 2, p. 868.

$$p_{max.}=\frac{\Delta M}{2M_{max.}-14}=\frac{1}{2n_{max.}-\frac{9}{7}}=\frac{1}{2\times 30-\frac{9}{7}}=1.27 \text{ per cent}$$

Example 2

Given:

$M_a=300$, $p_{max.}=0.1$

$h_a=0.0770$ $(\delta h)_{max.}=0.001$

$M_{min.}<300/1.1<272.6=274+\Delta$

$M_{max.}>300/0.9>333.3=332+\Delta$

$-x_{max.}>332\ [0.1666-1.1589\times 0.0760]>26.1=26$

$-x_{min.}<274\ [0.1666-1.1589\times 0.0780]<20.9=22$

$$n_{min.}<\frac{274+22}{14}<21.1=22$$

$$n_{max.}>\frac{332+26}{14}>25.6=24$$

$-r_{min}=0.98$; $-r_{max}=1.01$

Hence, $1.01>\frac{n}{-x}>0.98$

For

$x=-22$	$n=22$
-24	24
-26	26

The hydrocarbon must, therefore, belong to the type C_nH_n, for which $\Delta M=26$. The possibilities are

F	$-x$	M	h
$C_{22}H_{22}$	22	286.2	0.0775
$C_{24}H_{24}$	24	312.2	

To be certain of identifying the hydrocarbon by one additional M determination, it is evident [12] that

$$p_{max.} \text{ must be} < \frac{26}{286+312} < 4.3 \text{ per cent}$$

Example 3

Given:

$M_a=302$, $p_{max.}=0.1$

$h_a=0.0530$, $(\delta h)_{max.}=0.001$

$M_{min.}<302/1.1<274.5=276$

$M_{max.}>302/0.9>335.5=334$

$-x_{max.}>334\ [0.1666-1.1589\times 0.0520]>35.5=34$

$-x_{min.}<274\ [0.1666-1.1589\times 0.0540]<28.7=30$

$$n_{min.}<\frac{276+30}{14}<21.8=22$$

[12] See p. 235 of reference 2.

$$n_{max.} > \frac{334+34}{14} > 26.3 = 26$$

$$-r_{min.} = 0.742; \quad -r_{max.} = 0.757$$

$$0.757 > \frac{n}{-x} > 0.742$$

For

$x = -30$	$n =$ no possible integer
-32	$= 24$
-34	$=$ no possible integer

Hence, $n = 24$, $x = -32$ and the hydrocarbon is $C_{24}H_{16}$.

With the same values of h_a and $(\delta h)_{max.}$, the same result would have been obtained even though the maximum error in the molecular weight determination had been larger, as long as $M_{max.}$ was found to be <342 and $M_{min.}>266$. Similarly, with the same values of M_a and $p_{max.}$ the same result would have been obtained as long as $h \pm (\delta h)_{max.}$ was included within the limits 0.053 ± 0.002. Furthermore, by increasing the accuracy in the M determination the accuracy required in the h determination could be further materially lessened.

Example 4

In order to avoid the possibility of "mistakes,"[13] the investigator will usually run at least two combustion analyses, and, since M is being measured by a rapid method, at least two determinations of M might just as well be made. The following example illustrates a method which may be followed when more than one experimental value of h and/or of M is available.

Given:

$$M_1 = 542; \; M_2 = 539; \; p_{max.} = 0.1$$

$$h_1 = 0.0908; \; h_2 = 0.0916; \; (\delta h)_{max.} = 0.001.$$

$$M_{min.} < 542/1.1 < 492.27 = 492$$

$$M_{max.} > 539/0.9 > 599 = 598$$

$$-x_{max.} > 598\,[0.1666 - 1.1589 \times 0.0906] > 36.8 = 36$$

$$-x_{min.} < 492\,[0.1666 - 1.1589 \times 0.0918] < 29.6 = 30$$

$$n_{min.} < \frac{492+30}{14} < 37.3 = 38 \quad (a)$$

$$n_{max.} > \frac{598+36}{14} > 45.3 = 45$$

$$-r_{max.} = 1.256; \quad -r_{min.} = 1.227$$

Hence $1.256 > \frac{n}{-x} > 1.227$

For

$x = -30$	$n = 37$
-32	$= 40$
-34	$= 42$
-36	$= 45$

[13] See p. 225, 237 of reference 2.

The first set is ruled out by (*a*) above, leaving as possibilities:

F	$-x$	M	h
$C_{40}H_{48}$	32	528.34	0.0918
$C_{42}H_{50}$	34	554.38	.0909
$C_{43}H_{54}$	36	594.41	.0915

In order to identify the hydrocarbon it is obviously necessary to make additional measurements. What shall they be and how accurately must they be made? No definite single answer can be given to this question. For example, suppose the hydrocarbon were $C_{42}H_{50}$. With $(\delta h)_{max.}=0.001$ any value of h between 0.0899 and 0.0919 is an experimental possibility. If, therefore, the combustion analysis were repeated and any value not greater than 0.0904 were obtained, the hydrocarbon would be identified. If, however, the correct value, 0.0909, were obtained, identification would fail. Similarly, if the hydrocarbon were $C_{40}H_{48}$ and the M determination were repeated without increase of accuracy, identification would result if the value obtained in the measurement were less than $0.9\times 554.4=499$. In other words, if the investigator is fortunate in the error which he makes, he will obtain the desired answer.[14]

While a definite answer can not be given to the question as formulated above, the following formulation, which is that used in the preceding examples, will yield such an answer: How accurately must M or h be measured in order that a single measurement of either will be certain to lead to identification?

For M we use equation (32) of the preceding paper.[15] This gives us

$$p_1=\frac{554.38-528.34}{554.38+528.34}=2.4 \text{ per cent.}$$

$$p_2=\frac{594.41-554.38}{594.41+554.38}=3.5 \text{ per cent.}$$

The answer is therefore $p_{max.}$ must be <2.4 per cent.

For h we note that $\Delta h_{min.}=0.0003$. Hence $(\delta h)_{max.}$ would have to be <0.00015.

It is evident that our most certain procedure is to repeat the M determination, with an accuracy better than 2.4 per cent, if practicable.

V. POSSIBLE SUBSTITUTES FOR THE COMBUSTION ANALYSIS OR THE MOLECULAR WEIGHT DETERMINATION

1. GENERAL CONSIDERATIONS

From the foregoing discussion it is evident that the purpose of the molecular weight determination and the combustion analysis is to provide us with two independent mathematical relations involving n and x, each relation being given with a known accuracy. These two relations, together with the Diophantine characters of n and

[14] See p. 231 of reference 2.

[15] See p. 235 of reference 2.

lead to the complete identification of both n and x, if the accuracy is sufficient.

Now it is obvious that any mathematical relation involving either or both n and x should be similarly utilizable, either as additional information or in place of the M or the h functions. Furthermore, any clean-cut chemical reaction, series of reactions or set of reactions in which the hydrocarbon is involved should, in principle, be capable of furnishing a mathematical relation of this character. The expression "clean cut" in this connection means simply that all molecules of the hydrocarbon react stoichiometrically alike. The desired relation is obtained by determining any stoichiometric quantity associated with the process. For example, in the combustion analysis itself the stoichiometric quantity determined is the number of mols of water produced per gram of hydrocarbon burned.

It is hardly worth while to discuss in detail the various chemical reactions involving hydrocarbons which might conceivably be used to supply the desired type of information. It will suffice to discuss one such case as an illustrative example.

Let us first assume that we have made the customary determinations of molecular weight and combustion analysis with the following results:

$$M_a = 129 \qquad p_{max.} = 0.2$$
$$h_a = 0.0766 \qquad (\delta h)_{max.} = 0.001$$

This is a Group III hydrocarbon. Hence, we have

$$M_{min.} < 129/1.2 < 107.5 = 108$$
$$M_{max.} > 129/0.8 > 161.2 = 160$$
$$-x_{max.} > 160\,[0.1666 - 1.1589 \times 0.0756] > 12.6 = 12$$
$$-x_{min.} < 108\,[0.1666 - 1.1589 \times 0.0776] < 8.3 = 10$$
$$n_{min.} < \frac{108+10}{14} < 8.42 = 9$$
$$n_{max.} > \frac{160+12}{14} > 12.3 = 12$$
$$-r_{min.} = 0.976; \quad -r_{max.} = 1.00$$
$$1.00 > \frac{n}{-x} > 0.976$$

For

$$x = -10 \qquad n = 10$$
$$-12 \qquad 12$$

The hydrocarbon is therefore of the type C_nH_n and is either $C_{10}H_{10}$ or $C_{12}H_{12}$.

2. UTILIZATION OF THE BROMINE-ADDITION NUMBER

Now let us assume that instead of making a combustion analysis we have determined the bromine- (or other-) addition number of the hydrocarbon. The following discussion is applicable to any addition reaction. Our data will be, let us say

$$M_a = 129 \qquad p_{max.} = 0.2$$
$$u_a = 0.0307 \qquad (\delta u)_{max.} = 0.0003$$

where u is the number of equivalents of bromine stoichiometrically added by 1 gram of the hydrocarbon.

If we let Z represent the number of equivalents of unsaturation[16] which remain in the molecule after the bromine addition, it follows from the laws of valency that

$$x=2-Mu-Z$$

where Mu and Z are even integers.

As in the preceding example

$$M_{max.}=160 \text{ and } M_{min.}=108$$

Hence

$$(Mu)_{max.}\gtrdot 160\times 0.031\gtrdot 4.96=4$$
$$(Mu)_{min.}\lessdot 108\times 0.0304\lessdot 3.31=4$$

And

$$Mu=4$$

Also

$$M_{max.}\gtrdot \frac{Mu}{u_{min.}}\gtrdot \frac{4}{0.0304}\gtrdot 131.5=130+\Delta$$

$$M_{min.}\lessdot \frac{4}{0.031}\lessdot 129=130+\Delta$$

Hence, $M-\Delta=130$ and the hydrocarbon must be $C_{10}H_{10}$.

Complete identification has resulted because we have assumed a sufficiently small value for $(\delta u)_{max.}$ If we had assumed a larger value, say $(\delta u)_{max.}=0.001$, we would have found 6 possibilities, namely, (C_9H_{20}), $C_{10}H_8$, $C_{10}H_{10}$, $C_{10}H_{12}$, $C_{10}H_{14}$, and $C_{11}H_{12}$. C_9H_{20} is ruled out because it is a saturated hydrocarbon. It will be noticed that $C_{12}H_{12}$ is not included among the possibilities.

Let us now assume that we have made only the combustion analysis and the bromine-addition determination. These will yield the following information, taking the same numerical data as in the preceding examples.

$$1.00>\frac{n}{-x}>0.976$$

$$0.031>u>0.0304$$

$$x=(2-Mu-Z)>\frac{14-M}{6}$$

$$M=14.0156n+1.0078x$$

n is an integer and x, Mu and Z are even integers.

When solved for n and x the above relations, together with equation (9), give

$$x=\frac{(Z-2)\ (0.1666-1.159h)}{u-0.1666+1.159h} \tag{17}$$

$$n=-rx \tag{18}$$

[16] Saturation is here defined by the condition, $x=+2$.

Three cases are possible as follows:

1. If Z is actually zero, equation (17) will be found to yield a definite value for x.

2. If Z is actually 2, equation (17) will be found to become indeterminate. In this case the number of combination values possible for n and x is the same as though the bromine determination had not been made; that is, it is the number corresponding to the limiting values of h. The only utility of the bromine determination in these circumstances is to eliminate as possibilities certain structural formulas.

3. If Z is actually greater than 2, equation (17) will lead to a smaller number of possibilities than correspond to value of h alone.

In the present example we find

$$-x=\frac{(Z-2)\ [0.1666-1.159\ (0.0766\pm 0.001)]}{0.166-1.159\ (0.0766\pm 0.001)-(0.0207\pm 0.0003)}$$

The denominator is a positive quantity. Hence, Z must be >2. If we assume that $n \gtrsim 50$, a Diophantine analysis yields the following as the only possible formulas for the hydrocarbon: $C_{10}H_{10}$, $C_{20}H_{20}$, $C_{30}H_{30}$, $C_{40}H_{40}$, $C_{45}H_{44}$, and $C_{50}H_{50}$. For the same condition the value of h by itself leads to 30 possibilities.

3. CONCLUSIONS

The results obtained in the examples just discussed suggest that the bromine (or other) addition number may be a valuable aid in deducing the formula of a hydrocarbon. From a purely mathematical standpoint it has a material advantage over the combustion analysis because in many cases it enables us to deal with a small even integer instead of a large one, with a consequent gain in the precision required.

The writer has hesitated to include it definitely as a possible substitute for the combustion analysis, however, because he has been unable to satisfy himself that the present state of our knowledge of the reactions of any of the halogens with the hydrocarbons justifies the assumption that the reaction can be so controlled as to be always stoichiometric in character.[17] However, it should be valuable as additional evidence and should always be determined, if only for the purpose of accumulating additional evidence as to its stoichiometric reliability.

Whether or not it is stoichiometric in a given instance could in principle be determined by carrying out the bromination in steps, in such a way that the amount of bromine added by the hydrocarbon in each step is controlled by the known activity of bromine in some second nonmiscible phase (gas or liquid) containing it. The graph of the amount added against the activity of the bromine in the nonmiscible phase should exhibit a flat corresponding to each type of stoichiometrically added bromine.[18]

[17] This does not refer to the possibility that addition may be accompanied by some substitution, because the latter can, of course, be determined by an acid titration and corrected for.

[18] For recent applications of the principle of this method to another situation, see Bancroft and Barnett, Proc. Nat. Acad. Sci., **16**, pp. 118, 135; 1930.

VI. RÉSUMÉ AND GENERAL PROCEDURE

1. Make an approximate determination of the molecular weight.

(*a*) If M_a is less than 300, follow the procedure of Section III, 2, page 870.

(*b*) If M_a is of the order of 300 or greater, proceed to 2.

2. Make a combustion analysis.

(*a*) If $h-(\delta h)_{max.}>0.1438$, follow the procedure of Section IV, 4, page 878.

(*b*) If 0.1438 is included within $h\pm(\delta h)_{max.}$, follow the procedure of Section IV, 5, page 879.

(*c*) If $h+(\delta h)_{max.},<0.1438$, follow the procedure of Section IV, 8, page 880.

3. Determine the halogen- (hydrogen-, acid-, or other-) addition number and, if the result is not zero, check the deductions of 1 and 2 by the procedure explained in Section V, 2, page 885.

4. If there is reason to suppose that the hydrocarbon may be an equilibrium mixture of polymers, it should be further investigated as described in Section IX below.

VII. EFFECTS OF IMPURITIES

The procedure outlined in the foregoing pages assumes that the hydrocarbon is pure; that is, that it contains a single molecular species. In practice, however, the requirement in this respect is that, if impurities are present, they must be of such natures and magnitudes as not to alter the measured values of h and M by such amounts as will lead to erroneous deductions. Thus if the impurities are all isomers of the principal constituent, they are without influence. Likewise, an impurity having the same hydrogen content as the principal constituent would not lead to an erroneous result, if the quantity present did not affect the measured molecular weight by a significant amount. Since, however, in general the natures of the impurities present will not be known, it is necessary to establish the purity of the sample before proceeding to determine its formula.[19]

VIII. THE "AVERAGE FORMULA" OF A MIXTURE OF HYDROCARBONS

If the procedure of the preceding pages be applied to a mixture of hydrocarbons, it may lead to a definite formula. The hydrocarbon corresponding to this formula may not, however, be present in the mixture and the result is of no value. If it is desired to find the so-called average formula of a mixture, the procedure here outlined may be used, but with the omission of those features of it which result from the Diophantine characters postulated for n and x. The average formula thus obtained will be $C_{a\pm b}H_{c\pm d}$, the subscripts being evaluated numerically. In this way the data of example 1, page 881, would yield the formula

$$C_{37.1\pm3.7}H_{72.1\pm6.3}$$

In determining the "average molecular weight" of a mixture by any of the methods involving the use of a solvent, the determination

[19] Suitable tests for purity have been discussed elsewhere. See Ind. Eng. Chem., **22**, p. 985; 1930. It is obvious that the sample used for combustion must be carefully freed from all moisture.

should be made for at least two concentrations and preferably with at least two solvents in order to avoid the unnecessary and possibly erroneous assumption that the hydrocarbon mixture is free from the substance employed as the solvent.

IX. EFFECTS OF POLYMERIZATION

If the sample of the hydrocarbon is a mixture of polymers, certain precautions are necessary. If the polymers present are not in equilibrium with one another, the sample is a mixture. It may, in principle, be separated into its constituent hyrdocarbons by suitable methods of fractionation.

If, however, the sample is a mixture of polymers in equilibrium with one another, it will behave toward the phase rule like a pure substance, and may consequently meet the tests for purity as ordinarily applied.

If now the procedure of the preceding pages be applied to such a "pure substance," an erroneous result may be obtained. If it is desired to eliminate this possibility, it is necessary to make accurate molecular weight determinations and to demonstrate that the molecular weight is independent of concentration and/or temperature.

If the molecular weight varies appreciably with concentration and temperature, the hydrocarbon must be an equilibrium mixture of polymers of the general formula $(C_nH_{2n+x})_y$ where y is an integer. In such a case the information desired is the values of n and x, with, perhaps, the average value of y under some stated conditions.

To obtain the values of n and x, the combustion analysis should be made as accurately as possible and the molecular weight should be determined under conditions where the degree of polymerization is as small as possible. In this way it will be possible in many cases to determine n and x. If this proves not to be possible, recourse must be had to the information which can be obtained by converting the hydrocarbon into one or more of its chemical derivatives, a problem which will be specific for each case and can not be discussed in general terms.

X. OTHER CHEMICAL COMPOUNDS

The principles, which in the present paper have been developed in their application to the problem of determining the formula of a hydrocarbon, should be utilized in connection with the determination of the formula of any chemical compound. The widespread practice of reporting the results of a chemical analysis of a compound and comparing these results with the values calculated from an assumed formula should be abandoned. Instead, the investigator should deduce from the results of his analysis and their estimated accuracy, the set of chemical formulas consistent therewith. If then he can eliminate certain members of this set on the basis of auxiliary evidence, this evidence should be stated. Only when all but one member of the set can be thus eliminated can the formula be considered as established.

XI. CONCLUSIONS

By following the procedures described in the preceding pages it should be possible to determine the empirical formula of any molecularly pure hydrocarbon containing not more than, say, 100 carbon atoms.

The accuracy required in the molecular weight determination would never exceed that necessary to distinguish $C_{99}H_{198}$ from $C_{100}H_{20}$ and for this an accuracy of 0.5 to 1 per cent would be sufficient.

If the molecular weight can be determined with the required accuracy (which in no case need be better than ± 0.5 per cent), then the accuracy necessary in the combustion analysis would in no case be greater than that required to distinguish between $C_{100}H_{200}$ and $C_{100}H_{202}$. An accuracy of about ± 0.0008 unit in h is ample for this purpose. This degree of accuracy should be attainable in any instance.[20]

As regards the molecular weight determination, the required accuracy can probably be obtained in most cases where a molecular weight determination is possible. Hydrocarbons may exist, however, which are so nonvolatile and so insoluble in all solvents that it is not possible to determine their molecular weights. In such cases, however, it would be equally impossible to obtain them in the pure condition and/or to establish their purity. They are, therefore, not likely to be met with in practice. The special problems arising in connection with an equilibrium mixture of polymers are discussed in Section IX.

The writer desires to acknowledge the valued assistance of R. T. Leslie and S. T. Schicktanz for the computation of the M-table and for checking the computations throughout the manuscript.

WASHINGTON, June 24, 1930.

[20] The above statements are valid only if the sample is a molecularly pure hydrocarbon. In practice the possibility of definitely evaluating the formula of a hydrocarbon of high molecular weight will in many cases be determined, not by the accuracy attainable in the molecular weight and combustion determinations, but by the practicability of obtaining the hydrocarbon in the required degree of purity and of demonstrating the purity.

THE IMPORTANCE OF PARTICLE SIZE IN SAMPLES OF CERTAIN METALLURGICAL MATERIALS

By J. A. Scherrer and G. E. F. Lundell

ABSTRACT

The sampling of certain metallurgical materials gives rise to particles that differ in size and in composition. The extent of the differences is shown and the procedures that must be followed in selecting the sample for analysis are outlined.

CONTENTS

		Page
I.	Introduction	891
II.	Experimental	892
III.	Conclusions	895

I. INTRODUCTION

The segregation of metallic or nonmetallic elements in certain alloys, and its influence on methods of sampling for chemical analysis is well known. There is, however, another phase of the sampling of alloys that is often ignored; namely, that the large and the small sized particles of the sample may differ in composition.

If the particles differ in composition, it is evident that the sample for analysis must be taken with special care, and that analyses can not be expected to agree if some are made on coarse particles that have been obtained from the top of a container by pouring or by using pincers, and others are made on fine material left in the bottom of the container or scooped up from the edges of a poured-out sample by means of a spatula.

In preparing standard samples that are to be used in checking methods of chemical analysis, the chief requirements are that the samples be stable and of uniform composition. They need not represent the exact composition of the material from which they were obtained. A selected portion of the sample can, therefore, be taken for use as the standard, or the sample can even be prepared by a method which would be out of the question in selecting a sample for check analyses. Thus in the preparation of standard analyzed samples of cast iron it is customary to blow out all graphite dust and then to take a definite portion of the well-mixed sample, as, for example, the fraction that passes a No. 20 sieve and remains on a No. 35 sieve. Again, in the preparation of standard analyzed samples of bearing metals a uniform but not necessarily representative, sample is assured by atomizing the molten alloy and taking the fraction that passes a No. 100 sieve.

II. EXPERIMENTAL

Most of the following tests on the composition of the different size particles of certain materials were made in connection with the preparation of the bureau's standard analyzed samples. The samples of journal bearing, phosphor-lead bronze bearing metal, monotype metal, aluminum sand-casting alloy, duralumin, and samples 1 and 3 of zinc-base die-casting alloys were taken on a milling machine. The sample of cast iron and part of sample 3 of the zinc-base die-casting alloy were prepared on the lathe. The ferrotungsten sample was ground in a ball mill.

TABLE 1.—*Variations in the compositions of fine and coarse particles of the same sample*

JOURNAL BEARING

Constituent	Fineness			
	On No. 20	Through No. 20; on No. 30	Through No. 30; on No. 80	Through No. 80
Cu	70.0	70.2	67.6	62.1
Pb	24.4	24.1	27.9	31.2
Sn	4.9	4.9	4.7	4.6

PHOSPHOR-LEAD BRONZE BEARING METAL

Constituent	Fineness				
	On No. 20	Through No. 20; on No. 40	Through No. 40; on No. 60	Through No. 60; on No. 100	Through No. 100
Cu	81.2	79.8	77.1	71.5	66.1
Pb	11.9	13.5	16.3	22.6	28.4
Sn	5.2	5.1	5.0	4.5	4.2
Zn	1.4	1.4	1.3	1.2	1.1
P	.16	.14	.17	.16	.18

MONOTYPE METAL

Constituent	Fineness				
	On No. 20	Through No. 20; on No. 40	Through No. 40; on No. 60	Through No. 60; on No. 100	Through No. 100
Pb	71.5	71.4	71.6	71.1	67.1
Sb	19.1	19.2	19.1	19.3	21.7
Sn	9.3	9.3	9.2	9.4	10.9
Cu	.03	.05	.07	.08	.08

Each sample was put through appropriate sieves and the portions that are specified in the tables were analyzed for the constituents that are listed.

The data presented in Table 1 show that very great differences may exist between the compositions of fine and coarse particles of samples of alloys, such as journal bearings, bearing metals, and type metals. In fact, the differences may be so great that material meeting a speci-

fication might easily be rejected on the basis of an analysis made largely on the fine portions of the sample. For example, in the case of the journal bearings the analysis of the coarse portion (on No. 20 sieve) passes the A. S. T. M. chemical composition requirement as to Cu 70 ± 1.5, Pb 25 ± 1.5, and Sn 5 ± 0.5, while the portion that passes through the No. 80 sieve fails by a large margin.

The data shown in Table 2 indicate that different sized particles of alloys, such as zinc-base die-casting alloys, aluminum sand-casting alloys, and duralumin do not show as great differences in composition as are illustrated in Table 1. The distinctly higher iron content of the finer portions of the samples is, however, to be noted. In these samples all particles which were sufficiently magnetic to be picked up by a small permanent hand magnet were removed before making the analyses, but this procedure is not a sufficient guaranty that the higher iron content of the finer portions may not be due to iron abraded from the cutting tools during preparation of the samples. The more significant point for the purposes of the present consideration, is that the coarse and fine portions of the sample do not correspond in iron content.

TABLE 2.—*Variations in the compositions of fine and coarse particles of the same sample*

ZINC-BASE DIE-CASTING ALLOYS

Constituent	Fineness					
	Sample No. 1		Sample No. 2		Sample No. 3	
	On No. 40	Through No. 40	On No. 40	Through No. 40	On No. 40	Through No. 40
Cu	2.82	2.82	2.86	2.84	2.95	2.95
Pb	.03	.03	.32	.32	.60	.60
Cd	.007	.004	.29	.29	.10	.09
Al	4.04	4.01	4.04	3.99	.57	.56
Mg	.11	.10	.10	.10		
Fe	.048	.082	.056	.083	.032	.033
Sn					5.95	6.01

ALUMINUM SAND-CASTING ALLOY

Constituent	Fineness	
	On No. 14	Through No. 100
Cu	7.7	7.4
Si	.34	.42
Fe	1.58	1.62

DURALUMIN

Constituent	Fineness		Constituent	Fineness	
	On No. 14	Through No. 100		On No. 14	Through No. 100
Cu	4.1	4.0	Mn	0.55	0.55
Si	.45	.46	Mg	.40	.41
Fe	.43	.49			

Difficulties caused by segregation alone might be illustrated by the tin content of the zinc-base die-casting alloy No. 3. This alloy was cast as a slab (36 by 6 by 1 inch) and showed 0.3 per cent less tin (5.7 as against 6.0) in the middle than on the edge of the slab.

The variations in composition shown by coarse and fine particles of samples of cast iron and of ferrotungsten are shown in Table 3.

TABLE 3.—*Variations in the compositions of fine and coarse particles of the same sample*

CAST IRON

(Free graphite blown out before sieving)

	Fineness		
	Through No. 30, on No. 40	Through No. 20, on No. 30	Through No. 14, on No. 20
Percentage of total carbon	2.04	2.27	2.[illegible]

FERROTUNGSTEN

Sample	Fineness			
	On No. 100	Through No. 100, on No. 200	Through No. 200, on No. 325	Through No. 325
	Per cent W	*Per cent W*	*Per cent W*	*Per cent W*
A		82.8		71.6
B (100 pounds, as received)	77.6	80.2	79.5	70.4
B′ (90 pounds ground for 90 hours to pass No. 325 sieve)				77.8
B″ (10 pounds residue reground)		92.0	90.5	92.0

In the case of cast iron, sampling for analysis is complicated by the fact that while the fine particles of cast iron contain less carbon than the coarse particles, there is also present a goodly amount of graphite which has been torn from all of the particles.

The analyses of ferrotungsten illustrate difficulties that were encountered in the preparation of a standard sample of ferrotungsten. Sample A was ground to pass a No. 100 sieve and when it was thoroughly mixed and sampled no difficulty was experienced in getting concordant determinations of tungsten that averaged 77.8 per cent. The question of homogeneity was raised, however, and the sample was sieved and the sieved fractions analyzed. The fraction passing through a No. 100 and held on a No. 200 sieve showed 82.8 per cent tungsten, while that passing a No. 325 sieve gave 71.6 per cent tungsten. Its use as a standard analyzed sample was given up because of the difference between the compositions of the particles. In view of the difficulties that were incurred in the preparation of sample A, sample B was sieved at the start and tungsten was determined in each fraction. The results were as follows: The portion held on a No. 100 sieve 77.6 per cent, the portion passing a No. 100 and held on a No. 200 sieve 80.2 per cent, the portion passing a No. 200 and held on a No. 325 sieve 79.5 per cent, and the portion passing a No. 325 sieve 70.4 per cent. As the fractions showed con-

siderable differences in tungsten content and no fraction was large enough by itself, it was decided to crush and sieve the material until most of it passed a No. 325 sieve. Ninety out of the original one hundred pounds was so obtained and then thoroughly mixed and analyzed. The remaining 10 pounds were reground for a time and sieved. The fractions of this 10-pound lot were analyzed as a matter of interest, but were not added to the standard.

III. CONCLUSIONS

If the sampling of a metallurgical material gives rise to particles that differ in size and in composition, the analysis must be made either on a single piece, on the whole sample, on a carefully sampled portion of a specially prepared sample, or on a portion which is made up of proportionate parts of the varying sizes of the sample. As a general rule, a single piece can not be expected to represent the original material. Neither can a sample that is so small that all of it can be taken for the analysis. If the whole sample is to be used, it is better as a rule to get enough sample to make it representative and then to take an aliquot portion for analysis after dissolving the sample and diluting to a definite volume. If portions are to be taken from a large sample, the ideal sample is one in which there is no extreme variation between the sizes of the particles. If the particles are all comparatively small, a fairly representative portion for analysis can be obtained by spreading the sample out and taking small dab portions as in assaying. If it is not feasible to obtain small particles, a more representative analysis is obtained in most cases by taking the sample so as to get as little fine material as possible, sieving or shaking out the fines, and choosing particles of a size that is commensurate with the degree of segregation in the material and the weight of the portion to be taken for the analysis. Such a procedure fails if the composition of the fines differs very markedly from that of the coarse particles (as graphite in cast iron) and the formation of appreciable amounts of fines can not be avoided. In this case as well as for the most accurate sampling of material in which the composition varies with the size of particles, it is necessary to separate the sample into three or more parts by sieving without loss by dusting, then to weigh each part, and to take a proportionate part of each for the analytical sample. This has long been the practice in umpire determinations of carbon in cast iron, although in this case it is usually inferred that the only reason for the procedure is to take care of the accumulation of graphite in the fines.

WASHINGTON, July, 1930.

A RADIOBEACON AND RECEIVING SYSTEM FOR BLIND LANDING OF AIRCRAFT

By H. Diamond and F. W. Dunmore

ABSTRACT

A radiobeacon and receiving system is described for use at airports to permit the blind landing of aircraft under conditions of no visibility. The system comprises three elements to indicate to the pilot the position of the aircraft as it approaches and reaches the instant of landing. Lateral position (that is, landing field runway direction) is given by a small directive beacon of the same type as employed for guidance on the airways, differing only in the use of smaller loop antennas and lower power. Longitudinal position along the runway (that is, approach) is given by a marker beacon. Height is given by an inclined ultra-high-frequency radio beam, used in such a way as to provide a very convenient gliding path for the landing airplane, free of all danger from obstructions.

The same medium-frequency receiving set required for obtaining radiotelephone and radio range beacon service on the airways is utilized for receiving the runway localizing and marker beacon signals. The course indications of the runway localizing beacon are observed on the same vibrating reed indicator as employed on the main radio range beacon, automatic control of receiving set sensitivity being provided to maintain substantially constant reed deflections regardless of the distance between airplane and transmitting station. The marker beacon indications are received aurally. A special high-frequency receiving set is required to receive the landing beam signals. The rectified output current of this set is passed through a d. c. microammeter mounted on the instrument board. By keeping the deflection of this microammeter at a fixed value, the pilot directs the airplane along the curved path coinciding with the line of equal intensity of received signal below the axis of the beam. The relative position of the airplane with respect to this convenient landing path is indicated by the rise or fall of the microammeter deflection above the fixed value.

CONTENTS

	Page
I. Introduction	898
1. The need for this development	898
2. Previous work	899
(*a*) Field localizers	899
(*b*) Landing altimeters	899
II. Radio system of blind landing aids, first arrangement	900
1. Installation at College Park, Md	900
(*a*) Runway localizing beacon	902
(*b*) Boundary marker beacon	903
2. Demonstrations by Guggenheim fund	903
(*a*) Special navigation instruments, altitude indication	905
III. Radio system of blind landing aids, improved arrangement	905
1. Landing beam	906
2. Experiments leading to development of landing beam	907
3. Other improvements	908
(*a*) Runway localizing beacon	908
(*b*) Boundary marker beacon	909
4. Use of the improved system	910
5. Further developments	912
(*a*) Runway localizing beacon	912
(*b*) Boundary marker beacon	915
(*c*) Expansion of system to take care of wind direction	915

IV. Description and operation of apparatus
1. Runway localizing beacon
2. Boundary marker beacon
3. Receiving system for localizing and marker beacon signals
4. Landing beam
(*a*) Theory of operation
(*b*) Directive transmitting antenna system
(*c*) The ultra-high-frequency transmitting circuit arrangement
(*d*) The receiving system
V. Practical applications
VI. Acknowledgment

I. INTRODUCTION

This paper describes the research on a radio system for the blind landing of aircraft carried on in the research division of the Aeronautics Branch of the Department of Commerce at the National Bureau of Standards, during 1928 to 1930.

The object of the research was to provide a simple and effective radio system which, when combined with the usual navigational instruments, would permit the safe landing of aircraft in fog or any condition of visibility or no visibility. This system was to be adaptable for use in conjunction with the radio navigational aids being provided for point-to-point flying on the civil airways of the United States. In accordance with the practice already adopted in the development of the navigational aids for the civil airways, all the complicated and expensive parts of the system were to be used on the ground, the equipment required on the aircraft being kept as simple as possible.

The system developed fulfills these requirements. The pilot receives the desired information with a minimum of effort on his part. The additional equipment required on the aircraft (for use of the blind landing aids) is very simple, weighing approximately 15 pounds.

1. THE NEED FOR THIS DEVELOPMENT

The practicability of the use of directional radio as an aid to point-to-point flying has been demonstrated by nearly two years of service given by the radio range beacon system on the fixed airways. By means of this system [1] the pilot can keep accurately on his course, know approximately the points he is flying over, and proceed unerringly to his destination. Scheduled air transport operation is thus immeasurably aided; many flights are made which could not possibly be made without the use of radio direction facilities. Nevertheless, interruption of scheduled flying is still the rule whenever the landing field lies in an area completely inclosed by fog. The results secured by the development of instrument flying and radio navigational aids are then nullified through the lack of means for safe landing at the desired destination, under conditions of poor visibility. The system of radio aids to blind landing described in this paper removes this last great hazard to the reliability of airplane travel, and insures the rigorous maintenance of scheduled flying by day or night.

[1] J. H. Dellinger and H. Pratt, Development of Radio Aids to Air Navigation, Proc. I. R. E., **16**, p. 8[illegible] July, 1928. H. J. Walls, The Civil Airways and Their Radio Facilities, Proc. I. R. E., **17**, p. 2141; December, 1929. J. H. Dellinger, H. Diamond, and F. W. Dunmore, Development of the Visual Type Radio-beacon System, B. S. Jour. Research, **4** (RP159), p. 425; March, 1930; Proc. I. R. E., **18**, p. 796; May, 193[illegible]

2. PREVIOUS WORK

The present development differs from much of the earlier work in this field in its emphasis on directional radio transmission, thereby simplifying the receiving installation on the airplane. A system of blind landing aids must, in general, indicate to the pilot the position of the aircraft in three dimensions as it approaches and reaches the instant of landing. In practically all previous experimentation this problem has been resolved into two separate problems; namely, field localizing and means for securing suitable height indication.

(a) FIELD LOCALIZERS

The arrangement usually adopted for field localizing has involved the use of "leader cables." Typical installations are those of the British Government at Farnborough [2] and of the French Government at Chartres. The British installation employs a complete circuit around the landing field with a visual indicating device on the airplane instrument board. The French installation uses straight cables. The Loth Co., of Paris, and several agencies in this country, including the United States Air Corps at Wright Field, Dayton, Ohio, and the Ford Motor Co. at Detroit, Mich., are experimenting with various arrangements employing leader cables.

An obvious disadvantage of the leader-cable method of field localizing is its great cost. This method generally involved the burying of cables outside the limits of the landing field, thereby introducing the expense of securing right of way, in addition to the actual cost of equipment and installation.

(b) LANDING ALTIMETERS

In several of the leader-cable systems, the diminution of intensity of the magnetic field surrounding the cable for increasing distance from the cable is utilized for securing altitude indication. Theoretically, the intensity of the magnetic field varies inversely as the height above the cable. A suitable instrument on the airplane used for measuring the magnetic field intensity may therefore be calibrated directly in height above ground. Accurate altitude indication is then obtained, provided the airplane is neither banking nor turning when passing over the cable. This condition is rather difficult to achieve during blind flight, particularly since the airplane is at the same time being maneuvered to maintain a definite "course" in accordance with signals received from the leader-cable system. A second difficulty exists in the necessity for the instrument to have the same calibration for all landing fields. This requires close equality of the magnetic field intensities at different installations, and also requires that no distortion of the shape of the magnetic field exist.

The problem of securing reliable altitude indication, particularly during the last few hundred feet above ground, is a difficult one. The barometric altimeter, in common use on aircraft, is inadequate for the purpose, since it indicates primarily air pressure and not height above the ground.

Experiments are being undertaken by a number of organizations looking toward the development by several means of altimeters indicating the absolute height above ground. One is the development

[2] H. Cooch, J. Royal Aeronautical Soc., **30**, p. 365; 1926.

of a sonic altimeter.[3] The time taken by sound to reach the ground and return to the airplane is measured. Knowing the velocity of sound, the height of the airplane above ground may be determined. Another device is the capacity altimeter[4] which measures the distance from the ground by detecting the change in the electrical capacity between two plates on the airplane as the airplane approaches the ground. A third method is by the use of direct reflection with radio waves.[5] It is doubtful at the present time whether any of these instruments will be sufficiently sensitive or accurate for making normal landings in dense fog. These instruments when available will, however, be exceedingly valuable in maintaining a safe altitude during point-to-point flying, and may prove of some service during landing operations, as will appear below.

II. RADIO SYSTEM OF BLIND LANDING AIDS, FIRST ARRANGEMENT

The success obtained with the radio range beacon system in its application to point-to-point flying early suggested its possibilities as a field localizer. With the main beacon used for guiding an airplane to a given landing field, a low-power beacon with small loop antennas could be employed for marking out the major, or any desirable axis of the landing field. A low-power marker beacon could then be used for defining the hazard-free approach to the field (along the axis or runway selected), and for indicating the longitudinal position of the aircraft along that runway. This system offered two outstanding advantages: (1) The same equipment required on the airplane for utilizing the radio navigational aids on the fixed airways was sufficient for the reception of the signals from the runway localizing beacon and marker beacons; (2) the ground equipment was comparatively simple and inexpensive, a transmitter of moderate power for the runway localizing beacon being adequate for marking out a course for a distance range of approximately 15 miles. The marker beacon power requirements were also very small. In addition, all apparatus could be kept within the confines of the airport.

1. INSTALLATION AT COLLEGE PARK, MD.

The bureau accordingly began the installation of a system of this type at College Park, Md., in order to test its practicability. A series of flight tests demonstrated its complete feasibility for landing field localization. The problem of altitude indication still required solution at the time of these early tests.

Figure 1 illustrates the layout of the ground tansmitting equipment in this radio system for field localization. The 2 kw directive radiobeacon, with large loop antennas, shown at *A*, is the main radio range beacon of the type provided by the United States Department of Commerce for point-to-point flying on the fixed airways. This beacon is normally located just off the airport (so that the loop antennas may not constitute an obstruction to flying), and serves to

[3] Das Behmlot und seine Entwicklung als akustischer Höhenmesser für Luftfahrzeuge, A. Behm, Heft. 13, p. 56; May, 1926. Jahrbuch der Wissenshaftlichen Gesellschaft für Luftfahrt.
[4] L. A. Hyland, True Altitude Meters, Aviation, 25, p. 1322; October 27, 1928.
[5] E. F. W. Alexanderson, Height of Airplane Above Ground by Radio Echo, Radio Engineering, 9, pp. 34–35; February, 1929.

direct an incoming airplane to the vicinity of the airport. Utilizing the zero-signal zone directly over the beacon tower, it is possible to locate this beacon to within 100 to 1,000 feet, depending upon the altitude of the airplane. The drop to zero vibration amplitude of the reeds on his course indicator, therefore, gives the pilot his exact location with respect to the landing field and also with respect to the course radiated by the low-power (200-watt) runway localizing beacon *B*. The localizing beacon, using small loop antennas so that it may be located at one edge of the landing field without constituting an obstruction, directs a course along the major axis of the field. It operates on a radio-frequency separated by 50 to 60 kc from that of the main beacon *A*, thereby preventing interference from the main beacon.

Upon receiving the zero-signal indication when directly over the tower of the main beacon, the pilot retunes his receiving set to the frequency of the localizing beacon and through the use of his compass

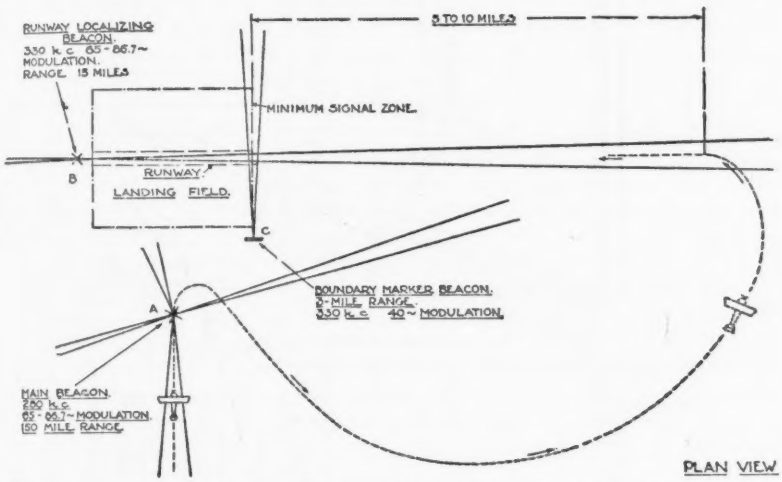

FIGURE 1.—*Layout of ground transmitting equipment for radio system of field localization*

and knowledge of the geography of the field, orients himself along the major axis of the field. The course indications received on the reed indicator greatly facilitate this maneuver. When crossing the boundary of the landing field a signal from the marker beacon *C*, operating on the same radio-frequency as the localizing beacon *B*, is obtained.

Summarizing, the complete system provides course and position indication by means of the main beacon *A*, landing field runway direction by means of the localizing beacon *B*, and longitudinal position (that is, approach) along the runway by means of the marker beacon *C*. On the airplane a simple receiving set is sufficient to receive all these indications. If accurate indications of the absolute height of the airplane above ground could have been secured in the early tests, the complete information necessary for the blind landing of aircraft (in addition to that obtained from the flight instruments) would have become available.

a) RUNWAY LOCALIZING BEACON

In the installation at College Park, the main beacon *A* and the localizing beacon *B* were of the visual type, the essential difference

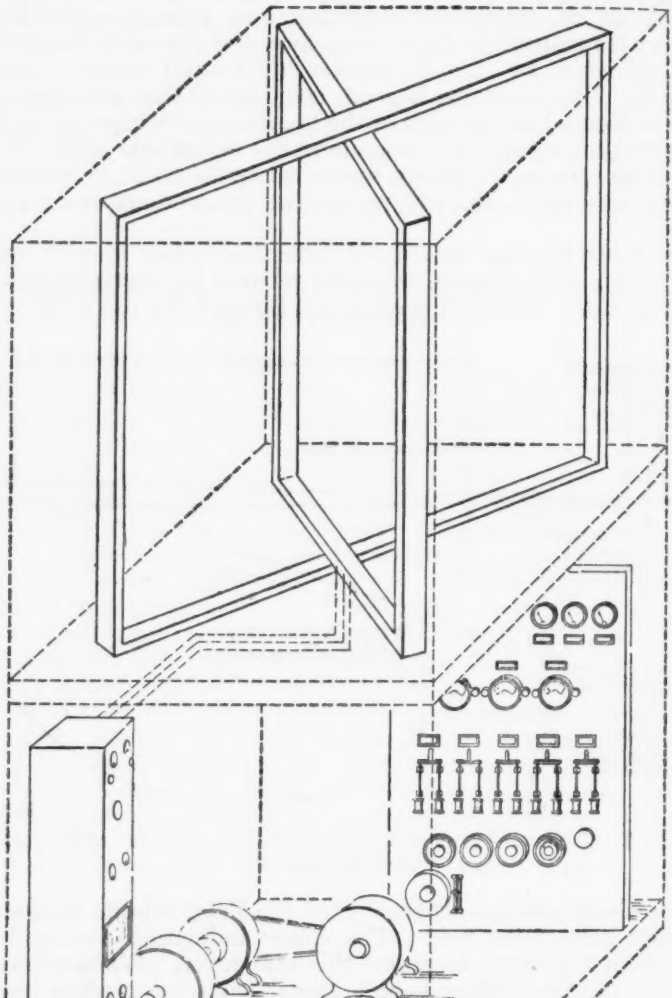

FIGURE 2.—*Runway localizing beacon set-up, showing location of loop antennas, transmitting set, and power equipment*

between the two being the number of beacon courses radiated, the power ratings of the final amplifying stages, and the dimensions of the loop antennas. A description of the visual-type beacon is given

in the third paper of footnote 1. This publication gives full details of the transmitting system for the main radio range beacon. Some idea of the set-up required for the localizing beacon may be had from the three-dimensional view given in Figure 2. The two loop antennas, crossed at 90°, carry currents of the same carrier frequency but modulated to different low frequencies, 65 and 86.7 cycles, respectively. These antennas are so oriented that the vertical plane containing the major axis of the landing field bisects the angle between the two antennas. An airplane flying in this plane, therefore, receives equal signals from the antennas. On either side of this plane the signal received from one antenna is greater than from the other. On the airplane a visual indicating instrument is employed,[6] consisting of two vibrating reeds mechanically tuned to the two modulation frequencies of the beacon and actuated by small electromagnets connected in the output circuit of the receiving set employed. When the beacon signals are received, the two reeds vibrate, comparison of their relative amplitudes of vibration serving to indicate the relative amount of signal received from the two loop antennas. On course (that is, along the plane bisecting the angle between the two antennas) the reed vibration amplitudes are equal. Off the course they are unequal, the reed vibrating with the greater amplitude being on the side to which the airplane has deviated. Figure 3 illustrates how the reed indications appear to the pilot, (*a*) when off the course to the left, (*b*) when on the course, and (*c*) when off the course to the right.

By adjusting the time phase displacement between the carrier currents in the two loop antennas, the number of courses provided by the beacon may be made either two or four. The four-course arrangement is more convenient for use on the long-range beacons on the fixed airways. The two-course adjustment is, however, more desirable for the localizing beacon, since in coming in for a landing the presence of the courses at right angles to the runway might prove confusing. A polar diagram corresponding to this adjustment, showing the relative deflections of the two reeds comprising the course indicator as a function of angular deviation from the beacon course, is given in Figure 4.

(b) BOUNDARY MARKER BEACON

The marker beacon *C* consisted of a 50-watt transmitter feeding a loop antenna, oriented as shown in Figure 1. Modulation of the radiated wave to the desired frequency, 40 cycles per second, was obtained by supplying the transmitting tube with a plate voltage of 40-cycle frequency. On the airplane a 40-cycle reed indicator (see fig. 5) connected in series with the main course indicator, was employed. The landing-field boundary line was thus defined by a zero signal zone, 2° or 3° wide. The pilot observed an increasing deflection of the marker beacon reed as he approached the edge of the landing field, a decrease to zero deflection as he passed over the boundary line, then an increasing deflection as he came within the landing-field area.

2. DEMONSTRATIONS BY GUGGENHEIM FUND

The practicability of the system of field localization outlined above, in application to actual blind landings, was demonstrated by Lieut.

[6] F. W. Dunmore, Design of Tuned-Reed Course Indicators for Aircraft Radiobeacon, B. S. Jour. Research, **1** (RP28); November, 1928.

J. H. Doolittle, of the Daniel Guggenheim Fund for the Promotion of Aeronautics, in tests carried on at Mitchel Field, Long Island, during July to December, 1929. During the latter part of 1928 the Guggenheim Fund conducted an extensive survey of methods likely to lead to the solution of the problem of landing in fog. The Bureau of Standards submitted a report to the Guggenheim Fund outlining essentially the system described above, and volunteered to make an installation at Mitchel Field similar to the one already under way at College Park. Arrangements for this cooperation were made in January 1929, the bureau agreeing to install a runway localizing beacon and

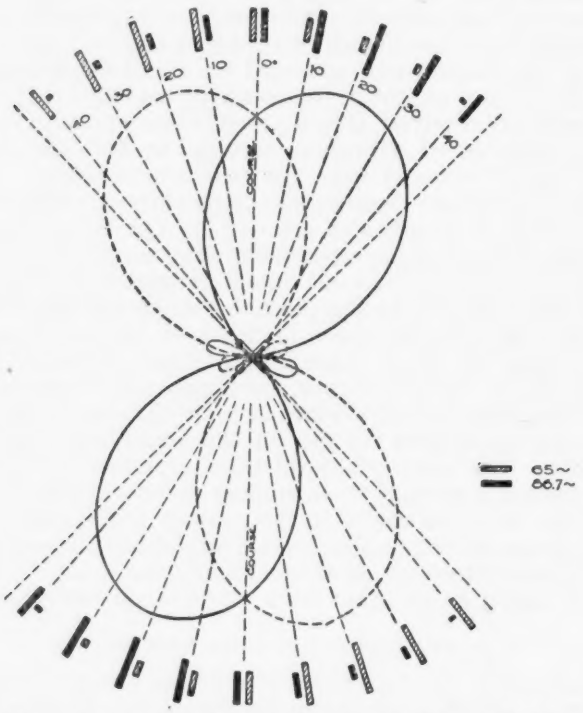

FIGURE 4.—*Polar diagram showing relative reed deflections as a function of angular deviation from the runway localizing beacon course*

suitable marker beacon. An aural type beacon, installed by the United States Air Corps, was to serve as the main directive radiobeacon.

The installation was completed in July, 1929, and was a material factor in enabling Lieutenant Doolittle, seated in a completely inclosed cockpit, to take off, circle the field, and make a satisfactory landing. A brief description [7] of the method of landing employed is considered of value here, particularly to serve as a basis of requirements for a blind landing system, and also as a comparison with the

[7] A complete description is given in the following two pamphlets issued by the Daniel Guggenheim Fund for the Promotion of Aeronautics: (1) Solving the Problem of Fog Flying, 52-page pamphlet; Oct. 9, 1929. (2) Equipment Used in Experiments to Solve the Problem of Fog Flying, 57-page pamphlet; Mar. 1930.

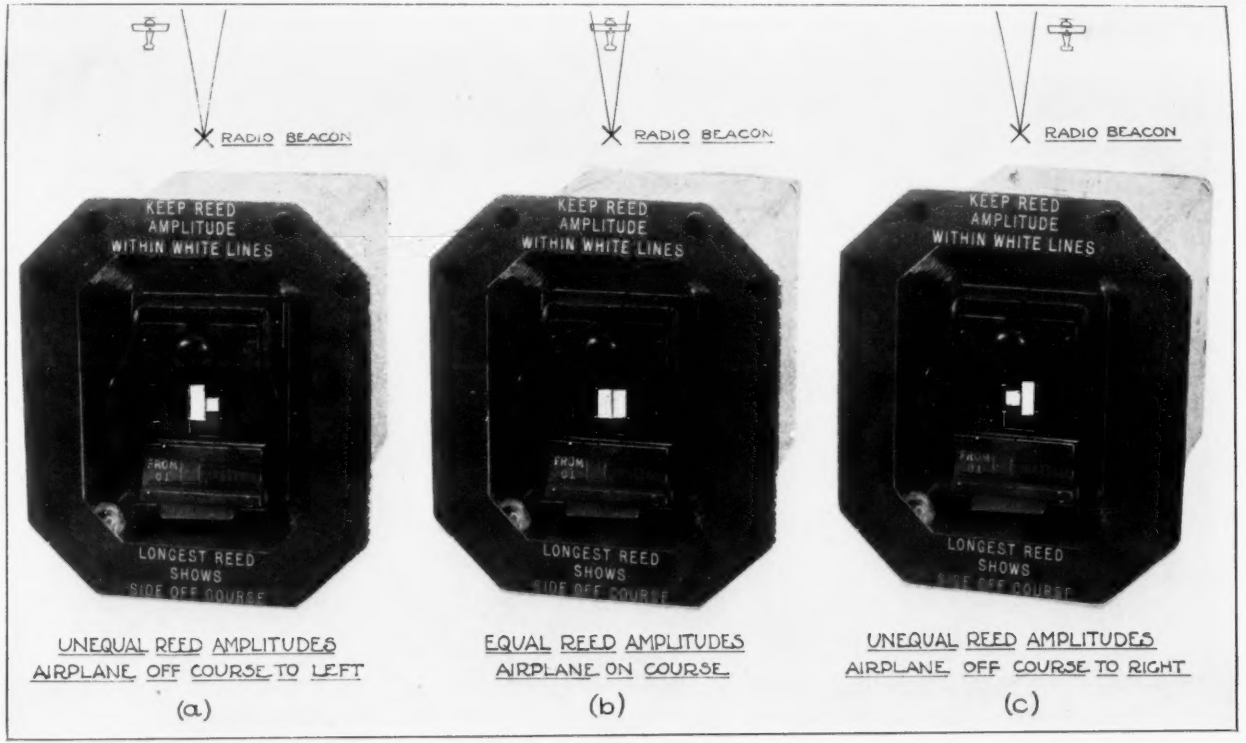

FIGURE 3.—*Course indications as received on vibrating reed-course indicator*

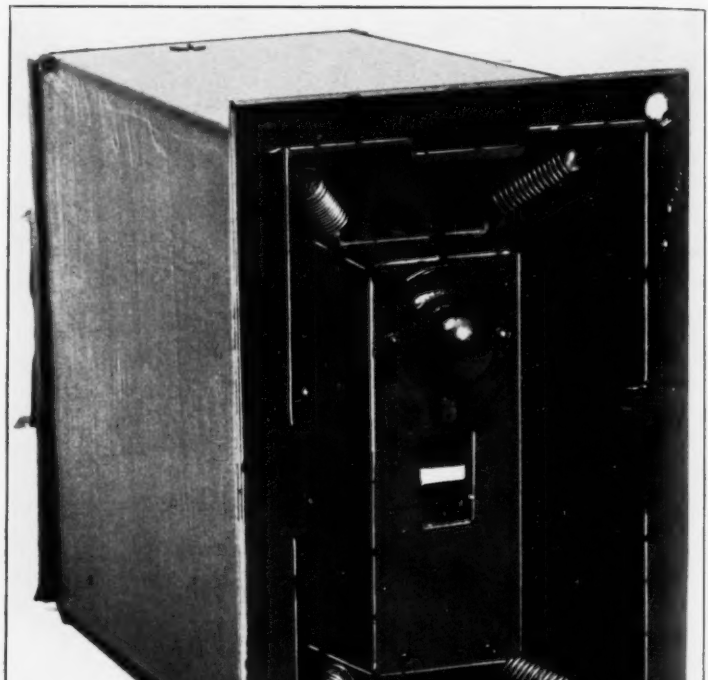

FIGURE 5.—*Marker beacon reed indicator*

Reed tuned to 40 cycles.

proved system of radio landing aids more recently developed by the Bureau of Standards at College Park, Md., and described in Section III below.

(a) SPECIAL NAVIGATION INSTRUMENTS, ALTITUDE INDICATION

In addition to the means for receiving the directional radio aids outlined, the airplane was equipped with standard engine and navigation instruments, including tachometer, compass, bank and turn indicator, air speed indicator, altimeter, rate-of-climb indicator, and three special instruments—an artificial horizon instrument, a directional gyroscope, and a sensitive barometric altimeter with a range of 20,000 feet graduated in 10-foot intervals.

The artificial horizon instrument gave at all times the attitude of the airplane with respect to the true horizon. The directional gyroscope was employed to maintain a steady course or to change the course by any desired amount. Lieutenant Doolittle used this instrument as an aid to flying on the localizing beacon course. He observed a natural tendency, when the beacon course narrowed, to fly a zig-zag course, first on one side of the beam and then on the other. He was better able to approximate a straight line by utilizing the directional gyroscope for making the necessary slight changes in the course as indicated by the reed indicator.

The sensitive altimeter was designed to secure height indications of the maximum possible accuracy. Provision was made for adjustment of the altimeter in the air, for any apparent change in ground altitude due to a change in barometric pressure, in accordance with information secured through two-way radio communication with the ground. In spite of these precautions, careful tests on the instrument indicated that a probable error of the order of 30 to 40 feet in reading absolute height above the ground was still obtained. The procedure of landing, therefore, resolved itself into maneuvering the airplane into a glide from a position in space of fixed bearing and altitude with respect to the landing field. The glide continued until contact with the earth was made, the oleo landing gear taking up the shock of contact. The lack of knowledge of the absolute height to the necessary accuracy prevented the usual "flattening out" in landing.

The lessons learned from these demonstrations were many. Perhaps the most important was that the problem of securing suitable indications of the true height above ground still required attention. The need for two-way communication with the ground in order to correct the altimeter to the proper barometric pressure seemed excessive. In addition, the absolute height could not be determined to the proper accuracy. When developed, it is probable that one of the absolute type altimeters, described in Section I above, would be preferable to the sensitive barometric altimeter for determining the altitude from which the glide should be started. The accuracy of height indication would probably be increased thereby, and the need for two-way communication with the ground obviated.

III. RADIO SYSTEM OF BLIND LANDING AIDS, IMPROVED ARRANGEMENT

Meanwhile, in the experiments carried on at College Park, the Bureau of Standards continued to work on improvements to the radio system of aids to blind landing. A general idea of the operation

of the improved system developed may be had by reference to

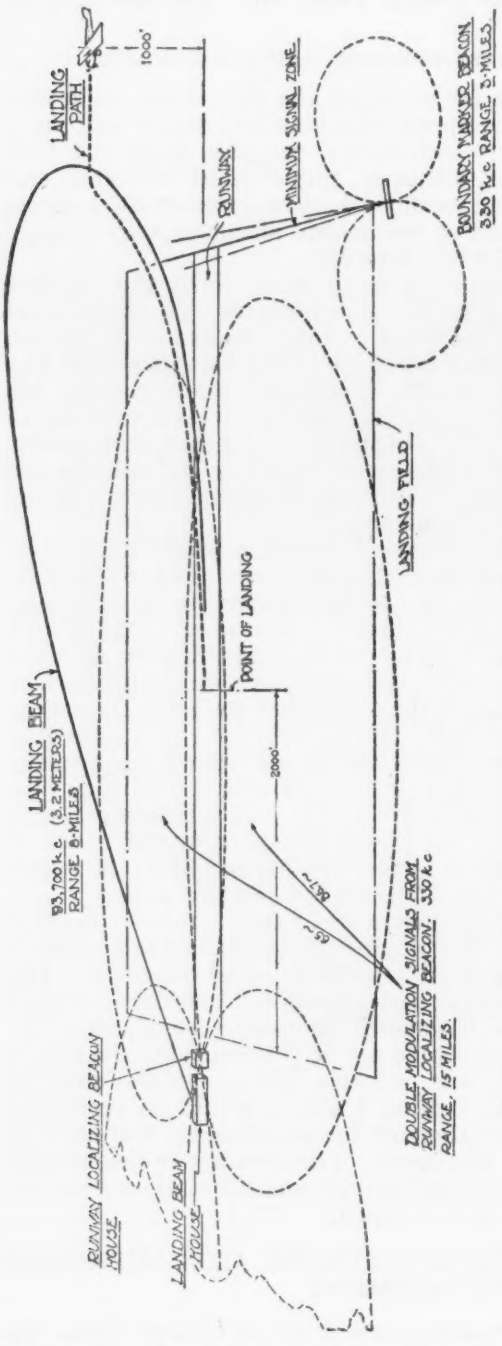

FIGURE 6.—*A 3-dimensional view showing improved radio system of blind landing aids*

three-dimensional illustration shown in Figure 6. The main range beacon (*A*, fig. is still employed, though not shown in Figure Lateral position (that is, landing-field runway direction) is still given by a runway localizing beacon, and longitudinal position (that approach) by a landing-field boundary-marker beacon. Numerous improvements in the operation and use of these elements have been effected. The major difference from the system illustrated in Figure 1 consists in the means provided for furnishing to the pilot accurate altitude position of the airplane as it approaches and reaches the instant of landing. A landing beam, utilizing directive transmission from the ground, is employed for this purpose.

1. LANDING BEAM

The landing beam transmitter operates on an ultrahigh-frequency of the order of 100 megacycles. The transmitting system employed, including the directive antenna array, is shown in Figure 7. The resultant beam is horizontally polarized, requiring the use of a horizontal doublet antenna on the airplane for its reception. (See fig. 8.) The beam is directed at a small angle above the horizontal,

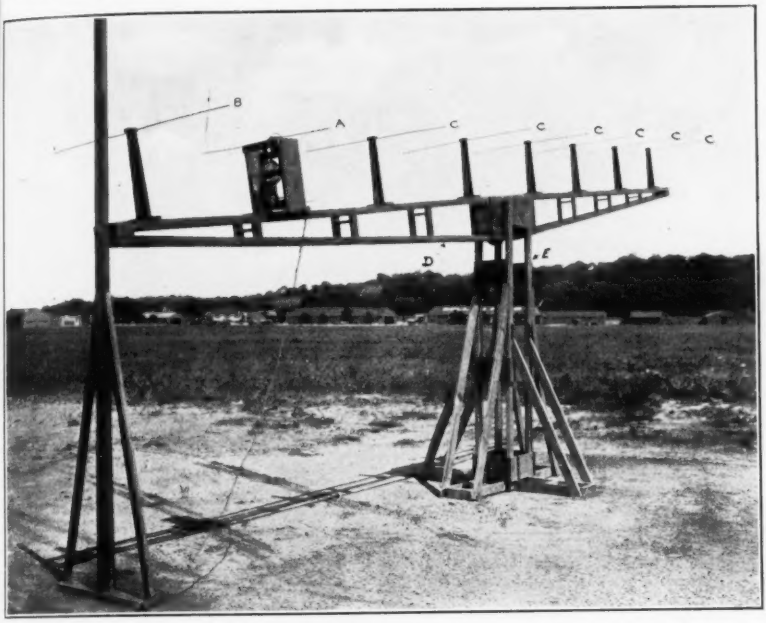

FIGURE 7.—*Landing beam transmitting system, showing electron-tube oscillator and directive antenna array*

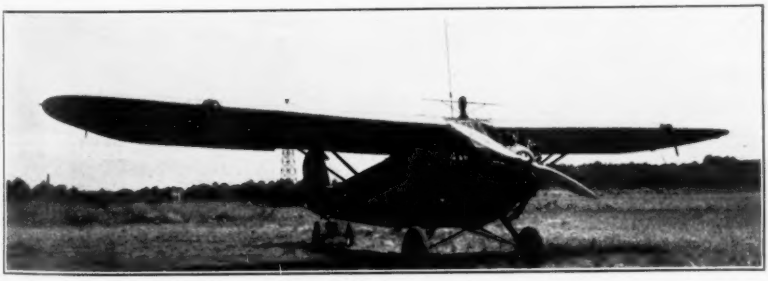

FIGURE 8.—*Bureau of Standards' experimental airplane showing horizontal doublet antenna used for receiving the landing beam signals*

FIGURE 9.—*Landing beam indicator used on the pilot's instrument board to show the relative position of the airplane with respect to the proper landing path*

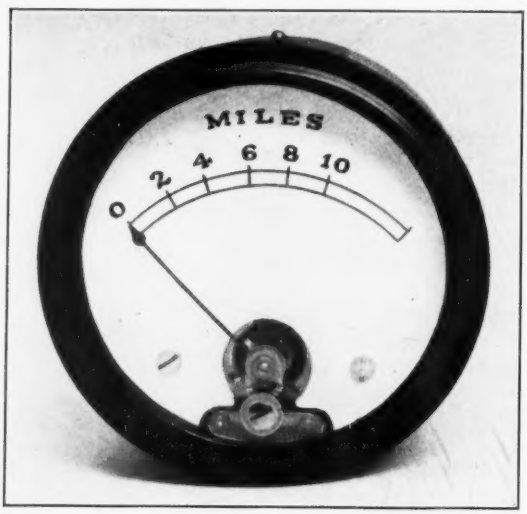

FIGURE 10.—*Rough distance indicator used on the pilot's instrument board to show the approximate distance of the airplane from the runway localizing beacon transmitter*

and is used in such a way as to provide a very convenient gliding path for the landing airplane, beginning at any desired elevation (within, say 500 to 5,000 feet) and at a corresponding distance from the landing field of 2 to 5 miles. Sixty-cycle modulation of the landing beam transmitter is provided to facilitate audio-frequency amplification at the receiving end.

On the airplane, a special high-frequency receiving set is used for receiving the landing beam signals. The signal current in the output circuit of the receiving set is rectified and passed through a d. c. microammeter mounted on the instrument board. The airplane does not fly on the axis of the beam, but on a curved path under the beam whose curvature diminishes as the ground is approached. The path is the line of equal intensity of received signal below the axis of the beam. The diminution of intensity as the airplane drops below the beam axis is compensated by the increase of intensity due to approaching the beam transmitter. Thus, by flying the airplane along such a path as to keep the deflection of the microammeter on the instrument board constant, the pilot comes down to ground on a curved line suitable for landing. Figure 9 shows the microammeter used for the landing beam indications. To facilitate its use by the pilot this instrument is mounted on its side so that the pointer moves vertically rather than horizontally. The deflection to be kept constant is chosen at half-scale reading, the instrument pointer being then in a horizontal position. A rise of the pointer above this position indicates that the airplane is above the proper landing path, while the reverse is true if the pointer falls below its horizontal position. The indications of the position of the airplane relative to the landing path are thus made readily comprehensible.

Several important advantages obtain for this method of furnishing altitude indication. The landing path may be so directed as to clear all obstructions. The pilot following the landing path is automatically kept above obstructions and no longer needs a thorough knowledge of the terrain in order to effect a safe landing. Secondly, the landing path may be of different shape to suit different landing fields. This is of particular importance in getting into a small field. A third advantage lies in the fact that in the act of following the landing path, the pilot automatically "levels off," thereby facilitating a normal landing, albeit somewhat fast. In following the landing path prior to receiving the marker beacon zero-signal zone, the pilot maintains an air speed somewhat above the landing speed of the airplane, insuring complete controllability with some margin to spare. Upon receiving the marker indication that he is passing over the boundary of the field, the margin over the landing speed may be reduced. The landing is therefore made at a speed more nearly approaching the normal landing speed of the airplane. A fourth advantage is that the landing glide may be begun at any desired altitude, within a rather wide range (say, 500 to 5,000 feet). A fifth advantage arises from the ease of using the landing beam indications. No manipulations on the part of the pilot are required. The tuning is fixed. Since a line of constant field intensity is followed no control of volume is necessary.

2. EXPERIMENTS LEADING TO DEVELOPMENT OF LANDING BEAM

At this point, it may be of interest to describe the experiments which led to the development of the landing beam. The object of the

first experiments along this line, early in 1929, was to mark out an equisignal path in space similar to that obtained with the visual-type beacon, but making a constant angle with the horizontal; that is, with the ground. To this end the same transmitting set-up as for the localizing beacon was employed, the two crossed loop antennas being turned over on their sides. This experiment proved unsuccessful because of ground reflection phenomena on the long waves used (about 300 kc).

The next step was to employ directed waves of higher frequencies. Ultrahigh-frequencies, of the order of 60 to 100 megacycles, were chosen in order to reduce the size of the antenna arrays. Two beams were required, both of the same radio-frequency but each modulated to a different low frequency, and its axis making a different small angle with the horizontal. The equisignal zone would, therefore occur where the two beams intersected; that is, along a line making an angle with the ground intermediate to the two angles formed by the axes of the two beams and ground. It was recognized that some difficulty would be met in setting up the transmitting circuit arrangement necessary for this system, on the ultrahigh-frequencies considered, since a common master oscillator feeding two balanced amplifier branches, each modulated to a different low frequency, was required. Moreover, making use of the equisignal zone, once it was set up, would add another volume control for the pilot to adjust as he approached the point of landing. The construction of suitable apparatus was, however, begun.

It was at this stage of the development that one of the authors[8] conceived the idea of using only one high-frequency beam in the manner described in Section III, 1, thereby eliminating the technical difficulties noted and at the same time providing a more suitable gliding path for the landing airplane. The obvious simplification of equipment both on the ground and on the airplane led to the adoption of this idea.

3. OTHER IMPROVEMENTS

(a) RUNWAY LOCALIZING BEACON

The runway localizing beacon employed in the improved system of blind landing aids, while still operating on the same principles as previously, has been made considerably easier to use. In the installation at Mitchel Field and the early installation at College Park, the equisignal zone or course was found to be somewhat broad, of the order of 4° to 5°. The use of small, multiturn loop antennas rendered it somewhat difficult to obtain exact 90° electrical displacement between the two. Some inductive coupling between the two antennas, therefore, existed, tending to broaden the course. The use of a small anticoupling device solved this difficulty, the width of the beacon course being reduced to 2°.

At the receiving end, some difficulty in following the course was experienced owing to the necessity for adjusting the receiving set sensitivity as the airplane approached the beacon transmitter. Since the beacon signals are followed from a distance of 10 miles from the transmitter to approximately 2,000 feet from the transmitter (the

[8] F. W. Dunmore.

point of landing), variations in the field intensity of the order of 50 to 1 obtain. Continuous adjustment of the receiving set volume control was therefore necessary, in order to keep the reed deflections within scale. The pilot, in making a landing, is, however, concerned with so many things that keeping the necessary close adjustment of the receiving set sensitivity becomes a troublesome task. To overcome this difficulty, an automatic volume-control device was developed for maintaining essentially constant receiving set output voltage regardless of the magnitude of the input voltage. The use of the runway localizing beacon thereby resolved itself simply to observing the course indications on the reed indicator and maneuvering the airplane to keep on the course.

The design of the automatic volume-control device was affected by the type of boundary marker beacon used, as will appear below. At this point it is sufficient to note that it operates through rectification of the alternating voltage across the reed indicator terminals and application of the rectified voltage, after filtering, as a negative biasing voltage on the grids of the radio-frequency amplifying tubes of the receiving set. An increase in the input voltage to the receiving set normally tending to increase the voltage across the indicator terminals is, therefore, accompanied by an increase in the negative bias on the radio-frequency amplifying tubes and, consequently, by a reduction in the receiving set sensitivity such as to maintain substantially constant voltage across the reed indicator.

The provision of this automatic volume-control device made possible the addition of an important instrument on the airplane instrument board, giving the pilot information as to his approximate distance from the localizing beacon transmitter. Since increasing input voltage to the receiving set is accompanied by increasing negative biasing voltage on the grids of the radio-frequency amplifying tubes, the deflection of a direct-current milliammeter connected in the plate circuit of these tubes will decrease as the airplane approaches the beacon transmitter. This meter (see fig. 10) may, therefore, be calibrated directly in approximate distance from the transmitter. Its calibration will hold roughly on different localizing beacons at different airports, provided these beacons are of approximately the same power ratings. Its chief function is, however, to give the pilot an added check that he is approaching or departing from the landing field and should aid materially in avoiding confusion during blind flight.

(b) BOUNDARY MARKER BEACON

In the first arrangement of blind landing aids, the boundary marker beacon signals were received on the airplane on a special reed indicator connected in series with the vibrating reed course indicator. Several factors combined to point out that aural indication might prove preferable in this case. The pilot, during landing, must focus attention on a number of instruments giving continuous information as to course, altitude of the airplane, air speed, etc. It was felt that he might easily miss the indications given by the marker beacon reed during the short period when he passed over the landing field boundary line. Aural indication would preclude this possibility. Aural indication also offered a further advantage. The ear is a

logarithmic device while the reed indicator has a linear response. Proper matching of the powers of the marker beacon and localizing beacon, so that signals from the two may be received at a given point or area for the same sensitivity adjustment of the receiving set, is therefore less exacting when aural marker beacon indications are employed. The marker beacon modulation was, therefore, changed from 40 to 1,000 cycles to facilitate aural reception.

A rather novel requirement comes up in connection with the use of the marker beacon. It will be recalled that the runway localizing and boundary marker beacons both operate on the same carrier frequency, and are both received simultaneously on the medium-frequency receiving set. Using automatic volume control, it is required to hold the voltage across the vibrating reed course indicator constant, while the marker beacon signal must be permitted to vary through a minimum. This requirement was met through the use of a filter circuit arrangement connected in the receiving set output which served to direct frequencies below 200 cycles to the reed indicator and frequencies above that value to the head telephones. The automatic volume control device is connected across the reed indicator terminals as before and, consequently, is operated only by the signals from the localizing beacon (no voltage of 1,000-cycle frequency appearing across the indicator). The 1,000-cycle marker beacon signal heard in the head telephones, since it does not affect the automatic volume control device, is therefore permitted to vary through a minimum, as required.

4. USE OF THE IMPROVED SYSTEM

Having outlined the function of each element of the complete system of blind landing aids, it is desirable at this point to consider the apparatus required on the airplane for making use of these aids. Figure 11 shows a complete airplane installation. The medium-frequency receiving set *A*, using mast antenna *B*, is normally employed for the reception of the weather broadcast and radiobeacon services. This set is also used for receiving signals from the runway localizing and marker beacons. To the output of this set is connected the filter unit *C* which directs the main and localizing beacon signals to the reed indicator *D*, and the boundary marker beacon signals to the head telephones. The automatic volume control device *E* is connected across the reed indicator terminals, its operation serving to maintain substantially constant reed deflections and at the same time governing the scale reading of the instrument *F*, which indicates roughly the distance from the beacon transmitter.

The receiving set for the reception of the ultrahigh-frequency landing beam signals consists of a detector unit *G* mounted in the stream-lined housing which supports the receiving dipole antenna structure *H*. *I* is the amplifier-rectifier unit. The rectified output current is fed to the landing beam indicator *J*. The remote control panels for the medium-frequency and ultrahigh-frequency sets are shown at *K* and *L*, respectively. *M* contains the batteries necessary for operating these sets.

The instrument board on the bureau's experimental airplane is shown in Figure 12. The reed indicator is shown at *A*, the landing beam indicator at *B*, and the rough distance indicator at *C*. At *D*

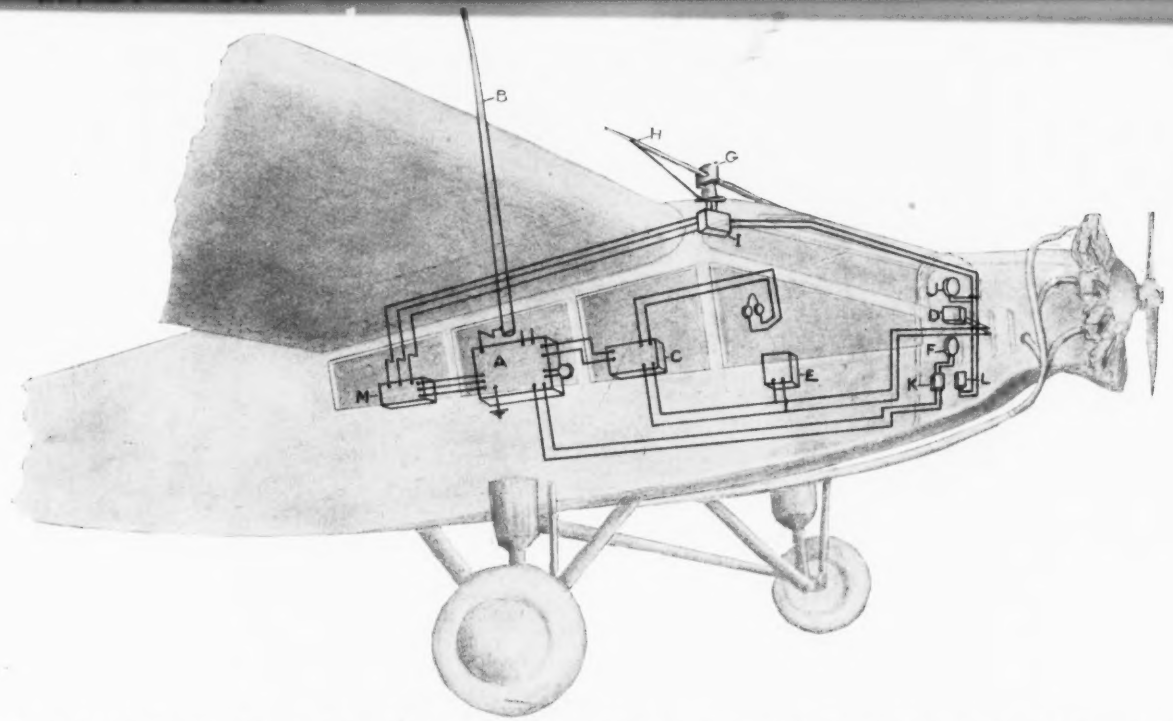

FIGURE 11.—*Complete airplane installation showing radio equipment required to make use of the radio system of blind landing aids*

Note that the medium-frequency receiving set is also employed for radiotelephone and radiobeacon service on the airways. *A*, Medium-frequency receiving set for voice and beacon signals; *B*, 6-foot vertical pole antenna; *C*, filter unit for separating voice and beacon signals; *D*, tuned-reed visual course indicator; *E*, automatic volume control for beacon signals; *F*, rough distance indicator; *G*, landing beam receiving set detector unit; *H*, horizontal doublet antenna for landing beam receiving set; *I*, landing beam receiving set amplifier unit; *J*, landing indicator, 0 to 500 microammeter; *K*, pilot's control unit for medium-frequency receiving set; *L*, pilot's control and test unit for landing beam receiving set; *M*, A, B, and C, batteries.

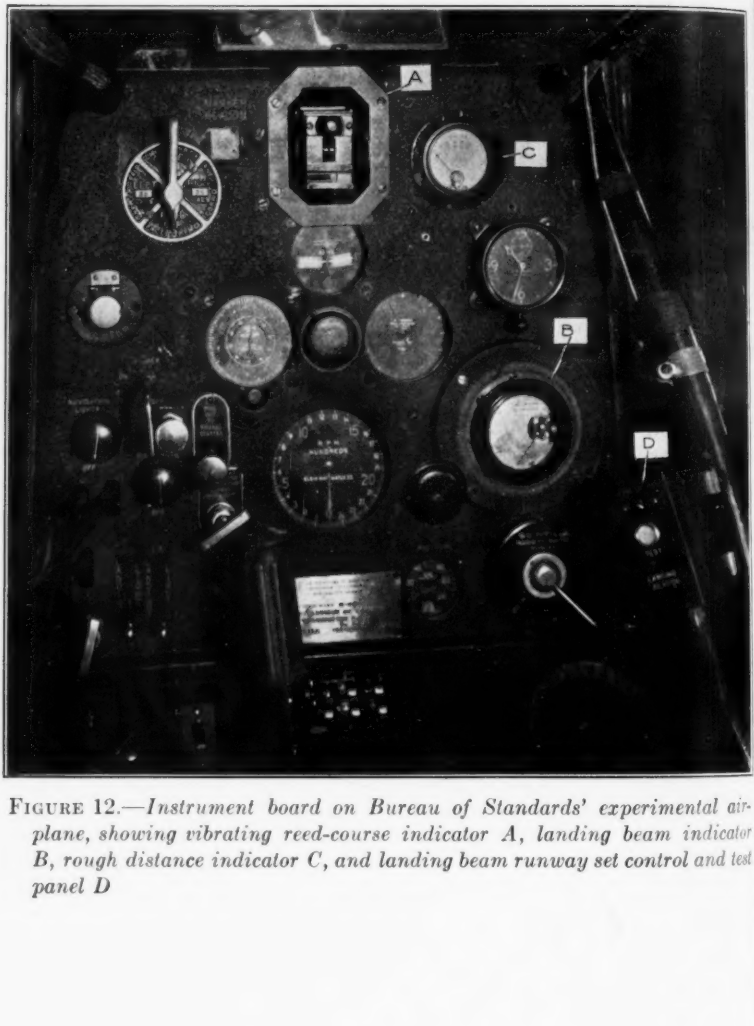

FIGURE 12.—*Instrument board on Bureau of Standards' experimental airplane, showing vibrating reed-course indicator A, landing beam indicator B, rough distance indicator C, and landing beam runway set control and test panel D*

is shown the control panel for the landing beam receiving set. The control panel for the medium-frequency receiving set is not shown.

Let us now consider the operations required on the part of the pilot in making a blind landing. It is assumed that the information necessary for maintaining the airplane in stable flight is available through the use of suitable flight instruments. The medium-frequency receiving set is tuned to the frequency of the main radio range beacon (say, 280 kc) and indications as to the correct course leading to the vicinity of the airport observed on the reed indicator. Since automatic control of volume is provided, these course indications are available to the pilot without manipulation on his part.

Upon receiving the zero-signal indication when directly over the tower of the main beacon, the pilot retunes the medium-frequency receiving set to the frequency of the localizing beacon (say, 330 kc) and throws a switch which places the landing beam receiving set in operation. These are the only adjustments of radio equipment required of the pilot during the entire landing maneuvers. The reed indicator now furnishes information as to the landing field runway direction, the provision of automatic volume control again relieving the pilot of the necessity for adjusting the receiving set sensitivity for variations in the distance between the airplane and the localizing beacon transmitter. The pilot next orients himself along the major axis of the landing field utilizing his compass indications, together with his knowledge of the geography of the field. As noted in connection with Figure 1, the reed indicator aids considerably in this maneuver. The airplane may be kept at any altitude within, say 500 to 5,000 feet. From time to time the pilot glances at the rough distance indicator and endeavors to get on the runway course at a point approximately 5 to 10 miles distant from the landing field. He now directs his airplane along the runway course and in the direction of the landing field, glancing occasionally at the landing beam indicator. When approximately half the distance to the field is covered, the pointer of the landing beam indicator begins to rise to midscale or horizontal position. When this position is reached, the pilot knows that he is at a point on the gliding path. To follow the gliding path he must maneuver the airplane to keep the pointer in the horizontal position. A pointer position above the horizontal indicates that the airplane is above the proper landing path, while the reverse is true if the pointer swings below the horizontal position.

It is necessary now that the pilot keep accurately on the runway beacon course, at the same time following down on the landing path. To facilitate this, he may reduce the airplane engine speed so that the air-speed indicator registers about 5 miles above the normal landing speed of the airplane. This also helps during the actual landing, as will appear below. The accuracy to which the runway beacon course should be followed is of the order of $\pm 3°$. This is necessary in order that the landing beam may be encountered head on; otherwise, a landing path somewhat steeper than the one desired would be followed. It should not prove difficult, however, to follow the course to the necessary accuracy, since a deviation of $\pm 1°$ may be observed on the reeds. It is felt that after some training a pilot may correct any tendency to fly a zigzag course by flying slightly off course and gradually bearing in toward the course.

Some distance from the landing field boundary line the pilot begins to hear a 1,000-cycle signal from the boundary marker beacon. This signal increases gradually, reaches a maximum, then decreases to zero, and begins to increase again. The instant of zero signal defines the landing field boundary line, and for a given field informs the pilot that he is at a definite distance above ground. Neither point of information is, however, essential to the pilot. The chief function of the boundary marker beacon is to establish a transition period after which the landing beam indications become of primary importance. He may now throttle down his engine to landing speed and maneuver his airplane to follow the landing path accurately to the point of landing.

In the foregoing analysis the direction of the wind has been assumed such as to permit landing along the major runway of the field, and in only one direction along that runway. The system as described, therefore, does not take into account the important factor of wind direction. While it is rare that dense fog is accompanied by a strong wind, blizzards and blinding snow storms often offer as great limitations to visibility as fog. The factor of wind direction can not, therefore, be neglected in the general problem of blind landing.

Developments now in progress with a view to making possible landing into the wind regardless of wind direction, will be considered below.

5. FURTHER DEVELOPMENTS

In addition to the work on expansion of the system of blind landing aids to take care of wind direction, other experiments are in progress at College Park looking toward still further simplification of the use of the system.

(a) RUNWAY LOCALIZING BEACON

Since indications of the position of the airplane with respect to the proper landing path are given the pilot by an instrument of the pointer type, it may prove desirable to furnish the localizing beacon-course indications on the same type of instrument. An instrument of this type has been developed, and numerous successful flight tests made. Whether it will prove superior to the reed indicator for use on the localizing beacon is now being determined. The instrument developed is of the zero-center type (see fig. 13), the movement of the pointer of this instrument from the zero-center position serving to indicate deviation to the left or right of the runway beacon course, as the case may be. The operation of this instrument depends upon the separation of the two frequencies of the double-modulation signal received from the runway localizing beacon (by means of a suitable filter circuit arrangement connected in the receiving set output), rectification of the separated signals, and the application of the resultant rectified voltages in opposition across the instrument terminals. When the two modulation signals are of equal intensity, as is true on the beacon course, the net voltage applied to the instrument is zero. The instrument pointer then assumes its zero-center position. An increase in relative magnitude of one signal over the other operates to deflect the instrument pointer in one direction or the other, depending upon which signal is the stronger. The direction of movement of the pointer may be made to correspond to the direction of deviation of the airplane from the runway course.

FIGURE 13.—*Pointer type localizing beacon course indicator*

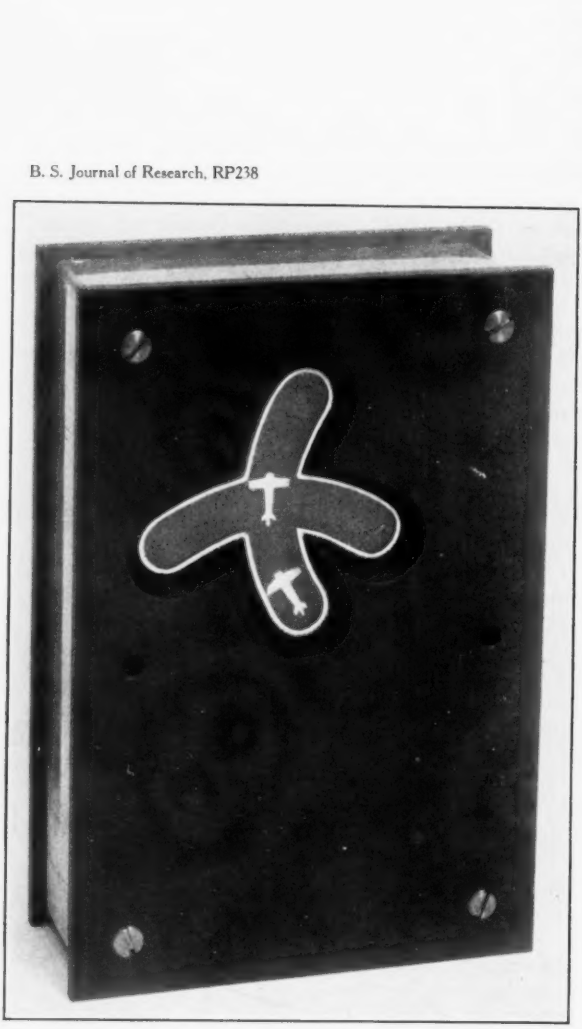

FIGURE 14.—*Combined instrument giving indications of the relative position of the airplane with respect to the runway and also with respect to the high-frequency landing beam path*

The use of this instrument presents a number of advantages, and also a number of disadvantages, over the use of the reed indicator. Among the advantages is included the fact that the course indications become considerably sharper, a deviation from the course of the order of $\pm 0.25°$ being readily detected. A second advantage is that the sharpness of course is adjustable at the receiving end, and may, therefore, be set at a value found most suitable in actual use. Another advantage is that, since the landing beam and runway localizing beacon indicators are now both of the same type, the two may be combined into a single instrument. (See fig. 14.) The resultant simplification is very similar to that obtained by combining rate-of-climb and bank indications in the artificial horizon instrument. Referring to Figure 14, the small airplane in the center is mounted on the pointer of the zero-center instrument connected to the output of the localizing beacon receiving set. This small airplane moves to the right or left of its central position, depending upon the direction of deviation of the airplane in flight from the runway course. The second small airplane shown on the instrument face is mounted on the pointer of the landing beam indicator, and moves vertically above or below its central position depending upon the position of the airplane in flight with respect to the landing path. During landing the pilot maneuvers his airplane to keep the two miniature airplanes, on the instrument face, exactly over each other and in the central position.

A modification of this indicator face is shown in Figure 15. The small airplane attached to the pointer of the landing beam indicator is here replaced by two yellow [9] dots. Two reference lines are provided on the face of the instrument, the white vertical line indicating the position of the runway, and the yellow horizontal line the position of the landing path. The position of the airplane during landing with respect to the runway is shown by the relative position of the white minature airplane with respect to the vertical white line. Similarly, the position of the landing airplane with reference to the proper landing path is shown by the relative position of the two yellow dots with respect to the horizontal yellow line. The indications in *A* show that the airplane is on both courses, while the indications in *B* show that the airplane is too far to the left and too high.

Among the disadvantages introduced through the use of the pointer-type instrument for securing localizing beacon-course indications is that this type of instrument does not possess the feature of selectivity and consequent freedom from interference inherent in the reed indicator. This disadvantage may be compensated for to some extent by increasing the power of the localizing beacon. A second disadvantage is evident from a study of the polar diagram given in Figure 4. If the small lobes shown are at all irregular, apparent courses may be obtained in a direction at right angles to the desired runway. This would be more serious with the pointer-type instrument than with the reed indicator, since the former depends only upon the balancing of the two modulation signals regardless of magnitude, while the reed deflections on these apparent courses would be too small for use.

[9] In Figure 15, yellow color is denoted by crosshatching.

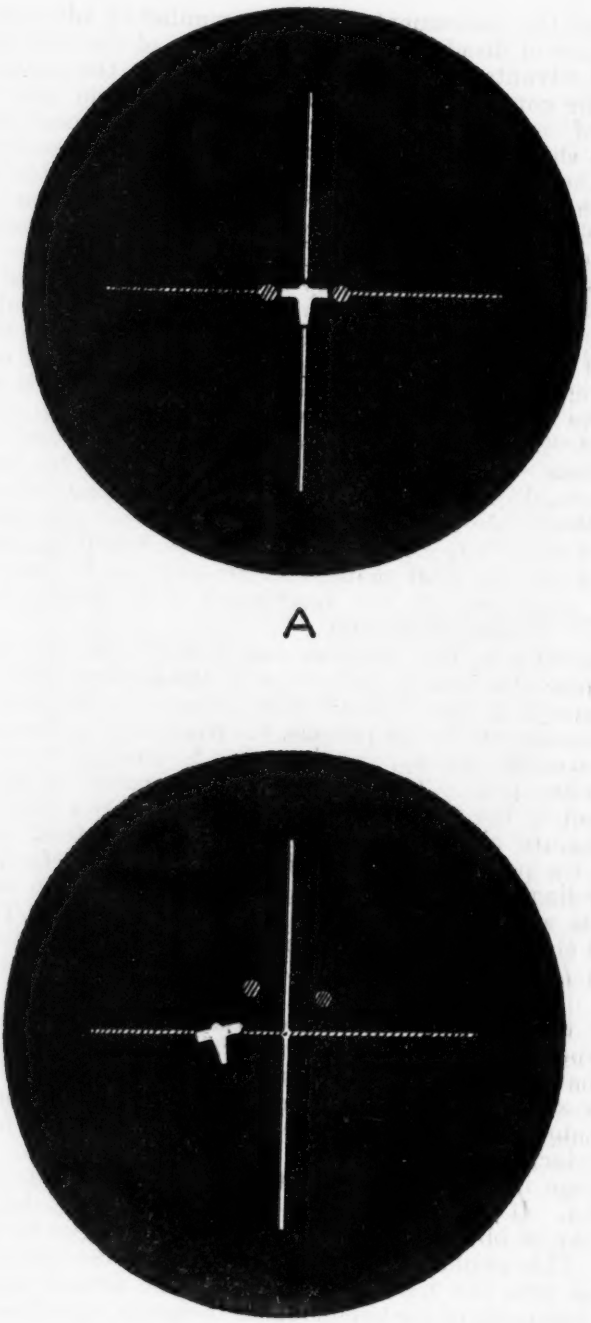

FIGURE 15.—*Modified face for combined localizing beacon and landing beam course indicator*

(b) BOUNDARY MARKER BEACON

A second field for investigation is the question of the best type of marker beacon signals to be furnished to the pilot. In the first system of blind landing aids, a 40-cycle reed indicator was employed for this purpose. It was later felt that aural indication would be preferable, since it would prevent any possibility for the pilot to miss the marker beacon indication during the short period when he passed over the marker. So many factors enter into consideration, however, that it is difficult to arrive at a definite decision as to whether aural indication is entirely satisfactory. With the present trend toward combined passenger and mail transportation, it is not possible to visualize the exact conditions on the airplane of the near future. Probably the copilot, who would also be the radio operator, will receive all voice and code messages, including weather reports, while the pilot will use radio only as a navigational aid. In that event, it would be unnecessary for the pilot to use head telephones except if the landing field boundary marker indications were aural. Visual indication, of the nature of a flashing light, such that the pilot could not miss the indications, would then perhaps be preferable. The complete system of radio navigational aids would then be furnished the pilot by visual indicating devices only.

(c) EXPANSION OF SYSTEM TO TAKE CARE OF WIND DIRECTION

A number of possible arrangements of the system of blind landing aids outlined above, whereby wind direction may be taken into account, are available. The problem is to determine the most economic arrangement; for example, it has been suggested that the localizing beacon and landing beam transmitters may be buried in the center of the field and oriented into the wind at all times by remote control from the operations office, or even automatically. Aside from the technical problems involved, the provision of a sufficiently large waterproof room with sturdy roof construction level with the surface of the ground, so that an airplane might roll over it, seems economically unfeasible. A second arrangement, somewhat less expensive, would be to mount the localizing beacon and landing beam transmitters on a truck, with provisions for operating the equipment from the 60-cycle supply used for the landing field boundary lights. Service into the wind could then be furnished by moving the truck to the proper position just off the field. In addition to the consideration of costs, each of the two arrangements noted is open to the objection that the landing beam transmitter would require special adjustment in each new position. The shape of the landing path should be convenient for landing and at the same time insure the clearance of all obstructions. Since the obstructions are quite different when coming into the average landing field from different directions, the need for the adjustment of the landing beam transmitter is apparent.

Perhaps the most feasible arrangement is the one shown in Figure 16. The transmitting equipment for both the localizing beacon and landing beam is so simple that the duplication shown appears warranted. It is estimated that the commercial cost of the complete installation would not exceed $15,000. An obvious advantage is that the equipment once set up remains in permanent adjustment.

Referring to Figure 16, the beacon arrangement shown is for a 3-runway field. Three-runway localizing beacons, *A*, *B*, and *C*, and six landing beam transmitters, *D*, *E*, *F*, *G*, *H*, and *I*, are required. Only three boundary marker beacons, *J*, *K*, and *L*, are necessary, since the drop in reed deflections directly over the localizing beacons, *A*, *B*, and *C*, may be used for that purpose in the three remaining positions where marker beacons are required. At any given time but one localizing beacon, one landing beam transmitter, and one

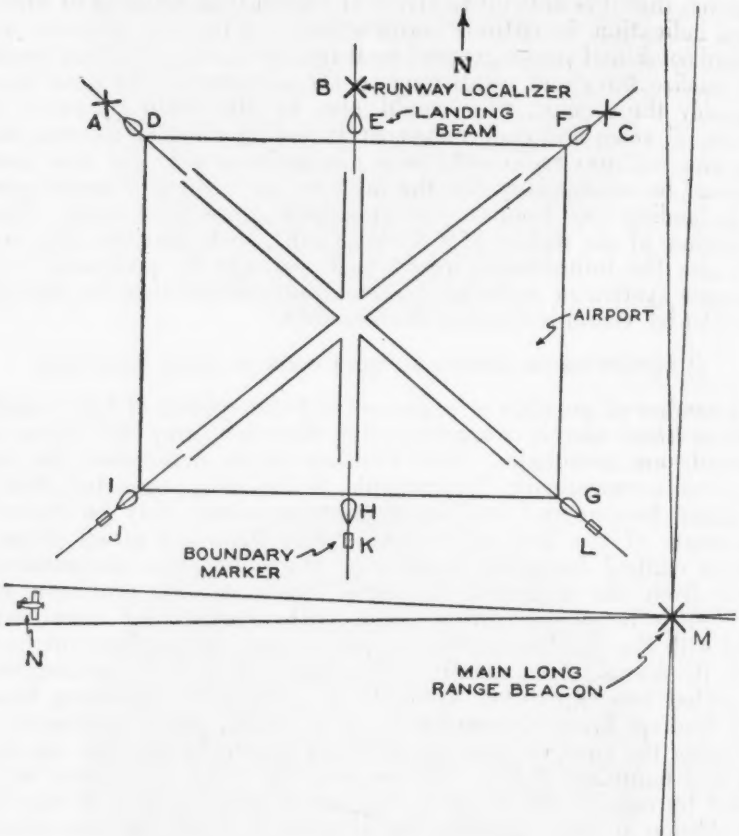

FIGURE 16.—*System of blind landing aids necessary to take care of wind direction on a 3-runway airport*

boundary marker beacon, are in operation, being so chosen as to require landing into the wind. In practice, this system would probably be used in the following manner. The radio operator or reserve pilot on an airplane approaching the field on a course of the main radio range beacon *M*, reports to the traffic control officer at the field (by radio) that the pilot wishes to land. The traffic control officer then informs him of the wind conditions at the field and the direction in which to land. He may also require that the airplane be maintained at a specified altitude in order to permit other air-

planes to land. This information is relayed to the pilot, who continues on the main radiobeacon course, at the specified altitude, until the drop in deflection of the reed indicator shows that he is passing over the main beacon tower. He then tunes the medium-frequency receiving set to the runway localizing beacon and, knowing the location of the main beacon relative to the field, heads the airplane on the compass course necessary to follow the particular localizing beacon in operation, in accordance with the information received from the traffic control officer. The pilot continues to travel back and forth along this course at the designated altitude, keeping the position of the field in mind by the zero deflection of the reed indicator each time the airplane passes over the localizing beacon transmitter. When orders are received to land, the radio operator relays the message to the pilot, who follows the localizing beacon course until he is about 5 miles away from the field in the proper direction, makes a 180° turn so as to head toward the field, places the landing beam receiver in operation, and proceeds to land in the manner described in Section III, 4, in connection with the single runway system.

IV. DESCRIPTION AND OPERATION OF APPARATUS

In the analysis given above, only such general details of the transmitting and receiving equipment have been introduced as were necessary to the understanding of the system as a whole. In this section the component parts making up the complete system are described in some detail.

1. RUNWAY LOCALIZING BEACON

This beacon was briefly described in Section II above. It is essentially a 200-watt, double-modulation beacon, employing small loop antennas so that it may be placed near the landing field without constituting an obstruction to flying. The course indications on the airplane may be obtained either on a reed indicator or on a zero-center pointer-type instrument. For the first case the modulation frequencies used at the beacon are 65 and 86.7 cycles, respectively; in the second case, 60 and 500 cycles, respectively. The beacon apparatus is housed in a 2-story shed located on the border of the landing field and in line with the runway along which the course is to be directed. (See fig. 2.) The transmitting set and machinery are shown on the first floor and the transmitting loop antennas on the second floor. These antennas consist of seven turns of wire wound on frames 6 by 8 feet, the turns being spaced 4 inches apart.

The transmitting set is shown in Figure 17. This transmitter is provided with a 250-watt power amplifier stage in each amplifier branch, but these stages were not used except in the early tests. The actual transmitting circuit arrangement employed is shown in Figure 18. To simplify apparatus, the transmitter is coupled to the antenna system through two coupling transformers, *C* and *D*, rather than by means of the goniometer employed in the usual radio range beacon set-up. The variometer *E* serves to neutralize any residual inductive coupling between loop antennas *A* and *B*.

2. BOUNDARY MARKER BEACON

The boundary marker beacon is shown in Figure 19. The transmitting loop antenna consists of 10 turns spaced 4 inches apart and wound on a wooden frame 6 by 8 feet, the plane of the antenna being so oriented that the minimum signal zone coincides with the landing field boundary line. In addition to the loop antenna, there are two

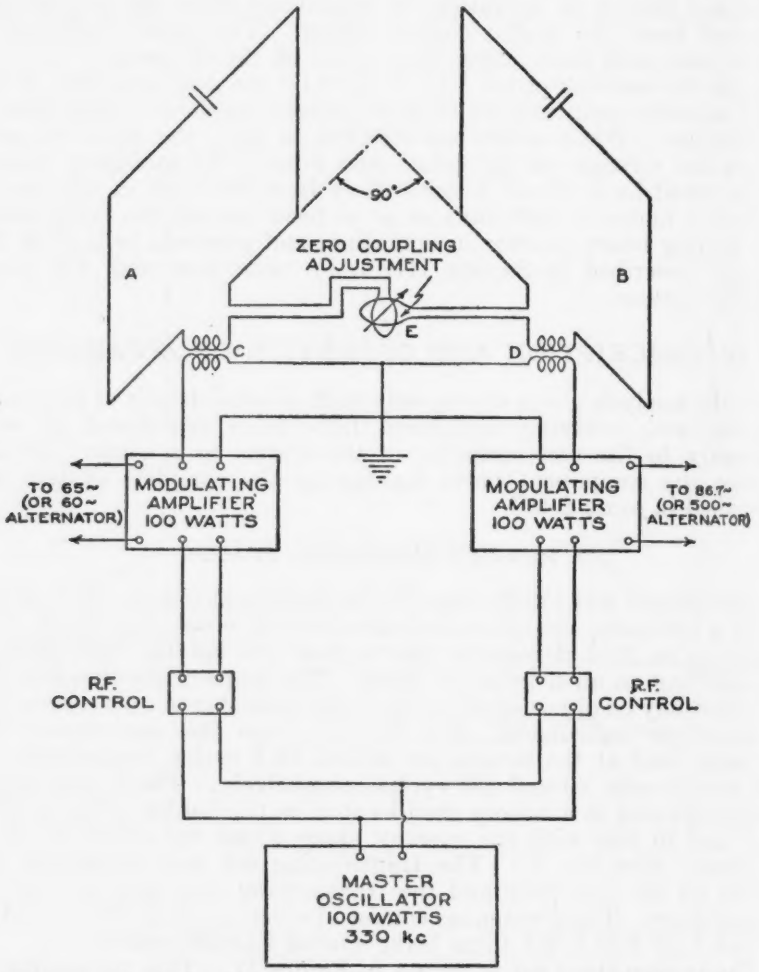

FIGURE 18.—*Transmitting circuit arrangement for runway localizing beacon*

small weatherproof boxes which contain the power supply unit and the transmitting set. The power supply unit is a converter for changing from 60-cycle to 500-cycle supply. The transmitting set employs two 50-watt tubes excited alternately from a 500-cycle plate supply transformer and feeding a common oscillatory circuit, coupled inductively to the loop antenna. (See fig. 20.) The tube filaments are also supplied from the 500-cycle source through a suitable winding

B. S. Journal of Research, RP238

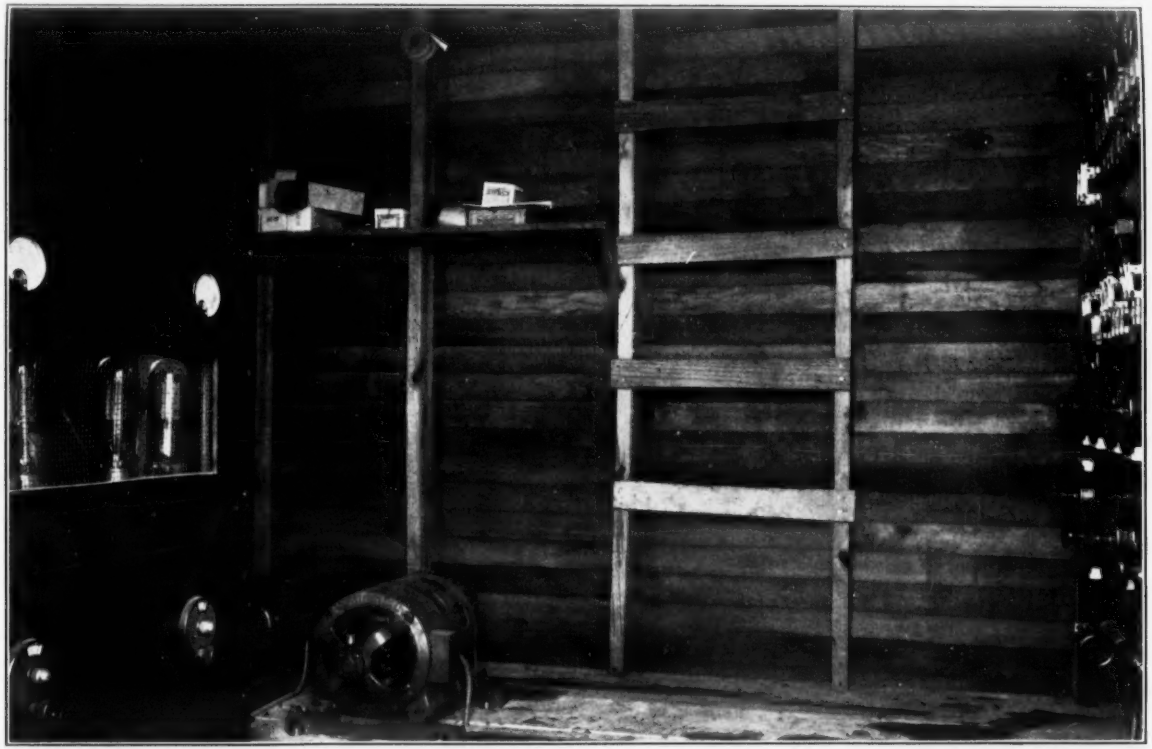

FIGURE 17.—*Runway localizing beacon transmitting set*

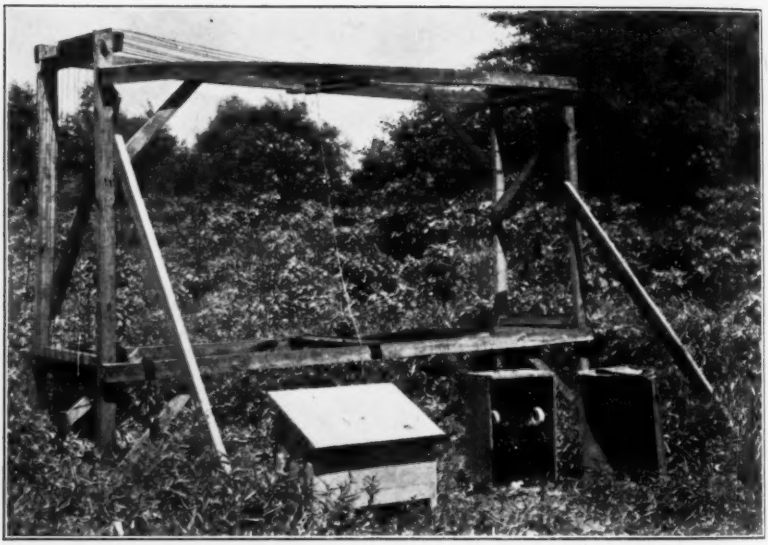

FIGURE 19.—*Transmitting system for airport boundary marker beacon*

on the 500-cycle transformer. Due to the alternate excitation of the 50-watt tubes, the resultant modulation has a frequency of 1,000 cycles. The boundary marker beacon operates on the same carrier frequency as the runway localizing beacon (330 kc).

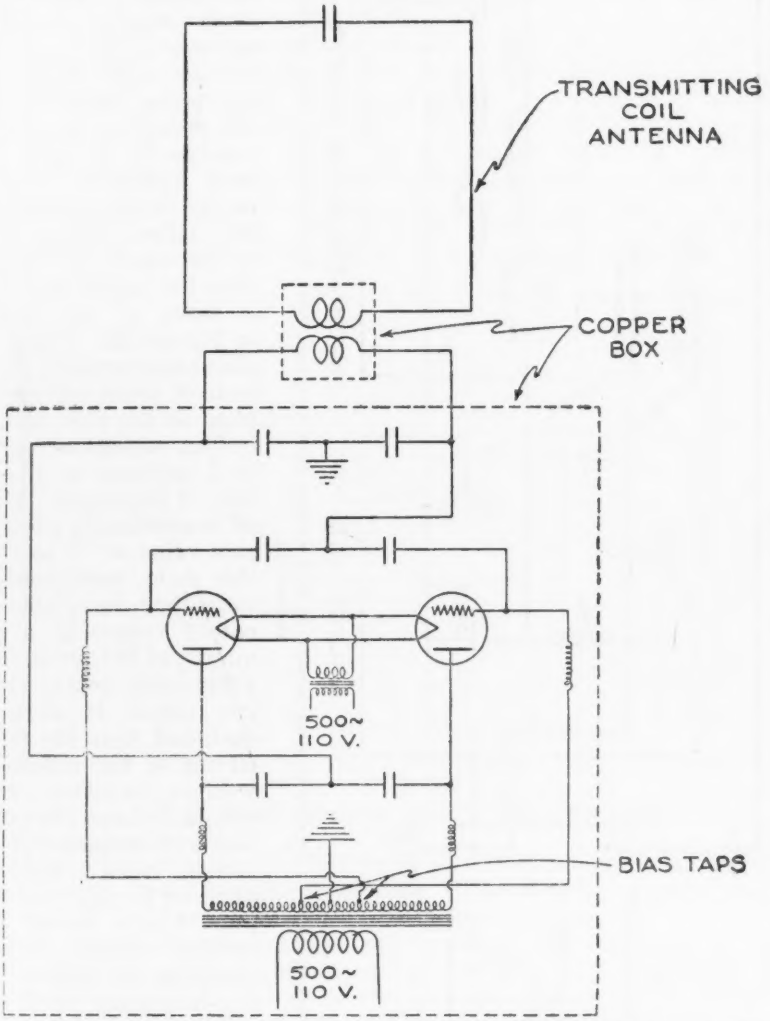

FIGURE 20.—*Transmitting circuit arrangement for airport boundary marker beacon*

3. RECEIVING SYSTEM FOR LOCALIZING AND MARKER BEACON SIGNALS

When the vibrating reeds are used as the course indicator on the runway localizing beacon, the receiving system on the airplane is as shown in Figure 21. The filter unit serves to direct the reed frequencies to the reed indicator and the 1,000-cycle marker beacon signals to the head telephones. The automatic volume control is

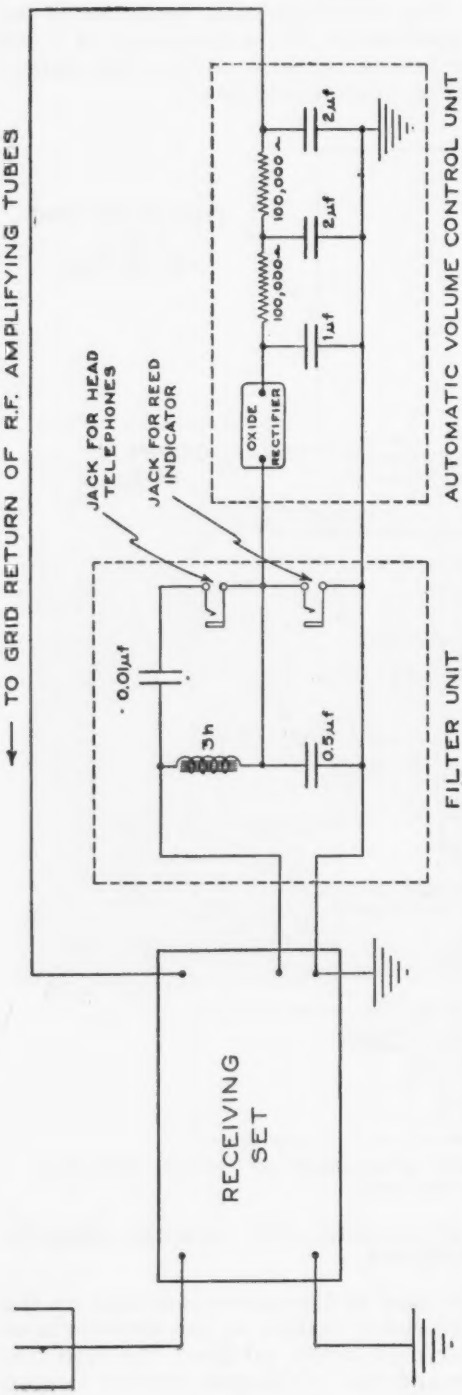

FIGURE 21.—*Circuit arrangement for receiving runway localizing and marker beacon signals when reed indictor is used for runway course indications*

connected across the reed indicator terminals and, consequently, is actuated only by the localizing beacon signals. The 1,000-cycle marker beacon signal is therefore permitted to vary through a minimum even though the receiving set output voltage (in so far as the reed indicator is concerned) is maintained substantially constant.

The operation of the filter unit is best seen from a study of the graphs in Figure 22. Graph *A* shows the variation of the ratio of input voltage applied to the filter unit to output voltage across the reed indicator as a function of frequency. Cut-off is arbitrarily assumed at a value of 10 to 1 for this ratio, corresponding to 20 decibels. Note that cut-off occurs at a frequency of 425 cycles. The 1,000-cycle marker beacon signal is therefore excluded from the input circuit of the automatic volume control unit. Graph *B* shows the variation with frequency of the ratio of input voltage applied to the filter to output voltage across the head telephones. Cut-off occurs at 140 cycles. The low-frequency reed signals (65 and 86.7 cycles) are, therefore, not heard in the head phones. The marker beacon signal is, however, received. In addition, code and intelligible speech may be received without adjustment of the filter unit.

This is of advantage when the receiving set is used to obtain aural radio range beacon and radiotelephone service on the fixed airways. Graph *C* shows the variation of the input impedence of the filter unit with frequency. This matches quite well the output impedance of the receiving set employed except in the narrow band, 125 to 300 cycles, which is unimportant.

The operation of the automatic volume control unit in conjunction with the particular receiving set used may be obtained from a study of the graphs in Figure 23. Graph *A* shows the variation of output voltage across the reed indicator with input voltage to the receiving set when no provision is made for automatic control of volume. Graph *B* shows the voltage across the reed indicator as a function of the input voltage to the receiving set when the automatic volume control connection is used. The variation of the plate current supply to the radio-frequency amplifying tubes as a function of the receiving

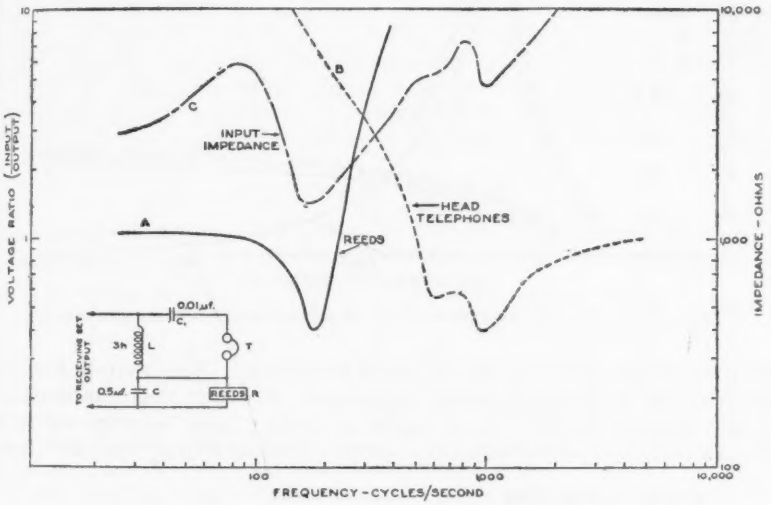

FIGURE 22.—*Performance characteristics of filter unit*

set input voltage is plotted in graph *C*. For a beacon station of given power, the instrument reading plate current supply may, therefore, be calibrated directly in distance.

When the zero-center pointer type instrument is employed as the runway beacon course indicator, a filter-rectifier unit is required at the receiving end for separating the two frequencies of the double-modulation signal received (60 and 500 cycles, respectively), then rectifying the separated signals and applying the resultant rectified voltages in opposition to the instrument terminals. The circuit arrangement for this unit is shown in Figure 24. The receiving set output signal is fed to terminals *AA* of this unit, the automatic volume control unit being connected across *AA*. Referring to Figure 24, the double-modulation signal is resolved into its component frequencies through circuit *BC*, voltage of 500-cycle frequency being applied to rectifier *D*, and voltage of 60-cycle frequency to rectifier *E*. The rectified output voltages from *D* and *E* are applied

in opposition across instrument F by means of the potentiometer G, the sliding contact H serving to balance the outputs so that the pointer of instrument F will be in zero-center position when the two

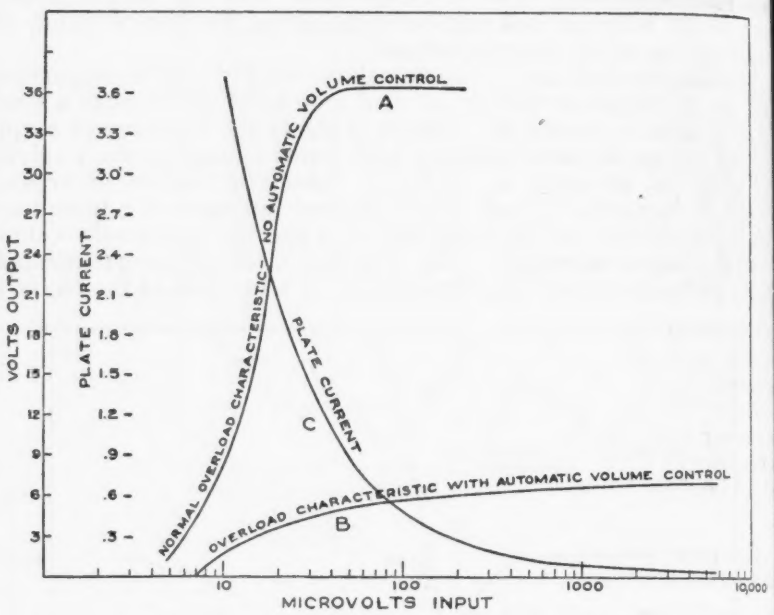

FIGURE 23.—*Performance characteristics of automatic volume control unit*

modulation frequencies are of equal intensity. The switch I permits the reversal of the instrument terminals, in order that the deflection of the pointer to the left or right of center may correspond to the direction of deviation from the course, whether flying "to" or "from"

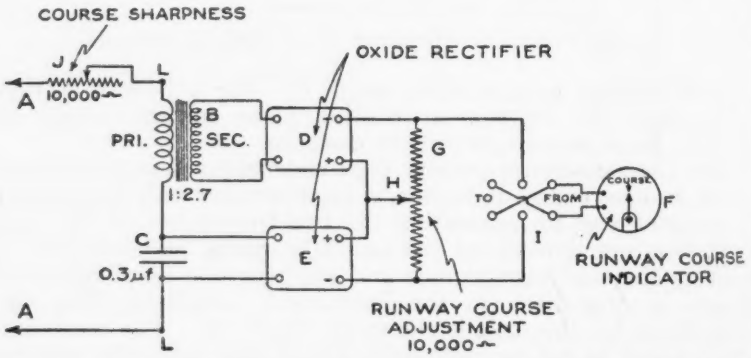

FIGURE 24.—*Circuit arrangement for filter-rectifier unit used with pointer type localizing beacon course indicator*

the beacon. The indicator F may be made to give any sharpness of course indication above $\pm 0.25°$, by varying the intensity of the signal delivered to the terminals LL. The series resistance J is

provided for this purpose. This arrangement permits the use of the same automatic volume control and setting (in parallel with *AA*) as is used for the reed indicator when receiving signals from the main radio range beacon.

4. LANDING BEAM

The use of the landing beam was outlined briefly in Section III above. The function of the landing beam is to furnish a pilot with the necessary vertical guidance to permit landing under conditions of no visibility. It consists essentially of a horizontally polarized beam directed at a small angle above the horizontal, this angle and the degree of directivity being so adjusted that a predetermined line of constant field intensity will mark out just the proper gliding path, clearing all obstructions and convenient for landing. In the set-up at College Park, Md., the beam is transmitted on a frequency of 93,700 kc (3.2 m) and is oriented in the same horizontal direction as the course of the runway localizing beacon. The beam transmitting system is shown in Figure 7. On the airplane, a horizontal dipole antenna feeding a detector-amplifier-rectifier unit is employed for receiving the landing beam signal. As will be evident below, the receiving equipment constitutes essentially a vacuum tube voltmeter arrangement for exploring the field intensity in different portions of the landing beam.

(a) THEORY OF OPERATION

The polar diagrams of Figures 25 and 26 show, respectively, the horizontal and vertical directive characteristics of the landing beam.

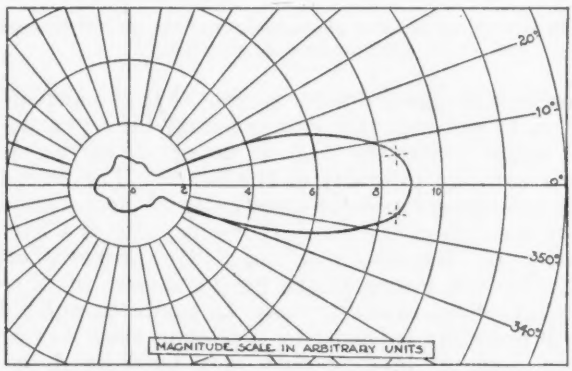

FIGURE 25.—*Horizontal directive characteristic of the 93,700 kc landing beam*

Referring to Figure 25, and recalling that an airplane is kept along the axis of the beam (in the horizontal plane) by means of the runway localizing beacon, it will be observed that a deviation from the runway course of $\pm 6°$ will result in but a 5 per cent drop in the landing beam signals. Since the reed indicator detects a course deviation of $\pm 1°$, it may be concluded that an airplane can readily be directed in a horizontal plane, head-on with the beam. In the analysis which follows it will be assumed at all times that the airplane is along the line of maximum intensity in so far as the horizontal characteristic is concerned.

Consider now the vertical directive characteristic shown in Figure 26. An airplane flying in a straight line from B to A directly into the region of maximum field intensity of the beam receives a signal which increases inversely as the distance from the beam transmitter. Such a rate of increase in received signal is of little help in landing. Suppose, however, that the airplane is directed into the beam along the line OC, until position G is reached, at which point the indicating instrument on the airplane reaches half-scale deflection. At a point directly above G, this deflection increases, since the airplane is nearer the line of maximum intensity of radiation of the beam. At a point directly below G, the deflection decreases, the airplane now being farther from the line of maximum intensity of radiation. The instrument deflection thus increases or decreases with any increase or decrease in the altitude of the airplane about the point G. If, now, a straight line were followed from G to A, the indicating instrument pointer would soon go off scale due to the approach of the receiving system to the transmitting source. However (and this is the basis of operation of the system), by dropping away from the line of maximum intensity of radiation as A is approached, the instrument pointer may be held at the half-scale deflection position at all times,

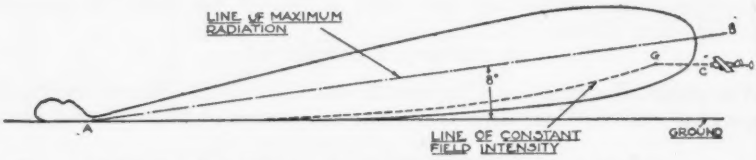

FIGURE 26.—*Vertical directive characteristic of the 93,700 kc landing beam showing landing glide path*

since the increase in signal due to the fact that the airplane is nearing the source A is continuously compensated for by a corresponding decrease in signal due to the angular departure of the airplane from the line of maximum intensity of the beam. The path followed by holding the instrument pointer constantly at half-scale deflection is indicated by the dotted line GA. Obviously this is a line of constant field intensity of definite magnitude. By properly orienting the beam vertically and giving it the proper degree of directivity, this line of constant field intensity may be made to coincide with the landing path normally followed by a pilot in clear weather.

This glide curve or landing path may be derived from a proper combination of two graphs, one of which shows the inverse variation of field intensity with distance from the beam transmitter, and the other the polar curve showing the beam directivity in the vertical plane. Referring to Figure 27 which shows the same vertical characteristic as Figure 26, the line of maximum intensity of radiation of the beam (OK) makes an angle of 8° with the horizontal. Assume that the field intensity at a point located on this line and 2,000 feet horizontally distant from the transmitter is 2,000 (in arbitrary units [10]). This corresponds to the magnitude OK. Then the field intensities at points the same horizontal distance from the transmitter

[10] These units are chosen to correspond to the reading of the landing beam indicating instrument in microamperes. This assumes that the detector-amplifier-rectifier is essentially linear in operation.

but located on lines making, respectively, 4°, 2°, and 1° with the horizontal, correspond to the magnitudes *OL*, *OM*, and *ON*, and are equal to 1,840, 1,600, and 1,200 (in the same arbitrary units). Consider, now, the variation of field intensity, along each of the lines

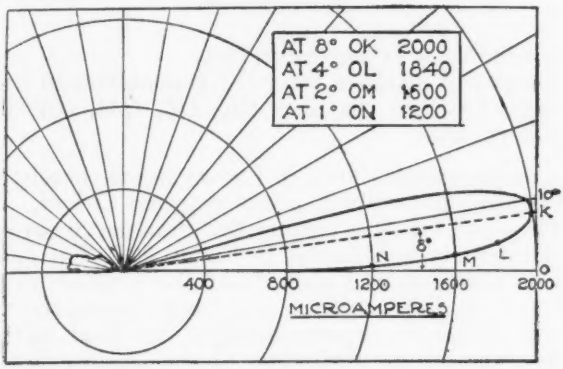

FIGURE 27.—*Vertical directive characteristic of the 93,700 kc landing beam giving experimental data used in the graphical determination of the landing glide path shown in Figure 29*

considered, for increasing distance from the transmitter. The graphs corresponding to the lines making 8°, 4°, 2°, and 1° with the horizontal are shown, respectively, by *K*, *L*, *M*, and *N* in Figure 28. In each case the field intensity is an inverse function of the distance. To

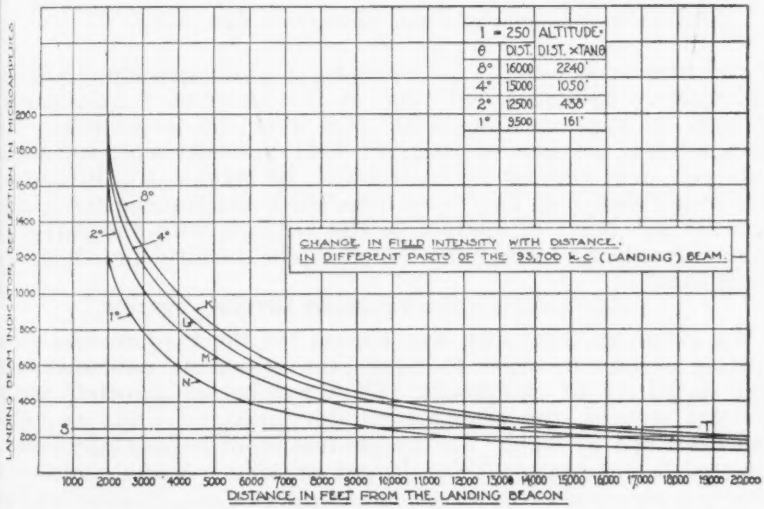

FIGURE 28.—*Graphical method of determining landing glide path from the data given in Figure 27*

determine the shape of any line of constant field intensity it is now simply necessary to draw a horizontal line, such as *ST* corresponding to the intensity desired (250 in this case, half-scale reading of the microammeter used in practice), determining the horizontal distance

from the transmitter corresponding to the points of intersection this line with the graphs K, L, M, and N, and computing the heig of these points above the ground from the relation

$$h = dx \tan \Theta \quad (1$$

where

h is the height above ground in feet,
d the horizontal distance from the transmitter in feet,
Θ the angle between the lines OK, OL, OM, ON (fig. 27), an the horizontal.

Four points on the graph shown in Figure 29 are thereby determine This is the landing path which it was required to find.

A second method for determining the glide curve corresponding t a given field intensity is indicated in Figure 30. The field intensiti are plotted as abscissas and altitude of the airplane as ordinates each 1,000 feet of distance from the beam transmitter. The da plotted were obtained experimentally, the field intensity bei measured in terms of the deflection of the landing beam indicato

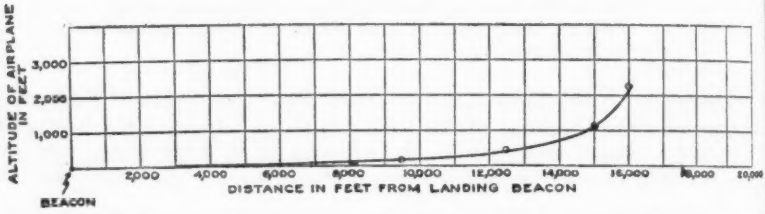

FIGURE 29.—*Landing glide path derived from data given in Figure 27*

It will be observed that a pilot coming in at an altitude of 1,000 fe will observe half-scale deflection of his instrument (250 μa) at distance of approximately 9,000 feet from the transmitter. If h then follows the line of constant field intensity corresponding t half-scale deflection on his instrument, he reaches an altitude of 1 feet at a distance of 2,000 feet from the beam transmitter. This i actually the point of contact of the airplane with the ground, th receiving antenna being mounted on top of the airplane, 10 feet fro the ground.

(b) DIRECTIVE TRANSMITTING ANTENNA SYSTEM

An ultrahigh frequency was chosen for the landing beam trans- mitting system in order to secure the attendant reduction in size and simplicity of equipment. Of a number of directive antenna systems studied, the arrangement developed by Unda and Okabe and described by Yagi,[11] for the production of horizontally polarized directed beams, was considered most suitable. A photograph of the directive antenna array, as set up at College Park, is shown in Figure 7. This was later housed in a shed for protection against weather. The ultrahigh frequency source (93,700 kc) is coupled to the horizontal doublet A (made of ⅛-inch copper tubing), which serves as the radiat- ing antenna and is accurately tuned to the frequency of the source. About 0.8 m behind the radiating antenna is placed a reflecting

[11] Hidetsugi Yagi, Beam Transmission by Ultrashort Waves, Proc. I. R. E., 16, p. 715; 1928.

ALTITUDE OF AIRPLANE IN FEET
10
9
8
7
6
5
4

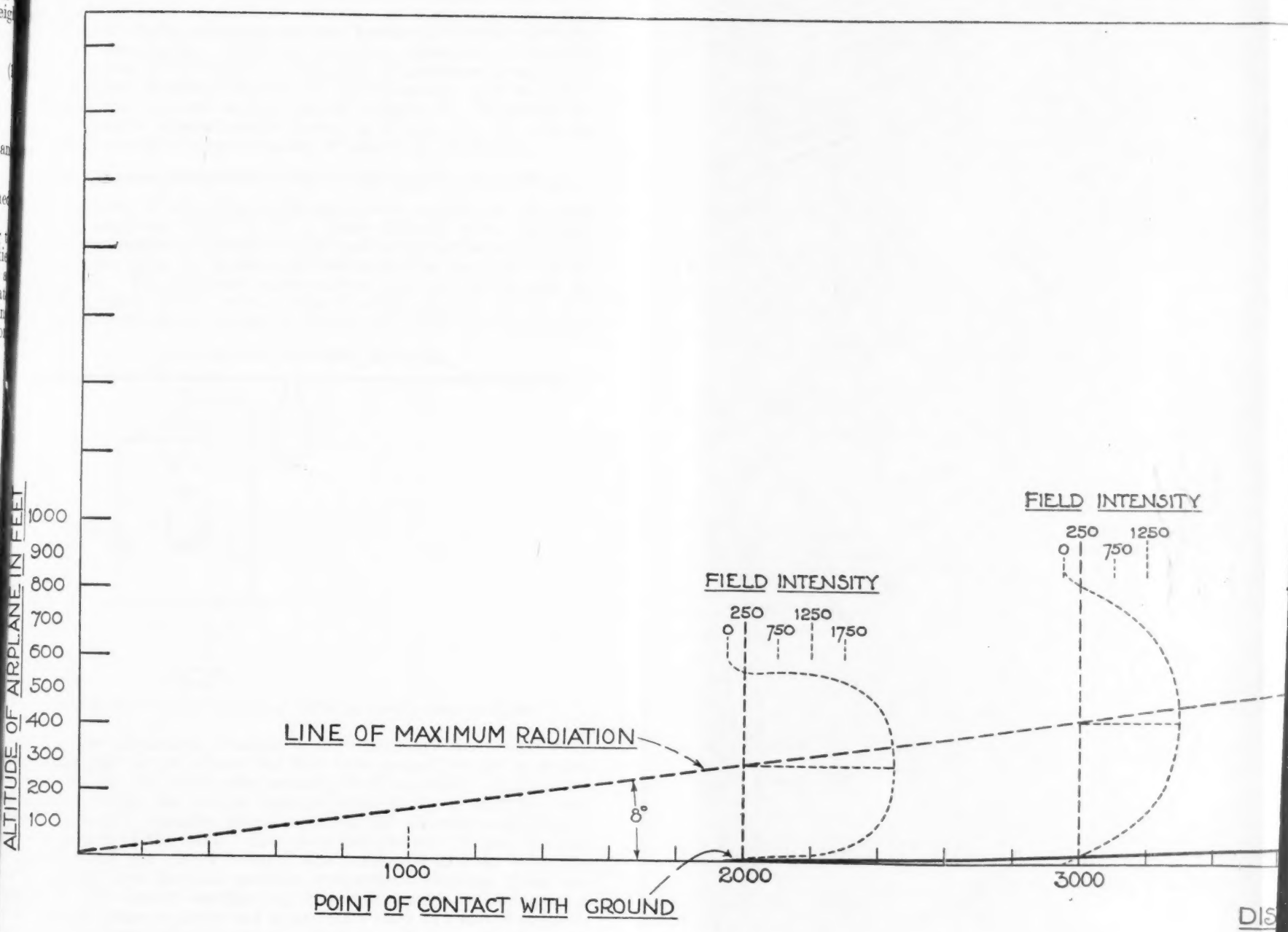
ALTITUDE OF AIRPLANE IN FEET
1000
900
800
700
600
500
400
300
200
100
FIELD INTENSITY
250
1250
0
750
FIELD INTENSITY
250
1250
1750
0
750
LINE OF MAXIMUM RADIATION
8°
1000
2000
3000
POINT OF CONTACT WITH GROUND
DIS

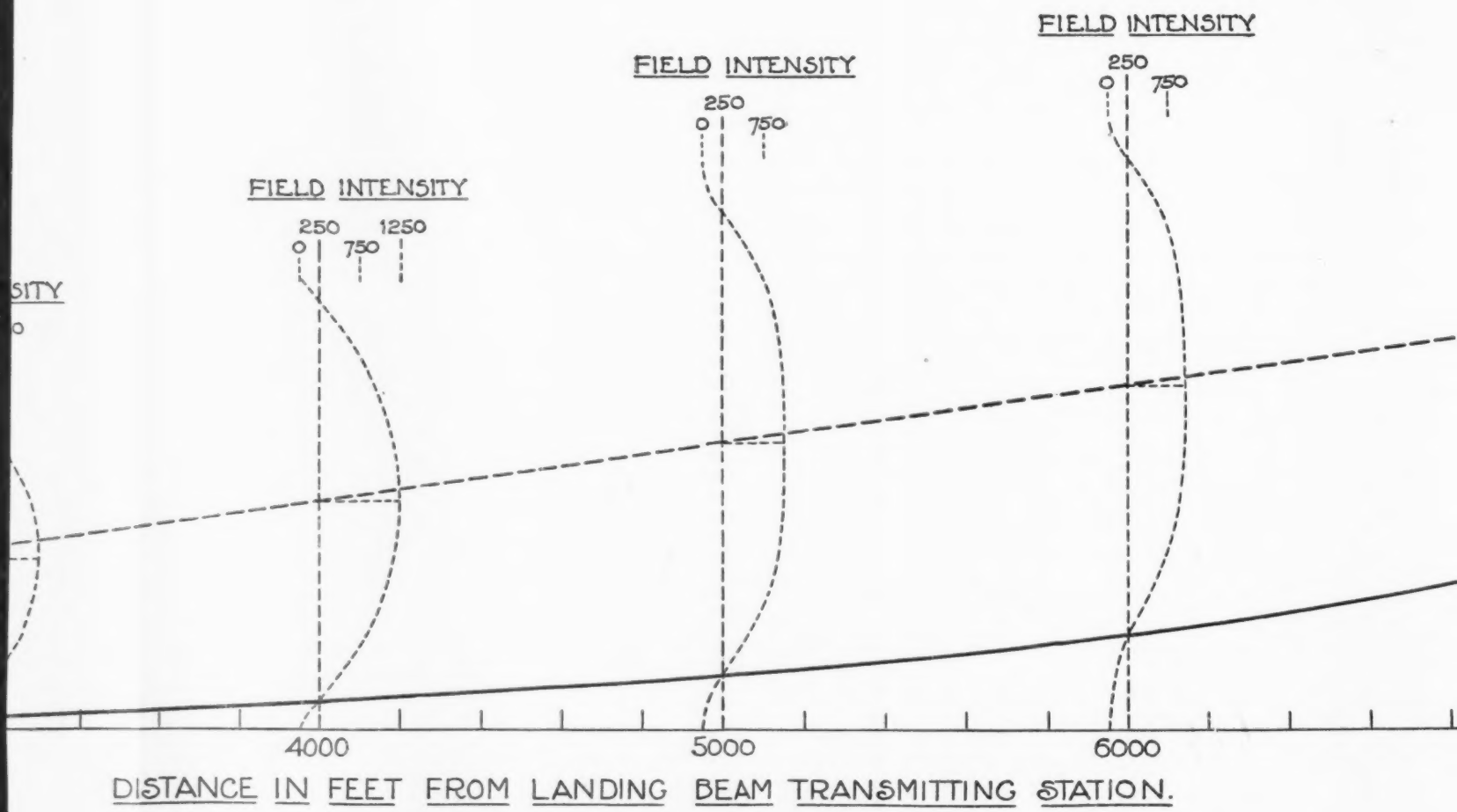

FIGURE 30.—*Experimental determination of landing glide path*

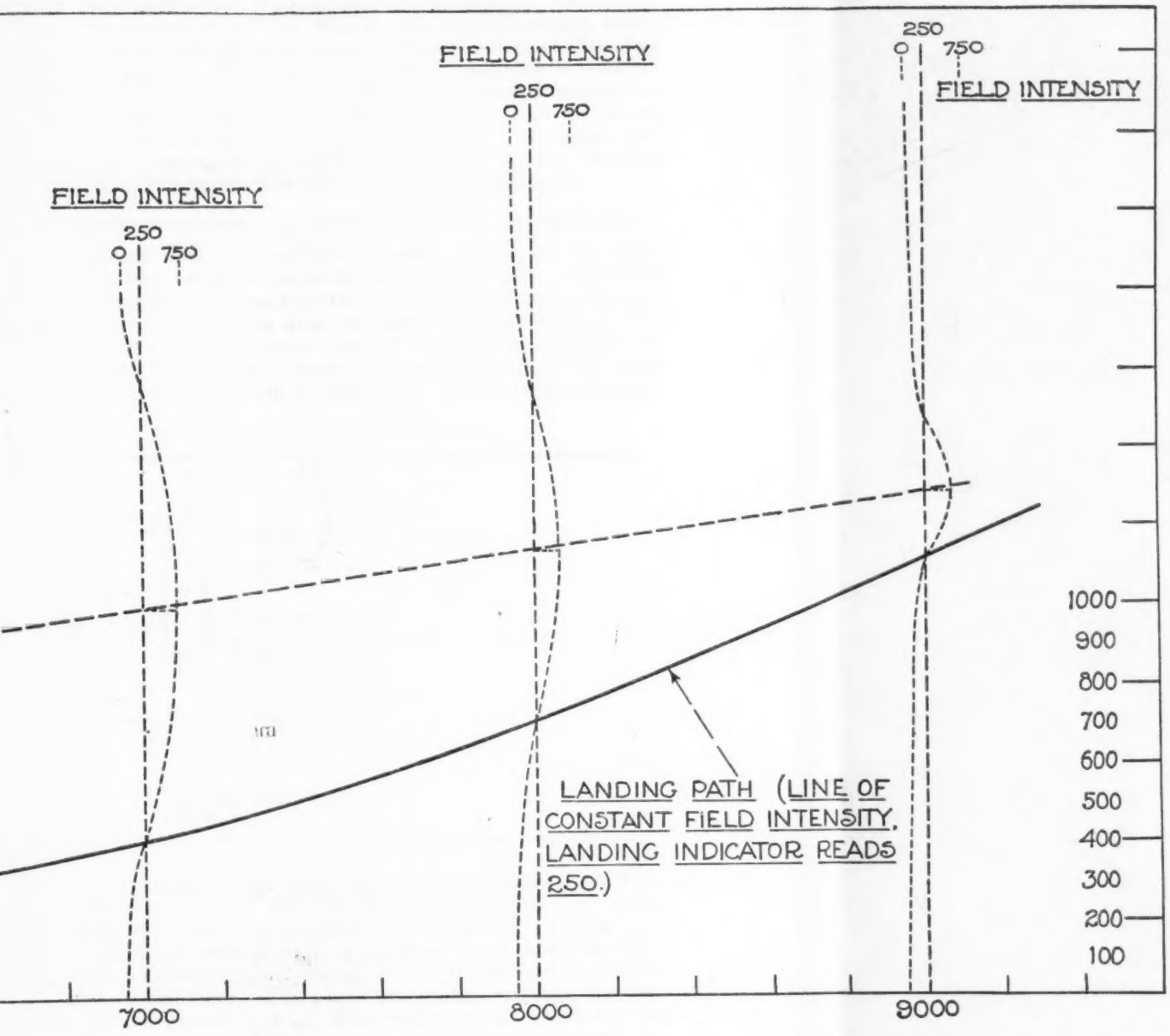
FIELD INTENSITY
250
750
FIELD INTENSITY
250
750
FIELD INTENSITY
250
750
LANDING PATH (LINE OF CONSTANT FIELD INTENSITY. LANDING INDICATOR READS 250.)
1000
900
800
700
600
500
400
300
200
100
7000
8000
9000

ntenna *B*, also a horizontal doublet, tuned to a frequency somewhat ower than the frequency of the source. At approximately every neter in front of the radiating antenna, horizontal-doublet directing ntennas *C* are placed. These are tuned to a frequency somewhat igher than that of the source. This array of antennas is supported n a horizontal wooden structure *D*, approximately 2.75 m. above he ground, and pivoted on the vertical support *E*. To obtain the ertical directive characteristic shown in Figure 27, the wooden tructure *D* was tilted approximately 8° above the horizontal.

(c) THE ULTRAHIGH-FREQUENCY TRANSMITTING CIRCUIT ARRANGEMENT

The problem of obtaining sufficient power output on the high requency used was found to be a rather difficult one. Sufficient adiation was desired to operate a visual indicating device at a distance f 5 to 8 miles from the source with not more than two tubes in the eceiving set. The necessary power output was secured through the se of a 500-watt three-element tube (General Electric ZP–2) used n the oscillatory circuit shown in Figure 31. This circuit arrange-

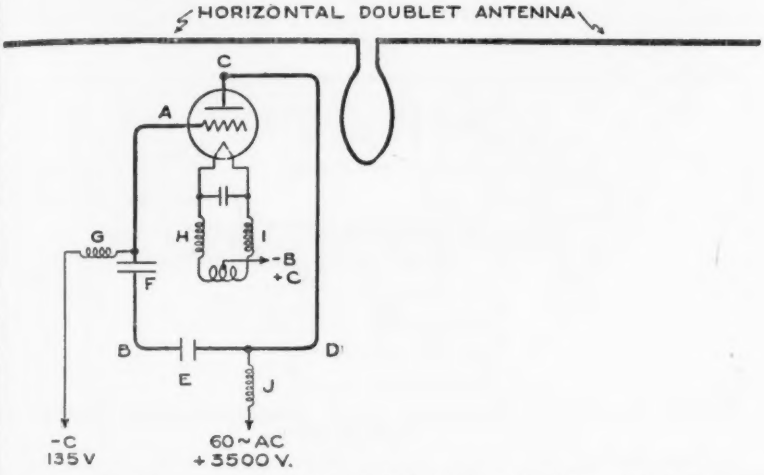

FIGURE 31.—*Circuit diagram of 93,700 kc landing beam oscillator*

ment has the advantage obtained in the customary short wave two-ube push-pull circuit where the two tube capacities are in series, hereby halving the total tube capacity in the circuit. In this new scillatory circuit the second tube is replaced by a small air con-enser *E*, with a capacity about equal to the interelectrode grid to late capacity of the tube. The plate inductance *CD* and the grid nductance *AB* are placed between this condenser and the tube, the eads making the shortest possible connections between these ele-ments of the circuit constituting the inductances. Condenser *F* s of relative large capacity and is necessary only as a safety measure n case of flashover of condenser *E*. *G*, *H*, *I*, and *J* are suitable choke oils to keep the oscillatory current out of the power supply leads.

Figure 32 shows the 500-watt tube and associated apparatus, in-luding the horizontal doublet radiating antenna. The tube is oper-

ated with 3,500 volts of 60-cycle frequency on the plate and a negati grid bias of about 135 volts. The tube circuit is tuned to the desi frequency within narrow limits by moving one of the plates of c denser E by means of an insulated adjustment screw. The f quency has proved sufficiently stable for use without external me for frequency control, due in part to the fact that but one broa tuned circuit is used at the receiving end.

(d) THE RECEIVING SYSTEM

Considerable time was devoted to the development of a simple a reliable receiving system for giving visual reception of the direc beam up to a distance of 5 to 8 miles. Early in the work it was fou that by placing a receiving tube in the center of a horizontal doub antenna, rather broad tuning was obtained. This was quite d sirable since slight changes in the transmitting frequency or receiv antenna constants then had no effect on the deflection of the receiv indicating instrument.

The circuit arrangement finally found to be the most stable a reliable as well as sensitive (see fig. 33) uses only two tubes with

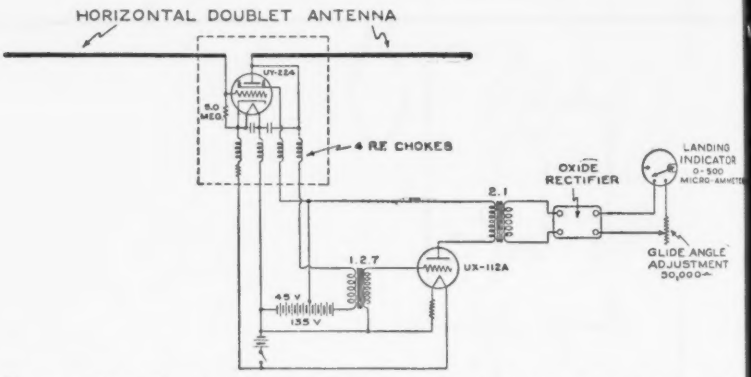

FIGURE 33.—*Circuit diagram of special ultrahigh-frequency landing beam receiving set*

regeneration. This receiving circuit requires no adjustments on t part of the pilot. Even the volume control is dispensed with, sin the path followed during the use of the receiving set constitutes a li of constant field intensity of the directed beam. The detecting po tion of the receiving circuit (within the dotted lines) is external the airplane, being mounted in a streamline weatherproof box abo 14 inches above the top wing. (See fig. 8.) The doublet anten is in the form of two copper rods housed in wooden streamlined su ports projecting from the streamlined detector box. The rest of t apparatus, which includes the audio amplifying tube and transform oxide rectifier, A and B batteries, and indicating instrument, a located within the airplane.

Figure 34 at *A* shows an inside view of the streamlined detect box. The amplifier-rectifier unit is shown in Figure 34 at *B*. T oxide rectifier shown eliminates one tube, and has been found pe fectly stable in its operation at the low frequency employed.

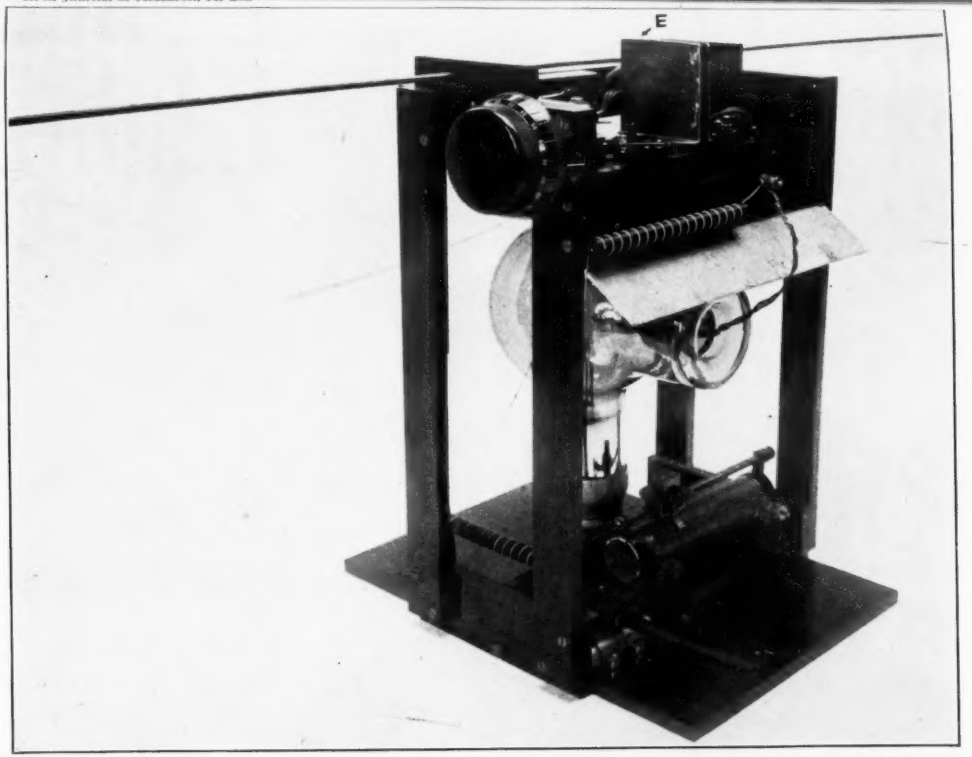

FIGURE 32.—*Electron-tube oscillator and radiating antenna for the 93,700 kc landing beam*

Shown at A, Figure 7.

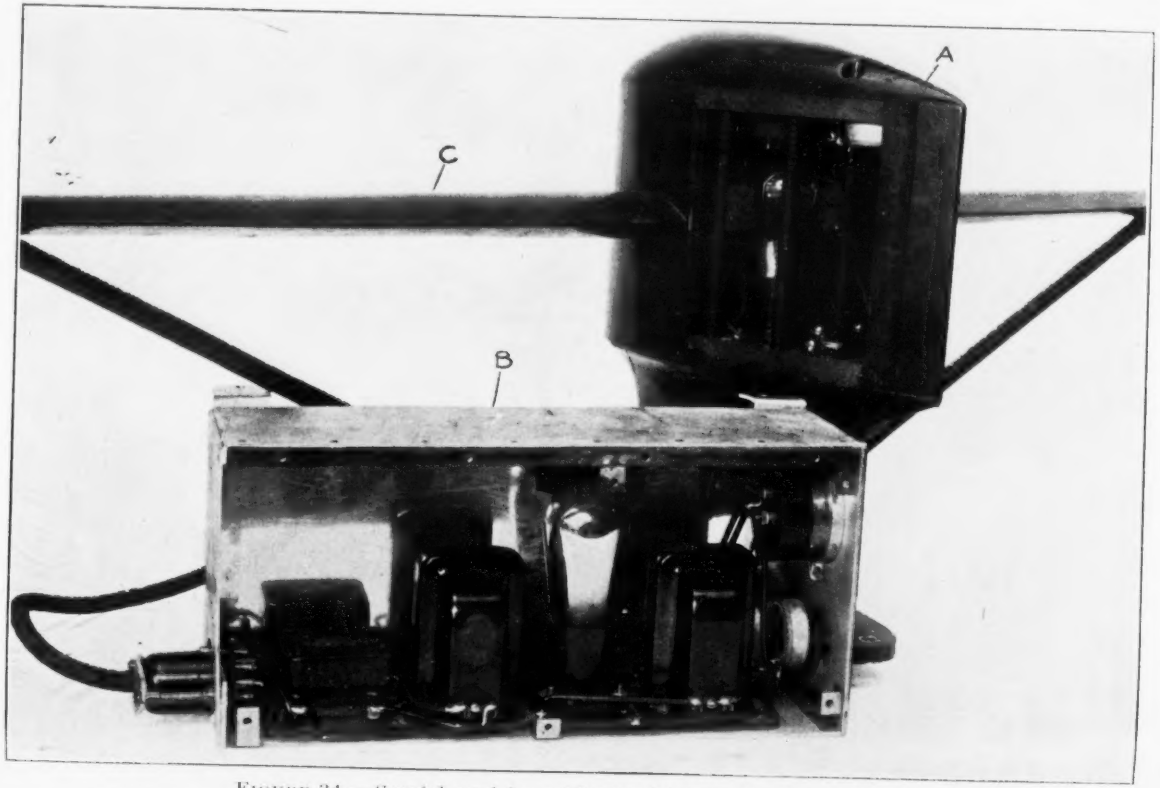

FIGURE 34.—*Special receiving set for receiving landing beam signals.*

A 224 heater-type screen-grid tube is employed for the detector, to afford the necessary high amplification without undue microphonic noises. To obtain good efficiency it was found desirable to connect the detector tube directly in the center of the horizontal doublet antenna. The detector tube was, therefore, located about 1 inch from the center of the antenna. The radio-frequency portion of the circuit is confined to the section above the four radio-frequency chokes. (See fig. 33.) The four leads running from the lower side of these chokes carry either direct current or the received audio modulation. The streamlined detector box and antenna system is arranged to plug in electrically to the supporting upright on the wing, a five-terminal plug making the necessary connections. The supporting upright also makes a plug connection to a socket in the wing.

Figure 35 shows the complete wiring diagram for the landing beacon receiver. It will be noted that the pilot has a small control box with a switch for controlling the receiving set filaments and a push button which operates a buzzer mounted in the detector box. The purpose of this buzzer is to produce a signal which operates the microammeter, provided the complete receiver is functioning properly. This button is pressed once before each landing to insure that the receiving set is functioning properly.

V. PRACTICAL APPLICATIONS

The practicability of the radio system of blind landing aids described has been partially demonstrated in numerous test flights on the bureau's experimental airplane. No difficulty has been experienced in following both the runway localizing beacon and the landing beam indications simultaneously. These tests have, however, all been made under conditions of good visibility, the bureau's airplane not being adapted for "blind" flying work. Arrangements are now being made for actual blind landing tests, the results of which it is felt will completely demonstrate the feasibility of the system.

Even in its simplest arrangement (see fig. 6), which does not take care of wind direction, this system should have numerous applications to scheduled flying. It should successfully prevent practically all interruptions to scheduled service due to dense fog, since fog is rarely accompanied by strong winds. Under special conditions of low visibility (for example, when the airport has a ceiling of 100 feet or more) the system may be used as an aid to landing regardless of wind conditions. A particularly interesting application consists of the use of this system for complete or partial blind landing on sea dromes or on airplane carriers, where the landing deck can at all times be oriented into the wind. A large number of conditions exist where a partial use of the system described appears practicable. The runway localizing beacon, in particular, seems to have possibilities of extensive use. This was demonstrated in the tests at Mitchel Field, under the auspices of the Guggenheim fund, where a special landing altimeter was employed in conjunction with the localizing beacon.

With the expansion of the system to take care of wind direction as shown in Figure 16, it is felt that the last great obstacle to flying under any conditions of weather is overcome.

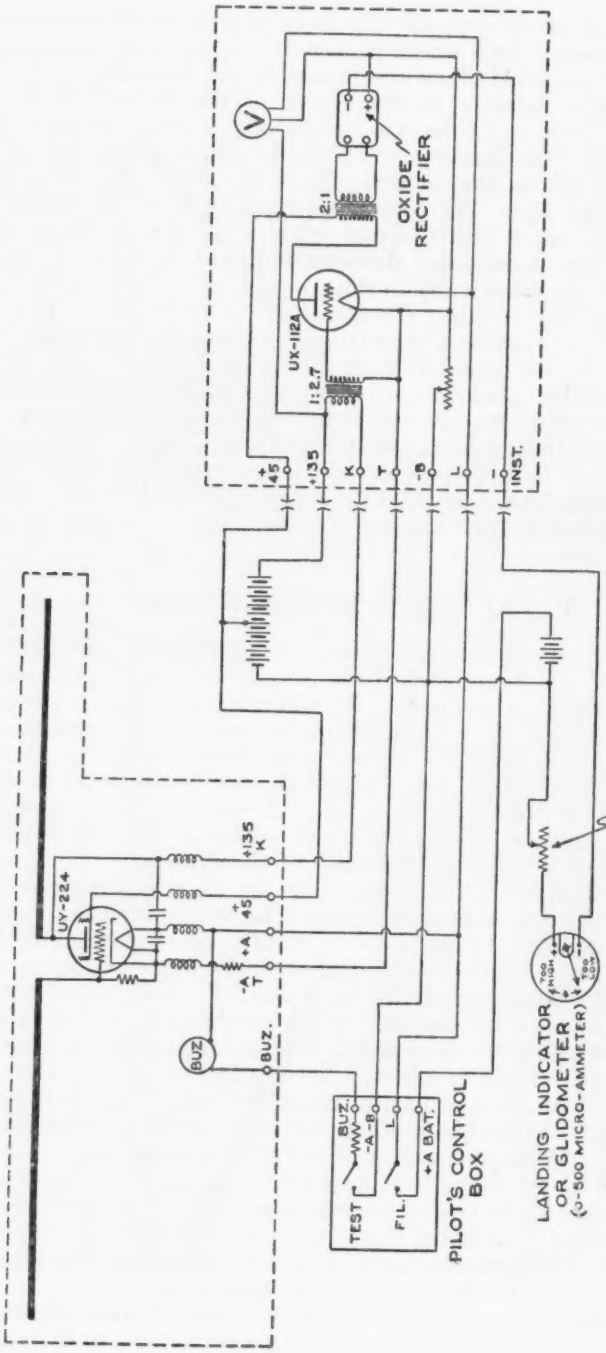

FIGURE 35.—*Complete wiring diagram for the special landing beam receiving set*

VI. ACKNOWLEDGMENT

The authors desire to acknowledge the parts played in this development by their coworkers in the Bureau of Standards. Appreciation of valuable contributions is extended to Lieut. D. H. Stuart, airplane pilot, for skillful flight tests of the system; to W. H. Orton for research incident to the operation of the landing transmitting and receiving apparatus; to W. S. Hinman for research in the design and construction of the automatic volume control and filter units; and to F. G. Kear and R. M. Green for field installations and tests. Special acknowledgment is due to Col. H. H. Blee, director of aeronautic development, Aeronautics Branch, and Dr. J. H. Dellinger, chief of the radio section, Bureau of Standards, for many helpful suggestions during the progress of the work.

WASHINGTON, July 29, 1930.

THE ISOLATION OF THE ISOMERS OF HEXANE FROM PETROLEUM [1]

By Johannes H. Bruun [2] and Mildred M. Hicks-Bruun

ABSTRACT

This paper describes the isolation of four of the five isomers of hexane from an Oklahoma crude petroleum. The fifth isomer, 2-2-dimethylbutane, was not found.

It was found that ordinary fractional distillation concentrated the hexanes in a cut of constant-boiling mixtures, the other constituents of which were ring compounds.

These constant-boiling mixtures were broken up by distillation after the addition of an alcohol which was later removed from the distillates by washing with water. In this way, aided by equilibrium melting, the following four hexanes were obtained and identified: 2, 3-dimethylbutane, 2-methylpentane, 3-methylpentane, and *n*-hexane.

The following constants were determined for each hexane: Boiling point, freezing point, specific gravity, and refractive index.

The freezing points found for two of the hexanes appear to be the only ones on record. They are, for the air-saturated hydrocarbon, $-143 \pm 0.5°$ C. for 2-methylpentane and $-118 \pm 0.5°$ C. for 3-methylpentane. The eutectic for the system CO_2-2-methylpentane is $-153 \pm 0.5°$ C.

CONTENTS

	Page
I. Introduction	933
II. Methods employed	934
III. Experimental procedure	935
1. Fraction containing the four higher-boiling isomers of hexane	935
2. A search for 2, 2-dimethylbutane	938
IV. Discussion of results	939
1. The 2, 3-dimethylbutane fraction	939
2. The 2-methylpentane fraction	941
3. The 3-methylpentane fraction	941
4. The *n*-hexane fraction	942
V. Acknowledgment	942

I. INTRODUCTION

A search through the literature reveals the reported isolation of four of the five isomers of hexane from petroleum.[3] The methods employed were usually a combination of distillation and strong chemical treatment, which yielded a mixture of the hexane isomers. By means of chlorination, bromination, or nitration of this mixture the

[1] This paper describes some of the results obtained in an investigation on The Separation, Identification, and Determination of the Chemical Constituents of Commercial Petroleum Fractions listed as project 6 of the American Petroleum Institute Research. Financial assistance in this work has been received from a research fund of the American Petroleum Institute donated by John D. Rockefeller. This fund being administered by the institute with the cooperation of the Central Petroleum Committee of the National Research Council. These results were communicated to the American Petroleum Institute April 1, 1929.

[2] American Petroleum Institute research associate.

[3] See the numerous references given in Engler-Höfer "Das Erdöl," **1**, p. 242 (Hirzel, Leipzig, 1913), and the literature cited by Brown and Carr, Ind. Eng. Chem., **18**, p. 718; 1926.

corresponding derivatives of the hexanes were obtained, and the derivatives, having larger differences in boiling points, were separated by means of fractional distillation. Some investigators attempted not only to prove in this way the presence of these isomers but actually to isolate them in pure condition. In this way Sidney Young[4] was able to isolate a small sample of *n*-hexane in fairly pure condition. With this exception, it seems that no one has obtained *n*-hexane or its isomers from petroleum in a demonstrably pure condition.

In recent years other investigators[5] have reported the isolation of the isomers of hexane by using efficient fractionating columns without the aid of chemical reagents. Although the fractions obtained were apparently of higher purity than those previously reported, the evidence as to purity and identity was, however, not complete.

The possibility of isolating pure hydrocarbons from petroleum by means of fractional distillation alone, seems to depend entirely upon the crude oil used. If this contains cyclic compounds which form constant boiling mixtures with the alipahtic hydrocarbons, complete separation can not be obtained in this way. If, for instance, methylcyclopentane or benzene is present, constant boiling mixtures with the hexanes will be formed.[6] Since cyclic compounds as a rule have higher densities and higher refractive indices than the aliphatic hydrocarbons, the presence of these ring compounds probably accounts for the fact that these physical constants are always higher for the hexanes reported from petroleum than for the synthetic ones.

II. METHODS EMPLOYED

For the purpose of separating the aliphatic from the cyclic hydrocarbons, it is desirable to avoid any chemical treatment which might destroy certain groups of hydrocarbons or convert them into new compounds from which they could not be readily recovered in the original form. In this investigation, therefore, use has been made only of physical methods.

In order to separate by distillation two liquids of nearly the same boiling point, it is customary to add a third component which alters materially the vapor pressure ratio of the original components; for example, by forming a constant boiling mixture with one of them. The general application of this principle is in practice not always feasible because difficulties are encountered in removing the added component after distillation. If, however, this component is selected so that it can be extracted by water or some other nonmiscible liquid it offers a very convenient method for separating cyclic from aliphatic hydrocarbons.[7]

In separating the ring compounds from the hexanes a liquid, such as absolute ethyl or methyl alcohol, is added in certain proportion and the mixture is subjected to fractional distillation, after which the alcohol is extracted from the distillates with water. Ethyl alcohol forms mixtures of constant minimum boiling point with the isomers of hexane, which all boil below 58.7° C. On the other hand, the com-

[4] J. Chem. Soc., London, **73**, p. 910; 1898.

[5] Anderson and Erskine, Ind. Eng. Chem., **16**, p. 263; 1924; Brown and Carr, Ind. Eng. Chem., **18**, p. 1926.

[6] Young, J. Chem. Soc., London, **73**, Trans., p. 905, 922; 1898.

[7] An industrial application of this method might be used for separating certain groups of (aromatic cyclic or unsaturated) hydrocarbons of high antiknock value from petroleum fractions.

nt boiling mixtures of ethyl alcohol and ring compounds have iling points somewhat higher as indicated by the following data, ich are taken from the International Critical Tables, Vol. III, ge 320.

C_2H_5OH with—	B. P.	Mole per cent of C_2H_5OH
	°C.	
Cyclohexene	66.7	49.5
Cyclohexane	64.9	44.5
Methylcyclohexane	73.0	70.0
Benzene	68.24	44.8
1, 3 Cyclohexadiene	66.7	47.3
n-hexane	58.68	33.2

III. EXPERIMENTAL PROCEDURE

FRACTION CONTAINING THE FOUR HIGHER BOILING ISOMERS OF HEXANE

In the present investigation about 30 liters of the naphtha fraction [8] th a boiling range from about +34° to 180° C. was subjected to stillation in a current of carbon dioxide in the 20-plate rectifying ill described in a previous paper.[9] Fractions from this distillation, ving a boiling range of 54° to 75° C., are represented by the ver- al row of rectangles on the left side of the chart shown in Figure 1. his diagram shows the further separation of these fractions.

Each rectangle represents a fraction and the numbers inside the ctangle indicate, respectively, the serial number (at the top) and e refractive index n_D^{20} (at the bottom). Boiling points are not in- rted as the distillation was carried out in different stills, in which ifferent thermometers and thermocouples were used, and also be- use the temperatures recorded were uncorrected and only of labo- tory value.

Fractions having similar refractive indices and boiling points were ixed and redistilled in smaller stills of Pyrex laboratory glass with ther steel "jack chain" columns or nonsiphoning bubbling-cap lates.[10] Referring to the upper left of the chart shown in Figure 1 ee letter *A* on chart), fractions Nos. 66^7 and 66^8 were mixed and dded to the still pot (indicated by the heavy horizontal line on the p), after which fractions Nos. 116^1, 116^2, 116^3, 116^4, 116^5, 116^6, and 16^7 were distilled off. In many cases the fractions were added to e still pot at intervals during the distillation. For instance, at the wer right of Figure 1 (see letter *B* on chart) fractions Nos. 126^7, 26^8, and 126^9 were initially mixed in the still pot. Fraction 126^{19} as then distilled off after which 126^{10} was added to the still pot, 26^{20} was next distilled off, etc.

The unbroken lines in the chart indicate that the distillation was arried out without the previous addition of a third component, the otted lines indicate that methyl alcohol was added to the still pot, hile the dashed lines show that ethyl alcohol was used as a third

[8] The crude was obtained from No. 6 well of the South Ponca Field, Kay County, Okla. See B. S. Jour. esearch, **2**, p. 469, Table 1; 1929.

[9] Washburn, Bruun, and Hicks, B. S. Jour. Research, **2**, pp. 470–473; 1929.

[10] J. H. Bruun, Ind. Eng. Chem., Anal. ed., **1**, p. 212; 1929.

component. For instance, referring to the center of the chart (fig. (see letter *C* on chart), fractions 117^5, 117^6, 114^4, 114^5, and 114^6 we mixed with methyl alcohol and added to the still pot. Fractio 117^{12}, 117^{13}, and 117^{14} were then distilled off after which fractio 117^7, 117^8, 114^7, 114^8, and 115^4 and more methyl were added to t still pot. Fractions 117^{15}, 117^{16}, 117^{17}, 117^{18}, and 117^{19} were th distilled off, etc. With this explanation, the chart is self-explanator

Freezing point curves were made for fractions 64^5, 64^6, 64^7, 6 64^9, and 65^1, which had refractive indices ranging from 1.387 to 1.4 The freezing ranges were from −95° to −60° C. This suggest that effective fractionation could be obtained by equilibrium me ing[11] (indicated by "D"). Therefore, each fraction was froze melted slowly, and separations made according to the melting poin In each case the fractions so obtained were classified into the grou shown in Table 1.

TABLE 1

Group	M. P. range	Refractive index n_D^{20}
I	−95° to −115° C	1.389 to 1.406.
II	−70° to −95° C	1.382 to 1.389.
III	−30° to +5° C	1.392 to 1.413.

Group II, which was the largest group, contained the hexanes, indicated by the melting point range, index of refraction, and boili point range. Fractionation of these three groups was continue in some cases alternating the equilibrium melting with distillati The ranges of the indices of refraction of the fractions contained Groups I and III in Table 1 are very similar, while their freezi points differ by more than 100° C. By further equilibrium melti the groups shown in Table 2 were obtained.

TABLE 2

Group	M. P. range	B. P. range	Refractive index n_D^{20}
I	−100° to −115° C	70° to 73° C	1.397 to 1.410.
II	−93° to −95° C	69° to 69.5° C	1.378 to 1.384.
III	−30° to +5° C	77.5° to 81° C	1.407 to 1.453.

The section of Group II in Table 2 containing compounds havi refractive indices from 1.380 to 1.383 was then mixed with fractio from serial Nos. 91 to 92. (See fig. 1.)

Concerning Group III in Table 2 it may be noted that althou no serious attempt was made to isolate the pure constituents, t odor resembled that of benzene. Also the freezing point (arou +5), the boiling point (about 81) and the refractive index (1.4 after several crystallizations approached more and more the valu of pure benzene. The presence of a constant boiling mixture (boili point around 69° C.) of benzene with the hexane would also expla why only small amounts of benzene would be obtained at the prop boiling point (79.6° C.) during a straight distillation of the crude c

[11] M. M. Hicks, B. S. Jour. Research, 2, pp. 483–486; 1929.

Group I in Table 2 will, perhaps, be found to consist mainly of methylcyclopentane which has the following physical constants: boiling point, 73° C.;[12] melting point, −140.5° C.;[12] and refractive index n_D^{20}, 1.410.[13]

As we approach the lower end of the diagram the refractive indices of the hexane fractions are decreasing, which indicates the separation of the cyclic and aromatic compounds. Compounds with high refractive indices were concentrated in the fractions on the right hand of the diagram and were gradually eliminated.

As a result of this procedure all the possible isomers of hexane were obtained with the exception of 2,2-dimethylbutane, the boiling point (49.7° C.) of which lies outside the range of this material. The search for this low boiling isomer is described below (p. 938).

The physical constants determined for the final fractions, together with some of the most reliable values recorded in the literature for the corresponding synthetic compounds, are given in Table 3. The data on refractive indices and specific gravities given by other investigators have been rounded off.

TABLE 3.—*Physical constants of the isolated hydrocarbons*

Compound	Boiling point corrected 760 mm	Freezing point °C. (in air)	Refractive index n_D^{20}	Specific gravity 20°/4°C.
2,2-dimethylbutane:				
(Series No. 114 [3]=40 ml)[a]	58.0	−135±1	1.378	0.668
(Series No. 126 [21]=40 ml)	58.3		1.376	.665
Synthetic:				
Data compiled by Edgar and Calingaert [b]	[c] 58.1		[d] [e] 1.377	[e] .662
Beilstein Erg. Bd. 1, p. 55; 1928	[f] 58.7	[g] −135		
2,3-methylpentane:				
(Series No. 119 [3]=100 ml)	60.4	−143±0.5	1.374	.659
(Series No. 126 [23]=120 ml)	60.6		1.373	.658
Synthetic:				
Data compiled by Edgar and Calingaert [b]	[c] 60.2		[d] [e] 1.371	[e] .654
Beilstein Erg. Bd. 1, p. 53; 1928			1.374	
3-methylpentane:				
(Series No. 110 [3]=60 ml)	63.3	−118±0.5	1.376	.665
(Series No. 127 [3]=50 ml)	63.2		1.375	.662
Synthetic:				
Data compiled by Edgar and Calingaert [b]	[c] 63.2		[d] [e] 1.376	[e] .665
Beilstein Erg. Bd. 1, p. 54; 1928	63.5 to 65.5		1.377	.667 [3]96
n-hexane (Ser. No. 126 [35])[h]	68.84	−97.2±0.5	1.379	.673
Synthetic:				
Timmermans [i]	68.80	−95.0	1.375	.659
Beilstein Erg. Bd. 1, p. 51; 1928 and Vol. I, p. 143; 1918	[j] 68.95	[k] −94.3	[l] 1.375	[e] .660
According to Mair [m]	68.68	−95.4±0.1	1.375	

[a] The molecular weight was found to be 85.7±0.5; theoretical=86.10. For method see B. S. Jour. Research, p. 575; 1930.
[b] J. Am. Chem. Soc., **51,** p. 1546; 1929.
[c] Chavanne, Bull. Soc. Chim. Belg., **31,** p. 331; 1922.
[d] Lowry, J. Chem. Soc., **105,** p. 91; 1914.
[e] Chavanne and Van Risseghem, Bull. Soc. Chim. Belg., **31,** p. 87; 1922.
[f] At 762 mm. pressure.
[g] From Int. Crit. Tables, **1,** p. 204.
[h] The molecular weight was found to be 85.6±0.3; theoretical=86.10.
[i] Timmermans, J. Chim. Phys., **25,** p. 411; (1928).
[j] Young, J. Chem. Soc., **73,** p. 906; 1898.
[k] Timmermans Chem. Zentr., **II,** p. 1015; 1911.
[l] Brühl Lieb. Ann., **200,** p. 184; 1880.
[m] Bureau of Standards, unpublished.

[a] From Int. Crit. Tables, **I,** p. 202.
[b] Kijner, J. Prakt. Chem., **56,** p. 364; 1897.

2. A SEARCH FOR 2, 2-DIMETHYLBUTANE

The physical constants of synthetic $(CH_3)_3C–CH_2CH_3$ are:[14]

Boiling point	49.7°C.
Refractive index $n\frac{20}{D}$	1.369
Specific gravity $\frac{20}{4}$	.649
Melting point	−98.2°C.

Six hundred gallons of crude oil[15] was distilled in a semicomme still in an oil refinery.[16] The lower boiling fractions from this tillation were fractionated in a 20-plate laboratory bubbling still.[17] The fractions from the laboratory still having boiling p ranges from 40° to 55°C. were subjected to distillation in sm Pyrex laboratory glass stills.[18] Between 40° and 52°C., 1,70 was obtained and after two more distillations in the glass fractions with the boiling points and refractive indices shown Table 4 were obtained.

TABLE 4.—*Properties of the final fractions obtained in a search for 2, 2-dimethylbutane*

Boiling range (°C.)	Volume	Refractive index at 20° C.
	ml	
36–38	100	
38–40	120	
40–42	240	1.367
42–44	270	1.372
44–46	135	1.377
46–47	110	1.376
47–48	140	1.381
48–49	120	1.379
49–50	74	1.384
50–51	30	1.390
51–57	150	1.381
Total	1,489	

Careful fractionation of the 1,700 ml of the combined frac with boiling point range 46° to 52° C. did not yield more th very small amount of liquid at the boiling point of 2, 2-dime butane. The comparatively high refractive indices of these hi boiling fractions indicate that they may be mixtures of cyclic hy carbons and the two isomers of hexane (boiling points 58° 60° C.), the presence of which has been shown on page 937.

Because of the fact that the fractions from our laboratory (equipped with condensers cooled with solid CO_2) contained sev liters of constituents boiling below 50° C., it seems reasonably to assume that the 2, 2-dimethylbutane was not lost by evapors before or during the industrial distillation in which ice water employed on the condenser. The very small amount (74 ml distillate which was obtained between 49° and 50° C. as well as

[14] International Critical Tables, 1, p. 204.
[15] From the well mentioned in footnote 8, p. 935.
[16] Acknowledgment for this distillation is made to A. E. Pew, jr., and R. B. Davidson, of the Sun
[17] See footnote 8, p. 935.
[18] See footnote 10, p. 935

A

D

Tab 2 Gr I 1397-1410

Tab 2 Gr II 1378-1384

1380-1383

Tab 2 Gr III 1407-1453

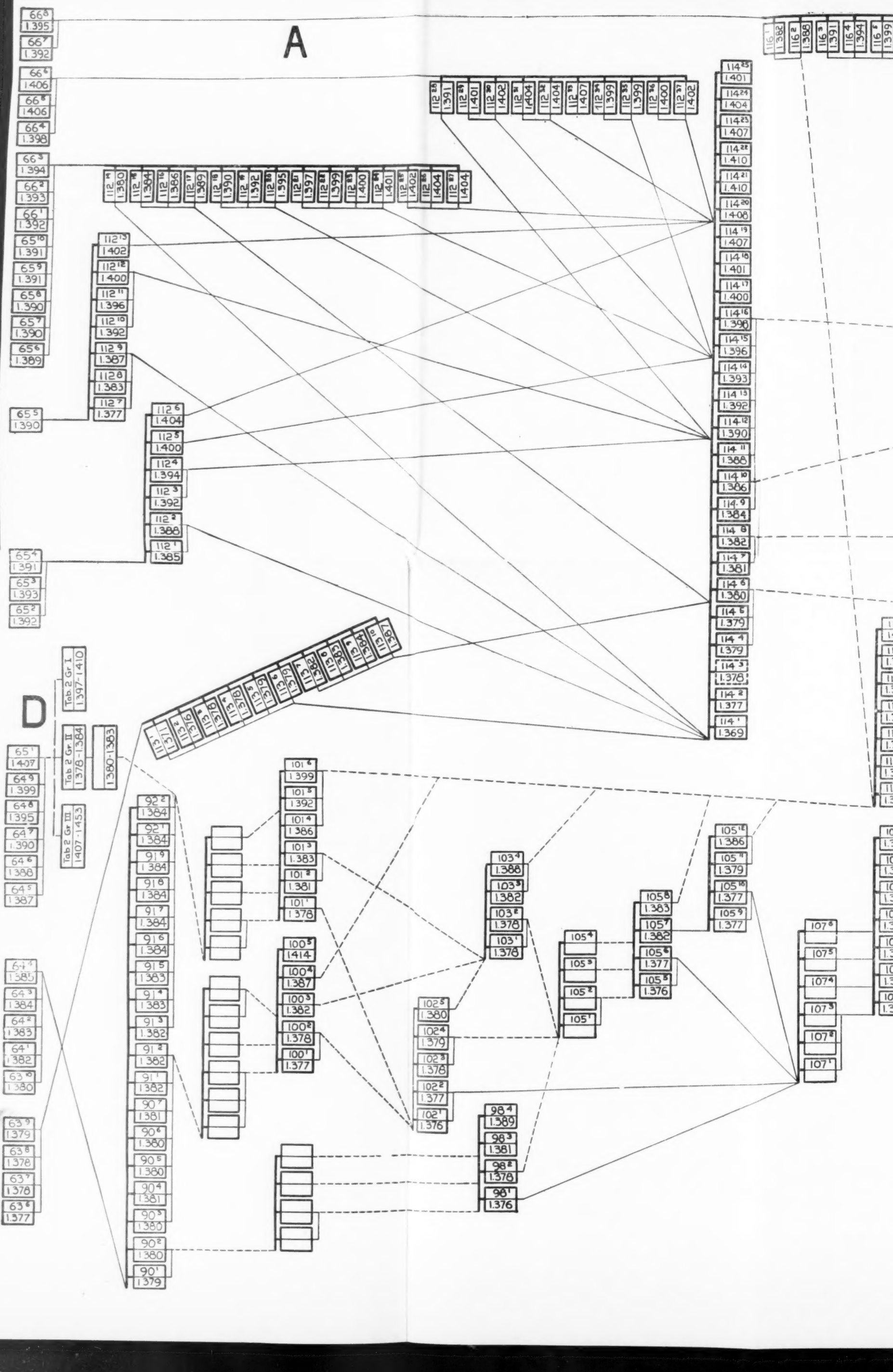

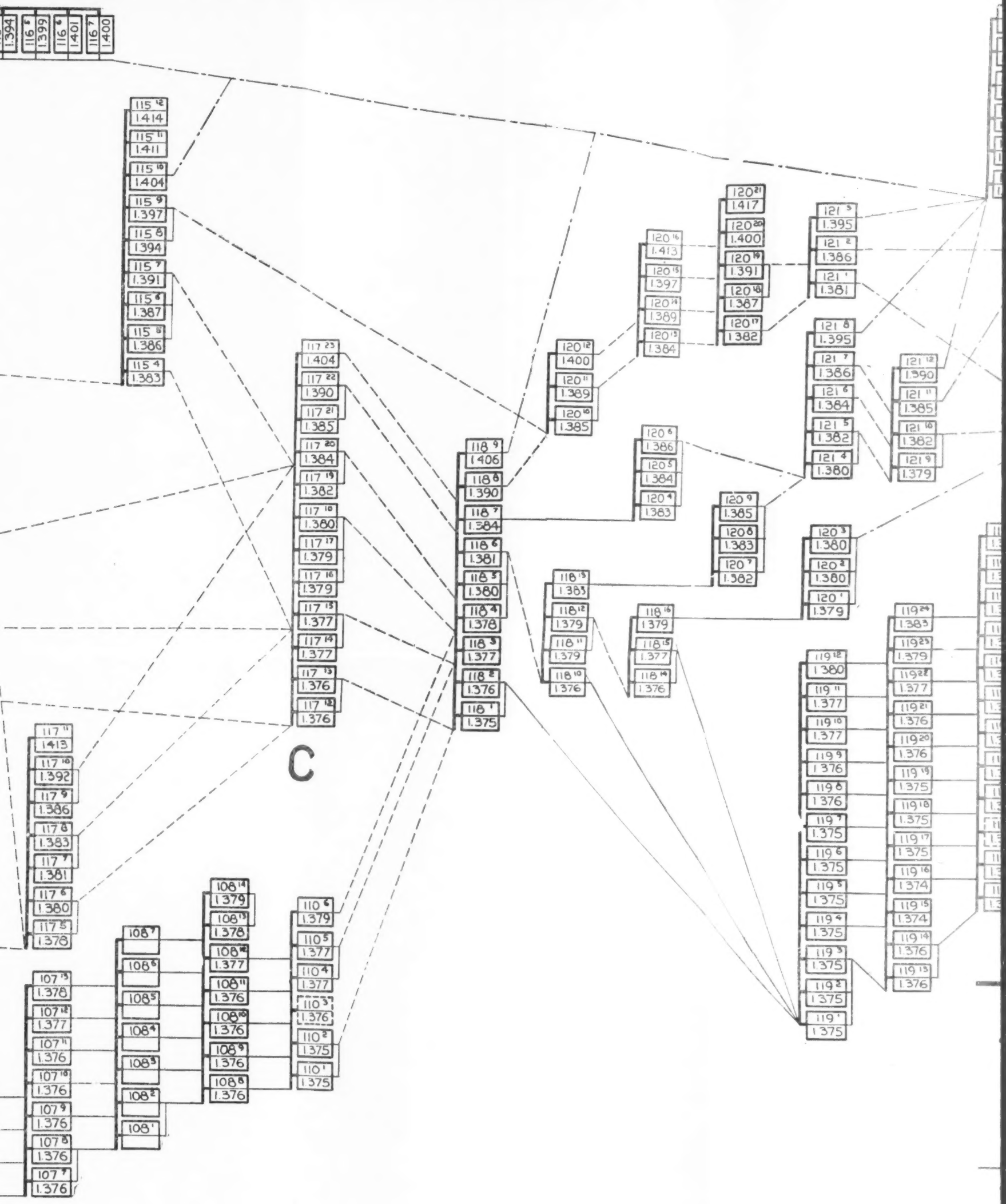

FIGURE 1.—*Ancestral chart of the hexanes*

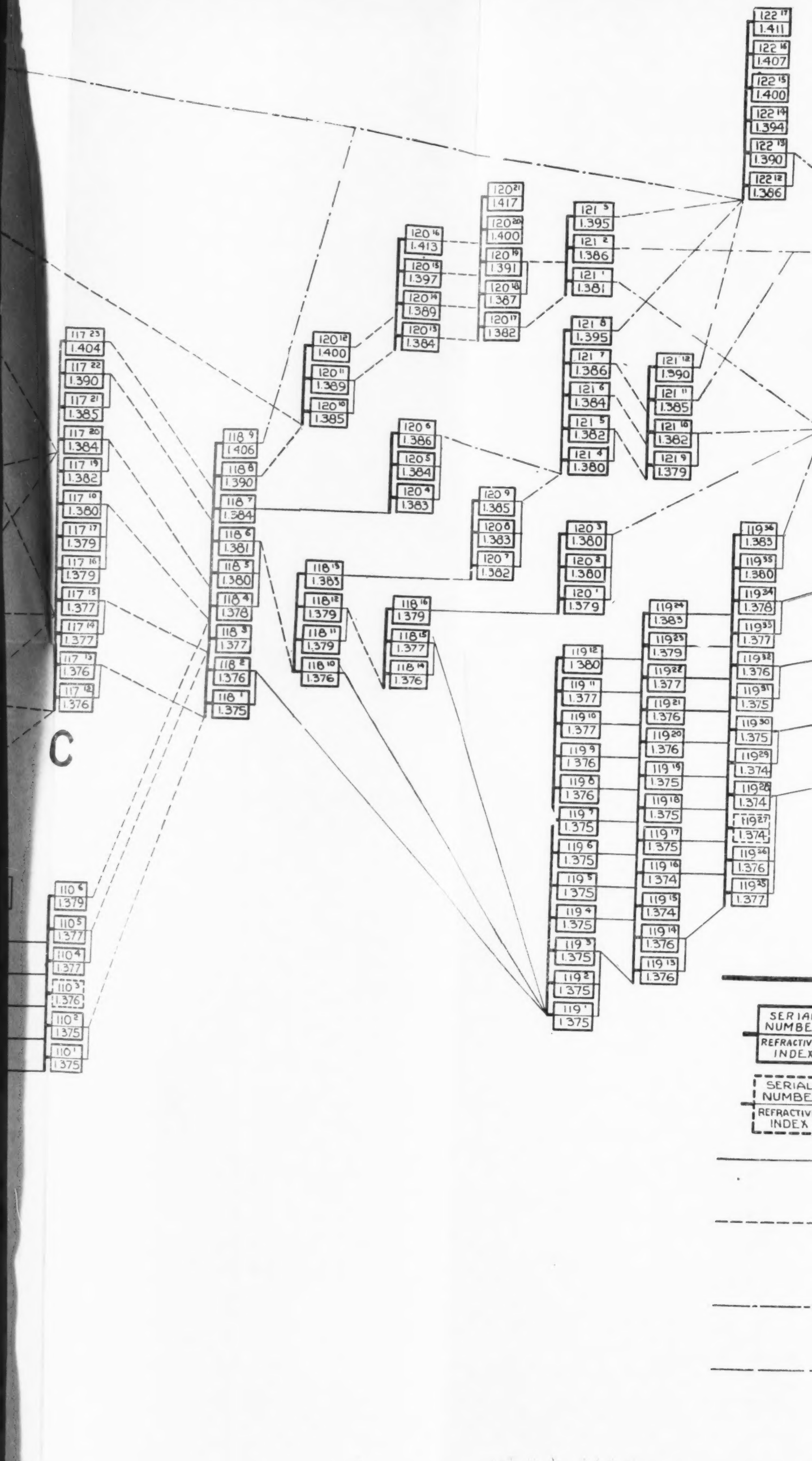

FIGURE 1.—*Ancestral chart of the hexanes*

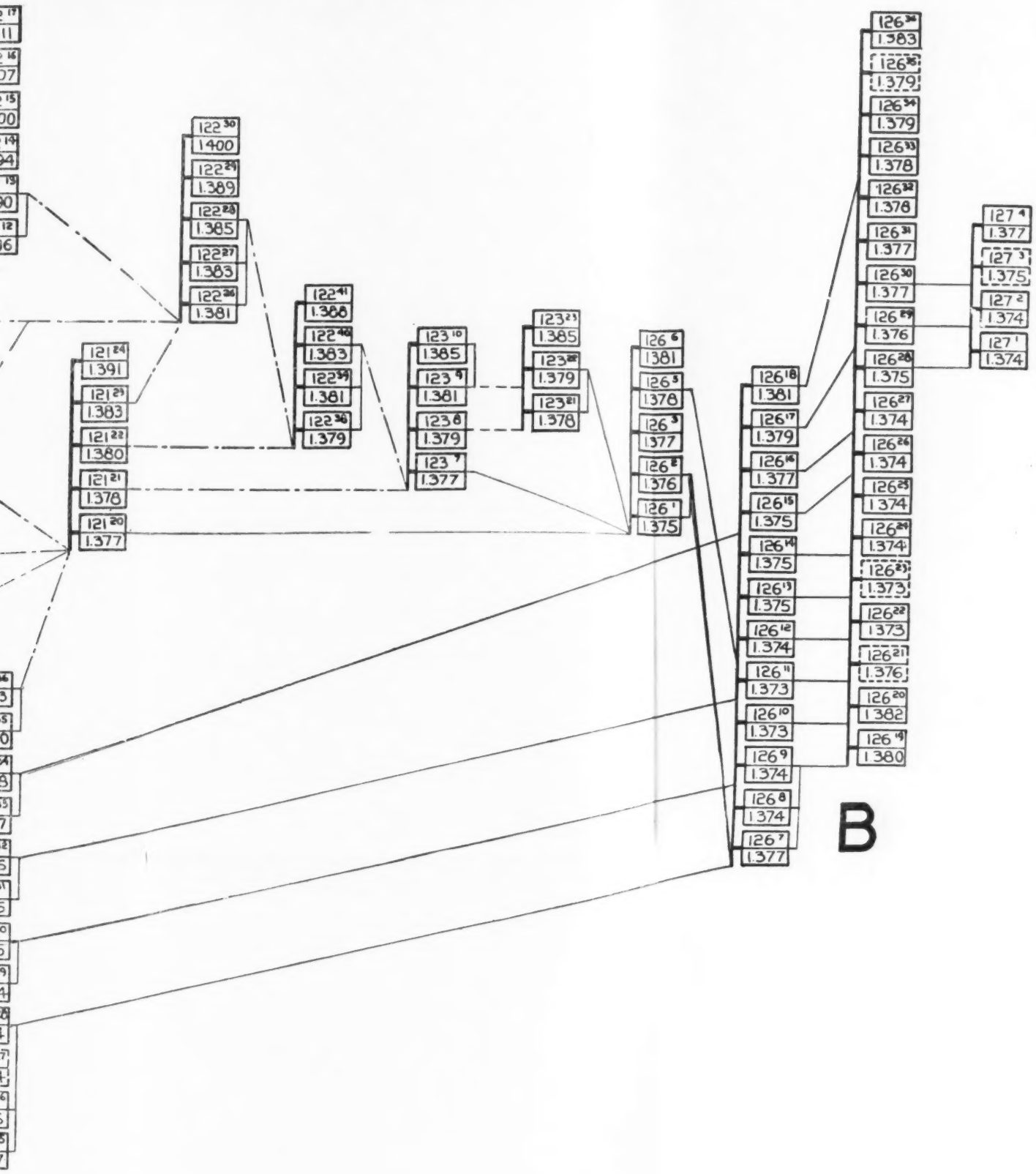

STILL POT

SERIAL NUMBER / REFRACTIVE INDEX

FRACTION DISTILLED OFF

SERIAL NUMBER / REFRACTIVE INDEX

FRACTION LISTED IN TABLE 3.

FRACTION ADDED TO STILL POT

FRACTION + METHYL ALCOHOL ADDED TO STILL POT

FRACTION + ETHYL ALCHOL ADDED TO STILL POT

FRACTION CRYSTALLIZED OFF

paratively high refractive index (1.384 against 1.369 for 2-dimethylbutane) of the distillate would indicate that the 2-dimethylbutane is absent or if present the percentage must be than 0.01 of the crude. It should be noted, however, that the sibility of the presence of 2, 2-dimethylbutane in the crude oil not completely excluded unless the absence of constant boiling xtures of this hexane with other constituents is proved.

IV. DISCUSSION OF RESULTS

1. THE 2, 3-DIMETHYLBUTANE FRACTION

The values of the five properties recorded in Table 3 for this ction show excellent agreement with those of the synthetic hydro-

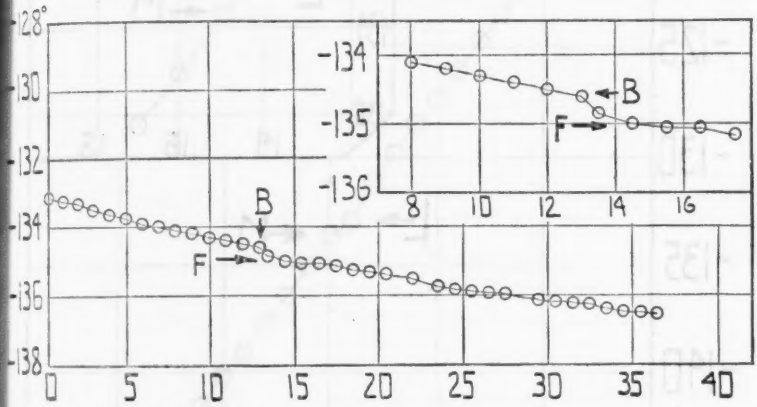

FIGURE 2.—*Cooling curve for 2, 3-dimethylbutane, C_6H_{14}*

Ordinates, temperature in ° C. Abscissas, time in minutes.

rbon. The agreement with respect to the freezing point is the ost significant, however, since the other four properties alone are t very distinctive for the hexane isomers. The cooling and heat- curves for this fraction are shown in Figures 2 and 3. At the oint *B* in Figure 2 crystallization begins. From *B* to *F* the tem- rature falls, owing to the increasing concentration of the dissolved r in the liquid phase. At *F* the liquid has become saturated with issolved air, and the system becomes nonvariant as evidenced by he three to four minute halting point at −135° C., which is the eezing point of the air-saturated hydrocarbon. On the heating urve (fig. 3) liquefaction does not begin until about −134°. The tent heat of fusion is evidently very small.

2. THE 2-METHYLPENTANE FRACTION

Here only three properties are available for comparison. The greement is satisfactory, but is not sufficient evidence of identity nless it can be demonstrated that the fraction is not a mixture. n order to obtain evidence on this point, the cooling curve was etermined with the results shown in Figure 4. These results are

satisfactory as far as they go, but it was noticed that the liqu became very viscous at its freezing point, so viscous in fact that t stirrer ceased to operate, and crystallization may, therefore, n have been complete.

In order to avoid this difficulty the hydrocarbon was cooled about $-50°$ and then saturated with solid CO_2. The dissolved C

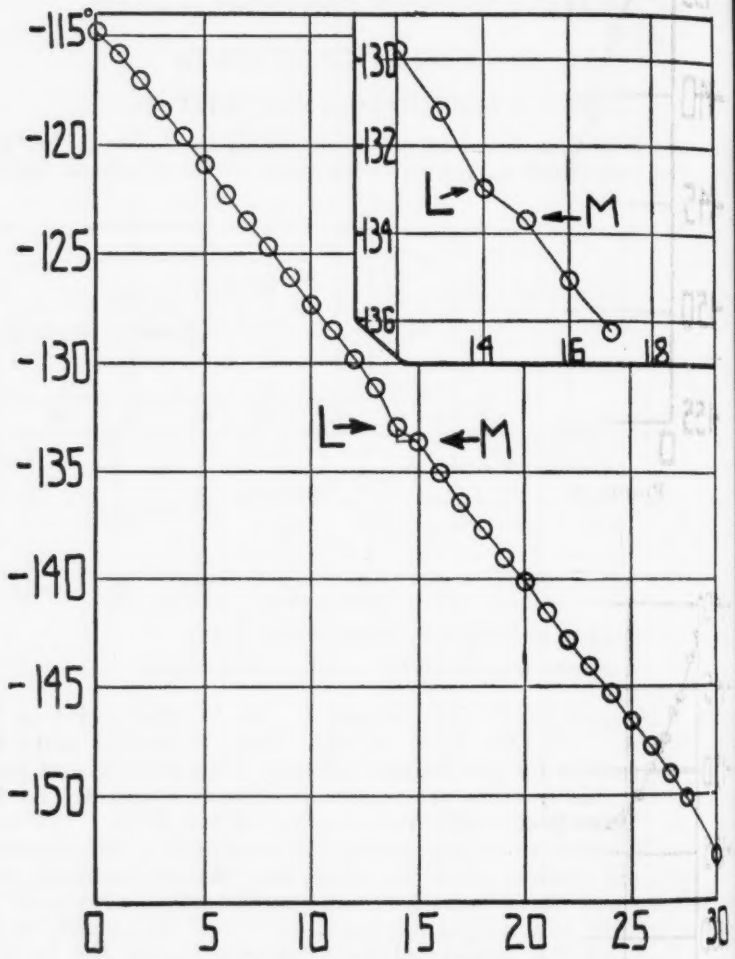

FIGURE 3.—*Heating curve for 2, 3-dimethylbutane, C_6H_{14}*

Ordinates, temperature in ° C. Abscissas, time in minutes

materially increased the fluidity. The cooling curve was then deter mined through the eutectic, with the results shown in Figure 3. The thermocouple was placed in the center of the sample, and freezing started on the walls of the container and proceeded toward the center. The long halting point followed by the sharp drop in tem perature at the completion of crystallization is evidence of purity.[19]

[19] The shorter halting point in the second experiment is due to the use of a heavier walled containing vessel and a consequent increase in the heat capacity of the system.

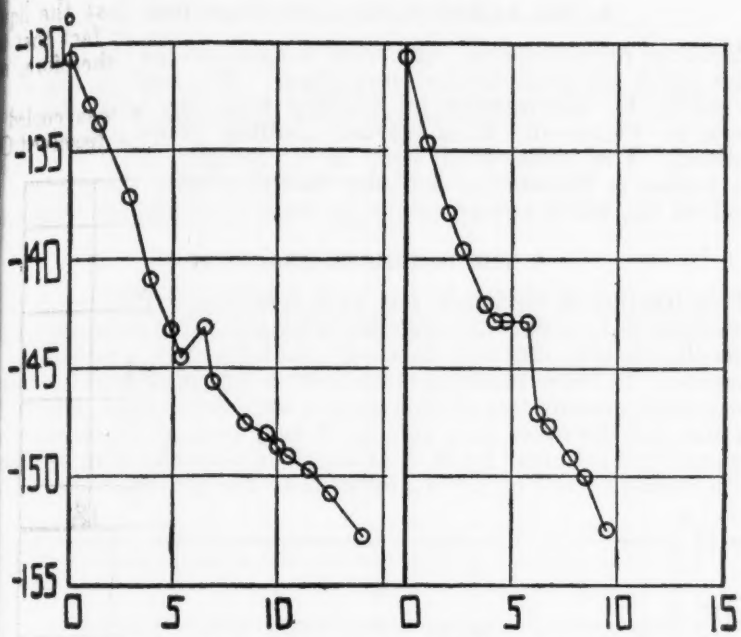

FIGURE 4.—*Two cooling curves for 2-methylpentane, C_6H_{14}*

Ordinates, temperature in ° C. Abscissas, time in minutes.

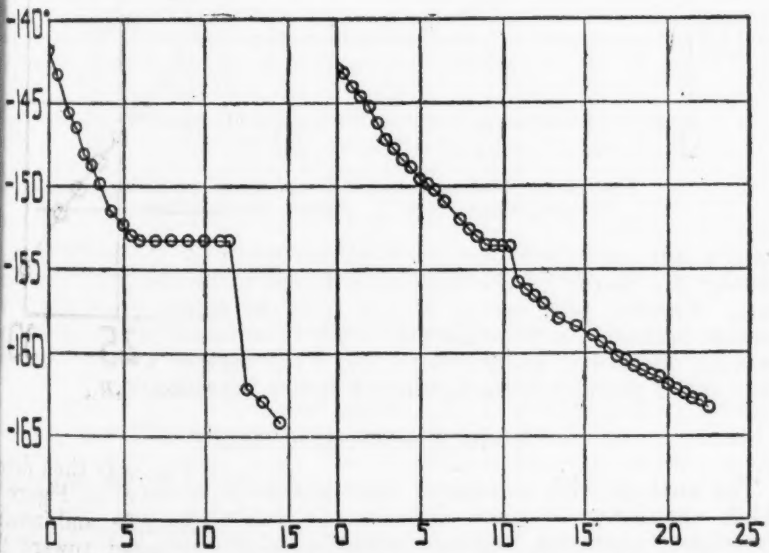

FIGURE 5.—*Cooling curve for carbon dioxide eutectic with 2-methylpentane, C_6H_{14}*

Ordinates, temperature in ° C. Abscissas, time in minutes.

3. THE 3-METHYLPENTANE FRACTION

As in the preceding case, agreement is excellent for the three properties which are available for comparison. The fraction was tested for purity by determining its freezing behavior, with the result shown in Figure 6. A satisfactory halting point was evidently obtained. The initial small drop in temperature after crystallization begins is the normal behavior resulting from the presence of dissolved air, which is very soluble in these hydrocarbons when cold.

4. THE N-HEXANE FRACTION

This fraction is obviously not pure *n*-hexane. The approximate agreement as to properties, together with the value obtained for the molecular weight indicate, however, that its major constituent is *n*-hexane. In order to obtain quantitative information as to amount of *n*-hexane present two cooling curves were determined, one on the fraction and the other on a sample of very pure synthetic *n*-hexane prepared in this bureau by B. J. Mair. The *n*-hexane from petroleum had a freezing point of 1.8° C. lower than the synthetic one. From

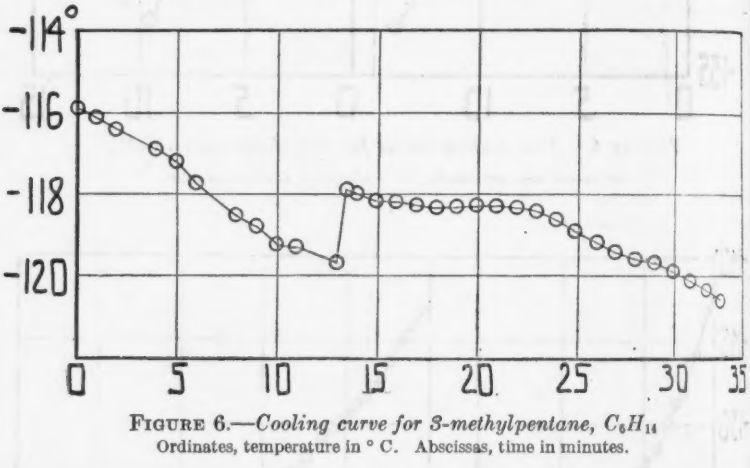

FIGURE 6.—*Cooling curve for 3-methylpentane, C_6H_{14}*
Ordinates, temperature in ° C. Abscissas, time in minutes.

these results and the value 34.89 cal. per gram for the molal heat of fusion,[20] the purity of the fraction is found to be about 92 mole per cent. Further purification of the fraction seems unnecessary at present because *n*-hexane has previously been found in petroleum and because additional quantities of this hydrocarbon will be obtained from other petroleum fractions now under investigation.

V. ACKNOWLEDGMENT

The authors wish to express their gratitude to E. W. Washburn, chief, chemistry division, Bureau of Standards, and director of American Petroleum Institute research project No. 6, under whose direction this investigation has been conducted. We are indebted to J. F. Fox for drawing the chart in Figure 1.

WASHINGTON, April 1, 1930.

[20] Parks and Todd, J. Ind. Eng. Chem., 21, p. 1236; 1929.

DETERMINATION OF CARBON IN HIGH SULPHUR STEELS BY DIRECT COMBUSTION

By H. A. Bright and G. E. F. Lundell

ABSTRACT

Oxides of sulphur are formed in the direct combustion method for carbon in steel and cause positive errors if they are not removed. The absorbents commonly used for this purpose, as well as promising new ones, have been tested. A description is given of the absorption train that has been developed at the National Bureau of Standards as well as one that has been developed by the Jones & Laughlin Steel Co.

CONTENTS

	Page
I. Introduction	943
II. Absorbents used for removing oxides of sulphur	944
III. Absorption train used at the National Bureau of Standards for high sulphur steels	948

I. INTRODUCTION

The method used largely at the present time for the determination of carbon in steel or iron is that of direct combustion in oxygen and absorption of the evolved carbon dioxide in soda-asbestos (ascarite) or soda lime. The increasing use of high sulphur steels (S > 0.10 per cent) has led to difficulties in securing accurate results for carbon, with consequent disagreements between different laboratories. This is caused by the fact that the sulphur in the steel burns to form oxides of sulphur. If these are not removed completely from the gas stream positive errors for carbon will result in the gravimetric method, and in any method in which the excess of barium hydroxide is titrated.

In the direct combustion of low sulphur plain carbon steels most of the sulphur is converted to sulphur trioxide. Some sulphur dioxide is also formed, and the amount will vary according to such factors as the rate of oxidation of the steel, the temperature, the type of furnace, and the kind of steel.[1]

In the present study it was desired to develop an absorption train which could be constructed readily in the ordinary laboratory. For this reason the possibility of using special apparatus such as electrical precipitators [2] was not investigated. It is doubtful in any case whether the oxides of sulphur could be quantitatively precipitated by electrical precipitation under the conditions prevailing in the direct combustion method for carbon.

[1] For example, from 2 to 10 per cent of their sulphur content was given off as sulphur dioxide when 2 g samples of steels containing 0.13 to 0.22 per cent of sulphur were burned. On the other hand, nearly 50 per cent was given off as dioxide sulphur from a stainless steel containing 14 per cent of chromium and 0.43 per cent of sulphur and from a plain carbon steel containing about 0.7 per cent of sulphur. It is evident that with low sulphur plain carbon steels the chief problem is to provide for the removal of sulphur trioxide, while with high sulphur steels the removal of the dioxide is as important as that of the trioxide. In fact it may be more important, for the absorption of the dioxide by alkaline reagents is more complete than is that of the trioxide.

[2] F. Oschwald, Determination of C in Al, thesis, Eidgenossiche Tech, Hochschule, Zürich, No. 356; 1923. J. Remy and C. Koch, Examination of Chemical Fogs for Electrical Charges, Z. anorg. allgem. Chem., 139. p. 69; 1924.

II. ABSORBENTS USED FOR REMOVING OXIDES OF SULPHUR

Asbestos.—A practice for removing oxides of sulphur that is employed by quite a few chemists [3] consists in packing the exit end of the combustion tube (usually 30 inches long) with a 6 to 8 inch section of ironized asbestos.[4] The ironized asbestos retains more or less sulphur trioxide in the cool section at the exit end and may also cause the oxidation of some sulphur dioxide to sulphur trioxide. If asbestos is used ferric sulphate will accumulate in the exit end of the combustion tube, and it is necessary, periodically, to draw the section containing the asbestos back into the hot zone of the furnace and burn out the sulphur trioxide by heating to about 900° C. while a stream of air or oxygen is passed through the tube. How often this must be done depends on the number and the sulphur content of the samples that are burned each day.[5] If this periodic burning out is neglected high and erratic results for carbon are obtained, particularly with steels containing more than 0.1 per cent of sulphur.

It is also well to mention that sulphur trioxide which has been fixed as ferric sulphate at a low temperature will be liberated again and carried along in the exit gas stream when the temperature becomes high enough to decompose ferric sulphate. Even though no trioxide is thus liberated, some may still remain in the gas stream through failure of the ironized asbestos to retain all of it. In addition, the ironized asbestos is not an efficient oxidizer of the sulphur dioxide that is always present.

The small amount of sulphur trioxide that may pass the asbestos when steels of less than 0.2 per cent sulphur are burned will usually be retained by the solid desiccant (phosphorus pentoxide, anhydrone of 20 to 25 mesh, etc.) interposed between the furnace and the absorption tower for carbon dioxide. If such provision is made to retain any sulphur trioxide which may pass by the asbestos and if the tube is burnt out regularly, it is believed that acceptable results for carbon in steels containing less than 0.2 per cent of sulphur can be obtained by this procedure. However, these precautions are not adequate to avoid high results for steels of higher sulphur content. For continuous runs on plain carbon steels containing more than 0.15 per cent of sulphur or on any high-sulphur stainless steels, it is probably better to omit the asbestos in the combustion tube and to absorb the oxides of sulphur after they leave the combustion tube.

Zn.—Granulated zinc of 20 to 80 mesh is used by a number of chemists for removing oxides of sulphur. Tests indicate that it acts as a baffle for condensing more or less sulphur trioxide, but does not remove sulphur dioxide. Like asbestos it has a limited value when used with low-sulphur steels (S<0.06 per cent), but is not satisfactory for high-sulphur alloys.

---

[3] Methods of the Chemists of the U. S. Steel Corporation for the Sampling and Analysis of Alloy Steels, Carnegie Steel Co., Pittsburgh, Pa., p. 9; 1921.

[4] Prepared by digesting asbestos in a solution of ferrous sulphate (150 g of the salt in 1 liter of 1 per cent sulphuric acid), drying and igniting at 1,000° C.

[5] W. D. Brown, chief chemist of the Carnegie Steel Co., Duquesne, Pa., informs us that they burn out combustion tubes every fifth day. About 75 determinations a day are made on a tube and approximately 10 per cent of the steels contain more than 0.10 per cent of sulphur. F. Garman, of the Pennsylvania R. R. Laboratories, Altoona, Pa., states that tubes are burned out after each 100 samples of plain carbon steels, none of which exceed 0.05 sulphur. With cast irons and screw steels a tube is burned out at least once a day.

P_2O_5.—In this laboratory and elsewhere it has been noted that phosphorus pentoxide, because of its fine state of subdivision, will also act as a baffle and condense and retain sulphur trioxide to a certain extent. It is not effective for sulphur dioxide.

PbO_2.—Tests made by passing a mixture of approximately 95 parts of oxygen and 5 parts of sulphur dioxide through a U tube containing specially prepared lead dioxide showed that sulphur dioxide is quantitatively absorbed. The lead dioxide was purified by digesting for several hours at 25°C. with nitric acid (1:3), filtering, washing with water, and drying at 105°C. Sulphur trioxide mist secured by passing dry oxygen through fuming sulphuric acid was also absorbed to a certain extent at 25° C. and very well at 250°C. It was found, however, that the lead dioxide absorbed small amounts of carbon dioxide at 25° C. and even at 100° C. No absorption of carbon dioxide was observed at 250° C.

The use of lead dioxide as an absorbent for oxides of sulphur was further tested by determining carbon in 2 g samples of steel to which 0.05 g portions of pyrite had been added. The exit gases from the combustion tube were passed through a 15 cm U tube, loosely packed with lead dioxide and heated to a temperature of 250° C. The gases from this tube were passed next through a 10 cm U tube filled with anhydrous magnesium perchlorate (anhydrone) and then into ascarite. Similar tests were made on 2 g samples of the

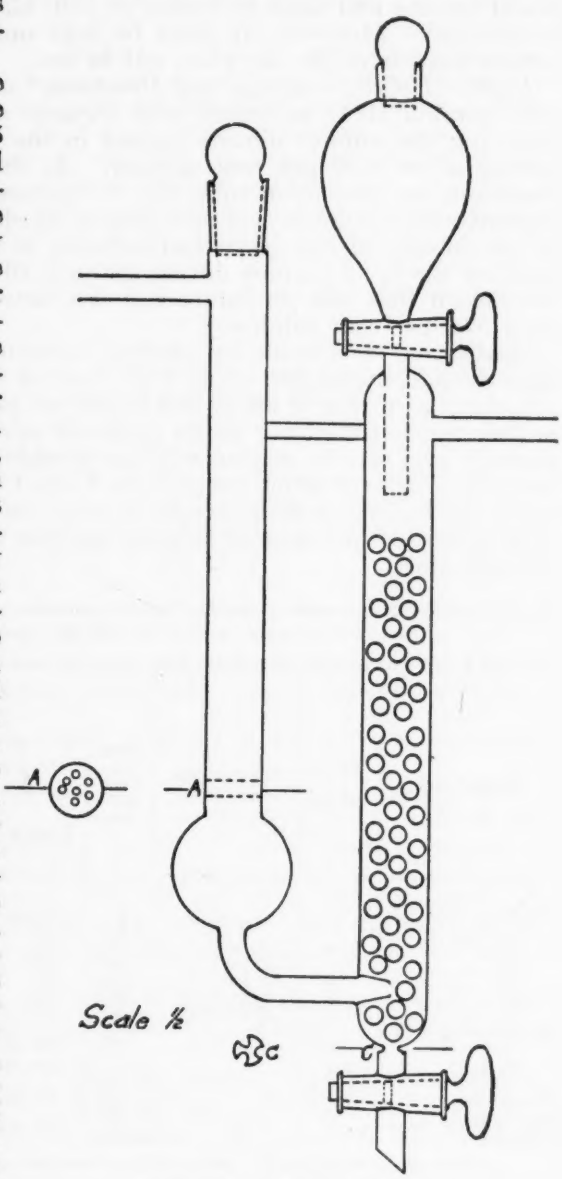

FIGURE 1.—*Absorption tube*

same steel to which 0.03 g portions of ferric sulphate were added. In both cases correct results for carbon were obtained.

Lead dioxide has certain disadvantages in that it requires an additional furnace and must be heated at 250° C. until a uniform blank is obtained. Moreover, it must be kept out of contact with the carbon dioxide of the air when not in use.

$H_2SO_4 - H_2CrO_4$.—Arnold and Ibbotston [6] used a dilute sulphuric acid solution (1:1) saturated with chromic acid for oxidizing and removing the sulphur dioxide formed in the burning of steels containing about 0.09 per cent sulphur. At the National Bureau of Standards an absorption tube (fig. 1) containing, in the right arm, concentrated sulphuric acid saturated with chromic acid and a 9 to 10 cm column of closely packed asbestos in the left arm has been used for the same purpose during the past 10 years. Previous tests had shown that this procedure was satisfactory for steels with less than 0.08 per cent sulphur.

Qualitative tests made by passing a mixture of dry air and sulphur dioxide, containing about 5 per cent of the latter, through the absorbent at a rate of about 200 to 250 ml per minute showed that neither concentrated nor dilute sulphuric acid (1:1) saturated with chromic acid would oxidize sulphur dioxide completely. Further tests, the results of which are given in Table 1, show that this absorbent is not entirely satisfactory for regular use with steels containing more than 0.10 per cent of sulphur and not at all for high sulphur stainless steels.

TABLE 1.—*Results for carbon obtained by using concentrated sulphuric acid saturated with chromic acid as an absorbent for oxides of sulphur*

[Figures in parentheses indicate the number of determinations from which the average was obtained]

Type of steel	Weight of sample	Sulphur compound added	Total sulphur present	Carbon			
				Per cent present		Per cent found	
				Average	Range of determinations	Average	Range of determinations
Bureau of Standards standard B. O. H.	*g*	*g*	*g*	*Per cent*		*Per cent*	
No. 11d	2		0.0008	[a] 0.202		0.201 (8)	0.200–0.204
Do	2	0.01 FeS_2	.0058	.202		.22 (8)	.201– .26
Do	2	.02 FeS_2	.0108	.202		.23 (5)	.22 – .30
Do	2	.05 FeS_2	.0258	.202		.43 (2)	.41 – .46
Do	2	.01 $Fe_2(SO_4)_3$	.0032	.202		.208 (2)	.203– .213
Do	2	.03 $Fe_2(SO_4)_3$	.0080	.202		.214 (2)	.21 – .218
Bessemer screw stock: [b]							
No. 1	2.73		.0036	[c] .088 (3)	0.086–0.092	.093 (3)	.092– .093
No. 2	2–3		.0024–.0036	[c] .131 (11)	.127– .138	.137 (21)	.134– .14
Plain carbon	2–2.73		.0044–.0060	[c] .171 (5)	.168– .175	.182 (11)	.17 – .187
High sulphur stainless steel [d]	1.5–2		.0064–.0085	[c] .090 (16)	.084– .096	.160 (6)	.124– .186

[a] Certificate value.
[b] Supplied through the courtesy of H. E. Slocum, chief chemist, Jones & Laughlin, Pittsburgh, Pa.
[c] Value obtained on the train adopted for high sulphur steels described on p. 948.
[d] Supplied through the courtesy of P. Tyson, chief chemist, Carpenter Steel Co., Reading, Pa.

[6] The Chemical Analysis of Steel-Works' Materials, 3d. ed., p. 35; 1907.

Aqueous solution of CrO_3 and dry chromates.—Blair [7] used a saturated aqueous solution of chromic acid for removing sulphur dioxide. This absorbent oxidizes sulphur dioxide completely, but does not remove all of the sulphur trioxide present in the exit gas stream when high sulphur steels are burned. Tests of crystals of potassium dichromate, dry barium chromate, and lead chromate showed that these substances do not absorb sulphur dioxide completely. Wetted crystals of potassium dichromate remove sulphur dioxide but because of lower solubility do not have as great an oxidizing capacity as a saturated aqueous solution of chromic acid.

Compounds added to the sample.—It is claimed by some that sulphur is retained in the slag if the drillings are mixed and burned with red lead (Pb_3O_4) or lead chromate. It is quite unlikely that lead sulphate or lead sulphite would be stable at the high temperature (>1,000° C.) occuring in the combustion boat.

Platinized silica gel and ironized asbestos.—For high sulphur steels H. E. Slocum [8] uses a train in which the gases from the combustion tube are passed first over platinized silica gel heated to 440° C. The catalyst,[9] of 6 to 8 mesh size, is contained in a pyrex glass U tube of a size to give a column approximately 1.2 cm in diameter and 30 cm in length. A small electric furnace with a rheostat is used to heat the catalyst. The gases are next passed through a tower containing a column (approximately 4 by 13 cm) of closely packed ironized asbestos for removing sulphur trioxide, on top of which is a 4 by 5 cm layer of anyhdrone for absorbing moisture. From the second tube the gases are passed to the usual carbon dioxide absorption tube.

Slocum also uses a specially designed combustion tube which is bent down at an angle of 90° at the point where it issues from the heating furnace. The exit end of the tube is tapered to facilitate connecting with the silica gel tube. It is claimed that there is less sulphuric acid condensed and collected in this form of combustion tube.

The chief function of the gel is to oxidize, catalytically, sulphur dioxide to the trioxide. A secondary function is to oxidize carbon monoxide to carbon dioxide should any have been formed in the combustion. With a properly functioning catalyst all of the sulphur that enters the tube containing the gel leaves the tube as sulphur trioxide and must afterwards be removed from the exit gases by collecting in a suitable absorbent, such as closely packed ironized asbestos.

This train has been tested by Slocum on samples of plain carbon steels to which sulphur had been added. Correct results for carbon were obtained.

It should be recognized that the efficiency of a catalyst may, and generally will, fall off in continued use. No data are available at present as to how long the platinized silica gel will function satisfactorily for this particular use. However, Slocum states that several catalysts have been in daily use in the Jones & Laughlin Co.'s laboratory for four months and have given satisfactory service. The use

[7] A. A. Blair, The Chemical Analysis of Iron, 8th ed., p. 128; 1918.
[8] The Laboratory, **3**, No. 2, p. 24 (1930); Fisher Scientific Co., Pittsburgh, Pa.; Burrell Bulletin 1017, Burrell Tech. Supply Co., Pittsburgh, Pa.
[9] Prepared according to Holmes et al., J. Ind. Eng. Chem., **21**, p. 850; 1929.

of red lead in the combustion boat is not recommended, since it tends to poison the catalyst.[10]

Tests of platinized silica gel made during this investigation indicate that it is entirely satisfactory if sufficient contact surface is provided. For example, with a 0.55 by 29 cm column of a silica gel containing 0.15 per cent of platinum [11] small amounts of sulphur dioxide were found in the gas stream issuing from the tube containing the catalyst when burning a 2 g sample of a stainless steel containing 0.43 per cent of sulphur, while with a 1.1 by 30 cm column of the same catalyst only negligible traces of sulphur dioxide were detected. Tests of a second catalyst of somewhat higher platinum content [12] and the smaller column referred to above showed a slight improvement over the same volume of the first catalyst, but did not show quite as complete oxidation of the sulphur dioxide as the larger volume of the first catalyst.

In using platinized silica gel it is therefore necessary to be sure that the particular lot of catalyst and the size of the column are adequate to oxidize all of the sulphur dioxide which may be present in the gases issuing from the combustion tube.

III. DESIGN OF COMBUSTION TUBE AND ABSORPTION TRAIN

As a result of the foregoing experimental work the following type of combustion tube and absorption train was developed for use in the determination of carbon in high sulphur steels. The porcelain combustion tube is about 48 cm long, of an internal diameter of 2.5 cm and is made with a rather sharply reduced diameter at the exit end. The reduced section is approximately 1 cm in outside diameter and 14 cm in length. The end of this section has a short taper to a 6 to 8 mm outside diameter. No asbestos packing is used in the tube, as with high sulphur steels less trouble is experienced from accumulations of sulphuric acid during the run. However, a short roll (3 to 4 cm) of oxidized copper gauze is placed in the 700° to 800° zone of the exit end to make sure that no carbon escapes as the monoxide. The gauze becomes coated with ferric oxide and copper sulphate and must be renewed occasionally.

The exit gases from the combustion tube are first passed through an absorption tube (fig. 1) containing about 8 to 10 ml of a 50 per cent aqueous solution of chromic acid [13] in the right arm and a 9 to 10 cm column of closely packed asbestos, plain or ironized,[14] in the left arm. All of the sulphur dioxide is removed by the chromic acid. Some, but by no means all, of the sulphur trioxide is condensed during the passage through the asbestos and the solution.[15] The first tube is followed by another of identical design which contains sulphuric acid (97 per cent) in the right arm and asbestos in the left arm. This tube serves to dry the gases and to remove more of the sulphur trioxide. The water vapor which is carried over from the aqueous chromic

[10] Private communication from H. E. Slocum.
[11] Grade 1 No. 150–G–1200–0. 15 Pt. 6 to 8 mesh, obtained from the Silica Gel Corporation, Baltimore, Md.
[12] Made by treating the 0.15 platinum, catalyst with H_2PtCl_6 as per Holmes et al., loc. cit. p. 947.
[13] A saturated solution tends to salt out and clog the tube.
[14] Our experience indicates that in this particular use, there is no difference in the absorbing or condensing efficiency of plain or ironized asbestos for sulphur trioxide.
[15] For the condensation of SO_3 mists see: H. Remy and Ruhland, Z. anorg. allgem. Chem., 139, p. 51; 1924; Z. agnew, Chem., 39, p. 147; 1926.

acid solution is not excessive (approx. 0.01 g per run). After passing through the second tube the gases enter a small U tube (12 cm) containing 20 to 30 mesh anhydrone. This tube serves to complete the drying of the gases and also to condense sulphur trioxide mist which may have passed through the first two tubes. From this third tube the gases are passed into a Fleming tube containing ascarite and anhydrone.[16] The chromic acid should be renewed about every 35 runs, the sulphuric acid about every 100 runs and the anhydrone should suffice for about 400 runs.

The pressure required for a gas stream of 200 to 250 ml per minute in a train of this construction is a little higher than in the ordinary train, but is not excessive and approximates about 4 cm of mercury. It is advantageous to use a mercury gage in the line as it serves to detect any leaks and also acts as a safety valve in case of a stop-up.[17]

TABLE 2.—*Results for carbon obtained by using a purifying train consisting of an aqueous solution of CrO_3, asbestos, 97 per cent sulphuric acid and anhydrone.*

[Figures in parenthesis indicate the number of determinations from which the average was obtained]

Type of steel	Weight of sample	Sulphur compound added	Total sulphur present	Carbon		
				Present	Average	Range of determinations
	g	*g*	*g*	*Per cent*	*Per cent*	
Bureau of Standards standard B. O. H. No. 11d	2		0.0008	[1] 0.202	0.201(12)	0.199–0.206
Do	2	0.05 FeS_2	.026	.202	.201(17)	.197–.208
Do	2	.03 $Fe_2(SO_4)_3$	.0080	.202	.200(5)	.197–.204
Do	2	.02 H_2SO_4	.0065	.202	.200(1)	

[1] Certificate value.

Results obtained for steels to which sulphur compounds had been added are given in Table 2. The data show that an absorption system containing asbestos, 50 per cent aqueous chromic acid, 97 per cent sulphuric acid and fine anhydrone is entirely satisfactory for removing oxides of sulphur in any steel that is likely to be analyzed for carbon. Values for carbon that were obtained with this train on high sulphur steels are shown in Table 1.

WASHINGTON, July 16, 1930.

[16] After the completion of the experiments incident to the adoption of the absorption system just described it was learned that P. Tyson, chief chemist of the Carpenter Steel Co., Reading, Pa., is also using a train consisting of 50 per cent aqueous chromic acid for removing sulphur dioxide, followed by sulphuric acid (98 per cent) and phosphorus pentoxide for removing sulphur trioxide and moisture.

[17] No trouble from leaks has been experienced by us. If desired the special tubes can be sealed together and a small tower substituted for the U tube.

RP241

SURFACE TENSION OF SOAP SOLUTIONS AND ITS RELATION TO THE THICKNESS OF ADSORBED FILMS

By Ronald Bulkley and F. G. Bitner

ABSTRACT

A sharp minimum in the surface tension-time curves of certain soap solutions has been interpreted in the literature as indicating the gradual formation of a surface film possessing the properties of a plastic solid and having a thickness equivalent to some 10,000 molecular lengths. In this paper the hypothesis is advanced that the formation of the thick film is brought about by chemical action between carbon dioxide from the air and dissolved soap. Surface tension experiments performed in the open air have confirmed the existence of the minimum point observed by previous investigators. However, when solutions prepared in exactly the same manner were tested by the same method in an atmosphere free from carbon dioxide no minimum point was found. The solutions behaved instead in the manner which is characteristic of colloidal solutions in general. These results support the hypothesis advanced above and leave the preponderance of evidence against the existence of a film of extraordinary thickness at the surface of soap solutions.

CONTENTS

	Page
I. Introduction	951
II. Experimental	952
III. Discussion	955

I. INTRODUCTION

In the course of an investigation [1] to determine the limiting distance to which a solid surface can affect the viscosity of a contiguous liquid, one of the authors had occasion to review the experimental work reported in the literature on the viscosity of liquids at the air-liquid interface. The most diverse conclusions as to the nature and magnitude of this property have been reached by different investigators even from the performance of the same experiment. Thus Plateau [2] observed that the surface viscosity of some liquids was higher than the viscosity in bulk, while the surface viscosity of other liquids was lower than in bulk. His experiments were repeated by Luvini [3] and, at a later date, by Lord Rayleigh,[4] both of whom arrived at the conclusion that the anomalous surface viscosities observed by Plateau were due to contamination. Stables and Wilson [5] measured the rate of damping of a torsion pendulum in the form of a thin disk suspended in the surface of a saponin solution, and found an abnormally high superficial viscosity.

[1] The Viscosity of Liquids as Measured in Fine Capillaries, Dissertation of Ronald Bulkley for degree of Doctor of Philosophy at Johns Hopkins University; 1930.
[2] Joseph A. F. Plateau, Statique des liquides, 8th series, 1873.
[3] Giovanni Luvini, On the Adhesion Between Solids and Liquids, Phil. Mag. (4), **40**, pp. 190 to 197; 1870.
[4] Lord Rayleigh, On the Superficial Viscosity of Water, Proc. Roy. Soc., **48**, pp. 127 to 140; 1890.
[5] W. H. Stables and A. E. Wilson, On the Viscosity of a Solution of Saponine, Phil. Mag. (5), **15**, pp. 406 to 414; 1883.

du Noüy,[6] with much more delicate instruments, found for organic colloids, in general, that the surface viscosity increased and the surface tension decreased as a function of time when the measurements were made always on the same surface layer instead of on "a continuously renewed layer." Both phenomena were explained by assuming an increasing concentration of the suspended colloidal material in the surface due to adsorption. By taking observations on solutions of various concentrations a decided minimum value for the surface tension was discovered which occurred always at the same concentration for a given material. This minimum value was postulated as occurring when the surface of the containing vessels and the free liquid surface as well were just covered with an oriented monomolecular layer of the solute.

Perhaps the most remarkable results in the literature are those reported by Wilson and Ries.[7] By several independent methods of attack these authors arrived at the conclusion that the surface of a soap solution is a film with the properties of a plastic solid, the thickness of the film increasing with time to reach a value of from 10 to 40μ. This is of the order of 10,000 molecular lengths as contrasted with the monomolecular film postulated by du Noüy. Wilson and Ries worked with much higher concentrations than du Noüy. They found a sharp minimum and a sudden rise in the surface tension-time curves for palmitate and stearate soaps, which they explained by assuming that the film has the properties of a plastic solid, and at a critical thickness the force necessary to overcome the increasing yield value becomes greater than the corresponding reduction of surface tension.

Wilson and Ries apparently were aware that carbon dioxide would react chemically with their soap solutions, but, as far as can be judged from their paper, their experiments were nevertheless conducted in open vessels exposed to the ordinary atmosphere of the laboratory. It is conceivable, therefore, that the film on their solutions was formed by complete or partial decomposition of the soap by carbon dioxide to give free acid or some of the numerous acid salts described by McBain.[8] These probably would be lighter than the solution and would float at the surface, the thickness of the partially rigid layer increasing as the carbon dioxide diffused deeper into the liquid and the products of the reaction accumulated. Since the surface tension measurements are easy of performance it seemed worth while to test out this hypothesis by determining the shape of the surface tension-time curves when the solutions were at all times carfeully protected against contamination with carbon dioxide.

II. EXPERIMENTAL

The surface tension measurements were made with a du Noüy tensiometer. This instrument measures directly the force exerted by the surface film of the liquid under test upon a platinum ring of known mean circumference when the ring is pulled away from the liquid in which it has been dipped. The usual container used for the liquid

[6] P. L. du Noüy, A Note on the Surface Viscosity of Colloidal Solutions, Sci., **61**, p. 117; 1925. See also Surface Tension of Colloidal Solutions and Dimensions of Certain Organic Molecules, Colloidal Chem., **1**, pp. 267 to 275, Chemical Catalog Co.; 1926.

[7] Robert E. Wilson and E. D. Ries, Surface Films as Plastic Solids, Coll. Sym. Mon., **1**, pp. 145 to 175; 1923.

[8] J. W. McBain, Colloidal Chemistry of Soap, B. A. A. S. Third Report on Colloid Chemistry; 192

with this instrument is an open vessel which exposes the liquid to the air, the composition of which varies from hour to hour and from day to day. Figure 1 shows some typical results of tests performed in open vessels under conditions similar to those of Wilson and Ries. The solutions were made by adding 1 part of sodium oleate, stearate or palmitate to 25,000 parts by weight of hot distilled water which had been boiled about 30 minutes to rid it of CO_2. The solutions were then stoppered and allowed to cool. The surface tension-time curves are almost identical with those found by Wilson and Ries. The curve for the oleate shows the decline to steady value, those for the stearate and palmitate the rise after minimum. The stock solutions were protected from CO_2 by passing all the air which entered the flask on cooling or while withdrawing samples through a soda-lime tube. All samples were withdrawn by a syphon from the center of the flask.

The container used in later experiments was a 3-necked Woulff bottle as shown in Figure 2. The tensiometer ring was suspended through the middle neck by an aluminum wire of sufficient diameter to give rigidity and of sufficient length to reach the bottom of the

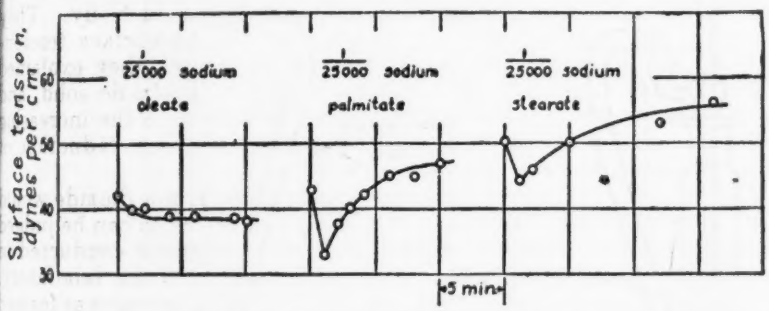

FIGURE 1.—*Surface tension-time graphs for solutions in open vessels*

bottle. This hole was then partly closed by a split-cork ring leaving a hole one-half centimeter in diameter through which the aluminum wire could move easily without touching the side. Air was supplied to the bottle through another neck by a glass tube which extended about halfway to the bottom. The solution was syphoned into the bottle through the third neck which was then stoppered. Air from the house pressure line was passed first through a wash bottle containing concentrated H_2SO_4 to indicate the rate of flow, through a drying tube containing P_2O_5 to remove moisture, and then to the Woulff bottle. When air which was free from CO_2 was desired, a tube containing soda lime was introduced between the indicator and the drying tube. The air stream was allowed to run through the bottle for about 15 minutes before the sample was introduced. The purpose of this circulation was to rid the bottle of CO_2-laden air.

The drying tube of P_2O_5 was used to insure approximately constant humidity in the Woulff bottle. That the initial decrease of surface tension with time was not due to evaporation from the surface was shown by making a few tests with the stearate and palmitate solutions while moist air was passed through the bottle. The air was moistened by bubbling through water near the boiling point and then through a column of distilled water about 50 cm deep which was kept

at room temperature. Under these conditions both solutions showed the characteristic drop in surface tension with time.

With the apparatus in place, a stream of air regulated to about 200 bubbles per minute was passed into the Woulff bottle. Since this air passed from the bottle through the small hole around the aluminum wire, there was little chance of backward diffusion into the bottle.

The sample was syphoned into the bottle after allowing some of the solution to run to waste, thus obtaining a better sample of the solution at the center of the flask. The first measurement was made as quickly as possible, and succeeding ones at measured time intervals. The air stream was stopped for each measurement, an operation of about 20 seconds.

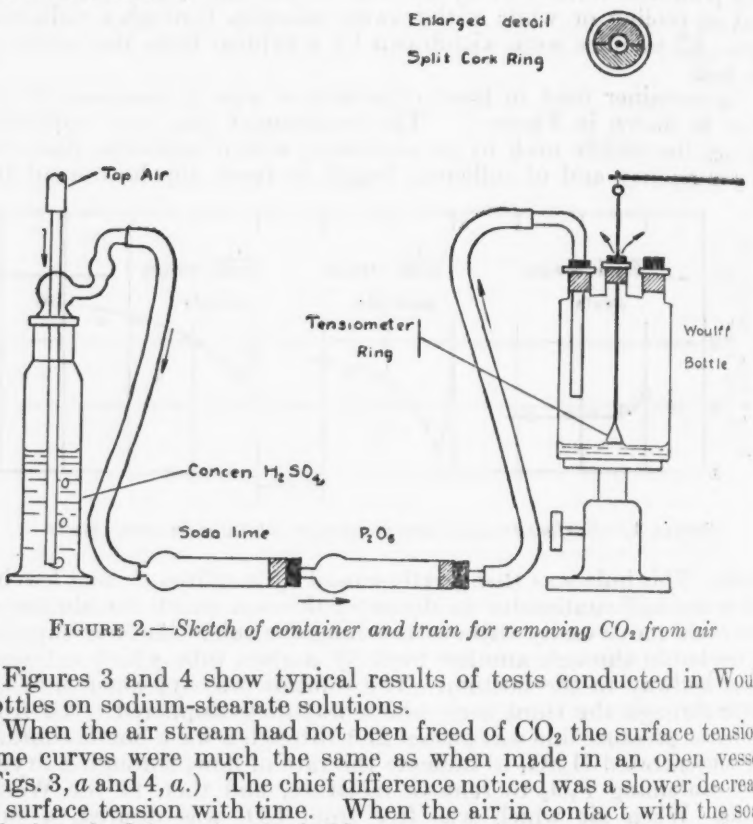

FIGURE 2.—*Sketch of container and train for removing CO_2 from air*

Figures 3 and 4 show typical results of tests conducted in Woulff bottles on sodium-stearate solutions.

When the air stream had not been freed of CO_2 the surface tension-time curves were much the same as when made in an open vessel. (Figs. 3, *a* and 4, *a*.) The chief difference noticed was a slower decrease in surface tension with time. When the air in contact with the soap solutions had been freed of CO_2, the surface tension decreased at a slower rate as shown by Figures 3, *b* and 4, *b*, reaching a steady value which held for about four hours or until the test was stopped. For the solution in Figure 4, the soda-lime tube was removed after the surface tension had remained steady for about four hours. Measurements then made at 10-minute intervals showed a sharp minimum.

Solutions of sodium stearate of high purity, made in the laboratory by titrating an alcoholic solution of chemically pure stearic acid with an alcoholic solution of NaOH, gave the same results as did the commercial product.

III. DISCUSSION

The authors offer no explanation of the observations here reported other than the hypothesis advanced earlier in the paper. This hypothesis is set forth merely as a tentative explanation, and it is supported only qualitatively by the meager evidence we have described. If the reaction of carbon dioxide with sodium oleate in the surface layer of a solution should proceed far enough to produce oleic

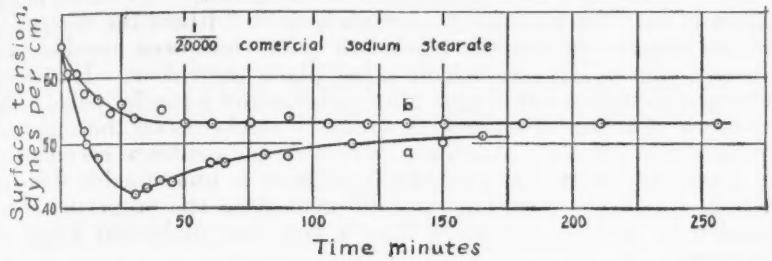

FIGURE 3.—*Surface tension-time graphs for soap solution in Woulff bottle*
a, CO_2 not removed from air stream; *b*, CO_2 removed by soda lime.

acid, the surface would be covered with a thin liquid film which would act only to lower the surface tension. No minimum in the surface tension-time curve would be expected for this solution exposed to the air and none was observed. On the other hand, the film resulting from the reaction of carbon dioxide with palmitate or stearate would be of a more or less solid nature and conceivably would acquire sufficient rigidity to produce the rise in the apparent surface tension which was found. In the absence of carbon dioxide all the solutions should

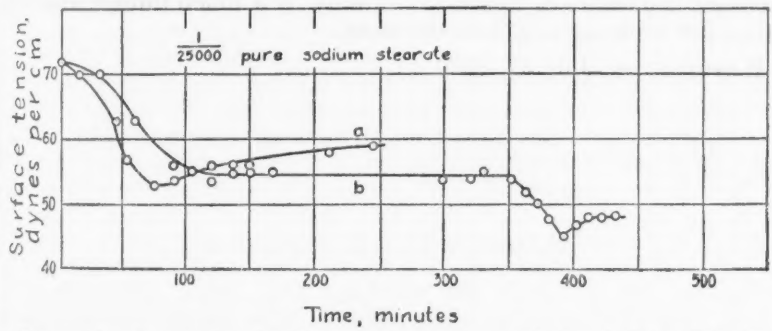

FIGURE 4.—*Surface tension-time graphs for soap solution in Woulff bottle*
a, CO_2 not removed from air stream; *b*, CO_2 removed by soda lime.

give a gradually decreasing surface tension as the concentration of the soap in the surface increased by adsorption. When equilibrium has been established between adsorbed soap in the surface and dissolved soap in the body of the liquid the surface tension should reach a low steady value as was actually observed.

Many disturbing factors enter to complicate the results, such as the age of the solution, the degree of hydrolysis of the dissolved soap, etc. The absolute values probably do not have much significance. In the

particular examples chosen here measurements made in the presence of carbon dioxide gave for commercial stearate a graph which is lower throughout its entire length than the corresponding graph for data taken in the absence of carbon dioxide. For pure sodium-stearate solutions the two curves crossed each other. Only the shape of the curves, that is, the relative values of the surface tension at different times for a single sample, are reliable as indicating the nature of the phenomena taking place. The one invariable observation which is common to all the graphs, including many not shown in this paper, is that the presence of carbon dioxide hastens the decrease in surface tension before the minimum point has been reached, and directly causes the rise which takes place thereafter. This seems sufficient to demonstrate that there is no sound basis for belief in the existence of a film of more than ordinary thickness on the surface of uncontaminated soap solutions. From ample evidence accumulated by investigators in the past the conclusion is unavoidable that this film, in which the properties are different from the properties of the solution in bulk, is not more than a very few molecular lengths in thickness.

Interesting results might be found by the further study of the surface tension of colloidal solutions by the capillary tube method or by other methods under carefully controlled conditions. Barring experimental difficulties the ideal situation would of course be to have the surface of the solution in contact only with its own vapor.

IV. CONCLUSIONS

1. There is no minimum point in the surface tension-time curve of soap solutions protected from carbon dioxide.

2. Such solutions are probably covered not by a plastic film several thousand molecules in thickness but only by a much thinner adsorbed film, a few molecules thick at the most.

WASHINGTON, July 31, 1930.

THE MEASUREMENT OF SOUND ABSORPTION

By V. L. Chrisler and W. F. Snyder

ABSTRACT

This paper contains a brief discussion of the theory of reverberation measurements. The reverberation room is described and details are given as to the method of measuring sound absorption by means of the ear.

Methods are also described by which sound absorption can be determined from oscillograph records or by the use of an attenuator box and vacuum tube voltmeter.

CONTENTS

		Page
I.	Introduction	957
II.	Methods available	957
III.	Theory of the reverberation method	958
IV.	Description of the reverberation room	960
V.	Reverberation time for an acoustically dead room	960
VI.	Source of sound	963
VII.	Calibration of the reverberation room	964
VIII.	Measurement of sound absorption coefficients by the ear method	966
IX.	Measurement of sound absorption by instrumental methods	967

I. INTRODUCTION

Since radiobroadcasting and sound pictures have become important the problem of the acoustical treatment of auditoriums has been greatly emphasized. If the acoustic quality of a room is to be determined in advance and is not to be a matter of cut and try, it is necessary to know the sound-absorption coefficients of the materials used in the interior finish of the room.

For some years past the National Bureau of Standards has realized the importance of this problem and has carried on experiments to determine the best method of measuring these coefficients. It is the purpose of the present paper to describe the theory and the method now in use at the bureau for this purpose.

II. METHODS AVAILABLE

Two methods have been used for the determination of sound absorption coefficients—the reverberation method of W. C. Sabine [1] and the tube method used by H. O. Taylor [2] and others. At the time this work was undertaken by the bureau, now some six years ago, the tube method, being entirely instrumental, appeared to be more desirable than the reverberation method, which involved the use of the ear. In addition, the tube method had the advantage that small samples could be used.[3] For these reasons this method was used for several years.

[1] W. C. Sabine, Collected Papers on Acoustics, Harvard University Press; 1922.
[2] H. O. Taylor, Phys. Rev., 2, p. 270; 1913.
[3] Transmission and Absorption of Sound by Some Building Materials, B. S. Sci. Paper No. 526, p. 61.

Notwithstanding the ease which such measurements could be conducted, it soon became evident that the results obtained by this method did not agree with those obtained by other observers using the reverberation method. In order to check and compare the two methods when carried out by the same observers, the National Bureau of Standards constructed a reverberation room which has now been in use for about two years.

As a result of this comparative study the bureau has discontinued the use of the tube method. The reasons for this change are discussed in an article entitled: "Absorption of Sound at Oblique Angles of Incidence," published in the Bureau of Standards Journal of Research for February, 1930.

III. THEORY OF THE REVERBERATION METHOD

W. C. Sabine,[4] the pioneer in the science of architectural acoustics, first developed and made use of a reverberation equation in making sound-absorption measurements. His discussion of the subject is spread at considerable length throughout his writings, and is not convenient for reference. A more compact and readable presentation is given by F. R. Watson [5] in a publication which is, perhaps, not generally accessible. For this reason it may be well to give here a brief summary of the theory, following the line of Watson's discussion.

The equation for the decay of sound in a room, as developed by Jaeger [6] is

$$E = E_0 e^{-Kt} = \frac{4A}{avS} e^{-\frac{avSt}{4V}}$$

where

E = energy of sound per unit volume in the room at time t.
A = rate of emission of energy from the source of sound.
a = average coefficient of absorption.
v = velocity of sound.
V = volume of room.
t = time at any instant after the source of sound is stopped.
S = total area exposed to sound waves.

In the practice of the reverberation method as heretofore conducted, sound is produced from any suitable source, and suddenly cut off. The time is measured from the instant of the stopping of the source until the residual sound becomes inaudible.

The object of reverberation experiments is to determine the quantity, a, and this involves a knowledge of all other quantities in equation (1).

E is determined, according to the precedure stated, by the threshold of hearing. This is assumed to be one physical unit for the normal ear, but may vary considerably from day to day with the same person. Over a short period of time, however, it may be fairly constant, though its absolute value is uncertain.

A is a quantity rather difficult to determine absolutely, though the ratio of two values of A may be determined quite accurately. This consideration, together with that in the preceding paragraph, sug-

[4] See footnote 1, p. 957.
[5] F. R. Watson, The Absorption of Sound by Materials, Bull. No. 172, Univ. of Ill. Eng. Exp. Sta. Nov. 29, 1927.
[6] Jaeger, "Zur Theorie des Nachhalls," Akad. Wiss. Sitz. Ber., **120**, 2a p. 613, 1911.

sts the advisability of making two experiments in close succession ith different values of A, and eliminating E. This is the procedure ctually adopted in the calibration of the reverberation room. For utput values of A_1 and A'_1, equation (1) gives the following for an mpty room of absorption coefficient a_1 and time of decay t_1.

$$\left.\begin{aligned} E &= \frac{4A_1}{a_1 vS} e^{-\frac{a_1 vSt_1}{4V}} \\ E &= \frac{4A'_1}{a_1 vS} e^{-\frac{a_1 vSt'_1}{4V}} \end{aligned}\right\} \tag{2}$$

liminating E we get

$$a_1 S = \frac{4V \times 2.3 \log_{10}\left(\frac{A_1}{A'_1}\right)}{v(t_1 - t'_1)} \tag{3}$$

he usual formula for calibration of a room by the reverberation-ear method.

Let us now introduce into the room a sample of material to be easured for sound absorption. Let its area be S_2 and its coefficient absorption a_2. This leaves an area $S_1 = S - S_2$ of the walls of the oom with a coefficient a_1.

Equation (1) gives in this case

$$E = \frac{4A_1}{(a_1 S_1 + a_2 S_2)v} e^{-\frac{(a_1 S_1 + a_2 S_2)\, vt_2}{4V}} \tag{4}$$

By introducing the absorbent material in the room the initial intensity has been reduced from

$$\frac{4A_1}{a_1 Sv} \text{ to } \frac{4A_1}{(a_1 S_1 + a_2 S_2)v}$$

nd therefore the measured time t_2 is a trifle shorter than it would be if the initial intensity were the same as that in the empty room. If it is now assumed that the initial intensity with the sample in room increased to the initial intensity with the room empty, equation (4) becomes

$$E = \frac{4A_1}{a_1 Sv} e^{-\frac{(a_1 S_1 + a_2 S_2)\, vt'_2}{4V}} \tag{5}$$

From the first of equations (2) and (5)

$$a_2 = \frac{a_1 St_1 - a_1 S_1 t'_2}{S_2 t'_2} \tag{6}$$

All of the quantities on the right have been measured except t'_2, ut this can be computed in terms of t_2. From equations (4) and (5)

$$t'_2 = \frac{4V}{(a_1 S_1 + a_2 S_2)}\, 2.3 \log_{10}\left(\frac{a_1 S_1 + a_2 S_2}{a_1 S_1}\right) + t_2 \tag{7}$$

To solve this equation a_2 must be known, but a sufficiently exact value can be obtained by assuming t'_2 equal to t_2 and solving for a_2

from equation (6). This approximate value of a_2 is used in equation (7) and thus obtaining t'_2. The exact value of a_2 can now be computed from equation (6).

The foregoing theory applies to the method of reverberation as heretofore applied, using the threshold of the ear as a fixed point of reference. The modification of this method now in use at the National Bureau of Standards eliminates the ear as a factor, and measures the time required for the sound intensity to decay from one fixed level to another, starting from any initial intensity. The two levels of reference between which the time is measured are indicated instrumentally.

The foregoing equations for the ear method need but slight change to be applicable to this modified practice. If the levels of measurement are E_1 and E_2 equation (1) gives for the empty room:

$$\left.\begin{aligned} E_1 &= E_0 e^{-\frac{a_1 v S t_1}{4V}} \\ E_2 &= E_0 e^{-\frac{a_1 v S t_2}{4V}} \end{aligned}\right\} \tag{8}$$

where t_1 and t_2 are now the times of passing the sound levels E_1 and E_2.

Eliminating E_0 and solving for a_1S, the total absorption of the empty room, we obtain:

$$a_1 S = \frac{4V \times 2.3 \log_{10}\left(\frac{E_1}{E_2}\right)}{v\,(t_2 - t_1)} \tag{9}$$

After introducing the test sample we obtain by modifying similarly equation (4) and denoting the new times by t_1' and t_2':

$$a_1 S_1 + a_2 S_2 = \frac{4V \times 2.3 \log_{10}\left(\frac{E_1}{E_2}\right)}{v\,(t'_2 - t'_1)} \tag{10}$$

from which a_2, the absorption coefficient of the sample may be calculated. It will be noticed that with the instrumental method it is not necessary to use two different output intensities, as E_0 is eliminated between the equations at the two levels E_1 and E_2.

IV. DESCRIPTION OF THE REVERBERATION ROOM

In planning this room two features were taken into consideration, first, the period of reverberation should be long, and second, the walls should be good sound insulators to eliminate the disturbance from outside noises. Figure 1 (*a*) and (*b*) show the construction of the room. It is a rectangular room 25 by 30 by 20 feet. The inner and outer walls are of brick, 8 inches thick and there is an air space of 4 inches between the inner and outer walls. The ceiling is of reinforced concrete supported on the inner walls. The roof is composed of a second reinforced concrete slab placed about 16 inches above the ceiling, and carried on the outer wall. In this way there is no con-

section between the inner and outer shells except at the foundation, and the sound insulation is excellent. Except for sounds, which are transmitted by ground vibration, the four doors at the entrance

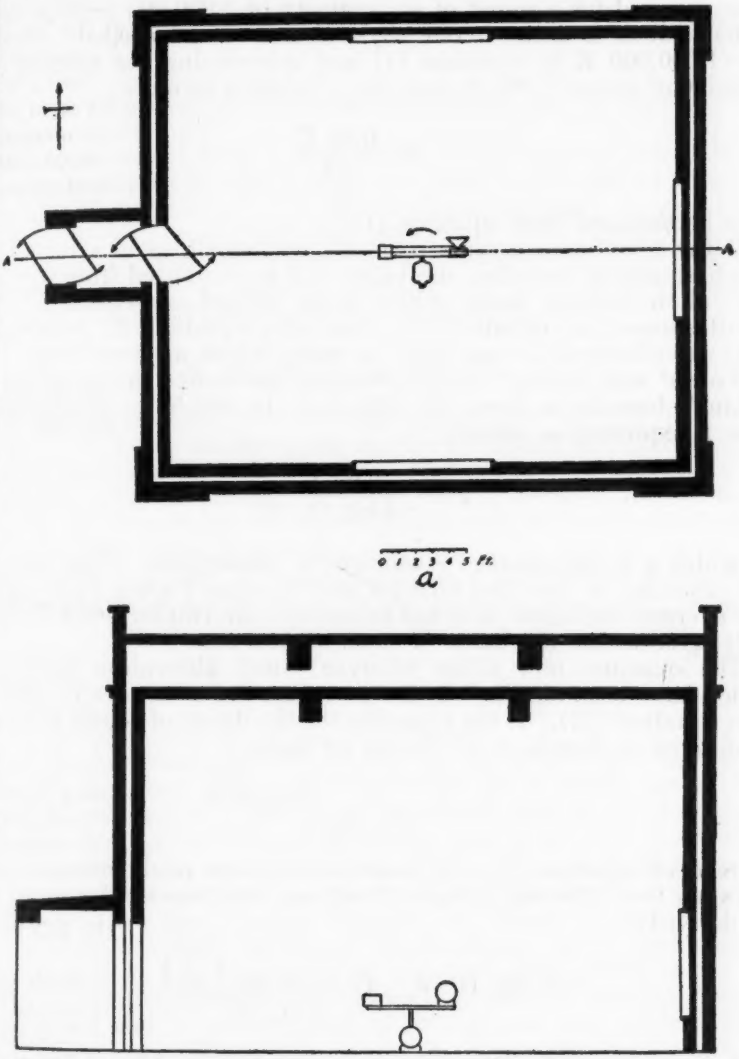

FIGURE 1.—*Plan and cross section of reverberation room*

(*a*) Plan; (*b*) Cross section.

permit more sound to pass through than any other portion of the building. It is seldom that enough sound comes through to disturb any measurements.

V. REVERBERATION TIME FOR AN ACOUSTICALLY DEAD ROOM

W. C. Sabine[7] defined the reverberation time of a room as the time required for a sound of an intensity of 1,000,000 physical units or 60 decibels to decay to one physical unit or zero decibels. Setting $E_0 = 1{,}000{,}000\ E$ in equation (1) and introducing the value of the velocity of sound, 1,088 ft./sec. for v, Sabine's formula

$$T = \frac{0.05\ V}{aS} \tag{11}$$

may be obtained from equation (1).

If the reverberation time becomes very small, as in a room with much absorbing material, the value of a as computed from equation (11) often exceeds unity, which is an absurd consequence. This result shows that equation (11), and also equation (1) from which (11) was obtained, do not apply to rooms which are very dead.

Norris[8] and Eyring[9] have developed theoretical modifications of Sabine's formula to meet this objection, in which the reverberation time is expressed as follows:

$$T = \frac{0.05\ V}{-S \log_e (1-a)} \tag{12}$$

in which a is the average coefficient of absorption. This removes the objection to the older formula, as a becomes 1 when $T = 0$. When the average coefficient does not exceed 0.1 the two formulas (11) and (12) agree within the limits of experimental error.

The question now arises whether sound absorption coefficients which have been obtained in the reverberation room can be used for a in equation (12). If the equation for the decay of sound is written as derived by Norris or by Eyring we have:

$$E = E_0 e^{\frac{vSt \log_e (1-a)}{4V}} \tag{13}$$

instead of equation (1). If measurements are made instrumentally between two different intensity levels an equation similar to (9) can be derived:

$$-S \log_e (1-a) = \frac{4V \times 2.3 \log_{10}\left(\frac{E_1}{E_2}\right)}{v\ (t_2 - t_1)} \tag{14}$$

and the average a for the empty room can be solved for as before. If this average a is defined as

$$\frac{a_1 S_1 + a_2 S_2 + \ldots}{S}$$

[7] See footnote 1, p. 957.
[8] R. F. Norris, of the Burgess Laboratories, Madison, Wis., private communication, as yet unpublished.
[9] Carl F. Eyring, Reverberation Time in Dead Rooms, Reprint B-465, Bell Telephone Laboratories.

where S is the total area and S_1, S_2, etc., the areas of the materials having coefficients a_1, a_2, etc., then when a sample is placed in the room equation (14) becomes:

$$-S \log_e \left(1-\frac{a_1S_1+a_2S_2}{S}\right)=\frac{4V\times 2.3 \log_{10}\left(\frac{E_1}{E_2}\right)}{v\ (t_2-t_1)} \qquad (15)$$

and a_2 can be solved for, as the other quantities are all known or can be measured.

The largest absorption coefficient which has been measured so far in the bureau's reverberation room is 0.94 as calculated by equation (9) or 0.91 by equation (15). The average coefficient for the whole room in this case was a trifle less than 0.04. It is therefore safe to say that in none of the measurements to date, which seldom rise above 0.50, has the reverberation room been dead enough to cause the result to depend appreciably on the formula used.

VI. SOURCE OF SOUND

In selecting a source of sound two features are desirable, first, that a pure note of any desired pitch can be produced, and second, that the intensity can be easily changed through a wide range. After considering various sources of sound it was decided that a loud-speaker with a suitable electric oscillator was the most satisfactory method of accomplishing the above results.

After deciding upon a loud-speaker as a source of sound it was found that care must be taken in the choice of the type, as many speakers do not faithfully reproduce what is put into them. The cone apparently breaks up into segments, and overtones are produced which are not present as harmonics in the current supplied to the loud-speaker. It is also desirable that the acoustical output be directly proportional to the electrical input.

The speaker finally chosen was of the dynamic type, and when tested for the above properties was found to be satisfactory. The quality of the tone was checked by receiving the sound electrically and then amplifying with a high-grade resistance-coupled amplifier and examining the output on an oscillograph. On viewing the image in a rotating mirror no appreciable harmonics were detected.

To determine the relation between the electric input and the acoustical output of the source of sound, the source (a loud-speaker was mounted in the room used for transmission measurements. To obtain as uniform a distribution of sound as possible the loud-speaker was rotated and a narrow band of frequencies used instead of a single frequency. Three different types of electric receivers were used, (1) a special telephone receiver made by the Bell Telephone Laboratories, (2) a loud-speaker in which a movable coil attached to a metallic diaphragm moved in an electromagnetic field, and (3) a condenser microphone. Several different strengths of current were applied to the source, and relative intensity was measured with the different receivers. In each case the square root of the sound intensity was found to be proportional to the current in the source. The results for one frequency are give in Figure 2.

In the first work a Vreeland oscillator was used as a source. The output of this oscillator was remarkably free from harmonics, but there were some undesirable features. A beat-frequency oscillator has been developed which is much more satisfactory. Figure 1 gives the wiring diagram. There are a few points about this circuit which may be of general interest although the ideas are not original.[10] To prevent the two oscillating circuits from being drawn together in frequency when the beat frequency is low, a stage of radioamplification has been added to each oscillator. With this loose coupling it is possible to go as low as 10 cycles without appreciable distortion. The freedom from distortion is also partly due to the careful shielding between the different sections of the oscillator. Special fixed condensers were used in the tuned circuits to prevent frequency drift with temperature changes. The results have been excellent. Over a period of an hour or more there has never been any appreciable frequency drift. The a. c. output voltage is about 4 volts, and approximately constant from 50 to 6,000 cycles.

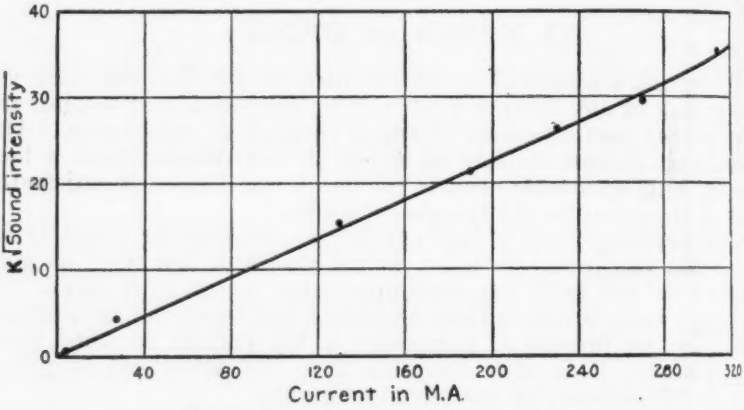

FIGURE 2.—*Intensity calibration of loud-speaker*

For some work it is desirable to use a tone which varies through a narrow band. To accomplish this, a small rotating variable condenser is placed externally in parallel with the condensers in the tuned circuit of one of the oscillators. The width of this band can be controlled by proper adjustment of the rotating condenser.

To obtain sufficient energy for the loud-speaker the output of the beat-frequency oscillator is fed into a high-grade resistance-coupled amplifier, the output of this amplifier going to the loud-speaker.

VII. CALIBRATION OF THE REVERBERATION ROOM

The reverberation room was first calibrated by the ear method, using equation (3). This is essentially the plan used by Sabine in his four-organ-pipe experiment. The principal difference in the two experiments is that by using a loud-speaker it is easy to vary the intensity ratio by as much as 1,600 instead of being limited to 4.

[10] G. F. Lampkin, Radio Broadcast, **13**, No. 3, p. 157; July, 1928. Cohen, Aldridge and West, J. Inst. Radio Engrs. (London), **64**, 1023; 1926.

Five stations for measurement were chosen, arranged in an irregular manner around the floor. The observer was seated in a box for the purpose of eliminating the absorption of his clothing.

To obtain the total absorption of the room at any given frequency observations were made for each intensity. Six intensities were

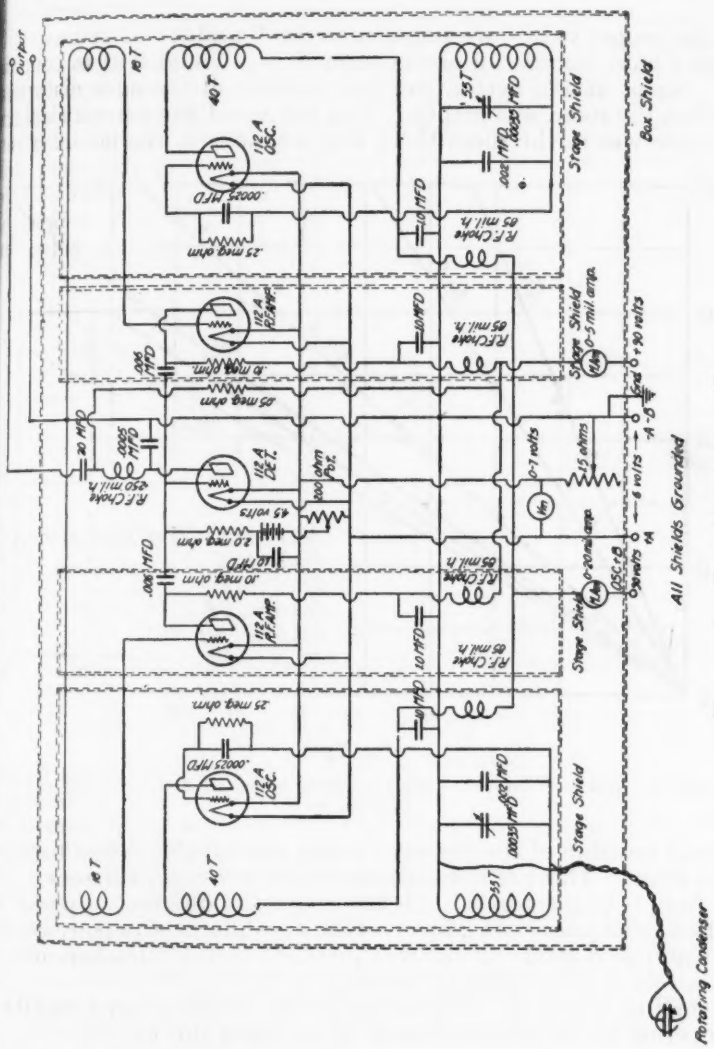

FIGURE 3.—*Beat frequency oscillator*

taken, the minimum corresponding to a 4 milliampere input to the loud-speaker and the maximum to 170 milliamperes input. This required the observer to make 300 observations to obtain the total absorption of the empty room for a single frequency. The figure finally used was the average of those obtained by two observers. The results of some of these observations are shown in Figure 4.

As the acoustical output of the loud-speaker is proportional to the square of the current, $E=KC^2$ and equation (9) becomes

$$a_1 S = \frac{120.9 \times 2 \log_{10}\left(\frac{C}{C_1}\right)}{t - t_1} \tag{10}$$

when the proper values are substituted for V and v.

After a large number of observations it was found that the time of decay, except at 128 cycles, was independent of the observer's position when the room was empty. In a few cases when a very absorbent sample was in the room there was a change in the period with

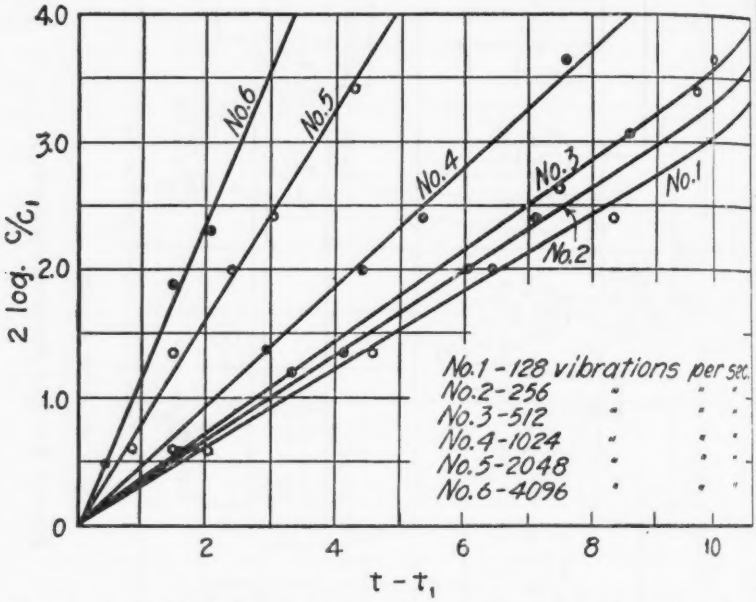

FIGURE 4.—*Relation between period of decay of sound and logarithm of current ratio*

change in position of the observer which was greater than the experimental error. This has not exceeded 0.2 of a second, the total period being from 6 to 8 seconds. At 128 cycles the difference under some conditions was somewhat larger. That the difference in period should be as small as possible at different positions in the room is of importance, as one of the conditions imposed in deriving the formula is that there shall be a uniform distribution of the sound energy at all times. If the period is not independent of the position this condition has not been met.

VIII. MEASUREMENT OF SOUND ABSORPTION COEFFICIENTS BY THE EAR METHOD

The usual method of determining the absorption coefficient of any material has been to determine the period of decay with the room empty and again with the test sample in the room. From equations (3), (5), and (6) the coefficients of the material could be computed

To determine experimentally whether equation (6) gave the proper correction a few sets of measurements were made on different samples at 512 cycles. The results are shown in Figure 5. The curves 1 and 3 intersect at $t=0$, as they should.

For an ordinary determination of time of decay 10 observations were made at each frequency, and this series repeated at a second station. The intensity was then changed and the whole set repeated. As a rule, the results from these measurements were in fair agreement. As a check determination, all of the measurements were repeated on a second day. This required not less than 960 observations to be made to determine the absorption coefficients at six frequencies for a single

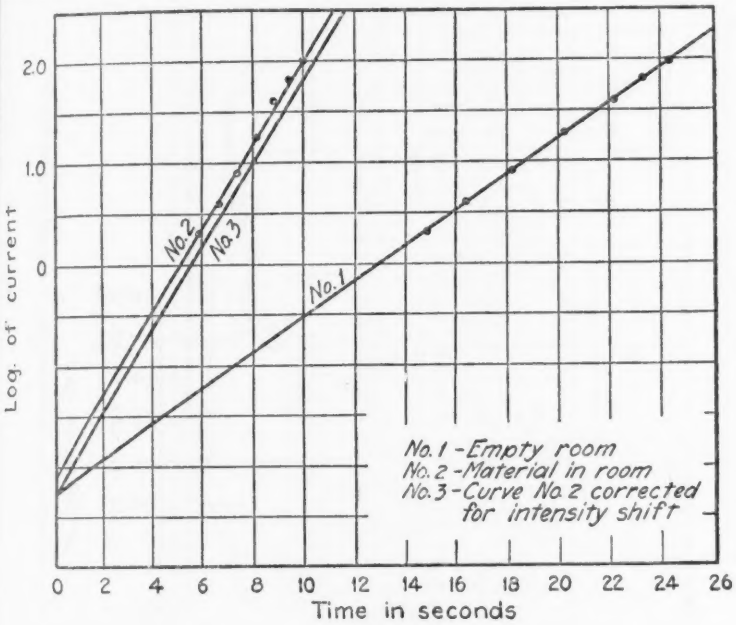
2.0
1.0
0
Log. of current
No. 2
No. 3
No. 1
No. 1 - Empty room
No. 2 - Material in room
No. 3 - Curve No. 2 corrected for intensity shift
0 2 4 6 8 10 12 14 16 18 20 22 24 26
Time in seconds

FIGURE 5

1. Relation between logarithm of current in loud-speaker and period of decay of sound without absorbing material in room.
2. Same with absorbing material in room.
3. Curve 2 corrected for intensity shift due to absorbing material.

sample, the equivalent of two days of strenuous work for a single observer. If the two sets did not check, additional measurements had to be made. As this involved entirely too much work it soon became evident that it was desirable to develop a method in which a single observation was more accurate, so that it would not be necessary to take so many measurements.

IX. MEASUREMENT OF SOUND ABSORPTION BY INSTRUMENTAL METHODS

From the results of ear measurements it was thought that the sound intensity decayed in a nearly uniform manner, and this suggested that an oscillograph record might be taken from which the absorption coefficient might be computed.

To obtain these records it was necessary to use a suitable electric receiver and amplifier. Various electrical receivers were used, but condenser microphone proved the most satisfactory. To obtain th necessary undistorted energy to operate the oscillograph a 5-stag

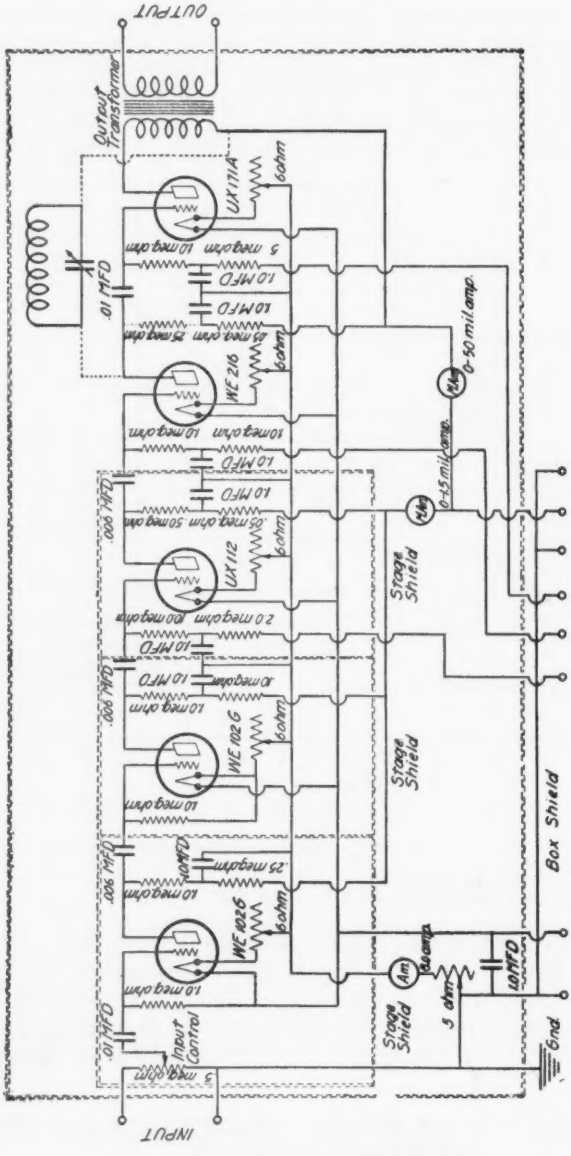

FIGURE 6.—*A 5-stage resistance capacity coupled amplifier*

resistance-coupled amplifier was built. A diagram of this circuit is shown in Figure 6. The next to the last stage contains a tuned circuit which can be used when desired. This aids in eliminating all sounds except those for which the circuit is tuned.

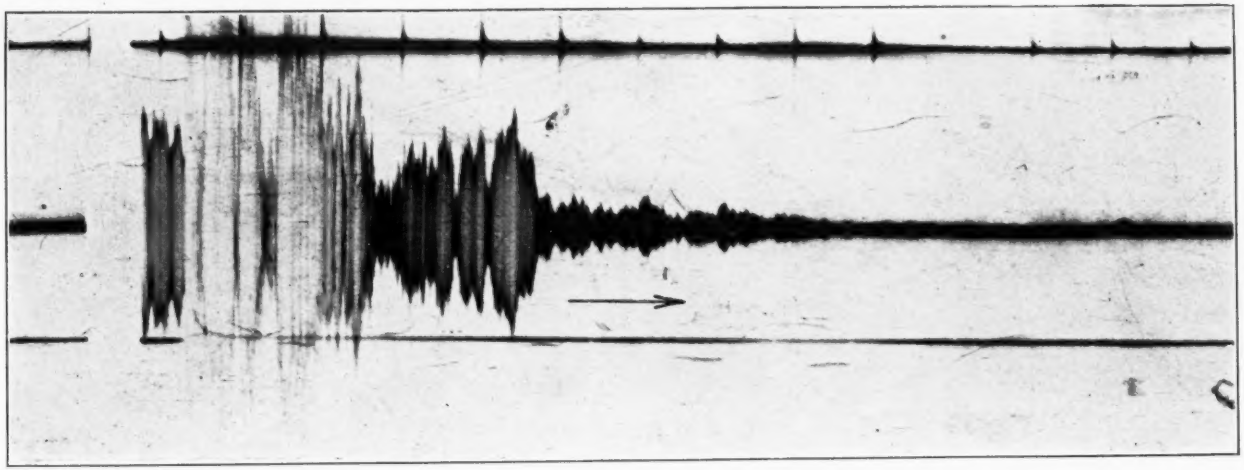

FIGURE 7.—*Decay of pure tone*

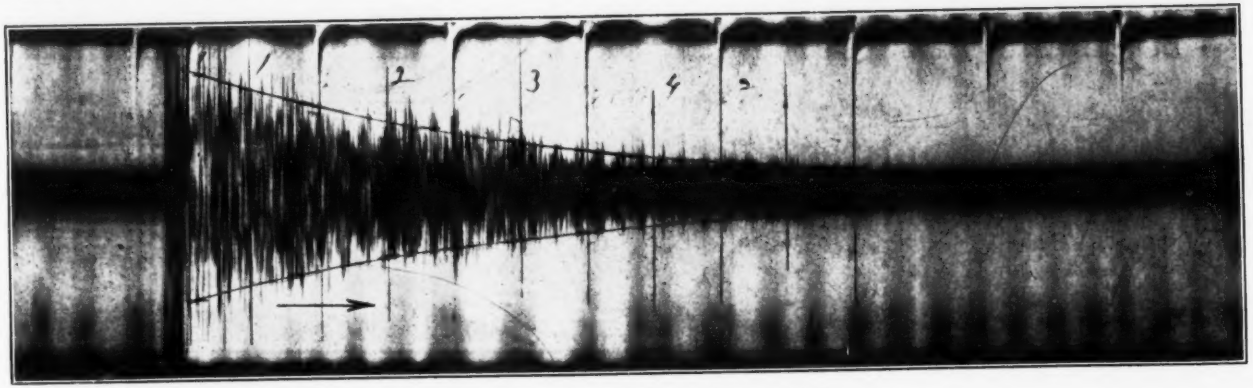

FIGURE 8.—*Decay of band-frequency tone*

Theoretically the curves recorded photographically should show a logarithmic decay for the sound energy; actually they do not always do so. Figure 7 illustrates the decay of a low-pitched note of a single frequency.

After obtaining a few films like this it became evident that steps must be taken to obtain a distribution of sound which was more nearly uniform at each instant. To accomplish this the source of sound was rotated and instead of using a single frequency, a band was used, its width being about 10 per cent of the average frequency. For example, at 512 cycles the lower end of the band was about 25 cycles below 512 and the upper about 25 cycles above. Jointly these two procedures produced a much more uniform distribution. Figure 8 shows one of the films obtained under these conditions. In this case it is possible to draw an envelope to the curve, and by measuring its ordinates at a number of values of the time the rate of

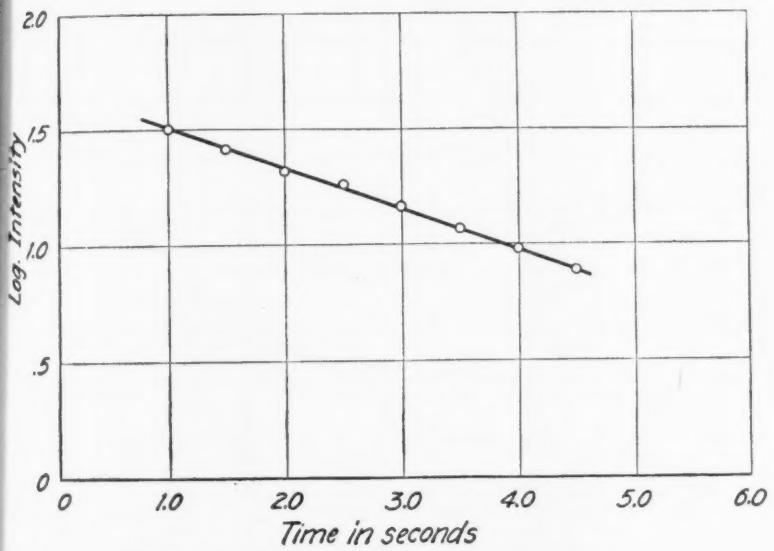

FIGURE 9.—*Rate of decay from oscillogram record*

decay can be computed. Knowing the rate of decay, the absorption can be computed from equation (3). To show that the rate of decay was logarithmic the ordinates of the above film have been squared and their logarithms plotted against the time. The results are shown in Figure 9.

In this manner a calibration of the reverberation room was made, which is shown in Figure 10 along with the calibration previously described, made by ear. There was a little additional equipment in the room when the calibration was made by the oscillograph, but it is doubtful if this would account for the difference of four or five units of absorption shown in the curves.

An attempt was also made to eliminate some of the irregularities by rectifying the current and using large chokes and condensers in the electrical circuit. Figure 11 shows the result. It is quite evident

there is no improvement; in fact, it would be easier to draw an envelope to Figure 8.

The results shown in Figure 10 are the average of a considerable number of films. It was found that the result of a single film was not dependable. The variation is probably caused by a gradual drift of the sound pattern in the room past the receiver as the sound dies away. It might be considered that two things are taking place. First, the sound is decaying, and second, the drift of the sound pattern either tends to increase or decrease the rate of decay. If the drift is such as to increase the rate of decay the apparent absorption is too large, while if the drift decreases the rate of decay, the apparent absorption is too small. If a sufficient number of films were taken this variation would probably average out, but the time required for this is greater than that required to take the measurements by ear.

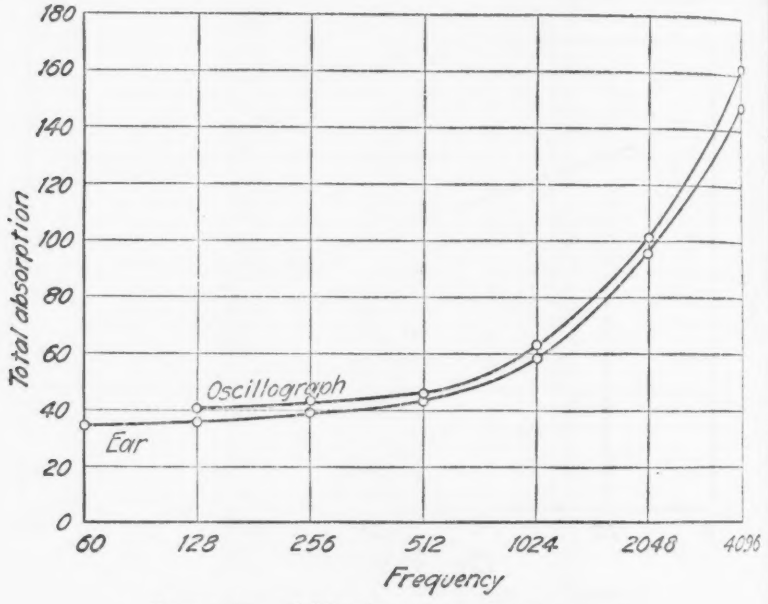

FIGURE 10.—*Calibration of reverberation room*

As the oscillograph gives a permanent record, which is always desirable, it seemed best to make further efforts to secure satisfactory records of the sound decay. If a record could be made through a sufficiently long-time interval it seemed possible that the drift of the sound pattern might be averaged out. To accomplish this it was necessary to change the amount of amplification while taking the record. This was accomplished by the use of an attenuator in the amplifier circuit. Figure 12 shows how such a record looks. By drawing envelopes to these two decay curves and then drawing parallel lines as shown we can determine the time that is required for the sound to decay a definite amount. The amount of this decay can be determined by using a calibrated attenuator box. The absorption can then be calculated as before from equation (9).

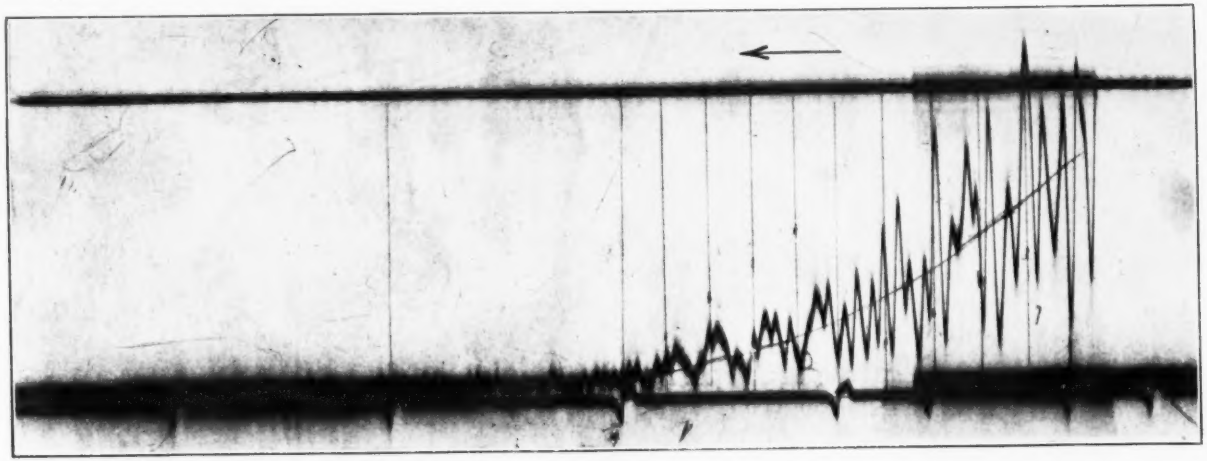

FIGURE 11.—*Decay with current rectified*

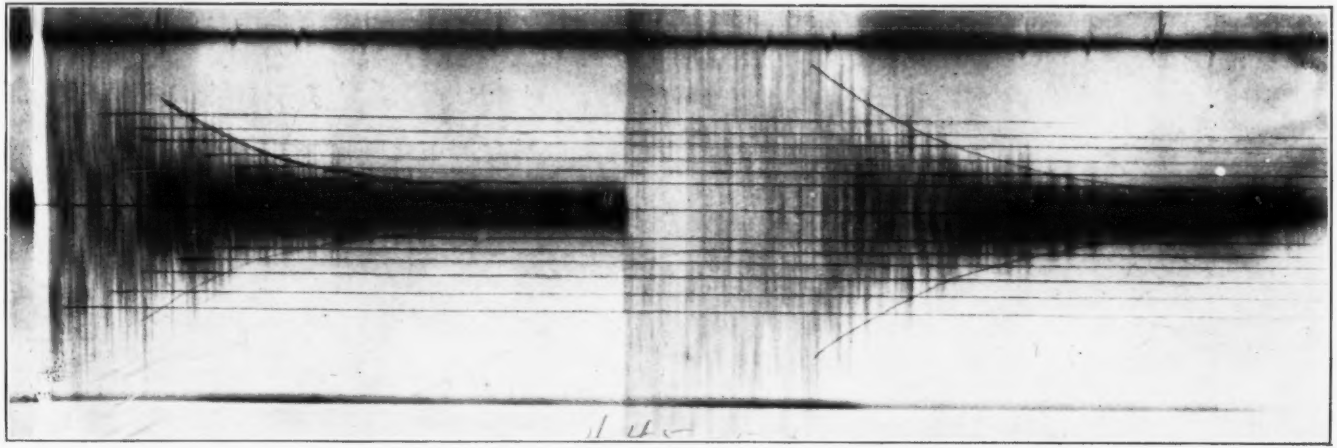

FIGURE 12.—*Oscillogram of sound decay*

This gives us a method which is very similar to the classical reverberation method. The principal difference lies in the fact that we no longer use the threshold of audibility, but determine the time of decay for a measured change of intensity. A large number of records have been made in this manner, but the results are somewhat disappointing when used to determine the absorption coefficients of materials. It was hoped that the time of decay of a given sound through a given change of intensity would be constant provided other conditions remained constant. It was found, however, that the time was not a constant due probably to the drift of the sound pattern. Variations were found which were somewhat smaller than those obtained by a good observer using a stop watch to measure the time of decay of the sound, as the error due to the personal element was eliminated. As a result of this it was found necessary to take a number of films and use the average if satisfactory results were to be obtained when measuring the sound absorption coefficient of samples of material.

As it is a slow process to take oscillograph records and work them up, the oscillograph has finally been abandoned and the process slightly modified. The oscillograph method as described consisted

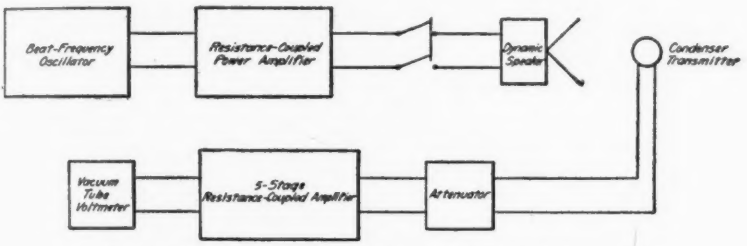

FIGURE 13.—*Schematic diagram of electrical apparatus*

Sketch shows entire arrangement

essentially in determining the length of time required for a sound to decay by a given amount. This can also be done by substituting a rectifying tube and microammeter.

The process of measurement is as follows. After the source has been on for a second or so the sound is cut off. Some arbitrary point is taken on the microammeter scale and as the sound dies away the microammeter needle passes this point. At that instant a timer is started by the observer and a helper changes the attenuator box a given amount so as to decrease the attenuation. The current is thus increased in the microammeter. As the sound continues to decay the needle again drops back through the same point and at this instant the timer is stopped. Knowing the change in attenuation and the time, the absorption can be computed from equation (10).

The measurements can be made much faster in this manner, although the accuracy of determining the time interval by a single measurement is not as good as that obtained from a single film taken with the oscillograph.

To obtain satisfactory results it is necessary to make a large number of measurements, just as when the ear is used as a measuring instrument, but it is believed that the accuracy of measurement is somewhat greater.

The results of some of the measurements are given in Table 1.

TABLE 1.

Sample No.	Method	Absorption coefficients at frequencies—					
		128	256	512	1,024	2,048	4,096
1	Instrument	0.14	0.27	0.53	0.62	0.60	0.54
	Oscillograph	.16	.30	.53	.63		
	Ear	.16	.28	.52	.66	.58	.42
2	Instrument	.08	.13	.25	.54	.67	.42
	Ear	.10	.14	.24	.55	.67	.40
3	Instrument	.19	.34	.63	.75	.77	.53
	Ear	.17	.31	.62	.75	.76	.44

WASHINGTON, July 8, 1930.